Differential functioning of deep and superficial lumbar multifidus fibres during vertebral indentation perturbations

by

Scott Apperley

B.H.K., University of British Columbia, 2005

A THESIS SUBMITTED IN PARTIAL FULFILLMENT OF
THE REQUIREMENTS FOR THE DEGREE OF

MASTER OF SCIENCE

in

The Faculty of Graduate Studies

(Human Kinetics)

THE UNIVERSITY OF BRITISH COLUMBIA

(Vancouver)

June 2008

Abstract

Introduction: Lumbar spine stability programs have been advocated to prevent and rehabilitate low back injury. Specifically, abdominal 'drawing in' has been used to train motor control deficits in individuals with low back pain. This technique requires differential activity within deep and superficial lumbar multifidus fibres, yet the ability of these fibres to act differentially has not been extensively examined. Deep fibres are hypothesized to act as spinal stabilizers while superficial fibres are hypothesized to act as global movers of the trunk.

Objective: To investigate differential excitation of deep and superficial lumbar multifidus fibres during segmental indentation loads to the lumbar spine.

Methods: Posterior-anterior indentation loads were applied to individual lumbar spinous processes of prone participants at three different velocities and three different indentation displacements. Indentations consisted of an initial downward displacement that was subsequently held for 500 milliseconds. Intramuscular electromyography (EMG) of deep and superficial lumbar multifidus fibres at L3, L4 and L5 was recorded. EMG was quantified by "average" root mean square (RMS), peak RMS of a sliding RMS window and time-to-peak RMS over the indentation phase and 500 millisecond hold phase.

Results: Increased indentation displacement at the slowest velocity resulted in increased "average" RMS of only the L5 superficial multifidus fibres. Increased indentation velocity produced differential effects in deep and superficial multifidus fibres. "Average" RMS and peak RMS significantly increased with increasing indentation velocity in most deep fibre recording sites, yet superficial fibre excitation did not significantly increase. In most EMG recording sites, the time-to-peak RMS increased with increasing indentation displacement and decreased with increasing indentation velocity.

Conclusion: Differential excitation of superficial and deep multifidus fibres was found with increasing indentation velocity; however, the result was opposite to that hypothesized. This result is clinically relevant because it suggests deep multifidus fibre excitation may increase in response to increased perturbation magnitude, possibly to restore vertebral body position. Differential excitation effects may also be related to different mechanical stimuli experienced by deep and superficial fibres due to vertebral body movement during indentation loads.

Table of Contents

Abstract ii
Table of Contents iii
List of Tables v
List of Figures vi
Acknowledgements viii

1. Introduction 1
2. Review of literature 5
2.1. Lumbar spine stability 5
2.1.1. The passive subsystem 5
2.1.2. The active subsystem 8
2.1.3. Trunk stiffness 12
2.1.4. The neural subsystem 14
2.2. The lumbar multifidus 16
2.2.1. Anatomy 16
2.2.2. Lumbar multifidus reflexes 18
2.2.3. Lumbar multifidus activity during voluntary trunk movements 23
2.3. The role of lumbar multifidus in lumbar spine stability 26
2.3.1. "Drawing in" and the "abdominal brace" 27
2.3.2 Differential functioning of lumbar multifidus 35
3. Statement of the problem 38
4. Hypotheses 39
5. Operational definitions 40
6. Methods and procedures 41
6.1 Study participants 41
6.2 Electromyography and multifidus imaging 42
6.3 Motor displacement and force 46
6.4 Respiration 48

6.5 Experimental protocol 49
6.5.1 Vertebral motion and participant experimental position 49
6.5.2 Indentation perturbations 50
6.6. Data analysis 54
7. Results 57
7.1 Experimental conditions validation 59
7.1.1 Trial exclusion 59
7.1.2 Perturbation velocity and displacement 59
7.2 Electromyography 66
7.2.1 Part A: The effect of perturbation displacement 68
7.2.1 Part B: The effect of low and high perturbation velocities 70
8. Discussion 75
8.1 Perturbation displacement 77
8.2 Perturbation velocity 81
8.3 Perturbation level 86
8.4 Limitations and trial exclusions 88
8.5 Clinical implications 90
9. Conclusion 92
10. References 93

Appendices 109
Appendix A: Fine-wire electrode fabrication 109
Appendix B: Lumbar multifidus imaging and fine-wire electrode insertion 118
B.1 Lumbar multifidus imaging 118
B.2 Fine-wire electrode insertion 120
Appendix C: Ethical approval and participant consent form 128
Appendix D: Statistical tests 130
Appendix E: Individual subject data 135

List of Tables

Table 6.1 List of participant ages and anthropometry. 41

Table 6.2 Experimental Design employed for analysis of each EMG channel (Note: The third dimension (perturbation level) of this 3x3x3 experimental design is not shown here). 55

Table 7.1 Mean perturbation velocities (m/s) across subjects for each perturbation displacement and velocity combination at each perturbation level. 60

Table 7.2 Mean perturbation displacements (mm) across subjects for each perturbation displacement and velocity combination at each perturbation level. 61

Table 7.3 Summary of statistical p values for Part A and B statistical tests. Statistically significant effects are denoted with **. 67

List of Figures

Figure 6.1 Transverse plane ultrasound image at the L4 vertebral level showing the fascial border of the lumbar multifidus..... 43

Figure 6.2 Example fine-wire electrode insertion locations. (A) L5 superficial needle used to insert the fine-wire electrode in Subject 06, (B) L3 superficial wire in Subject 08, (C) L5 deep needle used to insert electrode in Subject 10 and (D) L4 deep needle and L4 superficial wire in Subject 10. 45

Figure 6.3 The servo-motor used to deliver the indentation loads by manipulating the position of the indentation rod. The force transducer between the indentation rod and the cupped felt contact surface recorded force between the rod and skin..... 46

Figure 6.4 Schematic of digital servo-motor control during experimental posterior-anterior indentations..... 47

Figure 6.5 Experimental setup to deliver indentation perturbations while recording displacement, force and intramuscular electromyography. 51

Figure 7. 1 Displacement, force and electromyography of a (a) slow velocity, shallow displacement perturbation (V1-D1) and a (b) medium velocity, intermediate displacement perturbation (V2-D2) in Subject 03. For comparison purposes, both perturbations are plotted on the same scale of axis..... 58

Figure 7.2 Idealized perturbation velocity profiles for slow, medium and fast perturbation velocities (Note the x and y scales for each velocity profile are different). 63

Figure 7.3 Velocity profiles time-normalized to the length of the active indentation phase and expressed as a percentage of their target velocity. Perturbations to different displacements are expressed in different colours (D1=blue, D2=red, D3=black). Note that only Velocity 1 (V1) perturbations achieved 100% of their target velocity. 64

Figure 7.4 The revised experimental design excluding V3 and D3 perturbations..... 66

Figure 7.5 "Average" rms (top panel), peak rms (middle panel) and time-to-peak rms (bottom panel) for each EMG channel at D1 and D2 displacements. For comparison purposes, the "average" rms, peak rms and time-to-peak rms axes are consistent across Figures 7.5, 7.6, 7.7 and 7.8..... 69

Figure 7.6 Part B: "Average" rms for D1 (top panel) and D2 (bottom panel) perturbation displacements. For comparison purposes, the "average" rms, peak rms and time-to-peak rms axes are consistent across Figures 7.5, 7.6, 7.7 and 7.8. 71

Figure 7.7 Part B: Peak rms for D1 (top panel) and D2 (bottom panel) perturbation displacements. For comparison purposes, the "average" rms, peak rms and time-to-peak rms axes are consistent across Figures 7.5, 7.6, 7.7 and 7.8. 72

Figure 7.8 Part B: Time to peak rms for D1 (top panel) and D2 (bottom panel) perturbation displacements. For comparison purposes, the "average" rms, peak rms and time-to-peak rms axes are consistent across Figures 7.5, 7.6, 7.7 and 7.8..... 74

Figure 8.1 Indentation displacement during V1-D1 (orange dashed line) and V1-D2 (solid brown line) perturbation displacements across time. The dotted blue line at the top of the figure represents the length of the time interval between the onset of the active indentation phase and the end of the indentation hold phase..... 80

Figure 8.2 Conceptualized three vertebrae model of the relative stretch within the shorter deep lumbar multifidus fibres and longer superficial multifidus fibres. As the indentation load displaces the vertebral body, superficial and deep fibre attachments experience the same orthogonal displacement. Deep fibres experience a greater relative stretch and larger angular deviation than superficial fibres. 83

Acknowledgements

I was very fortunate to work with many terrific researchers whose knowledge and dedication to their research was truly inspiring. My graduate supervisor, Dr. David Sanderson, provided invaluable guidance throughout my graduate degree and without his support my personal and academic goals would not have been achieved. I am also grateful to my committee members for their insight and investment of time in this project. Drs. Jean-Sebastien Blouin, Timothy Inglis and David Sanderson, were influential to my academic development as a researcher and without their commitment and leadership this project would not have been possible.

I would like to thank my fellow graduate students, particularly my biomechanics lab members Ellexis, Ryan, Karine and Julia for their encouragement and friendship. I would also like to acknowledge Chris and Dan of the Spine Neurophysiology lab for their help during data collection. Thanks to Dr. Bill Sheel for providing and assisting with the pneumotachometer and Dr. Donna Ford in the Department of Anatomy for furthering my understanding of lumbar spine anatomy.

I would like to thank my family and friends for their support, reliability and honesty prior to and throughout my degree. Special thanks to Krista for looking out for me the entire way, providing emotional support and understanding. A graduate degree is an academic venture, yet the contributions of these individuals allowed this academic experience to become one of personal development.

1. Introduction

Low back pain (LBP) is a widespread and costly healthcare problem in today's society. LBP has been cited as the second most common reason for going to the doctor (Andersson 1999; Mengiardi et al. 2006). The lifetime prevalence of developing moderate or severe LBP in western populations has been estimated to be between 70% and 85% (Andersson 1999; Frymoyer et al. 1983). The majority of individuals who develop LBP are still experiencing symptoms one year after the initial episode (Croft et al. 1998). In a review of eighteen studies from eight different countries, the point prevalence of LBP was between 4.4% and 33% (Loney and Stratford 1999). In Canadians over the age of twelve, "back problems" were the second most prevalent chronic condition in 1996/1997 and affected more Canadians than asthma, high blood pressure or arthritis (Schultz and Kopec 2003). Based on Statistics Canada surveys in 1994/95 and 1996/97, Perez (2001) examined the two year prevalence of back problems in Canada. Of over 6,000 Canadian workers who reported their health as "very good", "good" or "excellent," 9% had developed "back problems" within the next two years (Perez 2000). LBP has special implications for individuals in the workforce and the elderly. During the 2003 calendar year, low back injuries were the second (16%) most commonly injured body part in Canadians aged 18-85 (Wilkins and Mackenzie 2007). Additionally, in Canadians over the age of 55, almost 20% of chronic conditions were attributed to "non-arthritic back problems" (Wilkins and Park 1996).

The costs of LBP to both the individual and society can be considerable. The direct annual costs of spine and back disorders in the United Kingdom were 1.6 billion pounds in 1998 (Maniadakis and Gray 2000), while in Canada these disorders cost approximately 670 million dollars annually (Coyte et al. 1998). These direct costs are dwarfed by the indirect costs such as lost work time and productivity (Lim et al. 2006). The yearly cost of lost work time due to LBP was estimated to be over 7.5 billion dollars in Canada (Coyte et al. 1998) and 28 billion dollars in the United States (Maetzel and Li 2002). Acute LBP often disappears spontaneously (Hides et al. 2001); however, in some individuals LBP can become chronic. Chronic LBP has the highest economical cost as

fewer than 10% of LBP claims make up 64.9-84.7% of LBP costs (Hashemi et al. 1998). LBP intervention programs have had some success, although many have been considered to be ineffective (Ebenbichler et al. 2001). In a comparison of national clinical guidelines for the management of LBP in eleven countries, Koes et al (2001) revealed discrepancies in management, particularly as they relate to the efficacy of exercise, when exercises are warranted and whether specific exercises (eg. McKenzie Back Exercises) should be prescribed (Koes et al. 2001). The rates of back surgery in eleven different countries varied considerably and appeared to be linearly associated with the number of available surgeons as well as the national rates of discretional (eg. tonsillectomy) surgeries (Cherkin et al. 1994).

Individuals with LBP form a heterogeneous group (Kang et al. 2007) making diagnosis of a specific cause problematic. Lumbar segmental instability has been implicated as significant cause of LBP (Panjabi 2003) and as a causative factor in 20-30% of chronic LBP cases (Taylor and O'sullivan 2000). Segmental instability that results in recurrent LBP in response to small, unpredictable or rapid disturbances to the lumbar spine is often referred to as clinical instability (Taylor and O'sullivan 2000), however exact definitions differ (Crisco et al. 1992). Clinical instability describes the inability of the vertebral column to preserve normal movement of individual vertebrae when exposed to common physiological loads (White 1990). The link between segmental instability and back pain is well established, however, the association is not unidirectional. Injury to anatomical structures in the low back can result in lumbar segmental instability; however, instability can also be the cause of back injury (McGill et al. 2003). Regardless of whether segmental instability is the cause or effect of LBP, many clinical researchers have investigated the contributing factors, deficits and mechanisms of lumbar spine stability (Cholewicki and McGill 1996; Cholewicki and VanVliet 2002; Granata and England 2006; Hodges and Richardson 1996; McGill 2001; McGill 2007; Moorhouse and Granata 2007; Richardson et al. 1999; Richardson et al. 2004).

Bergmark (1989) was one of the first researchers to mathematically model spinal stability by dividing the trunk muscles into two primary groups: local muscles with direct

attachments to the vertebral column and global muscles that act as prime movers of the trunk (Bergmark 1989). Until recently, electromyography (EMG) of the local muscles was challenging due to the depth of these muscles and lack of an objective method of ensuring needle electrode insertion accuracy (Donisch and Basmajian 1972; Floyd and Silver 1951; Floyd and Silver 1955; Morris et al. 1962). Fine-wire electrodes inserted using ultrasound guidance (Andersson et al. 1996; Andersson et al. 2002) have overcome these challenges and significantly increased our knowledge of intersegmental and deep trunk muscle function. A group of researchers from the University of Queensland in Australia have extensively examined the function of these muscles in people with healthy backs and those with LBP (Hides et al. 1995; Hides et al. 2001; Hodges and Richardson 1996; Hodges and Richardson 1997a; Hodges and Richardson 1997b; Hodges and Richardson 1999a; Richardson and Jull 1995; Richardson et al. 1999; Richardson et al. 2002). Based on observations of lumbar multifidus (Hides et al. 1994; Hides et al. 1996) and transversus abdominus impairments (Hodges and Richardson 1998; Hodges and Richardson 1999b) in individuals with LBP, these researchers developed a specific 'drawing in' technique designed to train and rehabilitated lumbar segmental instability (Richardson and Jull 1995; Richardson et al. 1999; Richardson et al. 2004). This 'drawing in' technique consisted of co-contraction between transversus abdominus and the deep fibres of lumbar multifidus (Richardson et al. 1999; Richardson et al. 2004). Randomized clinical trials have supported the use of specific segmental stabilization exercises to teach the 'drawing in' technique over conventional LBP treatment programs (Hides et al. 1996; O'Sullivan et al. 1997). Chronic LBP patients had reduced pain and disability after a ten week program of specific stabilizing exercises to train 'drawing in' (O'Sullivan et al. 1997), while acute LBP sufferers had a reduced recurrence rate of future LBP after these specific stabilizing exercises (Hides et al. 2001).

The 'drawing in' technique requires contraction of the deep fibres of lumbar multifidus while the superficial fibres are to remain electrically inactive (Richardson et al. 1999). The superficial fibres of lumbar multifidus are hypothesized to function with the global muscles and act as prime movers of the trunk (MacDonald et al. 2006). This would imply differential function of the superficial and deep layers of lumbar multifidus in situations

requiring spinal stability. Differential functioning within a single muscle has been observed between the long and short head of biceps brachii (Brown et al. 1993), while the feline splenius muscle is anatomically compartmentalized (Richmond et al. 1985). Rapid arm movement and trunk perturbation studies have supported the hypothesis of a functional differentiation between the superficial and deep layers of lumbar multifidus (Moseley et al. 2002; Moseley et al. 2003), however, controversy remains as to whether this differentiation exists (MacDonald et al. 2006).

This study will examine deep and superficial lumbar multifidus fibre excitation during segmental challenges to spinal stability. EMG from the deep and superficial lumbar multifidus fibres during perturbations of varying displacement and velocity will be examined to support or oppose the hypothesis that deep and superficial lumbar multifidus fibres have the ability to function differentially.

2. Review of literature

2.1. Lumbar spine stability

Lumbar spine stability has been proposed to be controlled by three subsystems: the passive, active and neural subsystems (Panjabi 1992a). Lumbar spine stability is task-specific (Reeves et al. 2007) and requires the integrated function of these subsystems to dynamically meet stability requirements. Manohar Panjabi (Panjabi 1992b) proposed that the goal of these systems was to maintain intervertebral joint motion within the non-elastic or neutral region of the total range of vertebral motion (Panjabi 1992b).

2.1.1. The passive subsystem

The passive subsystem is compromised of the lumbar vertebrae, ligaments of the lumbar spine, the intervertebral discs, the facet joints and capsules and the non-contractile, elastic components of muscle (Panjabi 1992a). The vertebral bodies in the lumbar spine are the larger and stronger than in the thoracic and cervical vertebral columns (Tortora 2000). The lumbar facet joint articular surfaces are oriented vertically at an oblique angle to the sagittal and coronal planes (Tortora 2000). The facet joints are surrounded by zygapophysial joint capsules that prevent the articular surfaces from separating (McGill 2007) and limit axial rotation (Panjabi 2003). These capsules are innervated by the superior and inferior medial branches of the lumbar dorsal ramus (Bogduk 2000a). Several ligaments in the lumbar spine restrict vertebral motion, particularly at the end of the joint range of motion (ROM). The anterior and posterior longitudinal ligaments run anterior and posterior to the vertebral bodies and are innervated by nerve plexuses (Bogduk 2000a). The anterior longitudinal ligament assists in preventing excess vertebral column extension, while the posterior longitudinal ligament assists in preventing sagittal plane flexion (McGill 2007). The supraspinous ligament extends along the spinous processes and also resists excessive vertebral column flexion (McGill 2007). The interspinous ligament is located just anterior to the supraspinous ligament and connects spinous processes of successive vertebrae (McGill 2007). Both the supraspinous and

interspinous ligaments are innervated by the lumbar dorsal ramus (Bogduk 2000a) and are formed in part by the posterior thoracolumbar fascia, lumbar multifidus and erector spinae tendons (Johnson and Zhang 2002). Short intertransversarii ligaments connect adjacent transverse processes, although their exact morphology is uncertain (McGill 2002).

The role of these passive structures and the intervertebral disc in sagittal plane motion has been investigated in porcine lumbar spines (Kaigle et al. 1995). Kaigle et al. (1995) introduced eight different surgical injuries to porcine spines including transverse process injury, interspinous ligament removal, intervertebral disc incision and facet joint injury. Facet joint injuries resulted in significantly greater sagittal rotation, while anterior intervertebral disc injuries were associated with greater vertebral movement along the longitudinal axis (ie. axial translation) (Kaigle et al. 1995). The combination of anterior intervertebral disc injury and interspinous ligament removal resulted in significantly greater sagittal rotation and anterior-posterior translation during flexion and extension (Kaigle et al. 1995). They concluded that the role of the intervertebral disc was to prevent excessive axial translation, while the interspinous ligament limited sagittal rotation (Kaigle et al. 1995). In addition, to their role in limiting axial rotation, the facet joints limited vertebral sagittal rotation and shear translation (Kaigle et al. 1995). Despite the actions of these passive structures, the ligamentous vertebral column is quite susceptible to buckling without muscular forces. When a mass is placed at the top of a vertebral column without muscles, the magnitude of the load causing the column to bend is referred to as the 'buckling load' (Crisco and Panjabi 1992). The thoracolumbar (T1-sacrum) buckling load in the coronal plane has been reported to be 20N (Lucas and Bresler 1961), while lumbar buckling loads have been measured to be 88N (L1-S1) and 98N (L2-S1) (Crisco et al. 1992). Surgical intervertebral disc injury decreased the buckling load by 17-50% and facet joint injury by 40-80% in the lumbar spine specimens (Crisco et al. 1992). These buckling loads are significantly less than the vertebral column experiences in vivo (Crisco and Panjabi 1992) which highlights the important role of muscles in spinal stability. The passive subsystem appears to exert its greatest effect in restricting spinal motion near the end of the normal ROM (Panjabi 1992a). In the sagittal

plane, this hypothesis was reinforced by Lee and Evans (2000) who applied posterior-anterior forces to spinal units consisting of two vertebrae. Dissection of the ligamentum flava, supraspinous ligament, interspinous ligament or zygapophysial capsule joints did not lead to significantly greater movement patterns (Lee and Evans 2000). These authors reasoned that this was because they did not fully load the vertebral units to their physiological ROM (Lee and Evans 2000).

It should be noted that many of these studies (Crisco et al. 1992; Kaigle et al. 1995; Lee and Evans 2000; Lucas and Bresler 1961) did not include the passive properties of muscle and the thoracolumbar fascia. The thoracolumbar fascia is composed of three layers (anterior, middle and posterior) that originate at the vertebrae and blend together to insert at the lateral raphe (Bogduk and Macintosh 1984). The anterior and middle layers encircle quadratus lumborum by originating at the lumbar transverse processes and passing anterior and posterior to quadratus lumborum, respectively (Bogduk 2000b; Hansen et al. 2006). The posterior layer attaches to the lumbar spinous processes and passes posterior to the dorsal back muscles to merge with the other layers at the lateral raphe (Bogduk 2000b). The posterior layer is composed of a deep lamina with fibres passing in a caudolateral direction and superficial lamina with fibres passing caudomedially (Bogduk and Macintosh 1984).

The posterior layer of the thoracolumbar fascia has been hypothesized to produce a trunk extensor moment through a hydraulic amplifier mechanism (Gracovetsky et al. 1977) or through lateral tension at the lateral raphe (Tesh et al. 1987). The hydraulic amplifier mechanism refers to paraspinal muscles expanding dorsally with active contraction which tensions the posterior thoracolumbar fascia and causes trunk extension (Bogduk and Macintosh 1984). The validity of this mechanism and its contribution to trunk extension remains in question (Bogduk 2000b). Due to the differing orientation of the deep and superficial lamina of the posterior thoracolumbar fascia, it has been hypothesized that lateral tension to all three layers at the lateral raphe could produce a lumbar extensor moment (Bogduk and Macintosh 1984). Lateral tension would produce a caudolateral force on the deep lamina and rostrolateral force on the superficial lamina. If the tension

was applied bilaterally the resultant forces would cause the lower lumbar vertebrae to move rostrally and the upper lumbar vertebrae to move caudally resulting in trunk extension due to the natural lordosis of the lumbar spine (Bogduk and Macintosh 1984). Barker et al. (2006) applied 20N of lateral tension to the transversus abdominus aponeurosis (which originates at the lateral raphe) of cadavers and observed increased trunk resistance and segmental stiffness to trunk flexion and decreased resistance and segmental stiffness to trunk extension. The authors concluded that lateral tension through the middle and posterior thoracolumbar layers has a stabilizing effect on the lumbar spine (Barker et al. 2006).

2.1.2. The active subsystem

Muscles and tendons spanning the vertebral column make up the active spinal stability subsystem (Panjabi 1992a). Many short muscles connect various parts of adjacent vertebrae. Each lumbar spinous process has bilateral interspinales muscles that attach the spinous processes of adjacent vertebrae (Bogduk 2000b; Richardson et al. 1999). There are three intertransversarii muscles that connect adjacent transverse processes (Bogduk 2000b). The intertransversarii mediales attaches at the accessory process of the superior vertebrae and at the mamillary process of the inferior vertebra (Hansen et al. 2006). Both the intertransversarii laterales dorsales and ventrales attach caudally at the transverse process, but dorsales attaches rostrally at the accessory process, while ventrales attaches rostrally at the superior transverse process (Bogduk 2000b). The exact function of these muscles is unknown (Bogduk 2000b); however, they have been proposed to have a proprioceptive function (McGill 2007).

The thoracic erector spinae muscles were originally thought to be continuous with the lumbar fibres; however, detailed anatomical studies have shown this is not the case (Bogduk 1980). The thoracic erector spinae consists of the longissimus thoracis pars thoracis and iliocostalis lumborum pars thoracis. Both of these muscles form tendons that merge to form the erector spinae aponeurosis, inserting at the sacrum and posterior superior iliac spine (Bogduk 2000b). The thoracic erector spinae muscles extend the

trunk (Tortora 2000), while longissimus thoracis pars thoracis also has a role in lateral flexion (Bogduk 2000b). The lumbar erector spinae muscles consist of the longissimus thoracis pars lumborum and iliocostalis lumborum pars lumborum. Longissimus thoracis pars lumborum fascicles arise from the L1-L5 transverse processes and attach to the posterior superior iliac spine with the L5 fascicle attaching most medial and each successive fascicle more laterally (Bogduk 2000b; Richardson et al. 1999). Iliocostalis lumborum pars lumborum fibres also arise from the transverse processes and insert at the ilium (Richardson et al. 1999), with both superior and inferior attachments lateral to the longissimus thoracis pars lumborum attachments (Bogduk 2000b).

Lumbar multifidus consists of superficial and deep fascicles that span between two and five vertebral levels (Macintosh et al. 1986). Deep fibres begin at the vertebral lamina and run two or fewer vertebral levels caudal to attach at the mamillary processes (Macintosh et al. 1986). Superficial fibres arise from the spinous processes and span greater than three vertebral levels attaching to caudal vertebrae, the sacrum and ilium (Macintosh et al. 1986). A more extensive discussion of lumbar multifidus anatomy will be presented in section 2.2.1. Psoas major also has direct attachments to lumbar vertebrae and consists of vertebral fibres and discal fibres (Hansen et al. 2006). Vertebral fibres attach to the vertebral bodies of T12 to L5 and become tendinous as they attach to the lesser trochanter of the femur (Bogduk 2000b; Jemmett et al. 2004). Discal fibres run from the T12 to L5 medial transverse processes and intervertebral discs to also attach at the femoral lesser trochanter (Bogduk 2000b; Jemmett et al. 2004). Psoas major functions to flex the hip (Hansen et al. 2006) while concurrently generates significant lumbar spine compression force (McGill 2007). The lateral fibres of quadratus lumborum are believed to weakly laterally flex the trunk (Bogduk 2000b; Richardson et al. 1999), while the medial fibres provide segmental stability (Richardson et al. 1999). McGill et al. (1996) recorded quadratus lumborum activity during upright standing as weight was progressively added bilaterally to the individual's hands. Even though the individual did not move from their upright posture, increases in the load held bilaterally caused increased quadratus lumborum activity and this lead the authors to hypothesize a stabilizing role (McGill et al. 1996).

The abdominal muscles also play a role in spinal stability. Transversus abdominus has received significant attention as a spinal stabilizer due to its ability to generate intra-abdominal pressure (Hodges et al. 2003), its attachment to the thoracolumbar fascia (Bogduk and Macintosh 1984) and its impairment in individuals with LBP during rapid arm (Hodges and Richardson 1996; Hodges and Richardson 1999a) and leg movements (Hodges and Richardson 1997a; Hodges and Richardson 1998). Transversus abdominus bilaterally originates at the iliac crests, lateral raphes and 12th ribs and wraps around the trunk blending with internal oblique fibres and the linea alba at the midline (Richardson et al. 1999). Muscular only through the anterior one-third of its course (Jemmett et al. 2004), this tendinous muscle can bilaterally contract to compress the abdomen (Tortora 2000).

The anatomy of biomechanical models has commonly been based on cadaver dissections (Bogduk et al. 1992), other models (Gardner-Morse et al. 1995) and data from The Visible Human Project® (Daggfeldt and Thorstensson 2003). These models have attempted to distinguish the stability roles and muscular moment contributions during trunk extensor efforts. Cholewicki and McGill (1996) used various imaging techniques, cadaver dissections and a previous model (Bogduk et al. 1992) to examine mechanical in vivo lumbar spine stability during a variety of tasks. To calculate a stability index, these authors developed a mathematical model that included the anatomy of 90 muscle fascicles, the pelvis, ribcage and lumbar vertebrae (Cholewicki and McGill 1996). Reeves et al. (2007) viewed one-dimensional stability as a ball sitting in a bowl where the steepness of the bowl walls determined how robust the ball was to instability. If a relatively small force acted on the ball, the steepness of the walls would prevent it from leaving the bowl (McGill 2002). Cholewicki and McGill (1996) extend a similar analogy to each lumbar vertebra for six degrees of freedom (an imaginary six-dimensional bowl) and looked for local potential energy minima of the resulting energy surface. In the analogy of Reeves et al. (2007), these local potential energy minima represent the ball being in a stable position at the bottom of the bowl. EMG was recorded from subjects performing various tasks and the resulting excitation profiles were input into their

stability model (Cholewicki and McGill 1996). These researchers found that the lumbar spine was more robust to instability (meaning a lesser risk of instability) in tasks with greater muscle excitation profiles than tasks with little active muscular input (Cholewicki and McGill 1996). Cholewicki et al. (1996) justified these findings on the basis that back injuries can occur in low muscular effort tasks such as bending over to retrieve an inanimate object from the floor. To determine how much each individual muscle contributes to lumbar spine stability, EMG was recorded from subjects performing a variety of isometric trunk movements (Cholewicki and VanVliet 2002). The resulting muscle excitation profiles were input into the stability model and individual muscles were sequentially removed from the calculation (Cholewicki and VanVliet 2002). These authors found that removal of an individual muscle resulted in a stability index reduction between 0-30%; however, no single muscle caused a greater reduction than 30% (Cholewicki and VanVliet 2002). It should be noted however, that this model (Cholewicki and McGill 1996) did not include transversus abdominus, nor did it consider intra-abdominal pressure as an extensor moment generating factor.

Anderson et al. (1985) first acknowledged that "better approximations of the attachments to the vertebrae, and more realistic values of resting length" (Anderson et al. 1985, p.577) are needed to improve spinal biomechanical models. More than twenty years later, this view was echoed by Hansen et al. (2006) who reviewed quantitative data on muscle lengths, moment arms, cross sectional areas (CSA) and joint ranges of motion. Due to the detailed anatomy of the lumbar spine, several researchers have examined the in vitro kinematic characteristics of cadaver lumbar spines with simulated muscle attachments (Kaigle et al. 1995; Panjabi et al. 1989; Quint et al. 1998; Wilke et al. 1995). Physiologically moments were applied to intact and injured lumbar two-vertebra units to examine the effects of intersegmental muscles on kinematic motion (Panjabi et al. 1989). Intersegmental muscles were artificially modeled as symmetrical vectors that pulled the superior vertebral body anterolaterally and in a caudal direction (Panjabi et al. 1989). The application of a 60N force through the simulated intersegmental muscles reduced intervertebral joint motion within the non-elastic region (or neutral zone) during flexion, extension and axial rotation moments (Panjabi et al. 1989). The authors concluded that

reducing motion within this non-elastic region was the functional role of intersegmental muscles. Wilke et al. (1995) carried out a more detailed in vitro study, attaching symmetrical cables to L4 to simulate the muscular action of lumbar multifidus, the lumbar erector spinae muscles and both the vertebral and discal fibres of psoas major. Intervertebral joint motion was examined during flexion, extension, lateral flexion and axial rotation moments with and without tension in one or all of the cables attached to L4 (Wilke et al. 1995). Simulated muscular tension in all muscles increased joint stiffness which decreased the ROM in all directions (Wilke et al. 1995). Lumbar multifidus was found to provide more than two-thirds of the segmental stiffness that caused this reduction in ROM (Wilke et al. 1995).

2.1.3. Trunk stiffness

Passive lumbar stiffness has been measured about sagittal, coronal and transverse planes (Brown and McGill 2008; McGill et al. 1994); however, this review of trunk stiffness will be limited to stiffness in response to posterior-anterior forces. Passive trunk stiffness to static or slowly applied posterior-anterior indentation forces has generally been calculated as the slope of a force-displacement graph over a specific force range. Posterior-anterior trunk stiffness in response to posterior-anterior forces applied to the skin overlying spinous processes has ranged from 12N/mm to 30 N/mm (Colloca et al. 2004; Keller et al. 2003; Latimer et al. 1996a; Latimer et al. 1996b; Latimer et al. 1998; Shirley et al. 2002; Shirley et al. 2003). Many possible variables could account for this wide variation in stiffness measures. Cyclic posterior-anterior forces (30-90N) applied to the skin overlying the L4 spinous process resulted in an average stiffness of 13.2N/mm; however, stiffness during the first cyclical load was significantly less than subsequent loads (Shirley et al. 2002). Additionally, Latimer et al. (1996b) measured posterior-anterior stiffness to forces up to 100N in LBP patients and observed a significant decrease in stiffness following resolution of pain symptoms. Lee et al. (1994) investigated the relationship between posterior-anterior stiffness and lumbar vertebral level in healthy back individuals and concluded that during both quasi-static and cyclical loading the stiffness at L5 was greater than at L4 and stiffness at L4 greater than at L3 (Lee and Liversidge 1994). The inverse relationship was found in patients with non-

specific LBP where average stiffness coefficients were 17.46N/mm at L3, 15.94N/mm at L4 and 15.14N/mm at L5 (Latimer et al. 1996a). Both of these studies calculated stiffness coefficients over similar linear force regions: 30-105N (Latimer et al. 1996a) and 20-100N (Lee and Liversidge 1994). Average stiffness to posterior-anterior forces in LBP patients was also greater when applied to vertebral spinous processes than vertebral transverse processes (Colloca and Keller 2001b).

The majority of the studies investigating posterior-anterior lumbar spine stiffness have done so at the end of normal expiration (functional residual capacity) to standardize lung volume (Colloca and Keller 2004; Latimer et al. 1996a; Latimer et al. 1998; Lee and Liversidge 1994; Lee et al. 1993; Shirley et al. 2002). Shirley et al. (2003) measured posterior-anterior stiffness to cyclic indentation loads (1Hz, 150N) applied to the L2 and L4 spinous processes during different phases of respiration. Inspiration and expiration significantly altered trunk stiffness; however, a greater increase in posterior-anterior stiffness was recorded during expiration (Shirley et al. 2003). For both L2 and L4, the largest average stiffness was recorded at residual volume and the lowest stiffness recorded at functional residual capacity (Shirley et al. 2003). At all lung volumes, the relationship between applied force and indentation displacement was linear over the force range 50-100N (Shirley et al. 2003). The active spinal stability subsystem also influences posterior-anterior stiffness. Isometric trunk extension efforts during the application of low frequency posterior-anterior indentation forces increased L3 stiffness by an average of 350% compared to resting values (Lee et al. 1993). Trunk extension also significantly increased dynamic stiffness to short duration (5 ms) indentation impulses applied to the L3 spinous process compared to the resting condition (Colloca and Keller 2004). Keller et al. (2007) applied mechanical stimulation directly to the anaesthetized ovine L3 spinous processes at variable frequencies (0.46-19.7Hz) with and without muscular stimulation. These authors found that trunk stiffness was modulated by the frequency of mechanical stimulation and the frequency of artificial multifidus muscle stimulation (Keller et al. 2007).

Respiration (Shirley et al. 2003), vertebral level (Lee and Liversidge 1994), muscular activity (Keller et al. 2007) and LBP (Latimer et al. 1996b) all appear to influence posterior-anterior trunk stiffness. Recent studies have also identified several other variables in the calculation of stiffness including subject position, the generation of intra-abdominal pressure and the range of forces over which stiffness is calculated (Kawchuk and Fauvel 2001; Latimer et al. 1998). These studies highlight the importance of a standardized experimental protocol to control for these variables when applying posterior-anterior indentation loads to the lumbar spine.

2.1.4. The neural subsystem

Dynamic spinal stability involves the coordination of the passive, active and neural subsystems to follow a "moving target" (McGill et al. 2003; Reeves et al. 2007). Active muscle contraction can increase lumbar spinal stability by increasing joint stiffness; however, this active contraction is context dependent and must occur in the correct muscles with appropriate excitation levels to achieve stability (McGill 2002; McGill 2007). This context dependency was demonstrated in an unstable sitting task with either minimal muscle activity or muscular co-contraction (increased active subsystem input) (Reeves et al. 2006). Increasing active stiffness through muscle co-contraction decreased the precision of the neural feedback system as larger forces meant greater force variability and greater 'over-corrections' (Reeves et al. 2006). Additionally, greater muscle co-contraction may produce greater compressive spinal loads that may lead to spinal injury (McGill 2002).

Feedback to the neural subsystem could stem from multiple structures in both the passive and active subsystems (Panjabi 1992a). Vertebrae receive innervation from long nerves that spread through the vertebral body (Bogduk 2000a) and many of the longitudinal and intersegmental spinal ligaments are also innervated (Bogduk 1983; Kang et al. 2001). The outer layers of intervertebral discs are innervated, especially in the lateral region (Indahl et al. 1995); however, the nucleus pulposus does not receive innervation (Kang et al. 2001). Paraspinal muscles contain sensory receptors that provide direct feedback to the

neural subsystem and have been shown to evoke reflexes in response to spinal manipulative-like perturbations in a feline model (Kang et al. 2003; Pickar 2002; Pickar and Kang 2006; Pickar et al. 2007). The short intersegmental muscles in particular have received attention as functioning primarily as length proprioceptors (McGill 2007). These fibres have small force producing capabilities and are consequently unable to produce significant trunk moments (McGill 2007); however, they appear to have larger concentrations of muscle spindles relative to other paraspinal muscles (Nitz and Peck 1986). Short medial muscles spanning only a few intervertebral joints contain much greater muscle spindle densities than more lateral longer muscles (Peck et al. 1984). These short intersegmental muscles may provide valuable feedback to the neural controller subsystem.

The importance of the neural subsystem in lumbar spine stability was evident in the motor control deficits seen in many individuals with LBP. Paul Hodges and colleagues (Hodges and Richardson 1996; Hodges and Richardson 1997a; Hodges and Richardson 1998; Hodges and Richardson 1999a) have uncovered transversus abdominus motor control differences between LBP patients and healthy controls. During rapid upper and lower limb movements, transversus abdominus onset appeared delayed in LBP patients and this deficit may have been a contributing factor to pain in these patients (Hodges and Richardson 1996; Hodges and Richardson 1998; Hodges and Richardson 1999a). LBP patients also do not normally display the typical 'flexion-relaxation phenomenon' observed in individuals with healthy backs (Geisser et al. 2005). This phenomenon is characterized by an absence of surface EMG at maximum trunk forward flexion which is absent in LBP patients (Geisser et al. 2005). Trunk repositioning accuracy was believed to be absent in LBP patients (Brumagne et al. 2000); however, a recent study showed that given adequate practice these LBP patients could accurately complete repositioning tasks, albeit by using a different motor control strategy (Descarreaux et al. 2005). Differing motor control strategies in some LBP patients were also observed during isometric trunk flexion and extension tasks (Descarreaux et al. 2004). Adopting maximally flexed postures for extended periods of time can result in biomechanical creep of spinal viscoelastic structures (McGill and Brown 1992). These postures are associated with

diminished paraspinal reflexes and thus may also affect the neural subsystem's ability to maintain lumbar spinal stability (Rogers and Granata 2006).

2.2. The lumbar multifidus

2.2.1. Anatomy

The lumbar multifidus is composed of five fibre groupings extending from each lumbar vertebrae caudolaterally to caudal vertebrae, the ilium and sacrum. These five groupings form overlapping layers such that multifidus fibres originating at superior lumbar vertebrae are superficial, lateral and rostral to multifidus fibres originating at inferior vertebrae (Hansen et al. 2006; Kim et al. 2005). At lower vertebral levels, lumbar multifidus is the most prominent back muscle (Bogduk 2000b) and contributes one-quarter of the total trunk extensor moment during maximal trunk extension efforts (Bogduk et al. 1992). There are five bilateral sets of deep (or laminar) lumbar multifidus fibres arising from each of the lumbar vertebral lamina. (Bogduk 2000b; Hansen et al. 2006; MacDonald et al. 2006; Macintosh et al. 1986). With the exception of the deep fibres arising from L5, these fibres insert at the mamillary processes and zygapophysial joint capsules two levels caudad (Bogduk 2000b; Hansen et al. 2006; Kim et al. 2005; Lewin et al. 1962; Macintosh et al. 1986). The deep fibres arising from the L5 vertebral lamina insert at a location superior to the sacral foramina between S1 and S2 (Hansen et al. 2006). Additionally, a comprehensive lumbar multifidus cadaver dissection study noted deep lumbar multifidus fibres attaching adjacent lumbar vertebrae in approximately 25% of cadavers studied (Macintosh et al. 1986). A recent anatomical study of a single male cadaver reported deep fibres originating at the vertebral laminae and inserting at the mamillary processes, yet the authors did not specify the actual number of vertebral levels between these attachments (Jemmett et al. 2004).

Superficial lumbar multifidus fibres originate bilaterally from each lumbar spinous process and insert at the ilium or sacrum (Bogduk 2000b; Jemmett et al. 2004; Macintosh et al. 1986). Two sets of superficial lumbar multifidus fibres originate from each of the

L1, L2 and L3 spinous processes: one set originating from the lateral base of the spinous process (referred to as 'base') and the other set from the dorsolateral tip of the spinous process (referred to as 'tip') (Bogduk 2000b; Macintosh et al. 1986). The 'L1-tip' fibres form a common tendon with the 'L2-base' fibres and insert at the posterior superior iliac spine (PSIS), L4/L5 zygapophysial joint capsule, and mamillary processes of L5 and S1 (Bogduk 2000b; Jemmett et al. 2004). The 'L1-tip' fibres may also attach to the erector spinae aponeurosis (Macintosh et al. 1986), while the 'L1-base' fibres insert at the L4 mamillary process (Bogduk 2000b; Macintosh et al. 1986). In an analogous fashion to the L1/L2 common tendon, the 'L2-tip' fibres and 'L3-base' fibres form a common tendon to insert at the PSIS, iliac crest and mamillary processes of L5 and S1 (Bogduk 2000b; Jemmett et al. 2004). The two common tendons share the same caudal attachment; however, the L2/L3 common tendon inserts mediocaudally to the L1/L2 common tendon (Macintosh et al. 1986). The 'L3-base' fibres insert at the S1 mamillary processes on the posterior sacrum (Bogduk 2000b; Macintosh et al. 1986). One set of superficial fibres arise from each of the L4 and L5 spinous processes' tips. The L4 and L5 superficial fibres insert at the sacrum lateral and medial to the sacral foramina, respectively (Macintosh et al. 1986). The sacroiliac attachments of superficial lumbar multifidus fibres follow a consistent directional pattern whereby fibres arising from successively lower vertebral levels attach medial to upper vertebral level fibres (Macintosh et al. 1986).

The caudolateral orientation of superficial multifidus fibres endows these fibres with vertical and horizontal force components (Macintosh and Bogduk 1986). The lateral obliquity of these fibres in the frontal plane increases from 13-15° at the L1 spinous process, reaching a maximum at L3 (20-23°) before decreasing to approximately 6° at L5 (Macintosh and Bogduk 1986). In the sagittal plane, superficial fibres inserting at inferior lumbar vertebrae form an approximate right angle (84-89°) to the anterior-posterior vertebral axis (Hansen et al. 2006; Macintosh and Bogduk 1986). Superficial fibres inserting at the ilium and sacrum form slightly more obtuse angles (94-103°), however, are still approximately orthogonal to the vertebral frontal axis (Macintosh and Bogduk 1986). These orientations imply that lumbar multifidus is ideally aligned to generate

compressive forces from each lumbar vertebra caudally (McGill 2007) and that fibres attaching to the ilium and sacrum are more suited for posterior sagittal rotation.

All lumbar multifidus fibres arising from a specific lumbar vertebra are innervated by the medial branch of the lumbar dorsal ramus immediately below the lumbar vertebra (Bogduk 1983; Bogduk 2000a). This innervation means that all multifidus fibres arising from a lumbar segmental level are innervated by the dorsal ramus of the same segmental number (Bogduk 2000a). A recent animal model reported that nociceptive afferents from lumbar multifidus at L5 were supplied by a bell shaped distribution of different dorsal root ganglia centered at L3 (Taguchi et al. 2007). These authors concluded that the innervation of lumbar multifidus was shifted two vertebral levels cranial (Taguchi et al. 2007), however, it is important to note that multifidus fibres from all lumbar levels cross the L5 vertebral body. Thus, a cranial shift would be expected when tracing afferent pathways from fibres spanning the L5 vertebral level and these findings do not refute the segmental innervation of lumbar multifidus. Nitz and Peck (1986) reported that the concentration of muscle spindles in the rotatores brevis at the L4/L5 level was 4.58-6.23 times the spindle concentration in lumbar multifidus (Nitz and Peck 1986). Anatomical studies of lumbar multifidus indicate that the rotatores muscles are absent in the lumbar spine (Macintosh et al. 1986) and thus these authors likely measured this increased spindle density in the deep laminar fibres of lumbar multifidus. Additionally, the work by Amonoo-Kuofi (1983) has been cited as evidence of a lower muscle spindle concentration in multifidus relative to iliocostalis and longissimus (McGill 2007). Contrary to this belief, close inspection of this report (Amonoo-Kuofi 1983) revealed that in the lumbar spine specifically, the muscle spindle concentration actually appeared to be higher than that of the erector spinae muscle columns (see figure 3 in the original manuscript).

2.2.2. Lumbar multifidus reflexes

Multifidus reflexes have been recorded following electrical stimulation of the lateral intervertebral disc (Indahl et al. 1995; Indahl et al. 1997), facet joint capsule stimulation

(Indahl et al. 1995; Kang et al. 2002), supraspinous ligament stretch (Solomonow et al. 1998) and during spinal manipulation therapy (Herzog et al. 1999; Symons et al. 2000). Lumbar multifidus reflexes have also been evoked by posterior-anterior forces to lumbar vertebrae (Colloca et al. 2003) and the skin overlying lumbar vertebral landmarks (Colloca and Keller 2001a; Colloca and Keller 2001b). Reflex latencies during these posterior-anterior forces have ranged from 2ms to 18ms using both intramuscular and surface EMG (Colloca and Keller 2001a; Colloca and Keller 2001b; Colloca et al. 2003). The very short latencies measured during these indentation loads have generally been measured between the time at peak indentation force and the initiation of lumbar multifidus electrical activity. Paraspinal muscle stretch reflex latencies have been reported to range from 8-16ms using tendon tap pulse durations of 8-19ms (Dimitrijevic et al. 1980; Tani et al. 1997). Stretch reflex latencies adjusted for pulse duration have hypothesized that a "zero pulse" tendon tap would produce an average reflex latency of 6.5ms, which is consistent with the conduction velocities and synaptic delays associated with a monosynaptic stretch reflex (Skotte et al. 2005).

Aage Indahl and colleagues (Indahl et al. 1995; Indahl et al. 1997) recorded lumbar multifidus EMG during electrical stimulation of the intervertebral disc and facet joint capsule. Electrical stimulation of the lateral L1/L2 intervertebral disc elicited bilateral EMG at multiple levels that was largest ipsilaterally at the L4 vertebral level (Indahl et al. 1995). Lidocaine injection into the facet joint capsule reduced this activity (Indahl et al. 1995) while the injection of physiological saline into the facet joint capsule also reduced EMG activity in response to intervertebral disc stimulations (Indahl et al. 1997). These authors hypothesized that stretching the joint capsule (with saline) may have caused afferent signals to facilitate inhibitory interneurons that produced motoneuron inhibition (Indahl et al. 1997). They further suggested that this reflex pathway may be responsible for the 'flexion relaxation phenomenon' commonly observed in healthy individuals using surface (Kippers and Parker 1984) and intramuscular EMG (Floyd and Silver 1955).

Indahl et al. (1995) also observed a localized EMG response during electrical stimulation of the L1/L2 facet joint capsules (Indahl et al. 1995). This stimulation produced a

response concentrated in the lumbar multifidus fibres at L2 and occurred with minimal contralateral activity (Indahl et al. 1995). This localized EMG response was also diminished after lidocaine injection into the facet joint and abolished after muscle detachment (Indahl et al. 1995). Based on these findings, Indahl et al. (1995) concluded that the observed EMG responses were reflexive; however, this conclusion has recently been challenged (Kang et al. 2002). Kang et al. (2002) stimulated the medial branch of the lumbar dorsal ramus or the facet joint capsule while recording compound action potentials from lumbar dorsal rami at multiple levels. These authors reported that facet joint capsule stimulation was associated with multifidus excitation that decreased after lidocaine injection into the facet capsule; yet persisted after cutting the nerve innervating the facet joint (Kang et al. 2002). They reasoned that Indahl et al. (1995) observed a multifidus reflex after facet joint stimulation because the stimulating current may have spread to adjacent spinal structures (including muscles). Additionally, lidocaine injection into the facet joint may have spread to lumbar multifidus resulting in a diminished muscle response (Kang et al. 2002). Kang et al. (2002) also documented intersegmental reflexes between lumbar segments. Electrical stimulation of the L3, L4 or L5 medial lumbar dorsal ramus branch evoked compound action potentials at the medial branches of lumbar segments one and two vertebral levels rostral or caudal (Kang et al. 2002).

Lumbar multifidus is also excited with electrical stimulation of the supraspinous ligament in human and feline spines (Solomonow et al. 1998; Stubbs et al. 1998). Stimulation of the feline supraspinous ligament from L1 to L6 produced bilateral EMG activity that was largest in multifidus fibres one level caudal to the stimulation site (Stubbs et al. 1998). When the vertebral bodies were fixated with metal rods, lumbar multifidus excitation was present during supraspinous ligament stimulation yet substantially reduced compared to the unbound condition (Solomonow et al. 1998). Bilateral reflexive activation of lumbar multifidus has been hypothesized as a "ligamento-muscular protective reflex" whereby supraspinous ligament stretch facilitates lumbar spine extensors to reduce this stretch (Stubbs et al. 1998). In addition to recordings in a feline preparation, this protective reflex has been demonstrated in vivo in humans undergoing lumbar spine surgery (Solomonow et al. 1998). Compatible with this proposed reflex pathway, supraspinous

ligament damage has been implicated as a possible reason that certain LBP patients present clinically with hyperlordotic postures (Dankaerts et al. 2006).

The amplitude of this multifidus reflex induced by stretch of the feline supraspinous ligament can be altered with prolonged ligament stretch at a constant load (Jackson et al. 2001; Solomonow et al. 2003a; Solomonow et al. 2003b). Reflexive lumbar multifidus activity declines quickly and subsequently exhibits bursts of excitation with prolonged supraspinous ligament stretch (Jackson et al. 2001; Solomonow et al. 2003a). The relationship between stretch magnitude and reduction of initial feline myoelectric activity appears to be an exponential decline with initial increases in stretch significantly reducing activity and subsequent stretch having a smaller effect (Solomonow et al. 2003a). The reflex pathway also does not immediately recover with rest periods as long as seven hours not being sufficient to restore initial excitation levels due to twenty minutes of static flexion (Jackson et al. 2001; Solomonow et al. 2003a). Studies in humans have shown four sets of seated maximal trunk flexion each four minutes long reduced paraspinal muscle reflex gain recorded by surface EMG (Rogers and Granata 2006). Reduced reflex gain was measured by pseudorandom perturbations to a chest harness worn by subjects and did not return to initial values after sixteen minutes of recovery (Rogers and Granata 2006).

Colloca, Keller and colleagues have examined multifidus reflexes to vertebral indentation loads in LBP patients undergoing back surgery operations (Colloca et al. 2003; Colloca et al. 2004). Indentation loads applied using the Activator II Adjusting Instrument (Keller et al. 1999) directly to vertebral processes and the skin overlying these processes produced positive EMG responses in lumbar multifidus (Colloca et al. 2003). Positive responses were defined as signals with peak-to-peak amplitudes greater than 2.5 times the baseline signal (Colloca et al. 2003; Colloca et al. 2004). EMG responses were seen in many trials; however, these responses were classified as positive responses in only 0-37.5% of indentation perturbations depending on indentation location (Colloca et al. 2003). These researchers also recorded compound action potentials from S1 nerve afferents just proximal to the S1 dorsal root ganglion (Colloca et al. 2003; Colloca et al. 2004). In all

but one LBP patient, when both positive EMG and compound action potential responses were noted, the latency of positive compound action potentials was shorter than the EMG response.

Similar to in humans, posterior-anterior indentation forces applied directly to exposed ovine L3 spinous processes produced positive EMG responses (Colloca et al. 2006; Colloca et al. 2007). Increases in indentation force at a constant duration (100ms) or increases in impulse duration at a constant force (80N) increased the peak-to-peak amplitude of EMG responses in these ovine models (Colloca et al. 2006). Compound action potentials showed different pattern relative to EMG responses. Instantaneous discharge frequency of spinal nerve afferents increased with decreasing impulse duration and showed a very slight decrease with increased force (although this was only noted between 100ms and 200ms impulse durations) (Colloca et al. 2007).

The inherent limitation of interpreting compound action potentials from afferent nerves entering the spinal cord is that these potentials represent global afferent activity from many sources (Colloca et al. 2004). This limitation clouds any relationship that may be hypothesized between afferent activity and lumbar multifidus excitation. Joel Pickar and colleagues have developed a feline model in which they are able to record and classify individual nerve afferent discharge during posterior-anterior spinal loads to the L6 spinous process (Ge et al. 2005; Kang et al. 2001; Pickar 1999; Pickar and Ge 2007; Pickar and Kang 2006; Pickar and Wheeler 2001; Pickar et al. 2007; Sung et al. 2005). The development of this model means that muscle spindle afferent responses to posterior-anterior loads of varying force (Kang et al. 2001; Pickar and Kang 2006; Sung et al. 2005), displacement (Pickar et al. 2007) and duration (Pickar and Kang 2006; Pickar et al. 2007; Sung et al. 2005) can be investigated. Sung et al. (2005) recorded changes in instantaneous discharge from six afferents arising from within multifidus or longissimus (all but one afferent was type I or II). Applied loads of 33%, 66% and 100% feline body weight did not systemically alter afferent instantaneous discharge (Sung et al. 2005). Contrary to this finding, a difference in mean instantaneous discharge was noted between the application of a 25% body weight preload force and a 100% body weight rapid

impulse force to the feline L6 spinous process (Pickar and Wheeler 2001). This may be due to the different durations of the preload force and rapid impulse force. The effect of posterior-anterior vertebral displacement was also recently investigated in a feline model (Pickar et al. 2007). Muscle spindle instantaneous discharge was significantly increased during posterior-anterior forces producing one millimetre of anterior vertebral translation compared to two millimetres (Pickar et al. 2007). The authors reasoned this may be due to the signal range properties of muscle spindles (Pickar et al. 2007).

The majority of work published by Joel Pickar and colleagues has focused on changes in afferent instantaneous frequency during spinal manipulative-like posterior-anterior impulses of varying durations (Pickar and Kang 2006; Pickar et al. 2007; Sung et al. 2005). These spinal manipulative-like impulses have been modeled as half-sine waves and have been applied to these authors' feline preparation. As impulse duration decreased from 800ms to 200ms, mean afferent instantaneous discharge remained fairly constant although may have exhibited slight increases with shorter impulses (Pickar and Kang 2006; Pickar et al. 2007; Sung et al. 2005). Between impulse durations of 100-200ms, an inflection point was found whereby further impulse duration decreases resulted in exponential increases in afferent discharge (Pickar and Kang 2006; Pickar et al. 2007; Sung et al. 2005). This inflection point has been noted for both primary and secondary afferent fibres (Pickar et al. 2007). The existence of this inflection point may have clinical relevance for high-velocity, low-amplitude (HVLA) chiropractic thrusts; however, may also play a role in lumbar multifidus reflexes.

2.2.3. Lumbar multifidus activity during voluntary trunk movements

A stability role has been attributed to the entire lumbar multifidus during many trunk movements (Ebenbichler et al. 2001). Biomechanically, the mechanical line of action of lumbar multifidus force suggests that this muscle's primary role is in posterior rotation of lumbar vertebrae in the sagittal plane (Macintosh and Bogduk 1986) Many researchers have recorded multifidus excitation during a number of gross trunk movements using both intramuscular (Andersson et al. 2002; Donisch and Basmajian 1972; Jonsson 1970;

McCook et al. 2007; Morris et al. 1962; Pauly 1966; Valencia and Munro 1985) and surface EMG (Arokoski et al. 2001; Danneels et al. 2002; McCook et al. 2007; Ng et al. 2001; Ng et al. 2002; Ng et al. 2003; O'Sullivan et al. 2002). Multifidus excitation measured using surface electrodes has recently been shown to be more closely related to longissimus excitation than multifidus excitation recorded using intramuscular electrodes (Stokes et al. 2003). These authors concluded that surface electrodes do not accurately record from lumbar multifidus (Stokes et al. 2003) and thus interpretation of surface EMG recordings must be made with caution.

Intramuscular EMG recordings of lumbar multifidus during upright standing have produced inconsistent results. Intramuscular EMG recorded from the lumbar spine just adjacent to the midline has found no activity (Andersson et al. 1996; Morris et al. 1962), intermittent activity (Valencia and Munro 1985) or slight activity (Donisch and Basmajian 1972; Jonsson 1970) during quiet stance. The discrepancy in results is not necessarily surprising because natural sway during quiet stance may produce different reactive forces on the trunk to maintain balance. Morris et al. (1962) reported that "a position of rest for iliocostalis dorsi and lumborum and the multifidus was easily found, although these muscles became active as the subject swayed slightly forward" (Morris et al. 1962, p.512). Increased multifidus excitation with forward sway appears to fit with the hypothesized biomechanical function of lumbar multifidus as a lumbar extensor (or posterior lumbar vertebrae sagittal rotator) (Macintosh and Bogduk 1986). Paraspinal muscle activity during forward trunk sway acts to resist the gravitational force acting on the trunk to sustain upright standing (Gupta 2001; Kippers and Parker 1984).

Multifidus excitation has also been recorded intramuscularly during controlled trunk flexion from upright standing (Andersson et al. 1996; Donisch and Basmajian 1972; Floyd and Silver 1955; Morris et al. 1962; Pauly and Steele 1966; Valencia and Munro 1985) to resist trunk gravitational force. In keeping with lumbar multifidus' role as a lumbar extensor, intramuscular activity has been recorded during upright trunk extension (Donisch and Basmajian 1972; Morris et al. 1962), sitting trunk extension (Jonsson 1970; McCook et al. 2007) and prone hyperextension (Valencia and Munro 1985). Bilateral

lumbar multifidus excitation has also been recorded during prone bilateral leg extension (Jonsson 1970; Valencia and Munro 1985).

Anatomy textbooks often describe multifidus as having one or more functions consisting of trunk extension, lateral flexion and rotation (Drake 2005; Martini 2006; Seeley 2003; Tortora 2003). There is strong evidence that lumbar multifidus produces lumbar extension, however, its role in lateral flexion is less clear. Jonsson et al. (1970) only noticed a slight increase in lumbar multifidus activity during upright standing while holding a weight on one side of the body. Macintosh et al. (1986) further concluded that the horizontal vector component of lumbar multifidus was too short to contribute significantly to lateral flexion. Lumbar multifidus excitation during axial rotation has been extensively study in sitting and standing postures (Andersson et al. 2002; Donisch and Basmajian 1972; Jonsson 1970; Morris et al. 1962; Ng et al. 2001; Ng et al. 2002; Ng et al. 2003; Valencia and Munro 1985). Unrestrained axial rotation during sitting produced greater lumbar multifidus intramuscular EMG activity on the side contralateral to the direction of rotation (Valencia and Munro 1985). When the same subjects adopted an upright standing posture, this directional pattern of activity remained; however, multifidus excitation levels were greater (Valencia and Munro 1985). Donisch et al (1972) reported that 14 of 25 subjects had increased contralateral intramuscular EMG during axial rotation, however, 7 of 25 did not display a directional bias and 3 of 25 had increased ipsilateral activity (Donisch and Basmajian 1972). Morris et al. (1962) predominantly found contralateral intramuscular EMG activity with rotation, but did note that occasionally ipsilateral activity was found in some subjects (Morris et al. 1962). Ng and colleagues (Ng et al. 2001; Ng et al. 2002; Ng et al. 2003) recorded lumbar multifidus surface EMG during standing isometric axial rotation and did not find excitation differences between ipsilateral and contralateral sides, but did report increased excitation with increased axial torque (Ng et al. 2001; Ng et al. 2002; Ng et al. 2003). As discussed previously, surface recordings of multifidus may be susceptible to crosstalk from the adjacent lumbar erector spinae muscles.

Andersson et al. (2002) attempted to resolve these literature contradictions by comparing trunk muscle excitation during easy unresisted, maximal unresisted and maximal resisted axial rotation while standing and sitting (Andersson et al. 2002). Intramuscular EMG of lumbar multifidus during unresisted sitting and standing rotation was greatest on the contralateral side and increased with rotation intensity (Andersson et al. 2002). During resisted rotations, this pattern switched with greater activity recorded on the side ipsilateral to rotation direction (Andersson et al. 2002). Multifidus excitation was also greater during standing rotation compared to sitting rotation for both unresisted and resisted conditions (Andersson et al. 2002). The abdominal oblique muscles appear to be the major trunk rotators (Andersson et al. 2002); however, contraction of these muscles produces a trunk flexor moment (Hansen et al. 2006). Several authors have suggested that the role of lumbar multifidus during rotation is to counteract the flexor moment generated by the oblique muscles (Hansen et al. 2006; Macintosh and Bogduk 1986; Ng et al. 2002). Thus, changes in bilateral lumbar multifidus excitation and may be in response to changes in the direction of the force generated by the oblique muscles at different trunk rotational positions.

2.3. The role of lumbar multifidus in lumbar spine stability

Comparisons between healthy control subjects and those with LBP reveal differences in trunk muscle morphology and motor control. Histological studies and studies of muscle CSA have noted lumbar multifidus differences in individuals with LBP (Hides et al. 1994; Rantanen et al. 1993). Additionally, altered motor control patterns were noted in the transversus abdominus muscle of LBP patients during tasks requiring spinal stability (Hodges and Richardson 1996; Hodges and Richardson 1998; Hodges and Richardson 1999a). The observed differences in LBP and hypothesized function of transversus abdominus and lumbar multifidus lead a group of researchers from the University of Queensland to develop the 'drawing in' technique to stabilize the lumbar spine (Richardson and Jull 1995; Richardson et al. 1999; Richardson et al. 2004). The development of this stabilization technique and challenges to its stabilizing potential will be discussed in the following section. The 'drawing in' technique requires differential

function of the superficial and deep fibres of lumbar multifidus (MacDonald et al. 2006). Evidence supporting and refuting the capability of multifidus to function differentially is discussed in section 2.3.2.

2.3.1. "Drawing in" and the "abdominal brace"

Muscle CSA has been associated with muscular strength (Tortora 2000) and evaluation of CSA may be a clinically useful tool in diagnosis. Julie Hides and colleagues have evaluated lumbar multifidus CSA using ultrasound imaging in numerous studies (Hides et al. 1994; Hides et al. 1995; Hides et al. 1996; Hides et al. 2001; Hides et al. 2006; Hides et al. 2007). One of their major findings using this technology was that lumbar multifidus CSA was asymmetric in unilateral acute LBP patients (Hides et al. 1994). This asymmetry involved a decreased CSA on the painful side and in 24 of 26 subjects was found to occur adjacent to the vertebral level clinically diagnosed as responsible for LBP symptoms (Hides et al. 1994). Bilateral chronic LBP patients were found to have decreased multifidus CSA at L4 and L5 compared to healthy controls using CT and ultrasound scanning (Hides et al. 2006; Kamaz et al. 2007). Unilateral chronic LBP patients presented with multifidus asymmetry at the clinically painful level and thus demonstrated the same pattern as unilateral acute LBP patients (Hides et al. 2006). Multifidus asymmetries were also found in 79% of unilateral lumbosacral radiculopathy patients; however, no differences in the ratio of pure muscle to total muscle area was found between patients and healthy controls (Hyun et al. 2007). Pure muscle was calculated as the total muscle area with the CSA of fatty deposits subtracted (Hyun et al. 2007).

Muscle biopsies of lumbar multifidus have reported muscle fibre type conversions (Demoulin et al. 2007), type I and type II fibre atrophy (Yoshihara et al. 2003), selective type II atrophy (Rantanen et al. 1993) or no differences (Demoulin et al. 2007) between LBP patients and healthy controls. Increases in the percentage of type I muscle fibres (Yoshihara et al. 2003) and a "moth-eaten" appearance of type I fibres has also been observed in LBP patients with intervertebral disc herniation (Rantanen et al. 1993).

Rantanen et al. (1993) compared muscle biopsy samples from LBP patients during laminotomy surgery and five years post-surgery. These researchers found that LBP patients who responded positively to surgery had type I and type II hypertrophy and a reduction in the "moth-eaten" appearance of type I fibres (Rantanen et al. 1993). This study was an important step in establishing a causal relationship between multifidus histological changes and low back injury. Lumbar multifidus CSA measured using ultrasound significantly decreased with only fourteen days of bed-rest, despite no significant decrease in erector spinae CSA after fifty-six days of bed-rest (Hides et al. 2007). This may indicate an increased susceptibility of lumbar multifidus to rapid atrophy with disuse (Hides et al. 2007). Hodges et al. (2006) introduced specific lesions in a porcine model to evaluate the time course of lumbar multifidus changes with low back injury. A segmental and unilateral reduction in lumbar multifidus CSA was detected within six days of unilateral intervertebral disc lesion and occurred ipsilateral to the lesion at the same segmental level (Hodges et al. 2006). The authors argued that the causal relationship between disc injury and localized segmental atrophy may be due to specific atrophy of the deep fibres of lumbar multifidus (Hodges et al. 2006). Superficial multifidus fibres span multiple vertebral levels and atrophy of these fibres would have likely resulted in a more generalized pattern of multifidus atrophy (Hodges et al. 2006). Deep multifidus fibres have short moment arms (McGill 1991) which primarily produce lumbar spine compression (Bogduk et al. 1992). Hodges et al. (2006) hypothesized that decreased neural drive to the deep multifidus fibres may reduce lumbar spine compression and cause selective segmental lumbar multifidus atrophy.

The motor control of transversus abdominus in human subjects performing rapid limb movements appears to be different in healthy back individuals and those with LBP (Hodges and Richardson 1996; Hodges and Richardson 1997a; Hodges and Richardson 1998; Hodges and Richardson 1999a). During rapid and intermediate velocity shoulder flexion, abduction and extension, the onset of transversus abdominus EMG activity preceded that of other trunk muscles in healthy controls but was delayed in LBP patients (Hodges and Richardson 1996; Hodges and Richardson 1999a). Transversus abdominus excitation latency with respect to deltoid EMG onset (prime mover) was not significantly

different between movement directions in healthy controls (Hodges and Richardson 1996; Hodges and Richardson 1997b). LBP patients did however exhibit differing transversus abdominus onset latencies with shoulder flexion, abduction and extension movements (Hodges and Richardson 1996). Transversus abdominus was the first trunk muscle excited during hip flexion, abduction and extension in healthy controls and displayed the same non-direction specificity as with arm movements; however, this did not occur in LBP patients (Hodges and Richardson 1997a; Hodges and Richardson 1998). Delayed onset of transversus abdominus and directional onset latency differences have been found during these rapid lower limb movements in individuals with LBP (Hodges and Richardson 1997a; Hodges and Richardson 1998).

Based on their observed deficits and differences in comparison to people without LBP, this group of researchers has contended that transversus abdominus and lumbar multifidus have specialized roles in lumbar spine stability (Richardson and Jull 1995; Richardson et al. 1999; Richardson et al. 2004). In addition to its early onset and non-direction specificity, transversus abdominus may directly or indirectly produce an extensor moment by increasing intra-abdominal pressure (Bartelink 1957; Daggfeldt and Thorstensson 2003). Cresswell and colleagues (Cresswell et al. 1992; Cresswell et al. 1994) recorded intramuscular transversus abdominus excitation and intra-abdominal pressure with an intra-gastric pressure transducer during different trunk movements (Cresswell et al. 1992). Transversus abdominus was excited during both isometric trunk flexion and extension with less than a 15% difference in excitation level between directions. Transversus abdominus was also most closely related to changes in intra-abdominal pressure relative to other abdominal muscles (Cresswell et al. 1992). These researchers also examined self-initiated and unexpected ventral loading of the trunk which consisted of a weight dropping onto the front of a harness worn by subjects (Cresswell et al. 1994). Early transversus abdominus onset with self-initiated loading was expected as a feed-forward response; however, transversus abdominus was also paradoxically active first with unexpected loading (Cresswell et al. 1994). Unexpected loading of the trunk was anticipated to result in early onset of the dorsal muscles to counteract the trunk flexor moment introduced by the load (Cresswell et al. 1994).

Transversus abdominus may pressurize the abdominal cavity to generate a trunk extensor moment or may provide a rigid cylinder by which diaphragm or pelvic floor muscle contraction increases intra-abdominal pressure and produces an extensor moment (Hodges et al. 2001). Hodges et al. (2001, 2003) simulated transversus abdominus tension using abdominal belts during unilateral or bilateral phrenic nerve stimulation to measure trunk extensor moment (Hodges et al. 2001) and posterior-anterior trunk stiffness (Hodges et al. 2005). Diaphragm evoked contraction by phrenic nerve stimulation produced an increase in intra-abdominal pressure and a side-lying trunk extensor moment in the absence of paraspinal muscle activity (Hodges et al. 2001). Phrenic nerve stimulation also increased posterior-anterior spine stiffness by 8-31% during indentation perturbations at L2 and L4 (Hodges et al. 2005). Anatomical cadaver studies of the human trunk have determined that transversus abdominus forms an attachment with the thoracolumbar fascia via the lateral raphe just superior to the ilium (Bogduk and Macintosh 1984). As discussed in section 2.1.1, lateral tension in the thoracolumbar fascia via transversus abdominus contraction may also increase trunk stiffness and generate a trunk extensor moment (Barker et al. 2006).

The evidence supporting the specialized role of lumbar multifidus in spinal stability is less clear. The deep fibres of lumbar multifidus are hypothesized to function as spinal stabilizers while the superficial fibres act as prime movers of the trunk (Richardson et al. 1999; Richardson et al. 2004). This hypothesis has been partly based on anatomical and biomechanical observations (Bogduk et al. 1992; McGill 1991; Richardson and Jull 1995) and in vivo recordings of the deep and superficial fibres during rapid limb movements and trunk perturbations (Moseley et al. 2002; Moseley et al. 2003). The small size of deep multifidus fibres suggests they do not produce enough force to significantly contribute to trunk movements (McGill 2002). Moreover, the proximity of these deep fibres to the longitudinal axis of the trunk and their biomechanical line of action suggests they produce primarily compressive spinal forces (Bogduk et al. 1992). The proximity of these deep fibres to the vertebral column likely means that they undergo small length changes with trunk movements (McGill 1991) and thus may be at an optimal contractile

length regardless of trunk position. In vitro studies have suggested that multifidus increases spine stability through increased stiffness (Quint et al. 1998; Wilke et al. 1995), reduced irregular vertebral motion (Kaigle et al. 1995) and that the deep fibres in particular control intersegmental vertebral motion (Panjabi et al. 1989).

Lorimer Moseley and colleagues (Moseley et al. 2002; Moseley et al. 2003) were the first to show in vivo differences in deep and superficial lumbar multifidus fibres during functional tasks. Deep lumbar multifidus fibre EMG onset was found to be consistent between rapid shoulder flexion and extension movements while superficial fibre onset varied with movement direction, occurring earlier in shoulder flexion (Moseley et al. 2002). Consistent EMG onset latencies in the deep fibres despite different movement directions paralleled transversus abdominus EMG onsets during arm movements and suggested a stability role (Moseley et al. 2002). Repetitive and rapid alternating shoulder flexion and extension produced two deep fibre EMG peaks just prior to shoulder flexion and extension (Moseley et al. 2002). Superficial multifidus fibre EMG traces primarily displayed a single peak prior to shoulder flexion (Moseley et al. 2002). A subsequent study examined the differential functioning of these fibres during predictable and unpredictable trunk perturbations (Moseley et al. 2003). Standing subjects were blindfolded and wore headphones while holding a bucket in front of their bodies with elbows flexed to ninety degrees (Moseley et al. 2003). A weight dropped into the bucket when subjects pressed a trigger button on the bucket (predictable condition) or at a random time (unpredictable condition) (Moseley et al. 2003). In six of seven subjects, the onset of deep multifidus fibre excitation was earlier in the predictable condition relative to the unpredictable condition; however, this difference was not statistically significant (Moseley et al. 2003). In the unpredictable condition all lumbar multifidus fibres were excited concurrently, yet in the predictable condition the deep lumbar multifidus fibres were excited prior to the superficial fibres (Moseley et al. 2003). When the deep fibre EMG amplitude in the predictable and unpredictable conditions was compared in the half second interval prior to the weight hitting the bucket, amplitude differences were noted as early as 400ms prior to the perturbation (Moseley et al. 2003). The amplitude of deep fibre EMG activity in the predictable condition was greater than the amplitude in the

unpredictable condition (Moseley et al. 2003). These studies concluded that the deep and superficial multifidus fibres were differentially active during these tasks and the deep fibres were responsible for lumbar spinal stability (Moseley et al. 2002; Moseley et al. 2003).

The hypothesized specialized role of transversus abdominus and lumbar multifidus formed the foundation of the abdominal 'drawing in' technique (Jull and Richardson 2000; Richardson and Jull 1995; Richardson et al. 1999; Richardson et al. 2004). The Queensland University group have advocated teaching this technique to retrain and correct "motor control deficits" (Jull and Richardson 2000) in LBP patients (Richardson et al. 1999; Richardson et al. 2004). This technique has been described as a 'segmental stabilization exercise' and involves gently drawing the lower abdominals dorsally through co-contraction of the transversus abdominus and deep fibres of lumbar multifidus (MacDonald et al. 2006; Richardson et al. 1999; Richardson et al. 2004). Biofeedback techniques involving ultrasound and EMG have been employed to train contraction of these muscles and to limit activity in more superficial abdominal and paraspinal muscles (Richardson et al. 1999; Richardson et al. 2004). Richardson and Jull (1995) have also advised clinicians to began teaching this technique in simple postures such as four-point kneeling and prone lying before progressing to performing functional tasks while 'drawing in.' This technique has been purported to ensure lumbar spine stability through increased control of intersegmental vertebral motion (Richardson et al. 1999; Richardson et al. 2004).

Recent clinical trials have examined the efficacy of this 'segmental stabilization exercise' in individuals with acute LBP (Hides et al. 1994; Hides et al. 1996; Hides et al. 2001; O'Sullivan et al. 1997). Hides et al. (1994) observed asymmetric CSA of lumbar multifidus at the clinically painful level in acute unilateral LBP subjects. These LBP subjects were randomly divided into two ten week LBP intervention groups: a 'medical management' group and an 'exercise therapy' group (Hides et al. 1996). The 'medical management' group received standard medical care, prescription drugs and medical advice whereas the 'exercise therapy' group was prescribed specific segmental exercises

to train these subjects in the 'drawing in' technique (Hides et al. 1996; Hides et al. 2001). Both intervention groups had decreased pain and disability; however, multifidus CSA asymmetries persisted in the 'medical management' group at ten weeks post injury (Hides et al. 1996). 'Exercise therapy' reduced multifidus asymmetry from 26% to 0.2% at ten week follow-up, whereas 'medical management' reduced asymmetry from 22% to 14% (Hides et al. 1996). Moreover, subjects in the 'exercise therapy' group had a reduced LBP recurrence rate as determined by phone questionnaires at one year and three years after the initial injury (Hides et al. 2001). O'Sullivan et al. (1997) randomly assigned chronic LBP subjects with spondylolysis and spondylolisthesis into two different exercises groups consisting of ten week long intervention programs while assessing pain, disability, lumbar spine and hip ROM (O'Sullivan et al. 1997). One exercise group consisted of weekly physiotherapy sessions to learn the 'drawing in' technique in previously painful postures while the other group received general aerobic and abdominal exercises (O'Sullivan et al. 1997). Following the ten week interventions the group learning the 'drawing in' technique reported significantly reduced pain and disability scores that were still present thirty months after the initiation of the intervention (O'Sullivan et al. 1997). The general aerobic and abdominal exercise group did not report any significant decreases in pain or disability at ten week, three month, six month and thirty month follow-ups (O'Sullivan et al. 1997).

Stuart McGill has opposed the practice of training LBP subjects to learn the 'drawing in' technique as a method of stabilizing the lumbar spine (McGill 2002; McGill 2007). McGill has acknowledged that motor deficits, particularly in transversus abdominus, may be present in LBP subjects warranting motor re-education programs; however, he has argued that the 'drawing in' technique does not stabilize the spine (Grenier and McGill 2007; McGill 2002; McGill 2007). McGill and colleagues (Cholewicki and McGill 1996; Cholewicki and VanVliet 2002; Cholewicki et al. 1997) have modeled the lumbar spine (Cholewicki and McGill 1996) and determined the stability index during a number of movement tasks (Kavcic et al. 2004a; Kavcic et al. 2004b). Analysis of individual muscle contributions to this model has shown that no one muscle is responsible for more than 30% of trunk stability (Cholewicki and VanVliet 2002). McGill contends that spinal

stability is a "moving target" and that a combination of many muscles work together to ensure stability in different tasks (McGill et al. 2003). This view opposes the hypothesis that lumbar multifidus and transversus abdominus have specialized stability roles. Using the analogy of the vertebral column as an antenna with muscles acting as "guy wires," McGill argues that tensioning a specific muscle will only improve spinal stability if that particular "guy wire" is slack (McGill et al. 2003).

Based on their research into lumbar spine stability and stability indices, McGill and colleagues have developed the 'abdominal brace' to stabilize the lumbar spine (Grenier and McGill 2007; McGill 2002; McGill 2007). The 'abdominal brace' consists of co-contraction of the transversus abdominus, internal oblique and external oblique at an intensity between 5-10% MVC (McGill 2002; McGill 2007). This technique is most effectively taught through self-palpation of the anterolateral abdominal wall after it is first demonstrated to subjects (McGill 2002). The use of an abdominal co-contraction technique with consequent paraspinal muscle contraction arises from the principle that increased joint stiffness increases joint stability (McGill et al. 2003). Comparative studies using the model developed by Cholewicki et al. (1996) have shown that the stability index of an electromyographically recorded 'abdominal brace' is far superior to the 'drawing in' technique (Grenier and McGill 2007). These authors also modeled both a perfect 'drawing in' technique using independent contraction of the transversus abdominus and a perfect 'abdominal brace' (Grenier and McGill 2007). Their findings indicated that transversus abdominus only contributed 0.14% to the 32% increase in stability index associated with the simulated 'abdominal brace' (Grenier and McGill 2007). A second study also demonstrated that during rapid trunk perturbations the 'abdominal brace' resulted in increased spinal stability; however, it was also associated with higher spinal compressive forces relative to the 'drawing in' technique (Vera-Garcia et al. 2007).

The Queensland group has also compared the 'drawing in' technique and 'abdominal brace' to assess which technique better stabilizes the lumbar spine (Richardson et al. 2002). Richardson et al. (2002) vibrated the anterior superior iliac spine of prone subjects

at 200Hz while they performed either the 'abdominal brace' or 'drawing in' of the lower abdominal wall (Richardson et al. 2002). Sacroiliac joint laxity was assessed by measuring the coupling between the ilium and sacrum using Doppler ultrasound (Richardson et al. 2002). These authors found that both stabilization methods decreased joint laxity (and hence increased joint stiffness), however; 'drawing in' resulted in significantly less sacroiliac joint laxity (Richardson et al. 2002).

2.3.2 Differential functioning of lumbar multifidus

The rapid arm movement and external trunk perturbation studies performed by Lorimer Moseley and colleagues (Moseley et al. 2002; Moseley et al. 2003) proposed that the deep and superficial lumbar multifidus fibres function differentially. During rapid arm movements, deep fibre EMG onset was consistent between movement directions; however, this onset was measured relative to the onset of surface EMG electrodes at different positions over the deltoid (Moseley et al. 2002). Predictable external trunk perturbations resulted in the onset of deep fibre excitation occurring earlier than during unpredicted perturbations, however, this difference was only a trend and did not reach statistical significance (Moseley et al. 2003). The ratio between deep fibre EMG amplitude during predicted perturbations and amplitude during unpredicted perturbations was significantly greater than one prior to the perturbation (Moseley et al. 2003). In other words, prior to predicted perturbations the amplitude of deep fibre excitation amplitude was significantly greater than excitation amplitude during unpredicted perturbations. It should be noted that unpredicted trials in which deep fibre excitation occurred prior to the perturbation were excluded from analysis and thus any significant deep fibre excitation during some or all predicted trials may have produced this result (Moseley et al. 2003). Moseley et al. (2003) acknowledge the possibility of a recruitment order effect whereby deep multifidus fibres are excited first and as neural drive increases superficial multifidus fibres are subsequently recruited (Moseley et al. 2003). They conclude this possibility is unlikely because if deep fibres contained a larger relative percentage of slow twitch fibres their burst duration would be longer than superficial multifidus fibres and their data do not support this (Moseley et al. 2003).

Differential deep and superficial lumbar multifidus EMG activity has been investigated during gait using different locomotor modes (walk, run) and at different velocities (1, 2, 3, 4, 5m/s) (Saunders et al. 2004; Saunders et al. 2005). Transversus abdominus excitation is relatively tonic throughout the gait cycle, yet superficial and deep lumbar multifidus fibres are phasically excited (Saunders et al. 2004; Saunders et al. 2005). Both superficial and deep lumbar multifidus fibres were modulated by the frequency of motion (Saunders et al. 2004) and there did not appear to be a consistent relationship between deep and superficial fibre excitation onsets (See Figure 4 in Saunders et al. 2004). The total percentage of muscle excitation through the gait cycle increased comparably in erector spinae, deep and superficial lumbar multifidus fibres (Saunders et al. 2004). These investigations concluded that during gait there was little evidence to support differential activity of the superficial and deep lumbar multifidus fibres (Saunders et al. 2004; Saunders et al. 2005). In a recent review, proponents of the 'drawing in' technique also concede there is no evidence to support deep lumbar multifidus fibre co-contraction with transversus abdominus during 'drawing in,' but there is also no evidence to refute this possibility (MacDonald et al. 2006). During training of the 'drawing in' technique, surface EMG has primarily been used to ensure superficial muscles are not electrically active while deep fibre muscle excitation has been assumed or imaged with ultrasound to view architectural muscle changes (Richardson et al. 1999).These architectural changes may reflect active or passive muscle properties due to active contraction or morphological changes of surrounding structures.

The hypothesis that deep muscle fibres stabilize the spine while more superficial muscles act as prime movers has also been attributed to the cervical and thoracic spines (Bexander et al. 2005; Lee et al. 2005). In an investigation of different eye positions during head rotation, multifidus and obliquus capitis EMG activity levels were independent of direction, suggesting a stabilizing role. Contrary to this finding, Blouin et al. (2007) observed direction specific excitation in multifidus during isometric sweep contractions. Furthermore, coherence analysis revealed a common frequency of neural drive to multifidus and other neck muscles, indicating that it was unlikely that separate neural

signals were sent to deep and superficial muscles functioning to stabilize and move the trunk, respectively (Blouin et al. 2007). Differential functioning of thoracic longissimus and multifidus has also been suggested to occur to move the trunk and stabilize the spine, respectively (Lee et al. 2005). In most subjects, thoracic multifidus was reported to be directionally non-specific (especially at T5) during slow seated axial rotation such that left or right rotation resulted in similar increases in muscle excitation (Lee et al. 2005). These authors acknowledged that there was considerable variability in the multifidus response (See Figure 4 in Lee et al. 2005), yet suggest that thoracic multifidus may have functioned as a stabilizer to control intersegmental motion (Lee et al. 2005). A second study investigating faster axial rotation tasks did not support their original study as thoracic multifidus EMG was significantly greater during contralateral rotation (Lee et al. 2007). In this second study the authors reconcile this apparent contradiction by stating that "close inspection of those data [the original study] suggest a trend for marginally greater activity with contralateral rotation" (Lee et al. 2007, p.7).

3. Statement of the problem

The abdominal 'drawing in' technique has been proposed to differential excite the deep fibres of lumbar multifidus, while the superficial fibres are not electrically excited. These deep fibres have been implicated as functional stabilizers during lumbar spine stability tasks. There is preliminary evidence to support this claim; however, the differential response of these fibres to varying perturbation magnitudes has not been quantified. Evidence against the proposed differential activity in the cervical and thoracic spines has further confounded these proposals. Additionally, differential lumbar multifidus activity has primarily been investigated at L4 and it is unknown if other lumbar vertebral levels produce similar results. To address these issues, we intend to introduce posterior-anterior indentation perturbations of varying amplitude and velocity to individual vertebrae and record the responses of superficial and deep lumbar multifidus fibres at multiple lumbar vertebral levels.

4. Hypotheses

Posterior-anterior indentation perturbations to the spinous processes of lumbar vertebrae are hypothesized to cause differential EMG responses in superficial and deep lumbar multifidus fibres. More specifically, the three primary hypotheses are as follows.

1. Deeper indentation displacements will cause larger EMG responses in superficial fibres whereas the response of deep fibres will not be affected by perturbation depth.
2. Higher velocity perturbations are expected to result in increased superficial and deep fibre EMG activity; however, the rate of superficial fibre activity increase will be greater than the rate of increase in deep fibres. The increase in deep lumbar multifidus fibre excitation with increased velocity will be in the form of increased stretch reflex amplitude which will occur very shortly after the initiation of the perturbation.
3. Lastly, it is hypothesized that indentation perturbations will result in similar but diminished EMG responses at adjacent vertebral levels due to the multi-level innervation of facet joint capsules.

5. Operational definitions

Deep lumbar multifidus fibres: Multifidus fibres arising from the vertebral laminae, inserting at the mamillary processes and spanning no more than two vertebral levels.

Superficial lumbar multifidus fibres: Multifidus fibres originating at the base or tip of a lumbar spinous process and inserting to the lumbar vertebrae, ilium or sacrum greater than two levels caudal to the fibres' origin.

Indentation start position: The indentation start position of the perturbation rod was defined as the displacement at which the indentation rod produces the required preload (20N).

Active indentation phase: This phase of the indentation perturbation began when the perturbation rod was in the indentation start position at the initiation of the perturbation. This phase ended when the perturbation rod reached its maximum downward displacement.

Indentation hold phase: This phase of the indentation perturbation followed the active indentation phase and commenced at the moment full indentation displacement was reached. This phase lasted for 500 milliseconds and ended at the beginning of the indentation resolution phase.

Indentation resolution phase: This phase followed the indentation hold phase and began when the indentation rod initiated upward movement away from the spinous processes and ended when the motor had reached its maximum upward displacement.

6. Methods and procedures

6.1 Study participants

Ten healthy participants (8 male, 2 female) without a history of neck, back, lower limb pain or neuromuscular pathology were recruited for this study. These participants had a mean (standard deviation) age of 28.6 (7.4) years old, height of 1.77 (0.10) metres and a body mass of 74.6 (9.9) kilograms. Individual participant anthropometric data are presented in Table 6.1. The experimental protocol including intramuscular electrode insertion technique and possible experimental risks and complications were explained to all participants prior to the start of the experiment. This study was approved by the UBC Clinical Research Ethics Board and all participants signed informed consent forms prior to participating.

Table 6.1 List of participant ages and anthropometry.

	Gender	Age (yrs old)	Height (metres)	Mass (kg)	BMI (kg/m^2)
Subject 01	M	47	1.73	78	26.14
Subject 02	M	26	1.83	82	24.37
Subject 03	M	22	1.76	75	24.30
Subject 04	F	23	1.55	58	24.12
Subject 05	F	25	1.68	61	21.70
Subject 06	M	35	1.76	71	23.12
Subject 07	M	26	1.75	81	26.37
Subject 08	M	30	1.88	86	24.37
Subject 09	M	25	1.83	85	25.52
Subject 10	M	26	1.82	67	20.34
Mean (SD)		28.5 (7.5)	1.76 (0.09)	74 (10)	24.03 (1.90)

6.2 Electromyography and multifidus imaging

Fine-wire electrodes were custom fabricated from insulated stainless steel wire with a 0.05mm diameter (Stainless Steel 304, California Fine Wire Company, California, USA). Two strands of bipolar stainless steel fine-wire were interwoven and guided through hypodermic needles. Fine-wire electrodes that were inserted into deep lumbar multifidus fibres were inserted using a 2" Monoject needle (Kendall, Massachusetts, USA), while electrodes inserted into superficial fibres were inserted using a 1.5" PrecisionGlide needle (Becton Dickson, New Jersey, USA). Both needles were regular bevel 25-gauge hollow hypodermic needles with the only functional difference between them being their cannula length. The exposed ends of the wire were hooked back onto the needle and each strand was transversely cut. One strand was cut to leave 4mm of wire hooked outside the cannula while the other wire was cut to leave 0.5mm outside the cannula. The opposite ends of the wire were soldered to nickel plated tip plug connectors (Emerson Canada, Ontario, Canada). All fine-wire electrodes were medically sterilized prior to insertion. For a detailed description of fine-wire electrode fabrication refer to Appendix A.

Participants were asked to lie prone on a comfortable and adjustable bed (Access model, Athlegen, Lewisham, Australia). The level of the L4 spinous process was determined by palpation either from the sacrum cranially or by moving caudally after identifying the L1 spinous process. The lumbar paraspinal musculature was imaged with an ultrasound transducer (Sonosite Micromaxx, 13-6MHz HFL38 Transducer) to locate the superficial and deep lumbar multifidus fibres. The ultrasound transducer probe was initially placed at the level of the L4 spinous process in the transverse plane (Figure 6.1). Personal observations of cadaver paraspinal anatomy, anatomical figures (Hides et al. 2007; Kamaz et al. 2007; Kang et al. 2007; Moseley et al. 2003) and axial images of the male Visible Human® show the multifidus as the most superficial and medial muscle at this level. The ultrasound transducer probe was translated superiorly and inferiorly to identify lumbar multifidus at the L3, L4 and L5 vertebral levels.

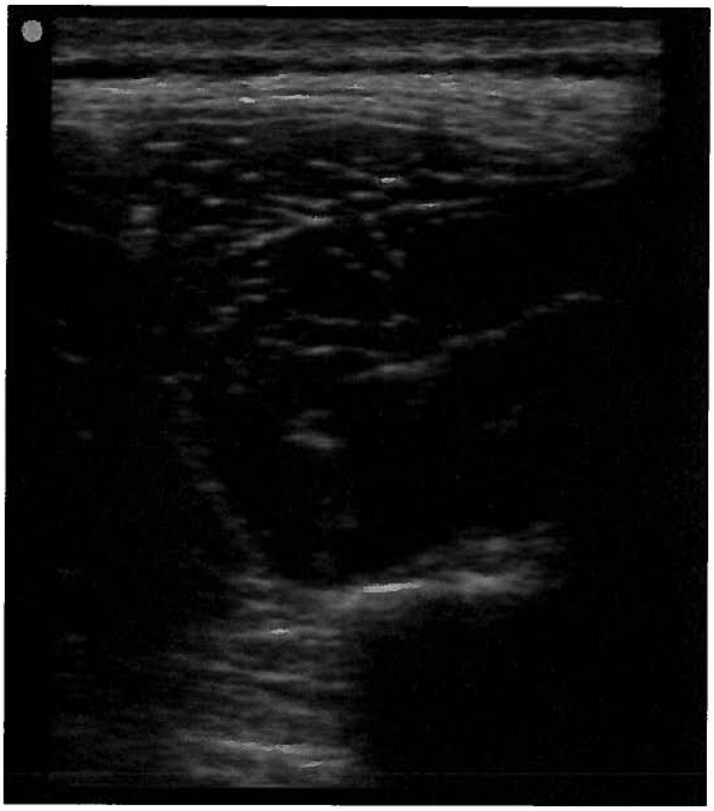

Figure 6.1 Transverse plane ultrasound image at the L4 vertebral level showing the fascial border of the lumbar multifidus.

Once the experimenter was satisfied that lumbar multifidus could be imaged accurately, the non-sterile ultrasound gel (Aquasonic 100, Parker Laboratories Inc, New Jersey, USA) was removed from the participant's lower back and the intended electrode insertions sites and surrounding skin was cleaned with Isopropyl alcohol. Sterile ultrasound transmission gel (Aquasonic 100 sterile, Parker Laboratories Inc, New Jersey, USA) was placed on the lower back and the ultrasound transducer probe was placed in a sterile probe cover (CIV-flex, 8.9x91.5cm telescopic fold, Cone Instruments, Ohio, USA). A total of six fine-wire electrodes were inserted unilaterally and under ultrasound guidance into the right superficial and deep fibres at the L3, L4 and L5 vertebral levels. Figure 6.2 displays ultrasound images of example fine-wire electrode insertion placements within lumbar multifidus. Once the needle reached its desired location, it was withdrawn and placed in a needle shield taped to the participant's skin. For a detailed description of multifidus imaging techniques and fine-wire electrode insertion refer to Appendix B.

The electrode connectors were plugged into a high impedance differential pre-amplifier (Digitimer Neurolog NL844, Hertfordshire, England, Input impedance: 100MΩ, Common mode rejection ratio: > 90db at 1kHz) that gained the EMG signals between 100x and 1000x (depending on the subject and recording electrode). The pre-amplifier was connected to a larger amplifier (Digitimer Neurolog NL820 housed in a NL820 Isolator, Hertfordshire, England, Input impedance: 100kΩ) which further gained the signals 1-5x. A Micro 1401 analog-to-digital converter (Cambridge Electronics Design, Cambridge, UK) sampled each EMG channel at 20,000Hz and these signals were recorded by a PC computer using Spike2 software (Cambridge Electronics Design, Cambridge, UK).

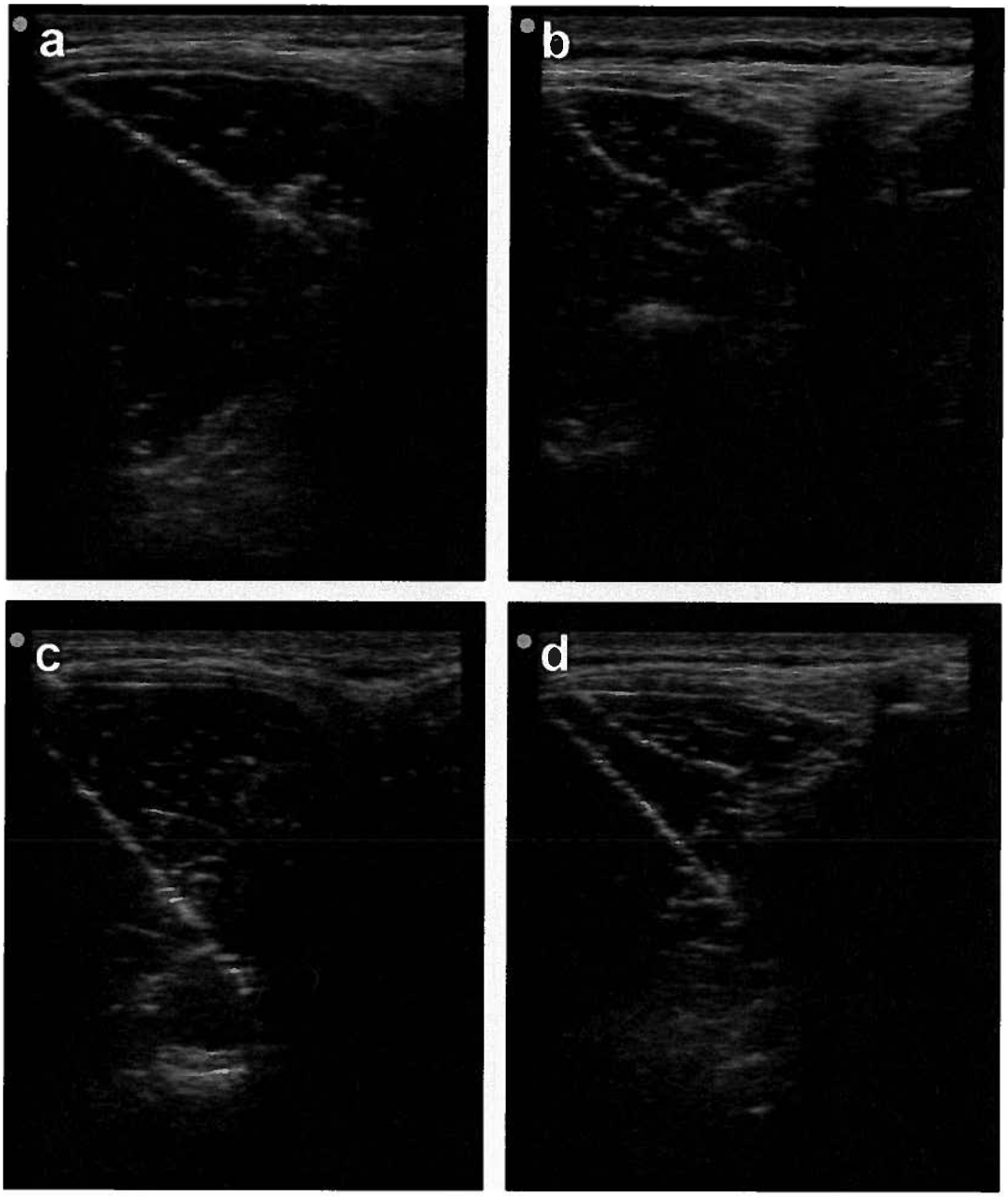

Figure 6.2 Example fine-wire electrode insertion locations. (A) L5 superficial needle used to insert the fine-wire electrode in Subject 06, (B) L3 superficial wire in Subject 08, (C) L5 deep needle used to insert electrode in Subject 10 and (D) L4 deep needle and L4 superficial wire in Subject 10.

6.3 Motor displacement and force

A linear brushless digital servo-motor (SimplIQ Bassoon, Elmo Motion Control, Westford, MA, USA) was used to apply poster-anterior indentation perturbations to individual lumbar spinous processes. The servo-motor had a peak force of 902.5N, peak current of 15.0A, a resistance of 8.6Ω and an electrical time constant of 0.0007 seconds. The servo-motor was affixed to a sturdy steel frame positioned over the Athlegen treatment bed. The servo-motor delivered indentation perturbations by manipulating the position of a long narrow rod with a cupped felt contact surface on the end (Figure 6.3). The cupped felt contact surface was used to cradle each spinous process and increase subject comfort.

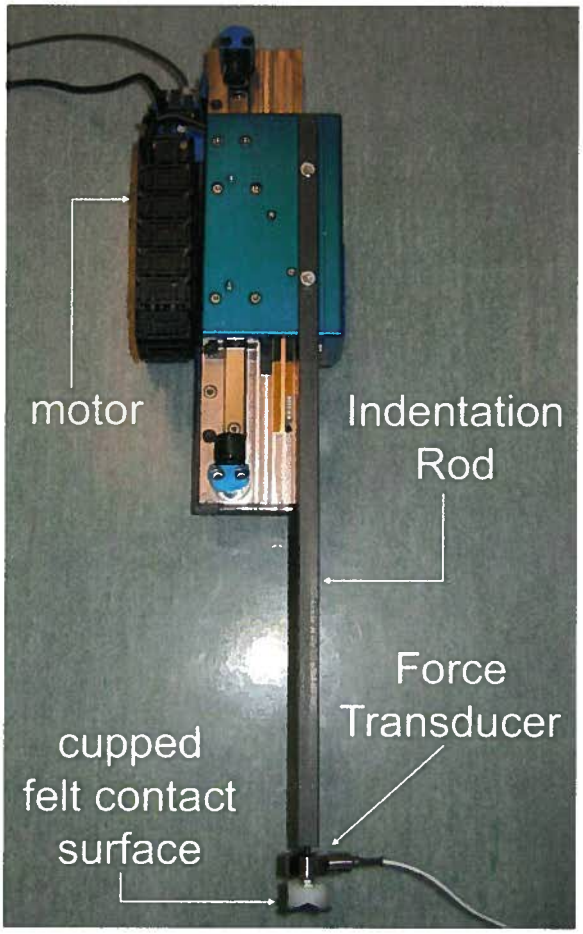

Figure 6.3 The servo-motor used to deliver the indentation loads by manipulating the position of the indentation rod. The force transducer between the indentation rod and the cupped felt contact surface recorded force between the indentation rod and skin

Two PC computers were used to control the digital servo-motor and deliver indentation perturbations. A custom computer program was written in Elmo Motion Studio software (Elmo Motion Control, Westford, MA, USA) and uploaded to the SimplIQ Bassoon controller using the first PC computer. This program contained perturbation subroutines with varying perturbation velocity and displacement and each velocity-displacement combination was triggered with a specific binary input to the controller. A second PC computer running Spike2 delivered the binary inputs to the controller through the digital output of the Micro 1401. This experimental setup allowed the experimenter to trigger perturbations by pressing a specific key on the second PC computer from within Spike2. A schematic of how the motor was controlled is presented in Figure 6.4.

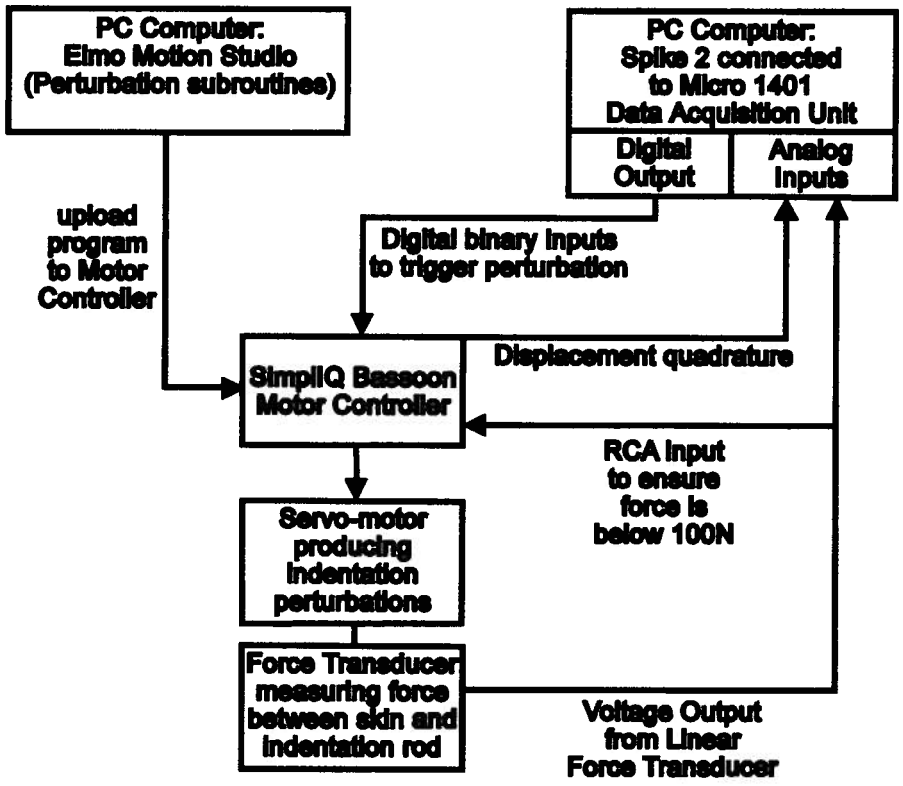

Figure 6.4 Schematic of digital servo-motor control during experimental posterior-anterior indentations.

Indentation rod displacement was measured by sampling the four quadrature channels from the SimplIQ Bassoon controller auxiliary feedback. Quadrature channels were sampled at 100,000Hz as event channels using Spike2 software and the Micro 1401 analog-to-digital converter. Displacement was calculated offline using a custom program written in MATLAB 7.4 (The Mathworks, Inc., Massachusetts, USA) that created a displacement channel sampled at 1000Hz. Force between the indentation rod and skin overlying the spinous process was measured with a small one-dimensional twenty-five pound load cell (Honeywell, Ohio, USA). The load cell had a force range of 111N and was fitted between the indentation rod and the cupped felt contact surface. Force was sampled by the Micro 1401 analog-to-digital controller at 1000Hz and recorded by Spike2 software.

6.4 Respiration

Respiratory flow was monitored during the experimental protocol to determine the time-point at the end of normal expiration corresponding to functional residual capacity. As discussed in section 2.1.3, trunk stiffness to posterior-anterior indentation forces directed at lumbar spinous processes is significantly modulated by lung volume (Shirley et al. 2003). Respiratory flow was be measured by a pneumotachometer (Hans Rudolph Inc, Series 1110, Kansas City, KS, USA) and sampled by an analog-to-digital converter (Micro 1401) at 1000Hz. Prone study participants breathed into a mouthpiece mounted in the face hole of the adjustable bed that was directly attached to the pneumotachometer. Respiratory gas collection was not required and thus expiratory gases were re-directed from the 'out valve' back into the pneumotachometer to record both inspiratory and expiratory flow.

Studies employing posterior-anterior indentation loads have primarily applied these loads at the end of normal expiration (Colloca and Keller 2004; Colloca et al. 2003; Hodges et al. 2005; Kawchuk and Fauvel 2001; Keller et al. 2003; McGill et al. 1994; Moseley et al. 2002). In the current study, pneuomotachometry was displayed online during indentation perturbations and the experimenter triggered each perturbation at the end of normal

expiration. Trials in which the perturbation was not delivered at the end of normal expiration were excluded from analysis (See Results section 7.1.1).

6.5 Experimental protocol

The experimental protocol was divided into two parts. The first part consisted of evaluating vertebral motion during slow velocity perturbations and determining the proper experimental position for each participant. The second part consisted of three experimental blocks of posterior-anterior indentation perturbations. The experimental protocol is described in the following sections.

6.5.1 Vertebral motion and participant experimental position

Participants lay prone on the Athlegen treatment table while three or four indentation perturbations of 7.5mm at 0.01m/s were applied to the skin overlying an individual lumbar spinous process. During these perturbations, the posterolateral aspect of the lumbar vertebrae being perturbed and the adjacent inferior vertebrae were imaged using ultrasound. Ultrasound video files of vertebral movement during these indentation perturbations were captured by the Sonosite ultrasound unit. The perturbation rod was placed directly over the spinous process being perturbed and thus the ultrasound probe was placed lateral to the perturbation rod and at an angle directed medially toward the vertebral body. This transducer probe orientation generally allowed the vertebral laminae and/or superior articular processes to be imaged clearly during these perturbations. These landmarks allowed sagittal plane movement to be assessed during perturbations. All videos were viewed real time and stored offline for later analysis.

Following these indentation perturbations during prone lying, both ends of the treatment table were inclined to extend the torso and hips, positioning study participants in hyperextension. The treatment table was inclined slowly and incrementally while asking participants how each increment felt and whether they would be comfortable in that position during the three experimental perturbation blocks. The treatment table was

inclined until participants were near their limit of "comfortable" hyperextension. Once a position of "comfortable" hyperextension was reached, ultrasound videos of the same three to four posterior-anterior indentation perturbations of 7.5mm at 0.01m/s were viewed in real-time. These ultrasound videos were stored on the compact flash drive of the ultrasound unit for additional off-line analysis. Vertebral movement during perturbations in the prone position and hyperextended position were compared. Pilot testing revealed that posterior-anterior perturbations in the prone position primarily produced vertebral rotation in the sagittal plane while perturbations in the hyperextended position resulted in anterior vertebral translation. If vertebral motion during the perturbations in the hyperextended position did not produce vertebral translation, the treatment bed was re-adjusted and vertebral movement during indentation perturbations was re-evaluated until the perturbation produced vertebral translation.

The treatment bed position was recorded and the bed was lowered back to prone after finding a position of "comfortable" hyperextension that produced vertebral translation during perturbations. Fine-wire electrodes were inserted under ultrasound guidance as described in section 6.2 and then participants were returned to the same hyperextended position by returning the treatment bed to the recorded position.

6.5.2 Indentation perturbations

A single block of indentation perturbations was delivered to each of the L3, L4 and L5 spinous processes resulting in a total of three perturbation blocks. The order of each block was randomly determined for each participant, however, all perturbations in each block were completed before the next block commenced. At the start of each block the long narrow indentation rod was positioned over the specified spinous process, oriented perpendicularly to the skin surface. Previous experimental protocols have oriented indentation perturbations perpendicular to the vertebral body anterior-posterior axis. This has resulted in perturbations being delivered to L2 and L3 at cephalad angles of 5.5-11.5°, to L4 at a caudad angle of 4.5° and to L5 at a caudad angle of 16° (Hodges et al. 2005; Latimer et al. 1996a; Lee et al. 1993; Shirley et al. 2003). We chose to orient the

indentation perturbation rod perpendicular to the skin surface of each prone participant to minimize any lateral distension of the skin surface during indentation perturbations. The experimental setup is shown in Figure 6.5.

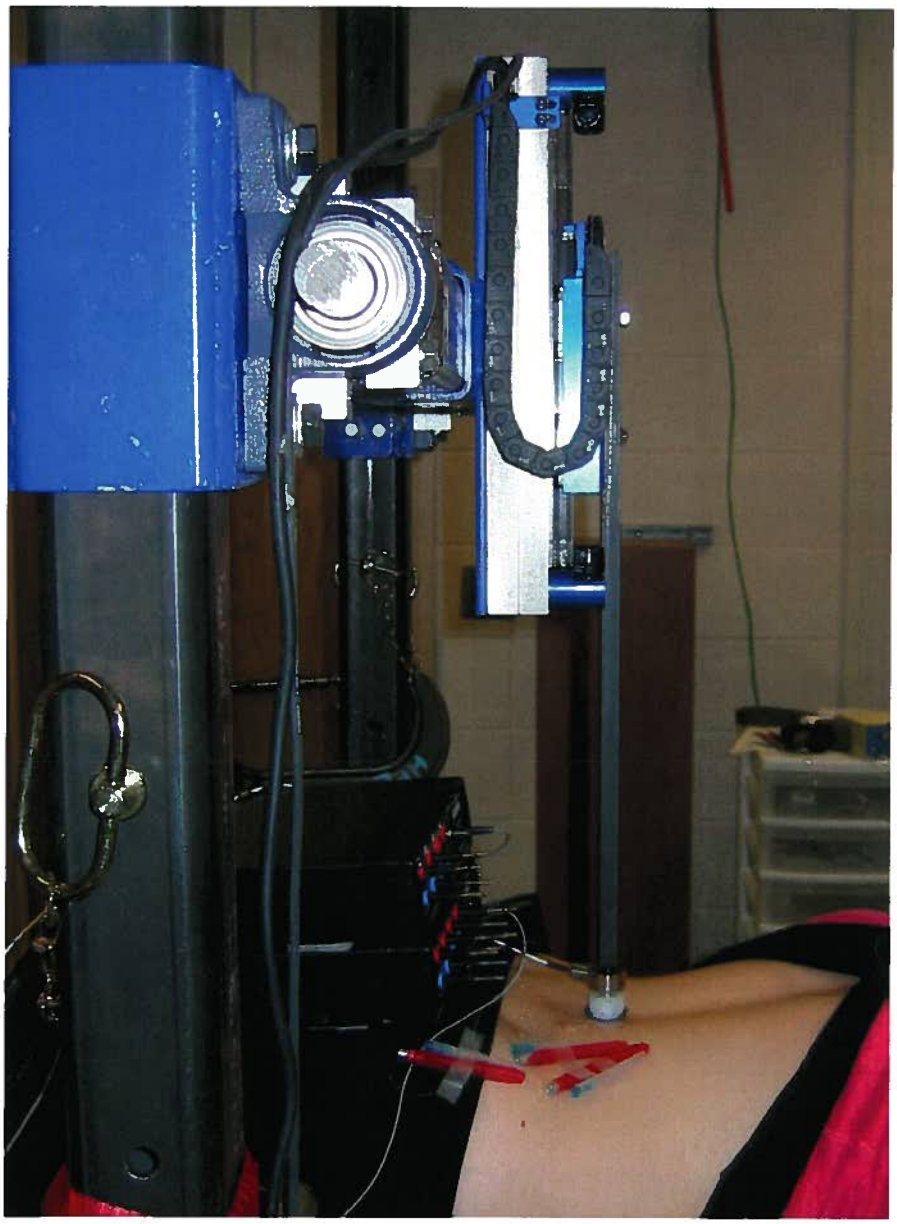

Figure 6.5 Experimental setup to deliver indentation perturbations while recording displacement, force and intramuscular electromyography.

Initially, a 5N preload was applied to the spinous process through the indentation rod prior to each indentation perturbation. When an indentation perturbation was triggered by the experimenter, the indentation rod displaced downward toward the spinous process at 0.0002m/s until the force between the rod and skin reached 20N. The indentation rod held this position for 200 milliseconds before delivering the indentation perturbation. Applying a preload to the specified target is the first phase of a HVLA thrust (Herzog et al. 1993; Pickar 2002) and has been routinely employed when applying indentation perturbations (Colloca and Keller 2001b; Colloca et al. 2004; Colloca et al. 2006; Colloca et al. 2007; Keller et al. 2006; Keller et al. 2007; Pickar and Wheeler 2001). Clinically, preload forces to the thoracic, lumbar spines and sacroiliac joints have ranged between 20N and 180N (Conway et al. 1993; Gal et al. 1997; Herzog et al. 1993; Herzog et al. 2001; Pickar 2002; Triano and Schultz 1997). The purpose of the preload was to reduce the effect of skin and soft tissue compliance by limiting the 'toe off' component of the stiffness curve (Keller et al. 2007) as well as moving the intervertebral joint being manipulated to the end of its ROM (Pickar and Ge 2007). The 20N preload employed in this study was small relative to those used in spinal manipulation therapy, yet still within the range of preload values reported for spinal manipulation therapy.

Perturbation displacements of 5.00mm (D1), 6.25mm (D2) and 7.50mm (D3) from the indentation start position were each paired with perturbation velocities of 0.01m/s (V1), 0.15m/s (V2) and 0.40m/s (V3). This resulted in a total of nine different perturbation displacement-velocity combinations. Indentation perturbations consisted of three phases: the active indentation phase, indentation hold phase and indentation resolution phase (defined in section 5). During the active indentation phase, the indentation rod moved downward at the specified velocity and stopped at the specified displacement. The indentation rod held this position for 500 milliseconds (indentation hold phase) before displacing upward (indentation resolution phase) at the specified velocity to a position two millimetres above the indentation start position.

Perturbation order within an experimental block was randomized; however, two perturbations of the same displacement and velocity did not occur in succession. Ninety

total perturbations of the nine displacement-velocity combinations were delivered to each vertebral spinous process which resulted in an average of ten perturbations at each displacement-velocity combination. These ninety perturbations were delivered in two sub-blocks of forty-five trials and after each sub-block, participants were allowed to remove the pneumotachometer mouthpiece and the indentation rod was removed from their lumbar spine. Each perturbation sub-block typically lasted between eight and twelve minutes with rest intervals between sub-blocks lasting two to three minutes. At the end of each perturbation sub-block, the participant was asked to bilaterally lift their legs to extend the hips and excite the lumbar multifidus. Pilot testing revealed that this movement elicited EMG activity at all multifidus EMG recording sites and was performed to ensure that the integrity of each EMG channel was maintained throughout the perturbation sub-block.

The use of a force-control or displacement-control experimental protocol has been debated for both in vitro and in vivo spinal biomechanical testing (Goel et al. 1995). Both force-control (Pickar and Kang 2006) and displacement-control protocols (Pickar et al. 2007) have been employed during posterior-anterior indentations. It has been argued that displacement-control protocols produce quickly rising forces during motion in the elastic zone and do not represent the intrinsic properties of increased stiffness with increased stretch (McGill 2007). On the other hand, displacement-controlled experimental protocols are better able to reproduce in vivo vertebral motions especially during low joint stiffness ranges (Goel et al. 1995). The current study employed displacement-control for two primary reasons. Firstly, posterior-anterior indentation loads to the skin overlying lumbar spinous processes have been shown to produce a linear relationship between force and displacement over the force range 50-100N (Shirley et al. 2003). Secondly, the motor controller can be pre-programmed to deliver specific displacements while force-control would necessitate feedback responses from the force transducer possibly resulting in increased processing time delays.

During cyclic indentation loads, trunk stiffness during the first cycle was reported to be significantly less than during four subsequent cycles (Shirley et al. 2002). To prevent

changes in trunk stiffness which may affect EMG responses, "habituation trials" were performed at each vertebral level prior to experimental perturbations at that level. Ten perturbations at the highest velocity (V3) and deepest displacement (D3) were delivered to the vertebral spinous process being perturbed in the current experimental block. During each experimental block of ninety indentation perturbations, indentation displacement and velocity combinations were randomized (as described above) to further guard against experimental order effects.

The servo-motor was equipped with a number of software and hardware precautions to ensure participant safety. The motor was programmed to limit the maximal force of each indentation to 100N, a hard rubber stop was placed at 10mm to prevent indentation rod displacement beyond this point and the experimenter could immediately cut power to the motor at any time using a manual kill switch.

6.6. Data analysis

Breathing, force, displacement and EMG channels were recorded using Spike2 software and data analysis procedures were performed in MATLAB 7.4. Posterior-anterior trunk stiffness was computed using the method of central differences as the change in force over the change in displacement. As described in section 6.3, perturbation velocity and displacement were controlled by the nine different perturbation subroutines; however, these independent variables were also computed from the displacement quadrature channels. Perturbation velocity was computed by the method of central differences by differentiating perturbation displacement. Breathing during each perturbation was examined online and offline and trials in which breathing did not occur at the end of normal expiration were eliminated.

EMG channels were bandpass filtered at 100-2000Hz using digital zero-phase fourth order Butterworth low and highpass filters. EMG channels were quantified by computing the "average" root mean square (RMS) of each channel over the combined active indentation and indentation hold phases for each perturbation. Despite experimental

precautions and bandpass filtering, EMG channels in some trials contained a small amount of electrical 'noise' due to the digital servo-motor. To eliminate this 'noise' from affecting experimental dependent measures, baseline electrical activity was subtracted from each "average" RMS value. Baseline activity was computed by taking the RMS value of the least variable 200 millisecond window within the two second window prior to the perturbation. This 200 millisecond interval was found by taking a sliding window of the standard deviation in each EMG channel during the two second interval prior to the perturbation and calculating the activity over the window with the lowest standard deviation. The motor was stationary over this interval and thus, this method was reasoned to be the most accurate in determining baseline motor 'noise.' Each EMG channel from each perturbation was individually examined and trials in which motor artifacts or non-random 'noise' contaminated EMG recordings were excluded from analysis. The "average" RMS of each EMG channel was averaged for each perturbation of the same velocity and displacement at each perturbation level. This produced a 3x3x3 matrix (perturbation velocity, displacement and level) for each EMG channel with a single value for each subject in each cell. The initial experimental design is presented in Table 6.2. Due to the nature of multifidus intramuscular recordings, it was not possible to accurately normalize EMG channels to a specific activity (i.e. maximal voluntary contraction). Consequently, each EMG channel was separately statistically tested using a 3x3x3 repeated measures ANOVA design with perturbation velocity, displacement and level as independent variables.

Table 6.2 Experimental Design employed for analysis of each EMG channel (Note: The third dimension (perturbation level) of this 3x3x3 experimental design is not shown here).

		Perturbation Displacement		
		D1 = 5.00mm	D2 = 6.25 mm	D3 = 7.50 mm
Perturbation Velocity	V1 = 0.01 m/s	V1-D1	V1-D2	V1-D3
	V2 = 0.15 m/s	V2-D1	V2-D2	V2-D3
	V3 = 0.40 m/s	V3-D1	V2-D2	V3-D3

Two dependent measures were added to the data analysis protocol aposteriori: peak RMS and time-to-peak RMS. A 20.05 millisecond sliding RMS window was computed for each EMG channel corresponding to 401 data-points at the EMG sampling frequency of 20,000Hz. The RMS over each 401 data-point window was computed and entered in the sliding RMS vector at the time value corresponding to the 201st data-point. The peak value of each sliding RMS vector and time-to-peak RMS were computed for each EMG channel during the time interval from the start of the active indentation phase to the end of the indentation hold phase. These dependent measures have been previously used to quantify the EMG response magnitude during horizontal simulated whiplash perturbations (Blouin et al. 2006). The peak RMS and time-to-peak RMS of each EMG channel was averaged for each perturbation of the same velocity and displacement at each perturbation level. In an analogous fashion to the "average" RMS dependent measure, averaging across trials produced a 3x3x3 matrix (perturbation velocity, displacement and level) for peak RMS and time-to-peak RMS with a single value for each subject in each cell.

Statistical tests were carried out using SPSS 14.0 for Windows (SPSS Inc, Illinois, USA). Mauchly's test of sphericity was tested prior to performing each ANOVA and the statistical significance level was set apriori at α=0.05. Greenhouse-geisser corrections were employed in statistical tests which violated the assumption of sphericity.

7. Results

Representative displacement, force and EMG responses for a slow velocity, shallow displacement (V1-D1) and medium velocity, intermediate displacement (V2-D2) perturbation are displayed in Figure 7.1 on the following page.

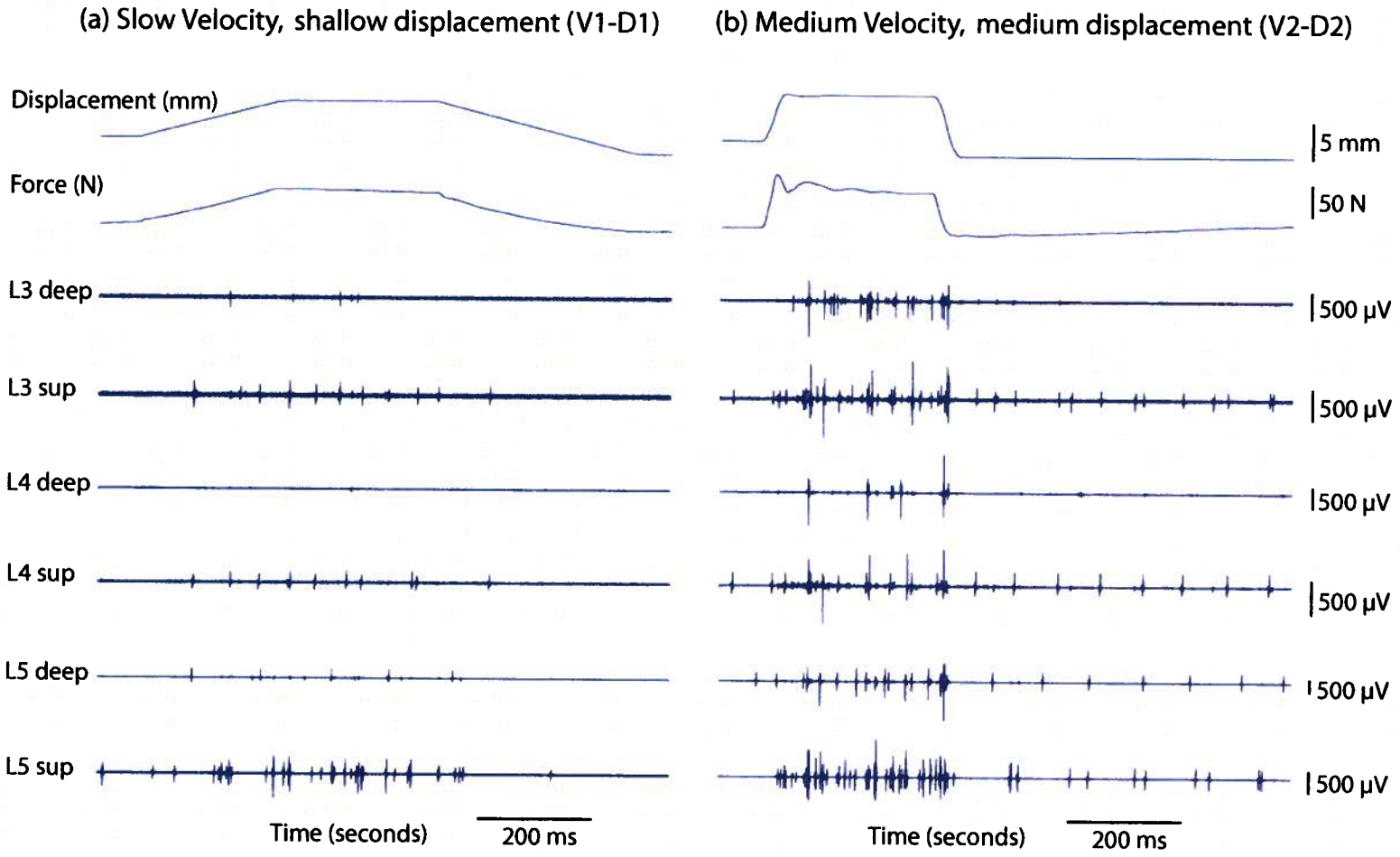

Figure 7. 1 Displacement, force and electromyography of a (a) slow velocity, shallow displacement perturbation (V1-D1) and a (b) medium velocity, intermediate displacement perturbation (V2-D2) in Subject 03. For comparison purposes, both perturbations are plotted on the same scale of axis.

7.1 Experimental conditions validation

7.1.1 Trial exclusion

A single subject was excluded from data analysis due to the presence of electrical artifacts in the EMG channels of many trials. These artifacts were initially observed during data collection and EMG electrodes, wires and connections were manipulated during collection in an attempt to reduce these artifacts. Despite these attempts, an experimental setup could not be found that completely eliminated all artifacts. This participant was male of average height and weight (1.75m, 81kg) and had these artifacts been eliminated, there is no reason to believe that this participant would have produced a different pattern of EMG responses.

A total of 2473 perturbations were delivered to the nine remaining subjects. All breathing, force and perturbation displacement channels of these perturbations were individually inspected for experimental protocol and equipment errors. Forty-eight trials were excluded due to the perturbation occurring at the wrong stage of breathing (1.98%), while thirteen trials (0.52%) were excluded to due the force transducer exceeding the maximum voltage output and five trials (0.20%) due to motor displacement command errors. Additionally, each EMG channel was inspected for non-random motor 'noise' or electrical artifacts and a conservative approach was taken such that any electrical activity that may not have been of physiological origin was excluded from analysis. This approach resulted in a total of 833 individual channels (5.61%) being excluded from analysis. A grand total of 8.28% of all channels were excluded from data analysis. A maximum of 13.85% of trials were excluded from any single subject.

7.1.2 Perturbation velocity and displacement

Perturbation velocity during the active indentation phase and maximum perturbation displacement for each subject were collapsed across trials by averaging all trials within a

single perturbation velocity, displacement and level combination. Perturbation velocity and displacement for each condition at each perturbation level are presented in Table 7.1 and 7.2. Two 3x3x3 matrices corresponding to perturbation velocity and perturbation displacement were statistically tested with repeated measures ANOVAs.

Table 7.1 Mean perturbation velocities (m/s) across subjects for each perturbation displacement and velocity combination at each perturbation level.

(A) Perturbation Level = L3

		Perturbation Displacement		
		D1	D2	D3
Perturbation Velocity	V1 (m/s)	0.011 (0.0008)	0.011 (0.0008)	0.011 (0.0007)
	V2 (m/s)	0.107 (0.003)	0.129 (0.002)	0.145 (0.002)
	V3 (m/s)	0.108 (0.004)	0.134 (0.004)	0.159 (0.004)

(B) Perturbation Level = L4

		Perturbation Displacement		
		D1	D2	D3
Perturbation Velocity	V1 (m/s)	0.011 (0.0004)	0.011 (0.0003)	0.011 (0.0003)
	V2 (m/s)	0.108 (0.002)	0.129 (0.002)	0.145 (0.003)
	V3 (m/s)	0.109 (0.003)	0.135 (0.003)	0.160 (0.003)

(C) Perturbation Level = L5

		Perturbation Displacement		
		D1	D2	D3
Perturbation Velocity	V1 (m/s)	0.011 (0.0005)	0.011 (0.0005)	0.011 (0.0004)
	V2 (m/s)	0.106 (0.003)	0.128 (0.003)	0.143 (0.003)
	V3 (m/s)	0.109 (0.003)	0.134 (0.004)	0.158 (0.004)

Table 7.2 Mean perturbation displacements (mm) across subjects for each perturbation displacement and velocity combination at each perturbation level.

(A) Perturbation Level = L3

		Perturbation Displacement		
		D1 (mm)	D2 (mm)	D3 (mm)
Perturbation Velocity	V1	4.96 (0.004)	6.20 (0.01)	7.13 (0.66)
	V2	5.02 (0.04)	6.24 (0.05)	7.46 (0.08)
	V3	5.01 (0.08)	6.23 (0.04)	7.49 (0.04)

(B) Perturbation Level = L4

		Perturbation Displacement		
		D1 (mm)	D2 (mm)	D3 (mm)
Perturbation Velocity	V1	4.95 (0.004)	6.20 (0.005)	6.99 (0.63)
	V2	5.03 (0.06)	6.26 (0.08)	7.48 (0.05)
	V3	5.01 (0.06)	6.29 (0.09)	7.53 (0.06)

(C) Perturbation Level = L5

		Perturbation Displacement		
		D1 (mm)	D2 (mm)	D3 (mm)
Perturbation Velocity	V1	4.95 (0.01)	6.21 (0.004)	6.78 (0.61)
	V2	4.99 (0.05)	6.29 (0.05)	7.50 (0.08)
	V3	5.01 (0.06)	6.28 (0.07)	7.48 (0.05)

The perturbation velocity ANOVA produced significant main effects of perturbation velocity ($F_{(2,16)}$=14632.41, $p<0.001$, MSe=0.00003, $\eta_p^2>0.99$), perturbation displacement ($F_{(2,16)}$=33768.12, $p<0.001$, MSe=0.0000005, $\eta_p^2>0.99$) and significant interactions between velocity and displacement ($F_{(4,32)}$ =10639.78, $p<0.001$, MSe=0.0000004, $\eta_p^2>0.99$) as well as displacement and level ($F_{(4,32)}$ =3.42, p=0.02, MSe=0.0000007, η_p^2=0.30). The significant interactions indicate that the magnitude of the perturbation velocity depended on the perturbation displacement and level. The perturbation velocities for each condition were qualitatively analyzed and it was observed that not all perturbation velocities reached their target velocity. The V2 (0.15m/s) and V3 (0.40m/s) perturbation velocities did not achieve their target velocities due to the short displacements required by the experimental protocol. The experimental protocol constrained perturbation acceleration and displacement and thus it was known that the time-to-target velocity would be different between perturbation velocities. A schematic of the idealized perturbation velocity profiles for the slow, medium and fast velocities are displayed in Figure 7.2. Perturbation velocities did not achieve their target values because the motor's maximum acceleration was not sufficient to accelerate the indentation rod to target velocity over the short displacements employed by this study.

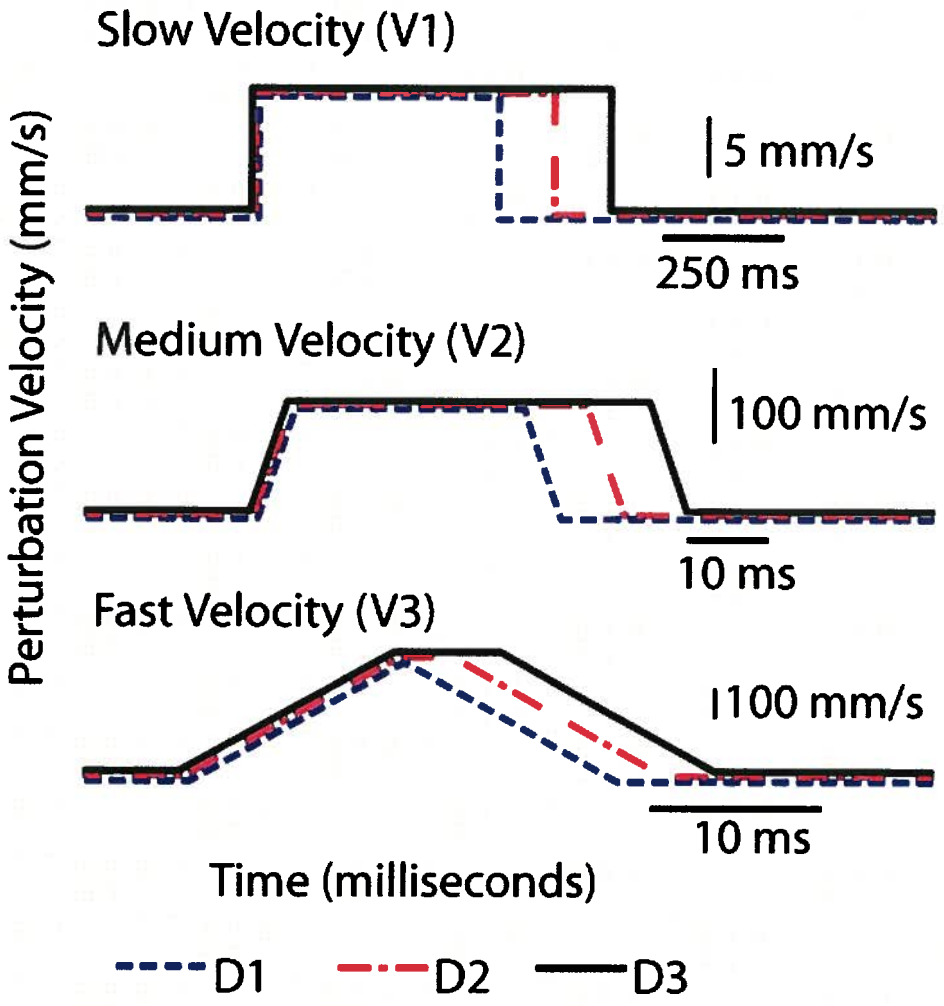

Figure 7.2 Idealized perturbation velocity profiles for slow, medium and fast perturbation velocities (Note the x and y scales for each velocity profile are different).

The perturbation velocity profiles for each condition were amplitude normalized to target velocity and time normalized to active indentation time and displayed in Figure 7.3.

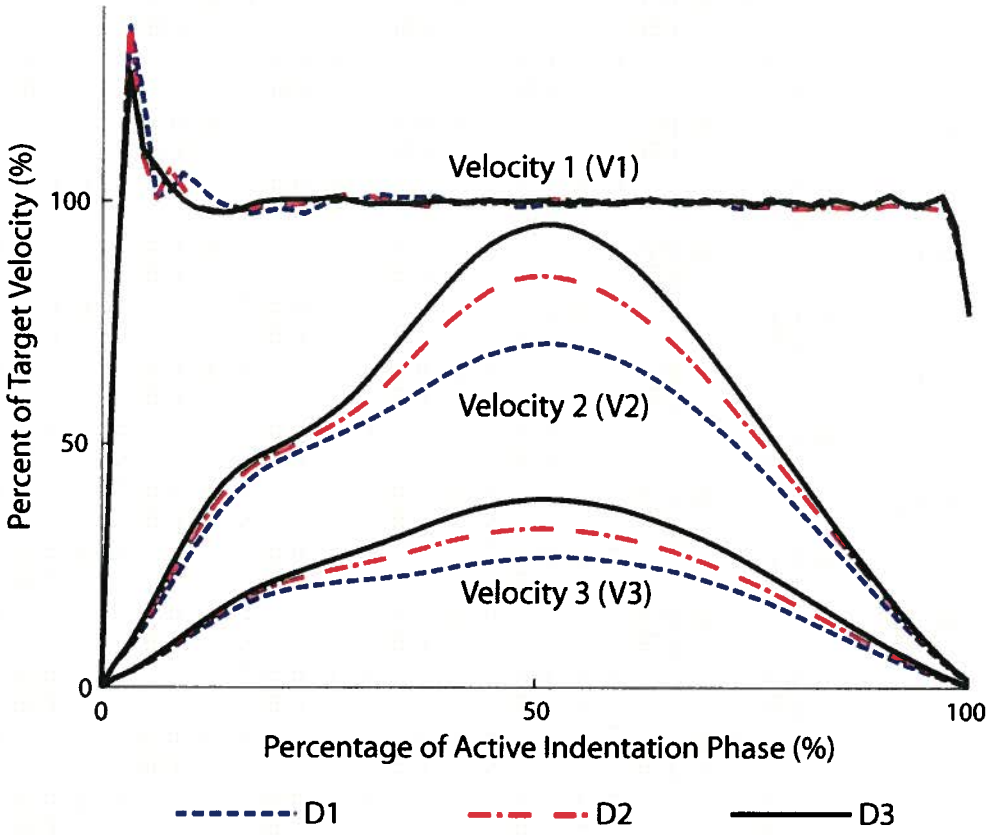

Figure 7.3 Velocity profiles time-normalized to the length of the active indentation phase and expressed as a percentage of their target velocity. Perturbations to different displacements are expressed in different colours (D1=blue, D2=red, D3=black). Note that only Velocity 1 (V1) perturbations achieved 100% of their target velocity.

The perturbation displacement ANOVA produced significant main effects of perturbation velocity ($F_{(2,16)}$=9.13, p=0.002, MSe=0.0000001, η_p^2=0.53), perturbation displacement ($F_{(2,16)}$ =832.53, p<0.001, MSe=0.0000001, η_p^2=0.99) and significant interactions between velocity and displacement ($F_{(4,32)}$ =5.99, p=0.04, MSe=0.0000001, η_p^2=0.43), displacement and level ($F_{(4,32)}$ =3.42, p=0.02, MSe=0.00000001, η_p^2=0.30) and velocity and level ($F_{(4,32)}$ =3.96, p=0.01, MSe=0.00000001, η_p^2=0.33). The significant interactions

suggest that the magnitude of perturbation displacement depended on the perturbation velocity and level. Close examination of perturbation displacement and force profiles revealed that indentation perturbations at the slowest velocity and deepest displacement (V1-D3) did not reach their target displacement. Target displacements were not reached because the force exceeded the 100N safety limit outlined in the experimental protocol (refer to section 6.5.2) and thus the perturbation displacement ceased when this safety limit was surpassed. The force safety limit was exceeded in three of nine subjects at L3, four of nine subjects at L4 and seven of nine subjects at L5.

Due to the motor limitations and safety precautions of this study, perturbations at the V3 target velocity (0.40m/s) and D3 displacement (7.5mm) were excluded from analysis and the design was modified. Additionally, perturbation velocities at V2 (0.15m/s) were not consistent across perturbation displacements because larger displacements permitted a longer period of positive and negative acceleration allowing the indentation rod to reach a higher peak velocity. Consequently, the effect of perturbation displacement could only be statistically tested at V1 and the effect of velocity could only be statistically tested at discrete perturbation displacements. To accommodate these constraints, data analysis was divided into part A and part B to test perturbation displacement and perturbation velocity, respectively.

Part A consisted of a 2x3 repeated measures ANOVA design with two perturbation displacements (D1, D2) and three perturbation levels (L3, L4, L5) at velocity V1 (0.01m/s). Perturbation velocities were only consistent across perturbation displacements at V1 and thus the effect of perturbation displacement could only be tested at this velocity. "Average" RMS, peak RMS and time-to-peak RMS were statistically tested using the 2x3 ANOVA design for each EMG channel. The effect of perturbation velocity could only be tested at discrete displacements and thus part B was divided into two separate analyses at the D1 and D2 perturbation displacements. The V2 velocity at each displacement was not consistent, however, V2 was consistently larger than V1 at each displacement and thus perturbation velocities could be labeled as "low" or "high" at each displacement. The "average" RMS, peak RMS and time-to-peak RMS at each

displacement were statistically tested with a 2x3 repeated measures ANOVA with independent variables perturbation velocity and perturbation level.

The exclusion of all conditions utilizing either the V3 velocity or D3 perturbation displacement did not significantly affect the number of trials excluded from analysis (8.28% vs. 8.26%). Limiting the number of conditions also did not affect the proportion of trials excluded for any specific reason (breathing 1.71%, motor displacement errors 0.20%, EMG artifacts 6.28%). The maximum number of trials excluded from a single subject in the new design was 13.42%. The following results are divided into part A and B to reflect the modifications made to the experimental design. The modified experimental design is summarized in Figure 7.4.

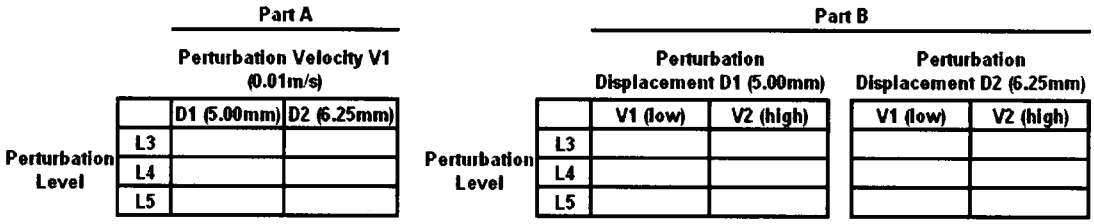

Figure 7.4 The revised experimental design excluding V3 and D3 perturbations

7.2 Electromyography

A summary of statistical probability values (p values) for each analysis is presented in Table 7.3. Statistically significant effects are denoted in this table by a double asterisk. The effect size, degrees of freedom, mean square error and statistic for each analysis are presented in Appendix D. The following sections describe only the significant main effects and interactions of each statistical test. All other statistical tests were not significant.

Table 7.3 Summary of statistical p values for Part A and B statistical tests. Statistically significant effects are denoted with **.

Part A (Velocity = V1)

Dependent Measure	"Average" RMS		Peak RMS		Time-to-peak RMS	
Independent Variable	Disp	Level	Disp	Level	Disp	Level
L3 deep	0.28	0.32	0.17	0.29	0.11	0.14
L3 superficial	0.15	0.38	0.1	0.46	0.01**	0.98
L4 deep	0.3	0.46	0.17	0.71	0.01**	0.48
L4 superficial	0.94	0.22	0.88	0.26	<0.001**	0.63
L5 deep	0.58	0.36	0.1	0.46	0.003**	0.07
L5 superficial	0.045**	0.33	0.23	0.34	0.1	0.38

Part B (Displacement = D1)

Dependent Measure	"Average" RMS		Peak RMS		Time-to-peak RMS	
Independent Variable	Vel	Level	Vel	Level	Vel	Level
L3 deep	0.006**	0.69	0.01**	0.83	Interaction =0.04**	
L3 superficial	0.63	0.39	0.75	0.43	<0.001**	0.77
L4 deep	0.08	0.56	0.047**	0.95	<0.001**	0.31
L4 superficial	0.3	0.39	0.15	0.34	<0.001**	0.3
L5 deep	0.47	0.37	0.12	0.48	<0.001**	0.048**
L5 superficial	0.18	0.21	0.16	0.26	<0.001**	0.18

Part B (Displacement = D2)

Dependent Measure	"Average" RMS		Peak RMS		Time-to-peak RMS	
Independent Variable	Vel	Level	Vel	Level	Vel	Level
L3 deep	0.01**	0.35	0.01**	0.33	<0.001**	0.89
L3 superficial	0.06	0.36	0.2	0.42	<0.001**	0.87
L4 deep	0.04**	0.58	0.04**	0.92	<0.001**	0.44
L4 superficial	0.18	0.36	0.14	0.38	<0.001**	0.82
L5 deep	0.02**	0.53	0.03**	0.81	<0.001**	0.17
L5 superficial	0.12	0.27	0.09	0.38	<0.001**	0.48

7.2.1 Part A: The effect of perturbation displacement

The "average" RMS 2x3 repeated measures ANOVA with independent variables displacement (D1, D2) and perturbation level (L3, L4, L5) produced a statistically significant effect of "average" RMS for the L5 superficial EMG recording electrode ($p=0.045$). This main effect indicated that "average" RMS increased with perturbation displacement in the L5 superficial fibres. The time-to-peak RMS 2x3 repeated measures ANOVA yielded significant main effects of perturbation displacement for the L3 superficial ($p=0.01$), L4 deep ($p=0.01$), L4 superficial ($p<0.001$) and L5 deep ($p=0.003$) electrodes. These main effects indicated that the time-to-peak RMS increased with increasing perturbation displacement. The mean time-to-peak RMS of all subjects was greater at D2 for every perturbation level in every EMG recording electrode. The "average" RMS, peak RMS and time-to-peak RMS collapsed across perturbation level are presented for each EMG recording site in Figure 7.5.

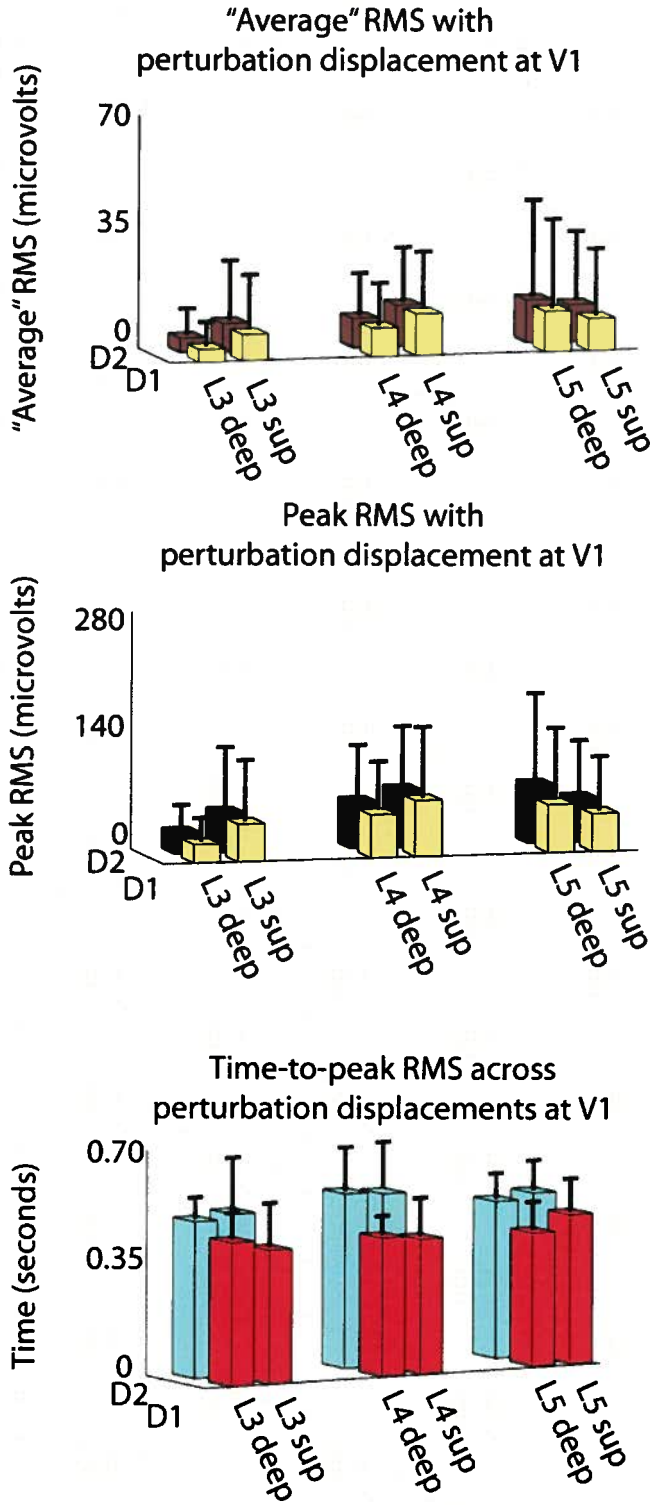

Figure 7.5 "Average" rms (top panel), peak rms (middle panel) and time-to-peak rms (bottom panel) for each EMG channel at D1 and D2 displacements. For comparison purposes, the "average" rms, peak rms and time-to-peak rms axes are consistent across Figures 7.5, 7.6, 7.7 and 7.8.

7.2.1 Part B: The effect of low and high perturbation velocities

The "average" RMS values of each EMG channel for low and high perturbation velocities during D1 and D2 perturbation displacements are displayed in Figure 7.6. The "average" RMS 2x3 repeated measures ANOVA at the D1 displacement produced a significant main effect of perturbation velocity in the L3 deep recording ($p=0.006$). This main effect indicated that in the L3 deep recording the "average" RMS increased with perturbation velocity. The "average" RMS 2x3 repeated measures ANOVA at the D2 displacement produced significant main effects of perturbation velocity in the L3 deep ($p=0.01$), L4 deep ($p=0.04$) and L5 deep ($p=0.02$) EMG recording electrodes. These main effects indicated that in deep multifidus recordings the "average" RMS increased with perturbation velocity.

Figure 7.7 displays the peak RMS of each EMG channel for low and high perturbation velocities during D1 and D2 perturbation displacements. The peak RMS 2x3 repeated measures ANOVA at the D1 displacement produced significant main effects in the L3 deep ($p=0.01$) and L4 deep EMG recordings ($p=0.047$). These main effects indicated that in the L3 and L4 deep recordings the peak RMS increased with perturbation velocity. The peak RMS 2x3 repeated measures ANOVA at the D2 displacement produced significant main effects of perturbation velocity in the L3 deep ($p=0.01$), L4 deep ($p=0.04$) and L5 deep ($p=0.03$) EMG recordings. These main effects indicated that in deep multifidus recording electrodes the peak RMS increased with perturbation velocity.

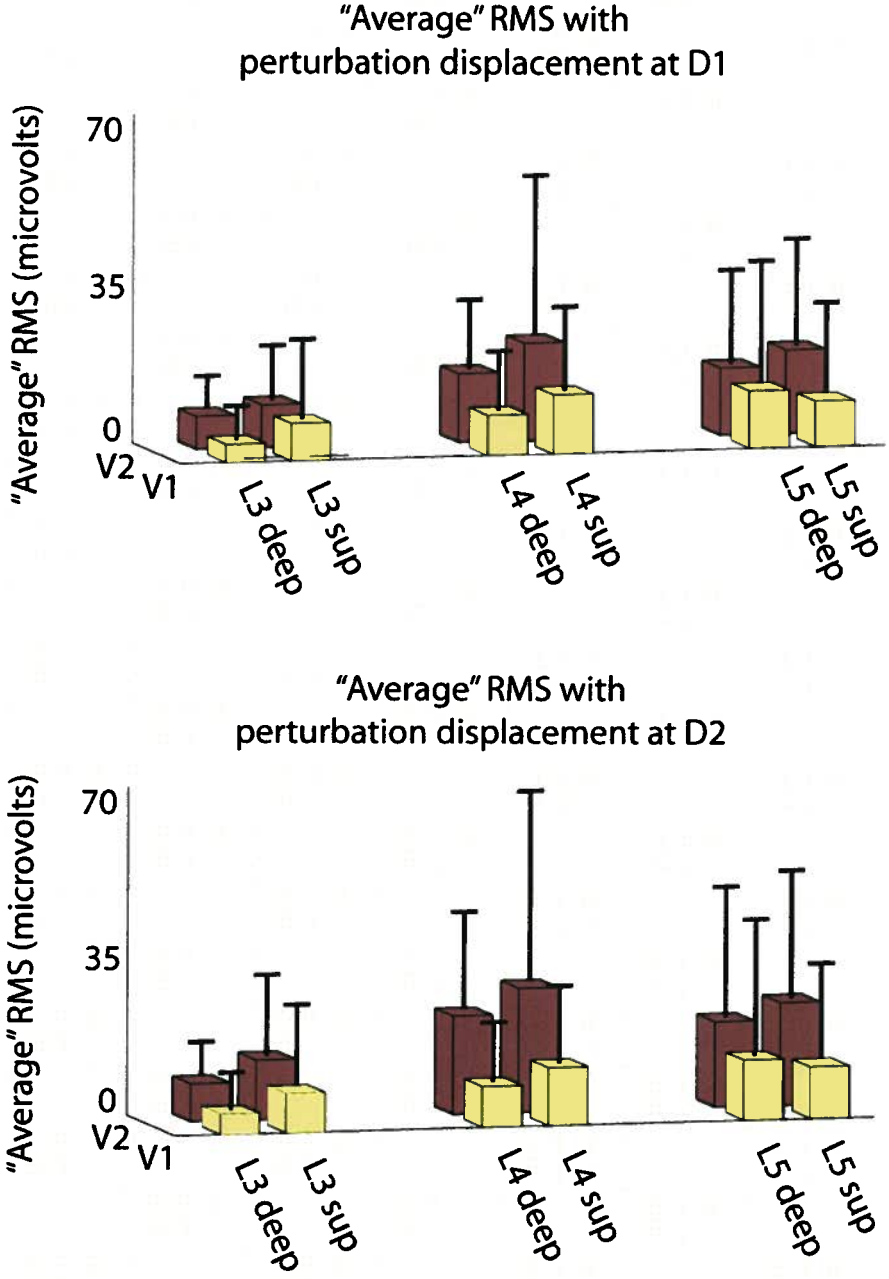

Figure 7.6 Part B: "Average" rms for D1 (top panel) and D2 (bottom panel) perturbation displacements. For comparison purposes, the "average" rms, peak rms and time-to-peak rms axes are consistent across Figures 7.5, 7.6, 7.7 and 7.8.

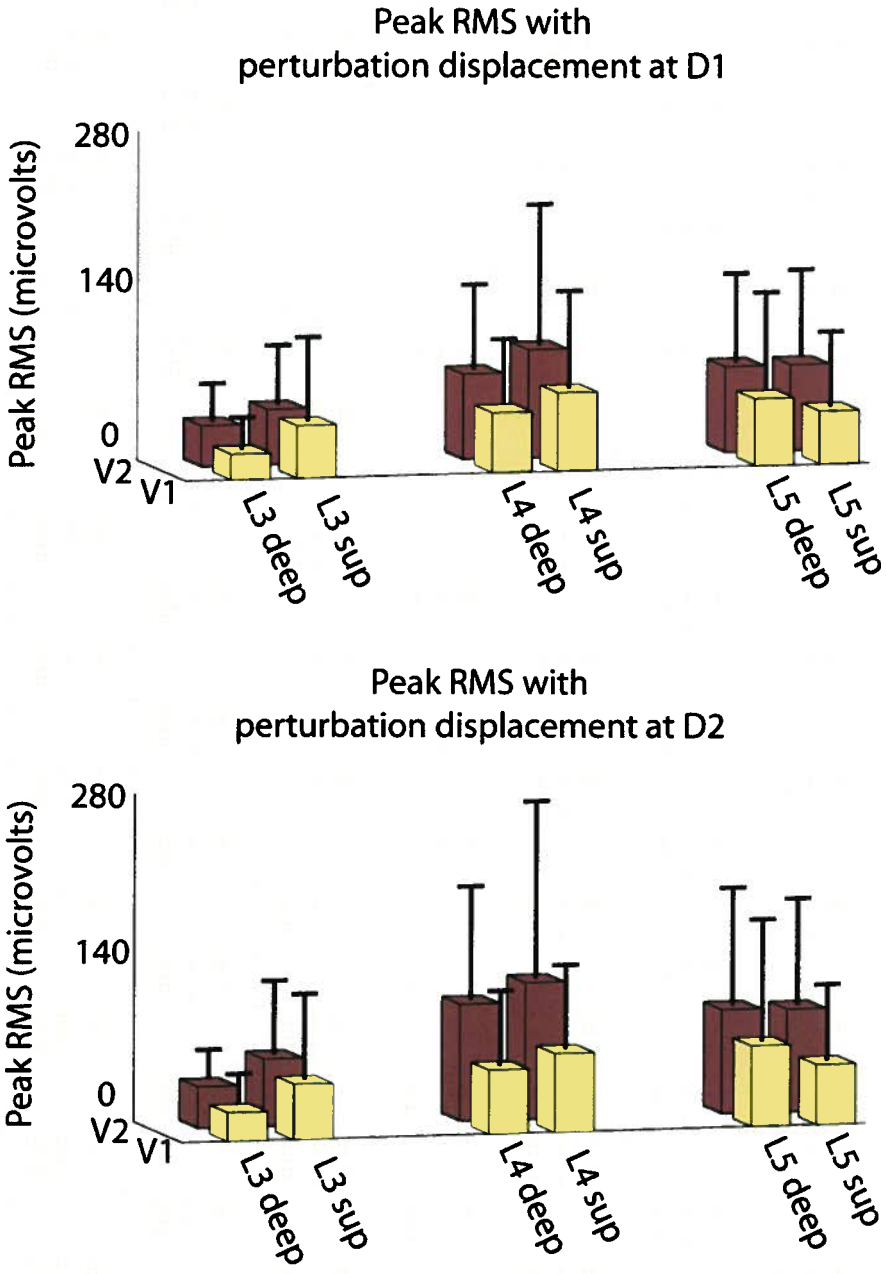

Figure 7.7 Part B: Peak rms for D1 (top panel) and D2 (bottom panel) perturbation displacements. For comparison purposes, the "average" rms, peak rms and time-to-peak rms axes are consistent across Figures 7.5, 7.6, 7.7 and 7.8.

The mean times-to-peak RMS at low and high perturbation velocities are displayed in Figure 7.8. The time-to-peak RMS 2x3 repeated measures ANOVA yielded significant main effects of perturbation velocity in all EMG recordings at the D1 and D2 displacements. There was a significant interaction between perturbation level and velocity at the D1 displacement in the L3 deep recording ($p=0.04$). Post-hoc Tukey test revealed that at each perturbation level there was a significant effect of perturbation velocity; however, there was only a statistically significant perturbation level difference between L3 and L4 at the low velocity ($p=0.02$). The time-to-peak RMS was significantly shorter at the L4 perturbation level relative to the L3 perturbation level at the low velocity. The main effects of perturbation velocity in all EMG recording sites indicated that the time-to-peak RMS decreased as perturbation velocity increased at both D1 and D2 displacements. There was a statistically significant main effect of perturbation level at the D1 displacement in the L5 deep recording ($p=0.048$). Post-hoc Tukey test indicated that the time-to-peak RMS was significantly shorter at the L5 perturbation level than at the L3 perturbation level at the low velocity ($p=0.04$).

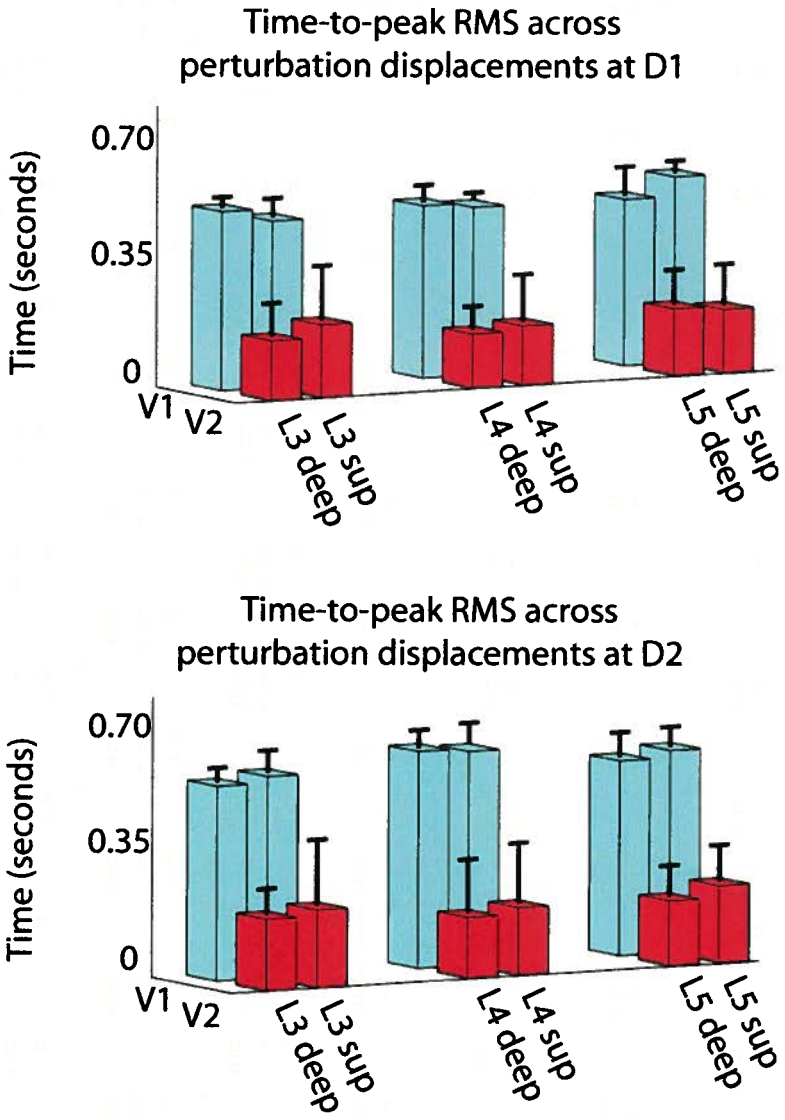

Figure 7.8 Part B: Time to peak rms for D1 (top panel) and D2 (bottom panel) perturbation displacements. For comparison purposes, the "average" rms, peak rms and time-to-peak rms axes are consistent across Figures 7.5, 7.6, 7.7 and 7.8.

8. Discussion

The overall findings were:

1. Perturbation displacement at the slowest velocity (V1) did not produce different "average" or peak RMS values for each EMG recording site. The exception to this trend was the "average" RMS of the L5 superficial EMG recording electrode which significantly increased with perturbation displacement. The time-to-peak RMS significantly decreased with increased perturbation displacement at all EMG recording sites except L3 deep and L5 superficial.
2. "Average" and peak RMS increased with perturbation velocity in the L3 deep recording electrode at D1 and all deep multifidus recording sites at D2. Peak RMS also increased with perturbation velocity in the L4 deep recording electrode at D1. Time-to-peak RMS significantly decreased with perturbation velocity in all EMG recording electrodes at both perturbation displacements (D1 and D2).
3. Perturbation level did not produce different "average" or peak RMS values for all analyses; however, perturbation level did produce statistically significant differences in the time-to-peak RMS at the D1 displacement. Time-to-peak RMS in the L5 deep electrode was shorter during D1 indentations to the L5 spinous process compared to the L3 spinous process. Additionally, time-to-peak RMS in the L3 deep electrode was shorter when V1-D1 indentations were applied to the L4 spinous process compared to the L3 spinous process.

This was the first study to record lumbar multifidus intramuscular EMG during posterior-anterior indentations to the skin overlying the lumbar spine of conscious humans. Intramuscular EMG responses to indentation loads have been previously reported in lumbar radiculopathy patients undergoing surgery (Colloca et al. 2003). Additionally, surface EMG has been recorded during posterior-anterior indentations to the skin overlying vertebral landmarks (Colloca and Keller 2001a; Colloca and Keller 2004) and during spinal manipulative therapy (Herzog et al. 1999; Symons et al. 2000). These studies allowed general comparisons to be made to the results of our study; however,

most previous studies applied indentation loads while participants were lying prone. The following paragraph provides an overview of the statistically significant results.

This study applied posterior-anterior indentation forces to participants in hyperextension to ensure anterior vertebral body translation (refer to section 6.5.1). During maximum trunk extension from upright standing, lumbar intervertebral joints extended (posterior sagittal rotation) approximately equal amounts (Lee et al. 2002; Wong et al. 2004). Maximal trunk extension also yielded horizontal intervertebral translations between adjacent vertebral bodies at L3, L4 and L5 (Kanayama et al. 1996). These vertebral movements during trunk extension may be similar to those experienced during posterior-anterior indentation forces. The application of a ten second posterior-anterior force (90-110N) to the skin overlying the L3, L4 or L5 spinous process produced concurrent lumbar vertebral extension at L3, L4 and L5 as measured by MRI (Powers et al. 2003). Lee and Evans (1997) applied a 150N posterior-anterior force to L4 producing an average of 10.2mm of skin surface movement, intervertebral extensions between 1.2-2.4 degrees and intervertebral translations of 2mm or less (Lee and Evans 1997). The apparent kinematic similarity between trunk extension and vertebral movement during posterior-anterior indentation suggests that the experimental position employed may have increased intervertebral translational prior to the perturbation. An experimental position with increased intervertebral translations may have resulted in specific perturbation displacements producing greater active or passive tissue stretch than the same depth of displacement would have produced in prone lying. This possibility necessitates caution when comparing specific posterior-anterior displacements in the hyperextended and prone lying positions.

8.1 Perturbation displacement

In the modified design (described in section 7.1.2), the effect of perturbation displacement on lumbar multifidus EMG was compared between the D1 and D2 displacements at the constant perturbation velocity of 0.01m/s (V1). We hypothesized that perturbation displacement would result in increased superficial fibre EMG activity and our result did not consistently support this hypothesis. "Average" RMS increased with perturbation displacement in the L5 superficial recording electrode, but no other perturbation displacement effects were noted. This may have been because the D1 and D2 displacements (separated by 1.25mm) were not sufficiently different enough to produce different EMG responses.

Pickar et al. (2007) acknowledged that indentation loads stretch paraspinal musculature only a fraction of the amount of the vertical indentation displacement. These authors modeled the stretch produced by one and two millimetre orthogonal displacements applied directly to feline lumbar vertebrae and concluded that these displacements only represented 0.17% and 0.35% stretch of a 50mm long paraspinal muscle (Pickar et al. 2007). Estimation of the amount of stretch applied to lumbar multifidus in the current study depended on the amount of displacement transferred through the skin to the spinous process as well as the length and orientation of lumbar multifidus fibres. As discussed above, a 150N indentation to the skin overlying the L4 spinous process produced an absolute skin displacement of 10.2mm, absolute vertebral displacements of 8.8-11.5mm and intervertebral translations of less than 2mm. The absolute displacement of the spinous process in the current study was difficult to estimate because displacement during the preload phase was not recorded and the nature of the relationship between intervertebral translations and perturbation force was not known. Regardless, perturbation force did not exceed 100N and thus it was assumed that even at the 6.25mm (D2) displacement intervertebral translations were likely less than 2 millimetres based on Lee and Evans' (1997) estimates. These intervertebral translations would have occurred orthogonal to the plane in which the muscles lie and using the cosine law a 2mm intervertebral translation would only produce a 16 micrometre stretch in a 119mm long

muscle (the length of the L3 superficial muscle fibre group as reported by (Hansen et al. 2006)). Additionally, the stretch produced by this intervertebral translation would have occurred within the muscle-tendon unit and the degree of stretch within the active multifidus fibres was unknown.

If the difference between perturbation displacements was sufficient to produce significantly different muscle stretches, increased perturbation displacement only increased the "average" RMS of L5 superficial multifidus fibres. This was the opposite result expected if muscle tension increased similarly in all superficial fibres. Superficial fibre groupings arising from the tip and shaft of the L4 spinous process and traversing the L5 vertebra to attach at the sacrum have been reported to have the largest physiological cross-sectional area (Hansen et al. 2006)). Superficial fibre recordings at the L5 vertebral level were likely within these fibres in most subjects because they make up the bulk of the superficial fibres at L5. Due to their larger cross-sectional area, these fibres produce greater tension than other superficial fibres with the same increase in muscle excitation. Consequently, L3 and L4 superficial fibres must receive a greater excitation increase to produce the same tension as a modest and possibly undetectable excitation increase in L5 superficial fibres. A significant increase in only the larger L5 superficial fibres implied that tension within these muscle fibres increased substantially relative to other multifidus fibres. This may have indicated that L5 superficial fibres behaved in a different manner than other superficial fibres, possibly related to their force producing capabilities. It must be noted that a larger muscle mass resulted in an EMG recording site that represented a smaller percentage of the muscle mass within the L5 superficial fibres. Nevertheless, with nine study participants it was assumed that EMG recording sites were different across participants and represented a random sample of muscle excitation. It was possible that deep and superficial lumbar multifidus excitation at other vertebral levels did not increase with perturbation displacement because other spinal structures resisted indentation loads. Passive spinal structures such as the anterior longitudinal ligament which resists lumbar extension (McGill 2007) and thoracolumbar fascia may have produced enough tension to make multifidus excitation unnecessary. Lumbar erector spinae muscle fibres also attach to lumbar vertebrae transverse processes and the ilium (Macintosh and Bogduk 1987) and

produce biomechanical extension moments about all lumbar vertebral levels (Bogduk et al. 1992).

The effect of posterior-anterior indentation displacement and force have produced mixed results in animal models (Colloca et al. 2006; Colloca et al. 2007; Pickar and Kang 2006; Pickar et al. 2007; Sung et al. 2005). Mean instantaneous frequency of feline paraspinal spindle afferents increased to a greater degree with one millimetre displacements compared to two millimetre displacements (Pickar et al. 2007). Sung et al. (2005) reported that half-sine wave loading profiles of increasing force magnitude at constant indentation duration did not produce significantly different mean instantaneous spindle frequencies in feline preparations. If indentation force and displacement were related in these preparations, larger posterior-anterior forces would produce larger displacements which did not appear to effect spindle discharge frequency. In an ovine preparation, forces of 20N, 40N and 60N at impulse durations of 100 milliseconds applied directly to spinous processes resulted in increased EMG responses with increased impulse force (Colloca et al. 2006; Colloca et al. 2007). Colloca et al. (2006) reported that greater forces resulted in increased EMG amplitudes as measured by the number of responses that exceeded peak-to-peak amplitudes of 1.5, 2.0 and 2.5 times baseline activity.

Collectively, animal model studies indicate that spindle afferent discharge may decrease or remain constant with perturbation displacement while muscular excitation increases. Detailed investigations of vertebral kinematics and models of lumbar multifidus muscle stretch during posterior-anterior indentations may clarify the effect of perturbation displacement on deep and superficial multifidus fibre excitation. Fortunately, the advent of ultrasonic indentation techniques (Kawchuk and Elliott 1998; Kawchuk et al. 2000; Kawchuk et al. 2001; Kawchuk et al. 2001; Kawchuk et al. 2006) to relate skin and spinous process movement during posterior-anterior indentations affords a method by which these vertebral movements can be assessed.

The time-to-peak RMS significantly increased with perturbation displacement in all but two multifidus recordings (L3 deep, L5 superficial). With perturbation velocity

constrained, displacement and velocity profiles for the D1 and D2 perturbation displacements were similar until the D1 perturbation displacement of 5.00mm was reached (Figure 8.1). Consequently, it was expected that the EMG responses would be similar until the D1 displacement was reached. The only kinematic event that would occur at a consistently longer latency between D1 and D2 perturbations would be the onset of the indentation hold phase. Longer times-to-peak RMS during D2 perturbations may indicate that peak RMS during D1 and D2 perturbations occurred at the onset of the indentation hold phase. This result suggests that even at the slow perturbation velocity peak muscle excitation occurred when there was a change in the velocity of muscle stretch.

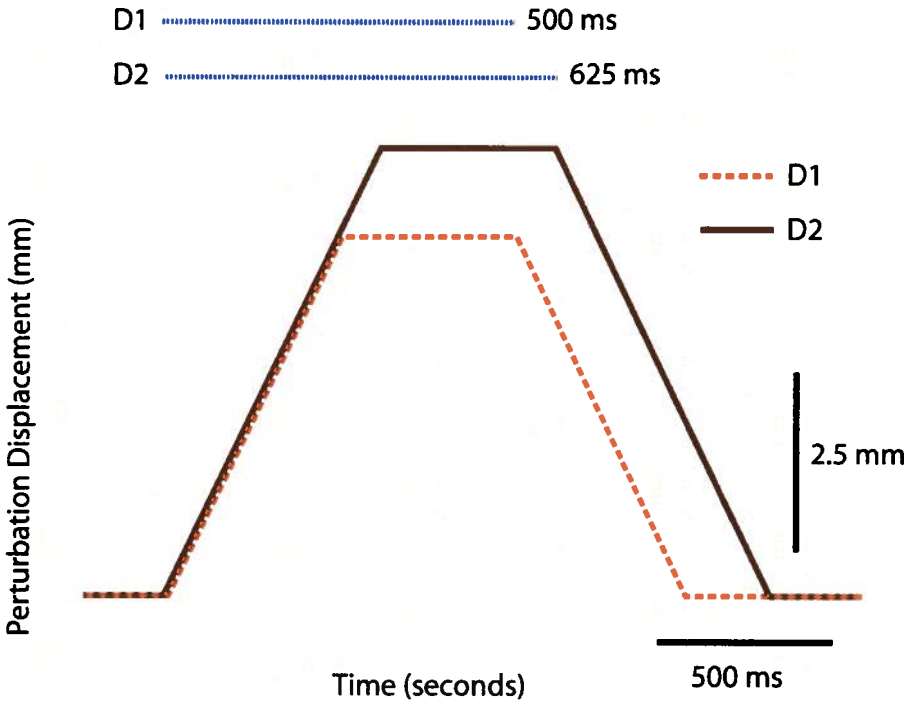

Figure 8.1 Indentation displacement during V1-D1 (orange dashed line) and V1-D2 (solid brown line) perturbation displacements across time. The dotted blue line at the top of the figure represents the length of the time interval between the onset of the active indentation phase and the end of the indentation hold phase.

In opposition to this view, the time interval between the onset of the active indentation phase and the end of the indentation hold phase was longer during D2 perturbations (625ms) relative to D1 perturbations (500ms). This is visually displayed by the dotted blue lines at the top of Figure 8.1. EMG responses were not always observed during V1 perturbations which may have resulted in peak RMS being chosen as the summation of different non-physiological electrical signals during some V1-D1 and V1-D2 indentations. If peak RMS was chosen in this manner, the location of peak RMS would be essentially random within the time interval over which peak RMS was calculated. Over many trials, the mean location of peak RMS would have tended toward the middle of the time interval between the onset of active indentation and the end of the indentation hold phase. This trend would have occurred for both V1-D1 and V1-D2 perturbations; however, because the time interval was longer for V1-D2 perturbations this would have resulted in longer times-to-peak RMS in the longer V1-D2 perturbations. Further analysis of the amplitude of the peak RMS values relative to baseline activity to determine if a response occurred would be required to substantiate or refute this possibility.

Time-to-peak RMS was not statistically significantly different between perturbation displacements at the L3 deep and L5 superficial recording sites. Lack of statistically significant differences did not mean that the times-to-peak RMS were the same; however, it suggested that if a difference existed, it was not as robust as in other multifidus fibres. As discussed above, L5 superficial lumbar multifidus fibres may have responded in a different manner to other superficial lumbar multifidus fibres.

8.2 Perturbation velocity

Higher perturbation velocities were generally observed to elicit greater EMG responses in most EMG channels as shown in Figures 7.6 and 7.7. Increased deep fibre EMG with perturbation velocity supported our deep fibre perturbation velocity hypothesis; however, the absence of a statistically significant increase in superficial fibre EMG activity did not support our superficial fibre velocity hypothesis. Differential velocity effects on deep and superficial fibres may have been due to differences in the magnitude and velocity of

stretch applied to deep and superficial fibres. Deep fibres span two or fewer vertebral segments while superficial fibres span three to five vertebral segments (Macintosh et al. 1986). If sarcomere lengths in deep and superficial fibres are similar, orthogonal displacements of deep and superficial fibre attachments may have produced greater relative musculotendinous stretch in deep multifidus fibre groupings. Greater relative stretch would have occurred because deep fibre groupings have shorter total distances between origin and insertion and experience greater angular deviations in response to indentations. Increased relative stretch of deep fibre muscle and tendon in the same time interval as lesser stretches in superficial fibre muscle and tendon would have resulted in greater deep fibre lengthening velocities. An abstract model of the different stretches produced in superficial and deep fibres is presented in Figure 8.2. The orthogonal displacement of the perturbed vertebra with each indentation rod displacement was unknown. Despite the orthogonal displacement being unknown, deep and superficial fibres attach to the vertebra at specific landmarks and thus their muscular attachments experienced the same orthogonal displacement.

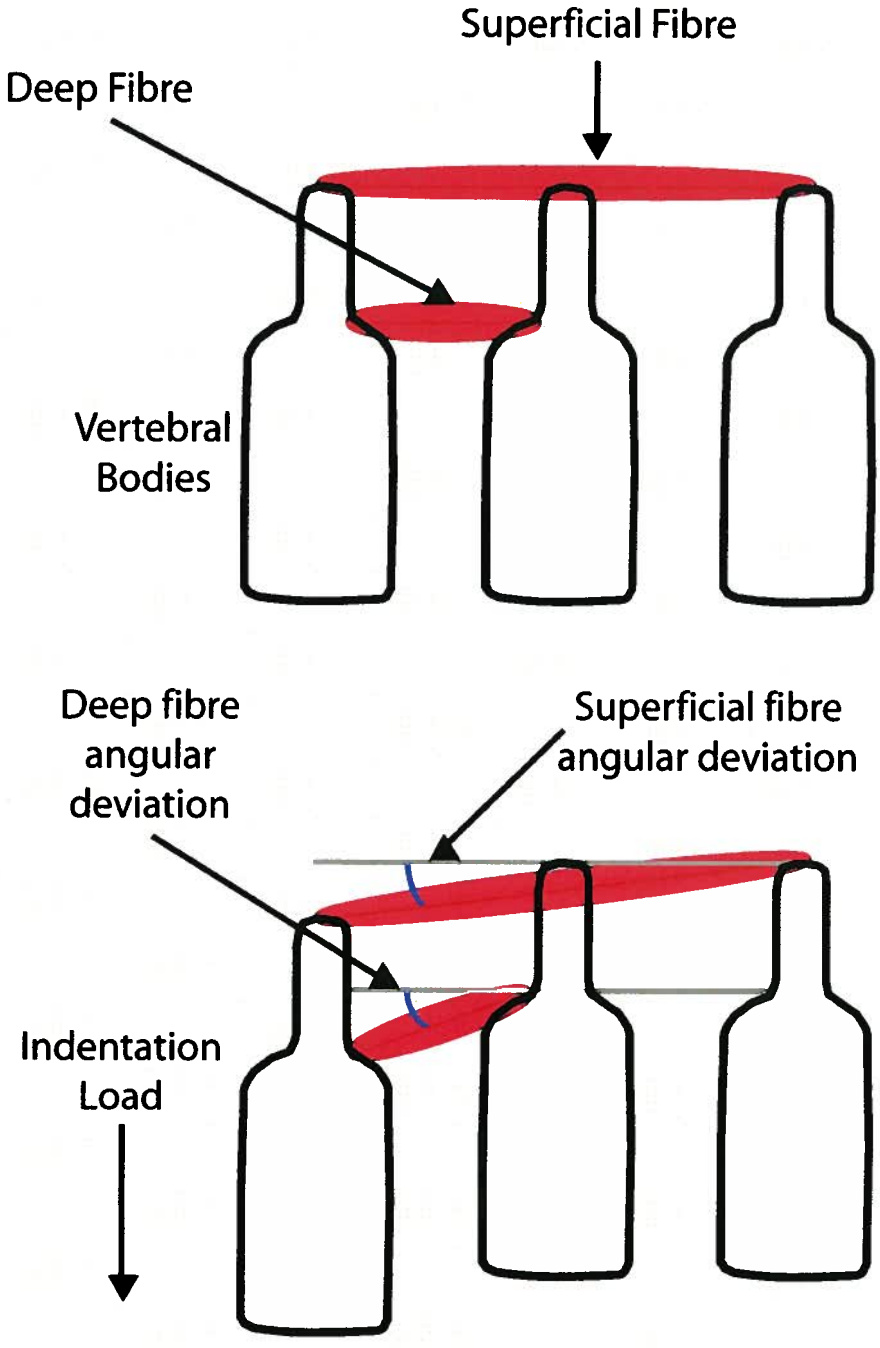

Figure 8.2 Conceptualized three vertebrae model of the relative stretch within the shorter deep lumbar multifidus fibres and longer superficial multifidus fibres. As the indentation load displaces the vertebral body, superficial and deep fibre attachments experience the same orthogonal displacement. Deep fibres experience a greater relative stretch and larger angular deviation than superficial fibres.

Half-sine wave impulses to feline lumbar vertebrae appear to have a threshold impulse duration at which spindle afferent discharge increases significantly and exponentially with decreasing impulse duration (Pickar and Kang 2006). The existence of a similar threshold in humans may have explained the differential EMG response of superficial and deep fibres to identical orthogonal indentations. This threshold may have been reached earlier in deep fibres than superficial fibres during posterior-anterior indentations and at lesser total orthogonal indentation velocities. With only two perturbation velocity levels, this design was not able to determine the perturbation velocity at this hypothetical "response threshold" or the relationship between EMG responses and velocity after this "threshold". We can not exclude the possibility that sensory receptors other than muscle spindle afferents are modulating or contributing to the EMG responses observed.

At the shallow perturbation displacement (D1), L5 deep multifidus fibres did not produce statistically significant differences in "average" RMS or peak RMS between low and high perturbation velocities. As discussed in section 2.1.3, posterior-anterior trunk stiffness of individual vertebrae to static and cyclic indentation loads increases with decreasing vertebral level (Lee and Liversidge 1994). Posterior-anterior trunk stiffness in response to indentation loads at the L5 spinous process is greater than in response to indentation loads at L3 and L4 spinous processes (Lee and Liversidge 1994). Increased stiffness may have resulted in less vertebral displacement at this vertebral level despite a constant indentation displacement at the skin surface. This was because if indentation stiffness at L5 was greater than other vertebral levels then greater compression of tissue between the L5 spinous process and skin may have occurred. During D1 perturbations, L5 deep fibres spanning the L5/S1 joint and attaching to the sacrum may not have been stretched enough to generate EMG responses during perturbations to L3, L4 or L5 spinous processes. It is also important to remember that peak velocities during V2-D2 perturbations were larger than V1-D1 perturbations due to longer time intervals over which the motor could accelerate at the D2 displacement.

The time-to-peak RMS decreased significantly with increasing perturbation velocity at both D1 and D2 perturbation displacements (Figure 7.8). This occurred for both

superficial and deep fibres despite the lack of a statistically significant increase in superficial fibre "average" or peak RMS with perturbation velocity. Higher perturbation velocities resulted in greater indentation displacements being reached earlier relative to perturbation onset. There may also have been a lag between the initiation of indentation and the onset of vertebral displacement due to compression of soft tissue between the indentation rod and vertebral spinous process. Higher velocity indentations may have decreased the latency of this 'soft tissue compression' lag and resulted in earlier vertebral displacement relative to lower velocity indentations. The total length of the combined active indentation and indentation hold phase over which this variable was calculated was also shorter during higher velocity perturbations due to the decreased length of the active indentation phase. Therefore, if perturbations did not elicit EMG responses in deep or superficial fibres, peak RMS would have been a summation of non-physiological electrical activity. Over many trials, the location of peak RMS would have tended toward the middle of time interval which would have been earlier in higher velocity perturbations. Peak RMS of deep fibres significantly increased with perturbation velocity and thus we can assume that at minimum, EMG responses to indentations consistently occurred in deep fibres at higher perturbation velocities.

Time-to-peak RMS changes may have also been a function of posterior-anterior stiffness changes with increased perturbation velocity. Cyclic posterior-anterior indentation loads of higher frequency (1-2Hz) have been reported to result in higher posterior-anterior trunk stiffness than lower frequency and quasi-static loads (loads applied over a twenty second interval) (Lee and Svensson 1993; Squires et al. 2001). These authors reasoned that this was due to the viscous behaviour of skin, ligaments, tendons, muscles and intervertebral discs (Lee and Svensson 1993; Squires et al. 2001). Higher perturbation velocities may have resulted in stiffness changes due to the viscosity of these tissues which changed the temporal relationship of kinematic events resulting in a shorter time-to-peak RMS.

In the context of the hypothetical "response threshold" paradigm, deep fibre peak RMS may have occurred earlier at higher indentation velocities because the "response

threshold" was not reached during low velocity perturbations. The "response threshold" may have also occurred earlier during high velocity perturbations due to decreased latencies between indentation initiation and vertebral displacement. Deep fibre time-to-peak RMS may have also decreased because of greater perturbation displacements being reached earlier at low velocity perturbations. Further analysis of the relationship between indentation initiation and vertebral displacement as well as the prevalence of EMG responses at each perturbation velocity would have been required to clarify interpretation of the decreased time-to-peak RMS.

8.3 Perturbation level

The results of the current study did not support the existence of segmental multifidus responses to posterior-anterior indentations. The "average" RMS and peak RMS were not statistically different between perturbation levels in all EMG channels for all analyses. In line with our results, intersegmental reflexes up to two vertebral levels rostral and caudal have been reported with electrical stimulation of medial dorsal ramus afferent pathways (Kang et al. 2002). This finding implies that regardless of the indentation location used in this study, the EMG response as measured by "average" RMS and peak RMS was the same in each of the deep and superficial fibres at L3, L4 and L5. This result may have been expected if no EMG response was produced by the indentation; however, it occurred for all analyses at all perturbation displacements and velocities. This result may have also been anticipated in deep lumbar multifidus fibres if they function as stabilizers, yet occurred in both superficial and deep fibres at all vertebral levels recorded. These results supported our hypothesis that similar EMG responses would be observed at adjacent vertebral segments.

A limitation of not measuring vertebral kinematics is that we were unable to quantify the amount of adjacent intersegmental motion during these segmental perturbations. Keller et al. (2003) applied posterior-anterior loads to the L2 spinous process of low back surgical patients at forces between 30-150N. These authors observed posterior-anterior and axial acceleration responses in the adjacent L3/L4 intervertebral joint as measured by bone

pins (Keller et al. 2003). In the current study, EMG activity at adjacent vertebral segments may have occurred in response to adjacent intersegmental motion rather than intersegmental spinal reflexes.

The time-to-peak RMS across perturbation levels may have provide insight into the likelihood of adjacent intersegmental motion as this motion would have likely occurred at a delayed latency with respect to the perturbed vertebra. If intersegmental motion occurred, the latency of EMG responses at adjacent segments would have likely been longer than at the perturbed segment. Time-to-peak RMS was significantly shorter in the L5 deep recording when D1 perturbations were delivered to the L5 spinous process compared to the L3 spinous process. This result was consistent with the expectation that perturbations to the L5 spinous process caused L3/L4 intersegmental motion at a delayed latency. L3/L4 intersegmental motion may have occurred if passive or active structures exerted forces on the L4 vertebrae due to the L5 indentation perturbation. Despite this possibility, the overall lack of differences in the time-to-peak RMS across perturbation velocities and displacements indicated that this measure may not have been sensitive enough to expose latency differences.

It was also not possible to determine whether EMG electrodes in superficial fibres were located in the same muscle fascicles. Superficial fibres from L3, L4 and L5 span the lower lumbar spine and attach to the sacrum and ilium (Macintosh et al. 1986), thus EMG electrodes inserted into these superficial fibres may have been located in the same fibre groupings. This possibility may explain the lack of a significant perturbation level effect in superficial fibres, yet perturbation level effects were also not consistently observed in deep lumbar multifidus fibres. Additionally, differences were noted between superficial fibre groupings with perturbation displacement (described in section 8.1) which opposed this possibility.

8.4 Limitations and trial exclusions

Revising the experimental design was necessary after examination of indentation rod kinematics. This study highlights the need of posterior-anterior trunk indentation studies to validate their perturbation parameters. Our attempted validation of these parameters revealed that slow velocity, deep displacement indentations (V1-D3) did not reach their maximum displacement in all subjects. Maximum displacement was not reached in three subjects at L3, four subjects at L4 and seven subjects at L5 due to perturbation force exceeding 100N. Stiffness to posterior-anterior indentations increases with decreasing vertebral level (Lee and Liversidge 1994) and hence fewer subjects reached maximum displacement at lower perturbation levels. This was only observed at the slowest movement velocity (V1) because the latency between full indentation displacement and the feedback response from low back tissue to the motor controller may have been too long for online corrective motion to occur before full displacement at V2 and V3.

Perturbation velocity profiles of the low (V1) and high (V2) velocities (displayed in Figure 7.3) were appreciably different because acceleration at each velocity was the same. Whether velocity or acceleration should be constrained during posterior-anterior perturbations is debatable as the precise biomechanical and neurophysiological mechanisms governing muscle responses to these perturbations are not known. Pickar and colleagues (Pickar 1999; Pickar and Kang 2006; Pickar and Wheeler 2001; Pickar et al. 2007) have employed half-sine wave displacement profiles during perturbations to feline lumbar vertebrae. Displacement, velocity and acceleration profiles are similar with each displacement-time perturbation combination, yet perturbation velocities and accelerations would have been different for each combination and would have changed throughout the perturbation.

The force limit of 100N was significantly less than typically experienced during posterior-anterior indentation loads. The Activator Adjusting Instrument used by Colloca, Keller and colleagues (Keller et al. 1999) produces maximum forces of 150N while Pickar and colleagues have applied indentation loads up to 100% body weight in their

feline preparation (Kang et al. 2002; Pickar and Kang 2006; Sung et al. 2005). The results of this study are only applicable at indentation forces up to 100N as stiffness responses may increase exponentially as intervertebral joint motion continues into the "elastic zone" (Panjabi 1992b). Increased joint stiffness may alter EMG responses making extrapolation of these results to larger forces invalid. These results are also not directly applicable to spinal manipulation therapy techniques employed in chiropractic therapy. During chiropractic HVLA thrusts to the lumbar spine and sacroiliac joint, peak impulse forces exceeded 500N (Triano and Schultz 1997). This peak impulse force represented a resultant force; however, the posterior-anterior component of this force was estimated to be approximately 300N (Triano and Schultz 1997) and was significantly larger than the maximum force delivered to participants in this study. The contact area of typical spinal manipulation impulses applied by a full-time clinician increased with impulse force while the point of peak pressure moved an average of 9.8mm (SD=9.4mm) (Herzog et al. 2001). The experimental protocol of the current study ensured that force was consistently applied through the contact surface; however, center of pressure movement within this contact surface may have occurred.

Force profiles were also different between perturbations of differing velocity. This was not surprising because differing rates of displacement would likely have resulted in different rates of force development. The most notable force profile difference other than rate of loading appeared to be the double peak generally observed in higher velocity perturbations near the cessation of the active indentation phase (see Figure 7.1b). As the indentation rod displaced anteriorly, active and passive spinal tissues were displaced in an anterior direction. At the cessation of indentation rod displacement, the momentum of the spinal structures being perturbed may have caused further anterior displacement before active contraction or passive stretch accelerated these tissues posteriorly. The anterior momentum of the lumbar spine generated by the indentation may have resulted in a local force minimum just after the active indentation phase due to the lumbar spine continuing to move anterior while the indentation rod stopped. This local force minimum would have caused the observed double peak in the force profile at the end of the active indentation phase. Close examination of the latency between EMG onset and the initial

upward deflection of the second force peak may have determined if active multifidus contraction provided all or part of the restorative force needed to accelerate the lumbar spine posteriorly. Perturbations at lung volumes other than the end of normal expiration normally resulted in the 100N force limit being exceeded. This observation supported the contention that trunk stiffness to posterior-anterior forces increased as lung volume increased or decreased from functional residual capacity (Shirley et al. 2003). Consequently, the results of this study are only valid during perturbations at the end of normal expiration.

8.5 Clinical implications

The possibility of a mechanical "response threshold" after which afferent and efferent pathways increase neural activity may be of clinical interest to the controversy surrounding lumbar stability. If the deep and superficial lumbar multifidus fibres are excited differentially due to differential timing of biomechanical thresholds, time-based EMG onset comparisons may not be optimal to determine differences in the functional role of these fibres. Frequency-based coherence analysis may be more useful to determine whether neural signals exciting deep and superficial fibres arise from the same or different neural structures. This is not to say that reports of differential multifidus excitation based on EMG onset latencies are invalid (Moseley et al. 2002; Moseley et al. 2003) as the experimental task and descending motor control in the current study was quite different. Moseley and colleagues (Moseley et al. 2002; Moseley et al. 2003) studied differential control during whole body movements requiring postural stability which most likely involved neural signals from supraspinal structures. The current study investigated multifidus excitation to segmental perturbations which may have been generated by neural circuitry within the spinal cord.

The results of the current study attest to the need to understand vertebral kinematics and excitation mechanisms during segmental and gross whole body movements. This need can be emphasized if we assume for the moment that a mechanical "response threshold" existed whereby multifidus excitation increased through supraspinal pathways. In the

unpredictable and predictable bucket experiment performed by Moseley et al. (2003) (described in section 2.3.2), subjects may have made slight postural adjustments prior to the weight dropping in the bucket during predictable perturbations. The impulse delivered to participants during predictable and unpredictable perturbations was the same; however, these adjustments may have been made to reduce the peak force of the external trunk perturbation while increasing the impulse duration. Increasing impulse duration may have resulted in a longer latency between "response thresholds" being reached in the deep and superficial fibres by increasing the time between vertebral kinematic events. This hypothetical example is purely speculative, yet may warrant further analysis of the existence and possible neural pathways of differential "response thresholds" in deep and superficial fibres.

If the differential multifidus fibre responses were due to different motor control strategies, then the current study suggests the opposite relationship between deep and superficial fibres to that contended by proponents of the 'drawing in' technique. Deep multifidus fibre EMG activity increased with perturbation velocity while superficial fibre EMG activity responded in a similar manner across perturbation displacements and velocities. This result opposes the view that deep multifidus fibres stabilize the spine while superficial fibres act as prime movers and respond to the different reactive forces imposed on the trunk. This is clinically significant because if deep fibres act as lumbar spine prime movers and restore vertebral position then they would be expected to increase their excitation response with increased perturbation magnitude. This may require clinical lumbar stability programs to focus on context-dependent excitation of these deep fibres rather than tonic co-contraction with transversus abdominus, as is mandated by the 'drawing in' technique.

9. Conclusion

Clinicians have used lumbar stability techniques in LBP rehabilitation programs as a method of relieving LBP and preventing initial or further injury. A specific lumbar stability technique, abdominal 'drawing in', requires tonic contraction of the deep multifidus fibres while superficial fibres are to remain inactive. Evidence of differential excitation to deep and superficial fibres has been reported, however, recent studies of the deep and superficial activity in the cervical and thoracic spine have disputed this evidence. The results of this study supported the hypothesis that deep and superficial fibres are differentially excited; however, the opposite pattern of differential activity was found. Deep multifidus fibres increased muscle excitation with increasing perturbation magnitude, while the same perturbations did not result in increased superficial fibre excitation. This differential effect may have been related to different mechanical thresholds being achieved in deep and superficial fibres because of their differing anatomy and geometric orientations. The segmental perturbations employed by this study are not directly applicable to whole body stability tasks, yet call attention to the need to understand vertebral kinematics and their resulting effects on lumbar multifidus fibres. A greater understanding of the biomechanical effects of different trunk movements on muscle architecture is important to maximize the potential of lumbar stability training programs to rehabilitate lumbar segmental instability or low back injury. Future research investigating concurrent superficial and deep multifidus electromyography and intervertebral movement is required to determine whether deep and superficial fibres have the capability to function differentially during lumbar stability tasks.

10. References

Amonoo-Kuofi HS. The density of muscle spindles in the medial, intermediate and lateral columns of human intrinsic postvertebral muscles. J Anat 136: Pt 3: 509-519, 1983.

Anderson CK, Chaffin DB, Herrin GD and Matthews LS. A biomechanical model of the lumbosacral joint during lifting activities. J Biomech 18: 8: 571-584, 1985.

Andersson EA, Grundstrom H and Thorstensson A. Diverging intramuscular activity patterns in back and abdominal muscles during trunk rotation. Spine 27: 6: E152-60, 2002.

Andersson EA, Oddsson LI, Grundstrom H, Nilsson J and Thorstensson A. EMG activities of the quadratus lumborum and erector spinae muscles during flexion-relaxation and other motor tasks. Clin Biomech (Bristol, Avon) 11: 7: 392-400, 1996.

Andersson GB. Epidemiological features of chronic low-back pain. Lancet 354: 9178: 581-585, 1999.

Arokoski JP, Valta T, Airaksinen O and Kankaanpaa M. Back and abdominal muscle function during stabilization exercises. Arch Phys Med Rehabil 82: 8: 1089-1098, 2001.

Barker PJ, Guggenheimer KT, Grkovic I, Briggs CA, Jones DC, Thomas CD and Hodges PW. Effects of tensioning the lumbar fasciae on segmental stiffness during flexion and extension: Young Investigator Award winner. Spine 31: 4: 397-405, 2006.

Bartelink DL. The role of abdominal pressure in relieving the pressure on the lumbar intervertebral discs. J Bone Joint Surg Br 39-B: 4: 718-725, 1957.

Bergmark A. Stability of the lumbar spine. A study in mechanical engineering. Acta Orthop Scand Suppl 230: 1-54, 1989.

Bexander CS, Mellor R and Hodges PW. Effect of gaze direction on neck muscle activity during cervical rotation. Exp Brain Res 167: 3: 422-432, 2005.

Blouin JS, Inglis JT and Siegmund GP. Auditory startle alters the response of human subjects exposed to a single whiplash-like perturbation. Spine 31: 2: 146-154, 2006.

Blouin JS, Siegmund GP, Carpenter MG and Inglis JT. Neural control of superficial and deep neck muscles in humans. J Neurophysiol 98: 2: 920-928, 2007.

Bogduk N. Innervation and pain patterns of the lumbar spine. In: Physical therapy of the low back, edited by Twomey L and Taylor JR. New York: Churchill Livingstone, 2000a, chapt. 3, p. 93-93-104.

Bogduk N. The lumbar muscles and their fascia. In: Physical therapy of the low back, edited by Twomey L and Taylor JR. New York: Churchill Livingstone, 2000b, chapt. 4,. 105-105-139.

Bogduk N. The innervation of the lumbar spine. Spine 8: 3: 286-293, 1983.

Bogduk N. A reappraisal of the anatomy of the human lumbar erector spinae. J Anat 131: Pt 3: 525-540, 1980.

Bogduk N and Macintosh JE. The applied anatomy of the thoracolumbar fascia. Spine 9: 2: 164-170, 1984.

Bogduk N, Macintosh JE and Pearcy MJ. A universal model of the lumbar back muscles in the upright position. Spine 17: 8: 897-913, 1992.

Brown JM, Solomon C and Paton M. Further evidence of functional differentiation within biceps brachii. Electromyogr Clin Neurophysiol 33: 5: 301-309, 1993.

Brown SH and McGill SM. How the inherent stiffness of the in vivo human trunk varies with changing magnitudes of muscular activation. Clin Biomech (Bristol, Avon) 23: 1: 15-22, 2008.

Brumagne S, Cordo P, Lysens R, Verschueren S and Swinnen S. The role of paraspinal muscle spindles in lumbosacral position sense in individuals with and without low back pain. Spine 25: 8: 989-994, 2000.

Cherkin DC, Deyo RA, Loeser JD, Bush T and Waddell G. An international comparison of back surgery rates. Spine 19: 11: 1201-1206, 1994.

Cholewicki J and McGill SM. Mechanical stability of the in vivo lumbar spine: implications for injury and chronic low back pain. Clin Biomech (Bristol, Avon) 11: 1: 1-15, 1996.

Cholewicki J, Panjabi MM and Khachatryan A. Stabilizing function of trunk flexor-extensor muscles around a neutral spine posture. Spine 22: 19: 2207-2212, 1997.

Cholewicki J and VanVliet JJ,4th. Relative contribution of trunk muscles to the stability of the lumbar spine during isometric exertions. Clin Biomech (Bristol, Avon) 17: 2: 99-105, 2002.

Colloca CJ and Keller TS. Active trunk extensor contributions to dynamic posteroanterior lumbar spinal stiffness. J Manipulative Physiol Ther 27: 4: 229-237, 2004.

Colloca CJ and Keller TS. Electromyographic reflex responses to mechanical force, manually assisted spinal manipulative therapy. Spine 26: 10: 1117-1124, 2001a.

Colloca CJ and Keller TS. Stiffness and neuromuscular reflex response of the human spine to posteroanterior manipulative thrusts in patients with low back pain. J Manipulative Physiol Ther 24: 8: 489-500, 2001b.

Colloca CJ, Keller TS and Gunzburg R. Biomechanical and neurophysiological responses to spinal manipulation in patients with lumbar radiculopathy. J Manipulative Physiol Ther 27: 1: 1-15, 2004.

Colloca CJ, Keller TS and Gunzburg R. Neuromechanical characterization of in vivo lumbar spinal manipulation. Part II. Neurophysiological response. J Manipulative Physiol Ther 26: 9: 579-591, 2003.

Colloca CJ, Keller TS, Harrison DE, Moore RJ, Gunzburg R and Harrison DD. Spinal manipulation force and duration affect vertebral movement and neuromuscular responses. Clin Biomech (Bristol, Avon) 21: 3: 254-262, 2006.

Colloca CJ, Keller TS, Moore RJ, Gunzburg R and Harrison DE. Effects of disc degeneration on neurophysiological responses during dorsoventral mechanical excitation of the ovine lumbar spine. J Electromyogr Kinesiol 2007.

Conway PJ, Herzog W, Zhang Y, Hasler EM and Ladly K. Forces required to cause cavitation during spinal manipulation of the thoracic spine. Clin Biomech (Bristol, Avon) 8: 210-214, 1993.

Coyte PC, Asche CV, Croxford R and Chan B. The economic cost of musculoskeletal disorders in Canada. Arthritis Care Res 11: 5: 315-325, 1998.

Cresswell AG, Grundstrom H and Thorstensson A. Observations on intra-abdominal pressure and patterns of abdominal intra-muscular activity in man. Acta Physiol Scand 144: 4: 409-418, 1992.

Cresswell AG, Oddsson L and Thorstensson A. The influence of sudden perturbations on trunk muscle activity and intra-abdominal pressure while standing. Exp Brain Res 98: 2: 336-341, 1994.

Crisco JJ,3rd and Panjabi MM. Euler stability of the human ligamentous lumbar spine: Part I. Theory Clin Biomech 7: 19-20-26, 1992.

Crisco JJ,3rd, Panjabi MM, yamamoto i and oxland tr. Euler stability of the human ligamentous lumbar spine: Part II. Experiment. Exp Clin Biomech 7: 26-26-32, 1992.

Croft PR, Macfarlane GJ, Papageorgiou AC, Thomas E and Silman AJ. Outcome of low back pain in general practice: a prospective study. BMJ 316: 7141: 1356-1359, 1998.

Daggfeldt K and Thorstensson A. The mechanics of back-extensor torque production about the lumbar spine. J Biomech 36: 6: 815-825, 2003.

Dankaerts W, O'Sullivan P, Burnett A and Straker L. Altered patterns of superficial trunk muscle activation during sitting in nonspecific chronic low back pain patients: importance of subclassification. Spine 31: 17: 2017-2023, 2006.

Danneels LA, Coorevits PL, Cools AM, Vanderstraeten GG, Cambier DC, Witvrouw EE and De CH. Differences in electromyographic activity in the multifidus muscle and the iliocostalis lumborum between healthy subjects and patients with sub-acute and chronic low back pain. Eur Spine J 11: 1: 13-19, 2002.

Demoulin C, Crielaard JM and Vanderthommen M. Spinal muscle evaluation in healthy individuals and low-back-pain patients: a literature review. Joint Bone Spine 74: 1: 9-13, 2007.

Descarreaux M, Blouin JS and Teasdale N. Repositioning accuracy and movement parameters in low back pain subjects and healthy control subjects. Eur Spine J 14: 2: 185-191, 2005.

Descarreaux M, Blouin JS and Teasdale N. Force production parameters in patients with low back pain and healthy control study participants. Spine 29: 3: 311-317, 2004.

Dimitrijevic MR, Gregoric MR, Sherwood AM and Spencer WA. Reflex responses of paraspinal muscles to tapping. J Neurol Neurosurg Psychiatry 43: 12: 1112-1118, 1980.

Donisch EW and Basmajian JV. Electromyography of deep back muscles in man. Am J Anat 133: 1: 25-36, 1972.

Drake RL. Gray's anatomy for students. Philadelphia: Elsevier/Churchill Livingstone, 2005, p. 1058.

Ebenbichler GR, Oddsson LI, Kollmitzer J and Erim Z. Sensory-motor control of the lower back: implications for rehabilitation. Med Sci Sports Exerc 33: 11: 1889-1898, 2001.

Floyd WF and Silver PH. The function of the erectores spinae muscles in certain movements and postures in man. J Physiol 129: 1: 184-203, 1955.

Floyd WF and Silver PH. Function of erectores spinae in flexion of the trunk. Lancet 1: 3: 133-134, 1951.

Frymoyer JW, Pope MH, Clements JH, Wilder DG, MacPherson B and Ashikaga T. Risk factors in low-back pain. An epidemiological survey. J Bone Joint Surg Am 65: 2: 213-218, 1983.

Gal J, Herzog W, Kawchuk G, Conway PJ and Zhang YT. Movements of vertebrae during manipulative thrusts to unembalmed human cadavers. J Manipulative Physiol Ther 20: 1: 30-40, 1997.

Gardner-Morse M, Stokes IA and Laible JP. Role of muscles in lumbar spine stability in maximum extension efforts. J Orthop Res 13: 5: 802-808, 1995.

Ge W, Long CR and Pickar JG. Vertebral position alters paraspinal muscle spindle responsiveness in the feline spine: effect of positioning duration. J Physiol 569: Pt 2: 655-665, 2005.

Geisser ME, Ranavaya M, Haig AJ, Roth RS, Zucker R, Ambroz C and Caruso M. A meta-analytic review of surface electromyography among persons with low back pain and normal, healthy controls. J Pain 6: 11: 711-726, 2005.

Goel VK, Wilder DG, Pope MH and Edwards WT. Biomechanical testing of the spine. Load-controlled versus displacement-controlled analysis. Spine 20: 21: 2354-2357, 1995.

Gracovetsky S, Farfan HF and Lamy C. A mathematical model of the lumbar spine using an optimized system to control muscles and ligaments. Orthop Clin North Am 8: 1: 135-153, 1977.

Granata KP and England SA. Stability of dynamic trunk movement. Spine 31: 10: E271-6, 2006.

Grenier SG and McGill SM. Quantification of lumbar stability by using 2 different abdominal activation strategies. Arch Phys Med Rehabil 88: 1: 54-62, 2007.

Gupta A. Analyses of myo-electrical silence of erectors spinae. J Biomech 34: 4: 491-496, 2001.

Haig AJ, Moffroid M, Henry S, Haugh L and Pope M. A technique for needle localization in paraspinal muscles with cadaveric confirmation. Muscle Nerve 14: 6: 521-526, 1991.

Hansen L, de Zee M, Rasmussen J, Andersen TB, Wong C and Simonsen EB. Anatomy and biomechanics of the back muscles in the lumbar spine with reference to biomechanical modeling. Spine 31: 17: 1888-1899, 2006.

Hashemi L, Webster BS and Clancy EA. Trends in disability duration and cost of workers' compensation low back pain claims (1988-1996). J Occup Environ Med 40: 12: 1110-1119, 1998.

Herzog W, Conway PJ, Kawchuk GN, Zhang Y and Hasler EM. Forces exerted during spinal manipulative therapy. Spine 18: 9: 1206-1212, 1993.

Herzog W, Kats M and Symons B. The effective forces transmitted by high-speed, low-amplitude thoracic manipulation. Spine 26: 19: 2105-10; discussion 2110-1, 2001.

Herzog W, Scheele D and Conway PJ. Electromyographic responses of back and limb muscles associated with spinal manipulative therapy. Spine 24: 2: 146-52; discussion 153, 1999.

Hides J, Gilmore C, Stanton W and Bohlscheid E. Multifidus size and symmetry among chronic LBP and healthy asymptomatic subjects. Man Ther 2006.

Hides JA, Belavy DL, Stanton W, Wilson SJ, Rittweger J, Felsenberg D and Richardson CA. Magnetic resonance imaging assessment of trunk muscles during prolonged bed rest. Spine 32: 15: 1687-1692, 2007.

Hides JA, Jull GA and Richardson CA. Long-term effects of specific stabilizing exercises for first-episode low back pain. Spine 26: 11: E243-8, 2001.

Hides JA, Richardson CA and Jull GA. Multifidus muscle recovery is not automatic after resolution of acute, first-episode low back pain. Spine 21: 23: 2763-2769, 1996.

Hides JA, Richardson CA and Jull GA. Magnetic resonance imaging and ultrasonography of the lumbar multifidus muscle. Comparison of two different modalities. Spine 20: 1: 54-58, 1995.

Hides JA, Stokes MJ, Saide M, Jull GA and Cooper DH. Evidence of lumbar multifidus muscle wasting ipsilateral to symptoms in patients with acute/subacute low back pain. Spine 19: 2: 165-172, 1994.

Hodges P, Holm AK, Hansson T and Holm S. Rapid atrophy of the lumbar multifidus follows experimental disc or nerve root injury. Spine 31: 25: 2926-2933, 2006.

Hodges P, Kaigle Holm A, Holm S, Ekstrom L, Cresswell A, Hansson T and Thorstensson A. Intervertebral stiffness of the spine is increased by evoked contraction of transversus abdominis and the diaphragm: in vivo porcine studies. Spine 28: 23: 2594-2601, 2003.

Hodges PW, Cresswell AG, Daggfeldt K and Thorstensson A. In vivo measurement of the effect of intra-abdominal pressure on the human spine. J Biomech 34: 3: 347-353, 2001.

Hodges PW, Eriksson AE, Shirley D and Gandevia SC. Intra-abdominal pressure increases stiffness of the lumbar spine. J Biomech 38: 9: 1873-1880, 2005.

Hodges PW and Richardson CA. Altered trunk muscle recruitment in people with low back pain with upper limb movement at different speeds. Arch Phys Med Rehabil 80: 9: 1005-1012, 1999a.

Hodges PW and Richardson CA. Transversus abdominis and the superficial abdominal muscles are controlled independently in a postural task. Neurosci Lett 265: 2: 91-94, 1999b.

Hodges PW and Richardson CA. Delayed postural contraction of transversus abdominis in low back pain associated with movement of the lower limb. J Spinal Disord 11: 1: 46-56, 1998.

Hodges PW and Richardson CA. Contraction of the abdominal muscles associated with movement of the lower limb. Phys Ther 77: 2: 132-42; discussion 142-4, 1997a.

Hodges PW and Richardson CA. Feedforward contraction of transversus abdominis is not influenced by the direction of arm movement. Exp Brain Res 114: 2: 362-370, 1997b.

Hodges PW and Richardson CA. Inefficient muscular stabilization of the lumbar spine associated with low back pain. A motor control evaluation of transversus abdominis. Spine 21: 22: 2640-2650, 1996.

Hyun JK, Lee JY, Lee SJ and Jeon JY. Asymmetric atrophy of multifidus muscle in patients with unilateral lumbosacral radiculopathy. Spine 32: 21: E598-602, 2007.

Indahl A, Kaigle A, Reikeras O and Holm S. Electromyographic response of the porcine multifidus musculature after nerve stimulation. Spine 20: 24: 2652-2658, 1995.

Indahl A, Kaigle AM, Reikeras O and Holm SH. Interaction between the porcine lumbar intervertebral disc, zygapophysial joints, and paraspinal muscles. Spine 22: 24: 2834-2840, 1997.

Jackson M, Solomonow M, Zhou B, Baratta RV and Harris M. Multifidus EMG and tension-relaxation recovery after prolonged static lumbar flexion. Spine 26: 7: 715-723, 2001.

Jemmett RS, Macdonald DA and Agur AM. Anatomical relationships between selected segmental muscles of the lumbar spine in the context of multi-planar segmental motion: a preliminary investigation. Man Ther 9: 4: 203-210, 2004.

Johnson GM and Zhang M. Regional differences within the human supraspinous and interspinous ligaments: a sheet plastination study. Eur Spine J 11: 4: 382-388, 2002.

Jonsson B. The functions of individual muscles in the lumbar part of the spinae muscle. Electromyography 10: 1: 5-21, 1970.

Jull GA and Richardson CA. Motor control problems in patients with spinal pain: a new direction for therapeutic exercise. J Manipulative Physiol Ther 23: 2: 115-117, 2000.

Kaigle AM, Holm SH and Hansson TH. Experimental instability in the lumbar spine. Spine 20: 4: 421-430, 1995.

Kamaz M, Kiresi D, Oguz H, Emlik D and Levendoglu F. CT measurement of trunk muscle areas in patients with chronic low back pain. Diagn Interv Radiol 13: 3: 144-148, 2007.

Kanayama M, Abumi K, Kaneda K, Tadano S and Ukai T. Phase lag of the intersegmental motion in flexion-extension of the lumbar and lumbosacral spine. An in vivo study. Spine 21: 12: 1416-1422, 1996.

Kang CH, Shin MJ, Kim SM, Lee SH and Lee CS. MRI of paraspinal muscles in lumbar degenerative kyphosis patients and control patients with chronic low back pain. Clin Radiol 62: 5: 479-486, 2007.

Kang YM, Choi WS and Pickar JG. Electrophysiologic evidence for an intersegmental reflex pathway between lumbar paraspinal tissues. Spine 27: 3: E56-63, 2002.

Kang YM, Kenney MJ, Spratt KF and Pickar JG. Somatosympathetic reflexes from the low back in the anesthetized cat. J Neurophysiol 90: 4: 2548-2559, 2003.

Kang YM, Wheeler JD and Pickar JG. Stimulation of chemosensitive afferents from multifidus muscle does not sensitize multifidus muscle spindles to vertebral loads in the lumbar spine of the cat. Spine 26: 14: 1528-1536, 2001.

Kavcic N, Grenier S and McGill SM. Determining the stabilizing role of individual torso muscles during rehabilitation exercises. Spine 29: 11: 1254-1265, 2004a.

Kavcic N, Grenier S and McGill SM. Quantifying tissue loads and spine stability while performing commonly prescribed low back stabilization exercises. Spine 29: 20: 2319-2329, 2004b.

Kawchuk GN and Elliott PD. Validation of displacement measurements obtained from ultrasonic images during indentation testing. Ultrasound Med Biol 24: 1: 105-111, 1998.

Kawchuk GN and Fauvel OR. Sources of variation in spinal indentation testing: Indentation site relocation, intraabdominal pressure, subject movement, muscular response and stiffness estimation. J Manipulative Physiol Ther 24: 2: 84-91, 2001.

Kawchuk GN, Fauvel OR and Dmowski J. Ultrasonic indentation: a procedure for the noninvasive quantification of force-displacement properties of the lumbar spine. J Manipulative Physiol Ther 24: 3: 149-156, 2001.

Kawchuk GN, Fauvel OR and Dmowski J. Ultrasonic quantification of osseous displacements resulting from skin surface indentation loading of bovine para-spinal tissue. Clin Biomech (Bristol, Avon) 15: 4: 228-233, 2000.

Kawchuk GN, Kaigle AM, Holm SH, Rod Fauvel O, Ekstrom L and Hansson T. The diagnostic performance of vertebral displacement measurements derived from ultrasonic indentation in an in vivo model of degenerative disc disease. Spine 26: 12: 1348-1355, 2001.

Kawchuk GN, Liddle TR, Fauvel OR and Johnston C. The accuracy of ultrasonic indentation in detecting simulated bone displacement: a comparison of three techniques. J Manipulative Physiol Ther 29: 2: 126-133, 2006.

Keller TS, Colloca CJ and Fuhr AW. Validation of the force and frequency characteristics of the activator adjusting instrument: effectiveness as a mechanical impedance measurement tool. J Manipulative Physiol Ther 22: 2: 75-86, 1999.

Keller TS, Colloca CJ and Gunzburg R. Neuromechanical characterization of in vivo lumbar spinal manipulation. Part I. Vertebral motion. J Manipulative Physiol Ther 26: 9: 567-578, 2003.

Keller TS, Colloca CJ, Harrison DE, Moore RJ and Gunzburg R. Muscular contributions to dynamic dorsoventral lumbar spine stiffness. Eur Spine J 16: 2: 245-254, 2007.

Keller TS, Colloca CJ, Moore RJ, Gunzburg R, Harrison DE and Harrison DD. Three-dimensional vertebral motions produced by mechanical force spinal manipulation. J Manipulative Physiol Ther 29: 6: 425-436, 2006.

Kim BJ, Date ES, Derby R, Lee SH, Seo KS, Oh KJ and Kim MJ. Electromyographic technique for lumbar multifidus examination: comparison of previous techniques used to localize the multifidus. Arch Phys Med Rehabil 86: 7: 1325-1329, 2005.

Kippers V and Parker AW. Posture related to myoelectric silence of erectores spinae during trunk flexion. Spine 9: 7: 740-745, 1984.

Koes BW, van Tulder MW, Ostelo R, Kim Burton A and Waddell G. Clinical guidelines for the management of low back pain in primary care: an international comparison. Spine 26: 22: 2504-13; discussion 2513-4, 2001.

Latimer J, Goodsel MM, Lee M, Maher CG, Wilkinson BN and Moran CC. Evaluation of a new device for measuring responses to posteroanterior forces in a patient population, Part 1: Reliability testing. Phys Ther 76: 2: 158-165, 1996a.

Latimer J, Lee M, Adams R and Moran CM. An investigation of the relationship between low back pain and lumbar posteroanterior stiffness. J Manipulative Physiol Ther 19: 9: 587-591, 1996b.

Latimer J, Lee M and Adams RD. The effects of high and low loading forces on measured values of lumbar stiffness. J Manipulative Physiol Ther 21: 3: 157-163, 1998.

Lee LJ, Coppieters MW and Hodges PW. Anticipatory postural adjustments to arm movement reveal complex control of paraspinal muscles in the thorax. J Electromyogr Kinesiol 2007.

Lee LJ, Coppieters MW and Hodges PW. Differential activation of the thoracic multifidus and longissimus thoracis during trunk rotation. Spine 30: 8: 870-876, 2005.

Lee M, Esler M, Mildren J and Herbert R. Effect of extensor muscle activation on the response to lumbar posteroanterior forces. Clin Biomech (Bristol, Avon) 8: 3: 115-119, 1993.

Lee M and Liversidge K. Posteroanterior stiffness at three locations in the lumbar spine. J Manipulative Physiol Ther 17: 8: 511-516, 1994.

Lee M and Svensson NL. Effect of loading frequency on response of the spine to lumbar posteroanterior forces. J Manipulative Physiol Ther 16: 7: 439-446, 1993.

Lee R and Evans J. An in vivo study of the intervertebral movements produced by posteroanterior mobilization. Clin Biomech (Bristol, Avon) 12: 6: 400-408, 1997.

Lee RY and Evans JH. The role of spinal tissues in resisting posteroanterior forces applied to the lumbar spine. J Manipulative Physiol Ther 23: 8: 551-556, 2000.

Lee SW, Wong KW, Chan MK, Yeung HM, Chiu JL and Leong JC. Development and validation of a new technique for assessing lumbar spine motion. Spine 27: 8: E215-20, 2002.

Lewin T, Moffett B and Vidik A. The morphology of the lumbar synovial interveertebral joints. Acta Morphol Neerl Scand 4: 299-319, 1962.

Lim KL, Jacobs P and Klarenbach S. A population-based analysis of healthcare utilization of persons with back disorders: results from the Canadian Community Health Survey 2000-2001. Spine 31: 2: 212-218, 2006.

Loney PL and Stratford PW. The prevalence of low back pain in adults: a methodological review of the literature. Phys Ther 79: 4: 384-396, 1999.

Lucas DB and Bresler B. Stability of the Ligamentous Spine Biomechanics Laboratory, University of California, San Francisco/Berkeley: 1961.

MacDonald DA, Moseley GL and Hodges PW. The lumbar multifidus: does the evidence support clinical beliefs? Man Ther 11: 4: 254-263, 2006.

Macintosh JE and Bogduk N. 1987 Volvo award in basic science. The morphology of the lumbar erector spinae. Spine 12: 7: 658-668, 1987.

Macintosh JE and Bogduk N. The biomechanics of the lumbar multifidus. Clin Biomech (Bristol, Avon) 1: 205-205-213, 1986.

Macintosh JE, Valencia FP, Bogduk N and Munro RR. The morphology of the human lumbar multifidus. Clin Biomech 1: 196-196-204, 1986.

Maetzel A and Li L. The economic burden of low back pain: a review of studies published between 1996 and 2001. Best Pract Res Clin Rheumatol 16: 1: 23-30, 2002.

Maniadakis N and Gray A. The economic burden of back pain in the UK. Pain 84: 1: 95-103, 2000.

Martini F. Fundamentals of anatomy & physiology. San Francisco, CA: Pearson Benjamin Cummings, 2006, p. 1. (arous pagngs) : co.. ; 29 cm. + 1nteracte physoogy CD-ROM (4 3/4n.) + 1 anatomy 360 degrees CD-ROM (4 3/4n.) + 1 student access kt (12.

McCook DT, Vicenzino B and Hodges PW. Activity of deep abdominal muscles increases during submaximal flexion and extension efforts but antagonist co-contraction remains unchanged. J Electromyogr Kinesiol 2007.

McGill S, Juker D and Kropf P. Quantitative intramuscular myoelectric activity of quadratus lumborum during a wide variety of tasks. Clin Biomech (Bristol, Avon) 11: 3: 170-172, 1996.

McGill S, Seguin J and Bennett G. Passive stiffness of the lumbar torso in flexion, extension, lateral bending, and axial rotation. Effect of belt wearing and breath holding. Spine 19: 6: 696-704, 1994.

McGill SM. Low back stability: from formal description to issues for performance and rehabilitation. Exerc Sport Sci Rev 29: 1: 26-31, 2001.

McGill SM. Kinetic potential of the lumbar trunk musculature about three orthogonal orthopaedic axes in extreme postures. Spine 16: 7: 809-815, 1991.

McGill SM and Brown S. Creep response of the lumbar spine to prolonged full flexion. Clin Biomech (Bristol, Avon) 7: 1: 43-46, 1992.

McGill SM, Grenier S, Kavcic N and Cholewicki J. Coordination of muscle activity to assure stability of the lumbar spine. J Electromyogr Kinesiol 13: 4: 353-359, 2003.

McGill S. Low back disorders : evidenced-based prevention and rehabilitation. Champaign, IL: Human Kinetics, 2007, p. 312.

McGill S. Low back disorders : evidence-based prevention and rehabilitation. Champaign, IL: Human Kinetics, 2002, p. 295.

Mengiardi B, Schmid MR, Boos N, Pfirrmann CW, Brunner F, Elfering A and Hodler J. Fat content of lumbar paraspinal muscles in patients with chronic low back pain and in asymptomatic volunteers: quantification with MR spectroscopy. Radiology 240: 3: 786-792, 2006.

Moorhouse KM and Granata KP. Role of reflex dynamics in spinal stability: intrinsic muscle stiffness alone is insufficient for stability. J Biomech 40: 5: 1058-1065, 2007.

Morris JM, Benner G and Lucas DB. An electromyographic study of the intrinsic muscles of the back in man. J Anat 96: Pt 4: 509-520, 1962.

Moseley GL, Hodges PW and Gandevia SC. External perturbation of the trunk in standing humans differentially activates components of the medial back muscles. J Physiol 547: Pt 2: 581-587, 2003.

Moseley GL, Hodges PW and Gandevia SC. Deep and superficial fibers of the lumbar multifidus muscle are differentially active during voluntary arm movements. Spine 27: 2: E29-36, 2002.

Moseley GL, Nicholas MK and Hodges PW. Pain differs from non-painful attention-demanding or stressful tasks in its effect on postural control patterns of trunk muscles. Exp Brain Res 156: 1: 64-71, 2004.

Ng JK, Parnianpour M, Richardson CA and Kippers V. Effect of fatigue on torque output and electromyographic measures of trunk muscles during isometric axial rotation. Arch Phys Med Rehabil 84: 3: 374-381, 2003.

Ng JK, Parnianpour M, Richardson CA and Kippers V. Functional roles of abdominal and back muscles during isometric axial rotation of the trunk. J Orthop Res 19: 3: 463-471, 2001.

Ng JK, Richardson CA, Parnianpour M and Kippers V. EMG activity of trunk muscles and torque output during isometric axial rotation exertion: a comparison between back pain patients and matched controls. J Orthop Res 20: 1: 112-121, 2002.

Nitz AJ and Peck D. Comparison of muscle spindle concentrations in large and small human epaxial muscles acting in parallel combinations. Am Surg 52: 5: 273-277, 1986.

O'Sullivan PB, Grahamslaw KM, Kendell M, Lapenskie SC, Moller NE and Richards KV. The effect of different standing and sitting postures on trunk muscle activity in a pain-free population. Spine 27: 11: 1238-1244, 2002.

O'Sullivan PB, Phyty GD, Twomey LT and Allison GT. Evaluation of specific stabilizing exercise in the treatment of chronic low back pain with radiologic diagnosis of spondylolysis or spondylolisthesis. Spine 22: 24: 2959-2967, 1997.

Panjabi M, Abumi K, Duranceau J and Oxland T. Spinal stability and intersegmental muscle forces. A biomechanical model. Spine 14: 2: 194-200, 1989.

Panjabi MM. Clinical spinal instability and low back pain. J Electromyogr Kinesiol 13: 4: 371-379, 2003.

Panjabi MM. The stabilizing system of the spine. Part I. Function, dysfunction, adaptation, and enhancement. J Spinal Disord 5: 4: 383-9; discussion 397, 1992a.

Panjabi MM. The stabilizing system of the spine. Part II. Neutral zone and instability hypothesis. J Spinal Disord 5: 4: 390-6; discussion 397, 1992b.

Panjabi MM, Duranceau JS, Oxland TR and Bowen CE. Multidirectional instabilities of traumatic cervical spine injuries in a porcine model. Spine 14: 10: 1111-1115, 1989.

Pauly JE. An electromyographic analysis of certain movements and exercises. I. Some deep muscles of the back. Anat Rec 155: 2: 223-234, 1966.

Pauly JE and Steele RW. Electromyographic analysis of back exercises for paraplegic patients. Arch Phys Med Rehabil 47: 11: 730-736, 1966.

Peck D, Buxton DF and Nitz A. A comparison of spindle concentrations in large and small muscles acting in parallel combinations. J Morphol 180: 3: 243-252, 1984.

Perez CE. Chronic back problems among workers. Health Rep 12: 1: 41-55 (Eng); 45-60 (Fre), 2000.

Pickar JG. Neurophysiological effects of spinal manipulation. Spine J 2: 5: 357-371, 2002.

Pickar JG. An in vivo preparation for investigating neural responses to controlled loading of a lumbar vertebra in the anesthetized cat. J Neurosci Methods 89: 2: 87-96, 1999.

Pickar JG and Ge W. Time course for the development of muscle history in lumbar paraspinal muscle spindles arising from changes in vertebral position. Spine J 2007.

Pickar JG and Kang YM. Paraspinal muscle spindle responses to the duration of a spinal manipulation under force control. J Manipulative Physiol Ther 29: 1: 22-31, 2006.

Pickar JG, Sung PS, Kang YM and Ge W. Response of lumbar paraspinal muscles spindles is greater to spinal manipulative loading compared with slower loading under length control. Spine J 7: 5: 583-595, 2007.

Pickar JG and Wheeler JD. Response of muscle proprioceptors to spinal manipulative-like loads in the anesthetized cat. J Manipulative Physiol Ther 24: 1: 2-11, 2001.

Powers CM, Kulig K, Harrison J and Bergman G. Segmental mobility of the lumbar spine during a posterior to anterior mobilization: assessment using dynamic MRI. Clin Biomech (Bristol, Avon) 18: 1: 80-83, 2003.

Quint U, Wilke HJ, Shirazi-Adl A, Parnianpour M, Loer F and Claes LE. Importance of the intersegmental trunk muscles for the stability of the lumbar spine. A biomechanical study in vitro. Spine 23: 18: 1937-1945, 1998.

Rantanen J, Hurme M, Falck B, Alaranta H, Nykvist F, Lehto M, Einola S and Kalimo H. The lumbar multifidus muscle five years after surgery for a lumbar intervertebral disc herniation. Spine 18: 5: 568-574, 1993.

Reeves NP, Everding VQ, Cholewicki J and Morrisette DC. The effects of trunk stiffness on postural control during unstable seated balance. Exp Brain Res 174: 4: 694-700, 2006.

Reeves NP, Narendra KS and Cholewicki J. Spine stability: the six blind men and the elephant. Clin Biomech (Bristol, Avon) 22: 3: 266-274, 2007.

Richardson CA and Jull GA. Muscle control-pain control. What exercises would you prescribe? Man Ther 1: 1: 2-10, 1995.

Richardson CA, Jull GA, Hodges PW and Hides JA. Therapeutic exercise for spinal segmental stabilization in low back pain : scientific basis and clinical approach. Edinburgh: Churchill Livingstone, 1999, p. 191.

Richardson CA, Snijders CJ, Hides JA, Damen L, Pas MS and Storm J. The relation between the transversus abdominis muscles, sacroiliac joint mechanics, and low back pain. Spine 27: 4: 399-405, 2002.

Richardson C, Hodges PW and Hides JA. Therapeutic exercise for lumbopelvic stabilization : a motor control approach for the treatment and prevention of low back pain. Edinburgh ; New York: Churchill Livingstone, 2004, p. 271.

Richmond FJ, MacGillis DR and Scott DA. Muscle-fiber compartmentalization in cat splenius muscles. J Neurophysiol 53: 4: 868-885, 1985.

Rogers EL and Granata KP. Disturbed paraspinal reflex following prolonged flexion-relaxation and recovery. Spine 31: 7: 839-845, 2006.

Saunders SW, Rath D and Hodges PW. Postural and respiratory activation of the trunk muscles changes with mode and speed of locomotion. Gait Posture 20: 3: 280-290, 2004.

Saunders SW, Schache A, Rath D and Hodges PW. Changes in three dimensional lumbo-pelvic kinematics and trunk muscle activity with speed and mode of locomotion. Clin Biomech (Bristol, Avon) 20: 8: 784-793, 2005.

Schultz SE and Kopec JA. Impact of chronic conditions. Health Rep 14: 4: 41-53, 2003.

Seeley RR. Anatomy & physiology. Boston: McGraw-Hill, 2003.

Shirley D, Ellis E and Lee M. The response of posteroanterior lumbar stiffness to repeated loading. Man Ther 7: 1: 19-25, 2002.

Shirley D, Hodges PW, Eriksson AE and Gandevia SC. Spinal stiffness changes throughout the respiratory cycle. J Appl Physiol 95: 4: 1467-1475, 2003.

Skotte J, Hjortskov N, Essendrop M, Schibye B and Fallentin N. Short latency stretch reflex in human lumbar paraspinal muscles. J Neurosci Methods 145: 1-2: 145-150, 2005.

Solomonow M, Hatipkarasulu S, Zhou BH, Baratta RV and Aghazadeh F. Biomechanics and electromyography of a common idiopathic low back disorder. Spine 28: 12: 1235-1248, 2003a.

Solomonow M, Zhou BH, Baratta RV and Burger E. Biomechanics and electromyography of a cumulative lumbar disorder: response to static flexion. Clin Biomech (Bristol, Avon) 18: 10: 890-898, 2003b.

Solomonow M, Zhou BH, Harris M, Lu Y and Baratta RV. The ligamento-muscular stabilizing system of the spine. Spine 23: 23: 2552-2562, 1998.

Squires MC, Latimer J, Adams RD and Maher CG. Indenter head area and testing frequency effects on posteroanterior lumbar stiffness and subjects' rated comfort. Man Ther 6: 1: 40-47, 2001.

Stein J, Baker E and Pine ZM. Medial paraspinal muscle electromyography: techniques of examination. Arch Phys Med Rehabil 74: 5: 497-500, 1993.

Stokes IA, Henry SM and Single RM. Surface EMG electrodes do not accurately record from lumbar multifidus muscles. Clin Biomech (Bristol, Avon) 18: 1: 9-13, 2003.

Stokes M, Rankin G and Newham DJ. Ultrasound imaging of lumbar multifidus muscle: normal reference ranges for measurements and practical guidance on the technique. Man Ther 10: 2: 116-126, 2005.

Stubbs M, Harris M, Solomonow M, Zhou B, Lu Y and Baratta RV. Ligamento-muscular protective reflex in the lumbar spine of the feline. J Electromyogr Kinesiol 8: 4: 197-204, 1998.

Sung PS, Kang YM and Pickar JG. Effect of spinal manipulation duration on low threshold mechanoreceptors in lumbar paraspinal muscles: a preliminary report. Spine 30: 1: 115-122, 2005.

Symons BP, Herzog W, Leonard T and Nguyen H. Reflex responses associated with activator treatment. J Manipulative Physiol Ther 23: 3: 155-159, 2000.

Taguchi T, John V, Hoheisel U and Mense S. Neuroanatomical pathway of nociception originating in a low back muscle (multifidus) in the rat. Neurosci Lett 427: 1: 22-27, 2007.

Tani T, Yamamoto H, Ichimiya M and Kimura J. Reflexes evoked in human erector spinae muscles by tapping during voluntary activity. Electroencephalogr Clin Neurophysiol 105: 3: 194-200, 1997.

Taylor JR and O'sullivan PB. Lumbar segmental instability: Pathology, diagnosis and conservative management. In: Physical therapy of the low back, edited by Twomey LT and Taylor JR. New York: Churchill Livingstone, 2000, chapt. 7, p. 201-201-247.

Tesh KM, Dunn JS and Evans JH. The abdominal muscles and vertebral stability. Spine 12: 5: 501-508, 1987.

Tortora GJ. Principles of anatomy and physiology. New York: Wiley, 2003, p. 1104.

Tortora GJ. Principles of anatomy and physiology. New York: John Wiley & SonsInc., 2000, p. 1055.

Triano J and Schultz AB. Loads transmitted during lumbosacral spinal manipulative therapy. Spine 22: 17: 1955-1964, 1997.

Valencia FP and Munro RR. An electromyographic study of the lumbar multifidus in man. Electromyogr Clin Neurophysiol 25: 4: 205-221, 1985.

Vasseljen O, Dahl HH, Mork PJ and Torp HG. Muscle activity onset in the lumbar multifidus muscle recorded simultaneously by ultrasound imaging and intramuscular electromyography. Clin Biomech (Bristol, Avon) 21: 9: 905-913, 2006.

Vera-Garcia FJ, Elvira JL, Brown SH and McGill SM. Effects of abdominal stabilization maneuvers on the control of spine motion and stability against sudden trunk perturbations. J Electromyogr Kinesiol 17: 5: 556-567, 2007.

White AA. Clinical biomechanics of the spine. Philadelphia: Lippincott, 1990, p. 722.

Wilke HJ, Wolf S, Claes LE, Arand M and Wiesend A. Stability increase of the lumbar spine with different muscle groups. A biomechanical in vitro study. Spine 20: 2: 192-198, 1995.

Wilkins K and Mackenzie SG. Work injuries. Health Rep 18: 3: 25-42, 2007.

Wilkins K and Park E. Chronic conditions, physical limitations and dependency among seniors living in the community. Health Rep 8: 3: 7-15(Eng); 7-15(Fre), 1996.

Wong KW, Leong JC, Chan MK, Luk KD and Lu WW. The flexion-extension profile of lumbar spine in 100 healthy volunteers. Spine 29: 15: 1636-1641, 2004.

Yoshihara K, Nakayama Y, Fujii N, Aoki T and Ito H. Atrophy of the multifidus muscle in patients with lumbar disk herniation: histochemical and electromyographic study. Orthopedics 26: 5: 493-495, 2003.

Appendices

Appendix A: Fine-wire electrode fabrication

The following steps outline the fine-wire electrode custom fabrication process employed by this study to make lumbar multifidus intramuscular electrodes. The specifications of the materials used and where these materials were commercially available is included in each step.

1. Approximately three feet of a fine-wire was measured from the spool and the two loose ends were held together to form a loop. A single strand of annealed stainless steel wire coated with liquid enamel insulation was used. Further specifications of the wire were:

- Stainless steel 304
- Material No: cfw-100192
- Diameter: 0.002
- Temper: annealed
- Insulation: H-ML liquid enamel
- Color: Natural

This wire was purchased from California Fine Wire Company in the United States.

- California Fine Wire Company
- P.O. Box 446
  Grover Beach, CA 93483-0446
- Phone: 805-489-5144
- Fax: 805- 489-5352
- website: www.calfinewire.com

2. The wire was looped through a paper clip that was fitted into a drill (Figure A.1). The loose ends of the wire were held firmly using tweezers while the drill was spun to coil the two strands of fine-wire around each other. While the wire was held tightly, the two coiled strands were intermittently smoothed by running one's fingers over the coiled wire moving in a direction from the drill towards the tweezers. The drill was used to coil the two strands of fine-wire until they were almost indistinguishable from a single strand.

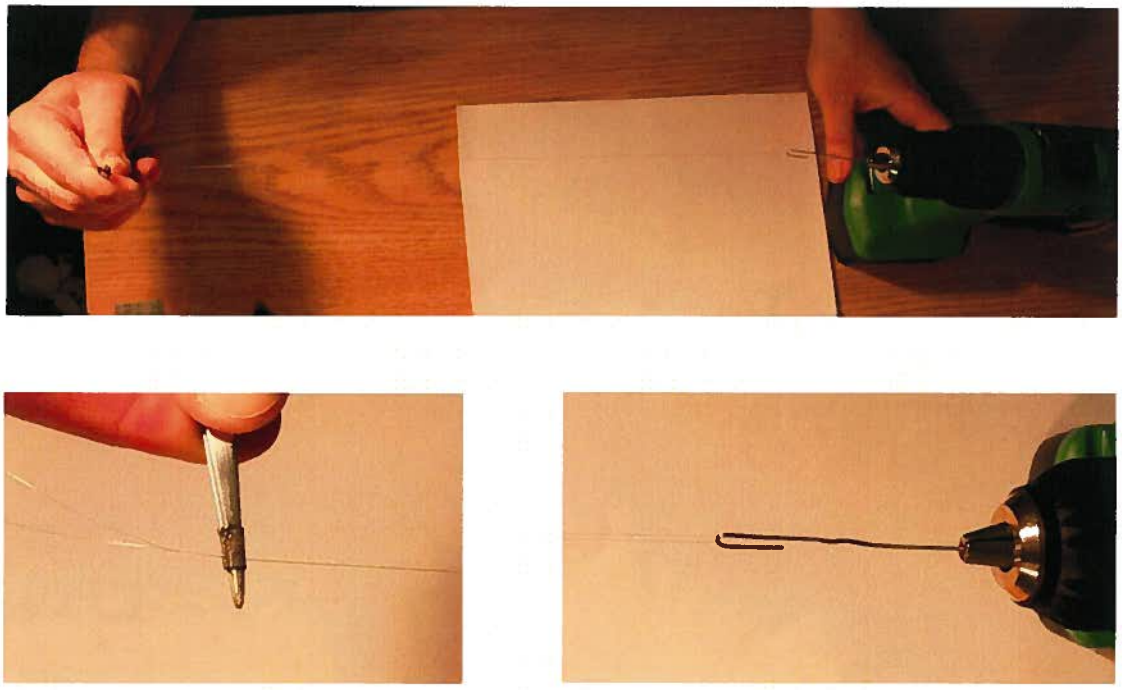

Figure A.1 The top panel displays the fine-wire looped around the paper clip with the loose ends being held by tweezers. The bottom left panel is a close-up view of the wire being held with tweezers while the bottom right panel is a close-up view of the wire looped around the paper clip drill bit.

3. The coiled wire was removed from the paper clip (Figure A.2) and fed through a hollow hypodermic needle by guiding the loose ends of the wire through the tip of the cannula (Figure A.3).

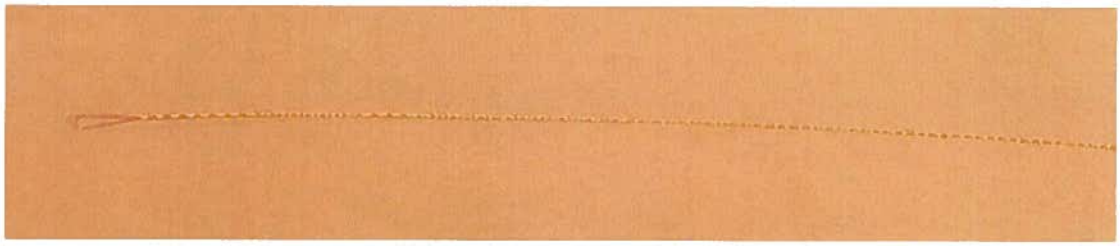

Figure. A.2. The coiled fine-wire was removed from the paper clip once the two strands of wire are tightly intertwined. Note that the loop that was wrapped around the paper clip was still intact.

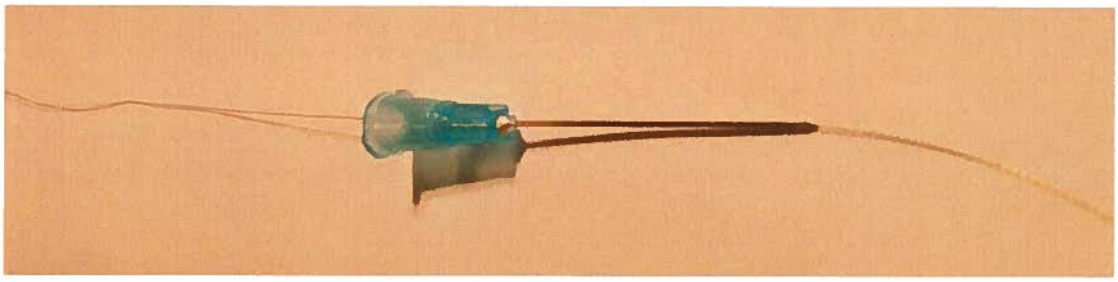

Figure. A.3. The coiled fine-wire was fed through the cannula of the hollow hypodermic needle (Becton-Dickson PrecisionGlide 1.5" needle shown here).

4. Two types of sterile single-use 25-gauge hypodermic needle were used in the current study. Kendall Monoject 2" (25-gauge) hypodermic needles (Figure A.4 left panels) were used to insert fine-wire electrodes into deep lumbar multifidus fibres. These needles (Product number: 537-200441) were purchased from:

- The Stevens Company
- 8188 Swenson Way
  Delta, B.C. V4G 1J6
- Phone: 604-634-3088
- Fax: 604-585-0193
- website: www.stevens.ca

Becton Dickson (Franklin Lakes, NJ USA) PrecisionGlide 1.5" regular bevel needles (Figure A.4 right panels) were used to insert fine-wire electrodes into superficial muscle locations. These needles were purchased from:

- Kerrisdale Pharmacy
- 5591 West Boulevard
  Vancouver BC, V6M 3W6
- Phone: 604-261-0333
- Fax: 604-261-0311

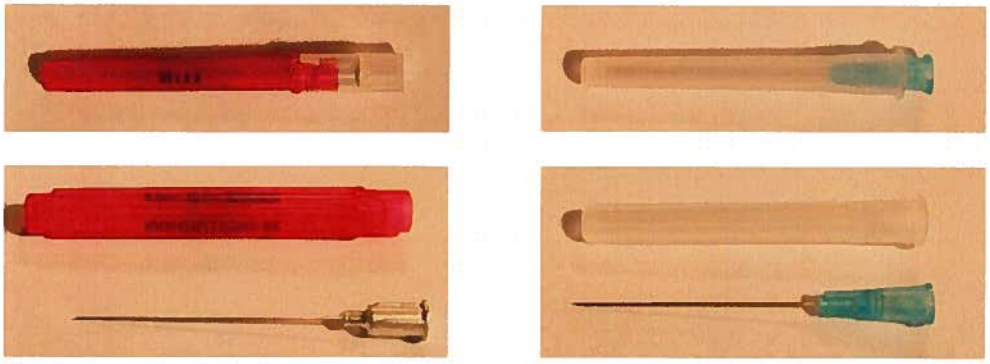

Figure A.4 The two types of hypodermic needles used in this study. A Kendall 25 gauge Monoject 2" hollow hypodermic needle is shown in the left panel while a Becton Dickson 25 gauge 1.5" PrecisionGlide hollow hypodermic needle is shown in the right panel.

4. The wire loop that was previously hooked onto the paper clip was cut at its midpoint, perpendicular to the wire, with a sharp blade (Figure A.5). The wire was then bent backwards around the tip of the hypodermic needle to form two hooks protruding from the needle tip (Figure A.6).

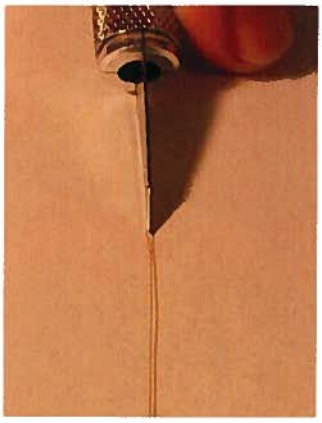

Figure A.5. The wire loop being cut with sharp blade.

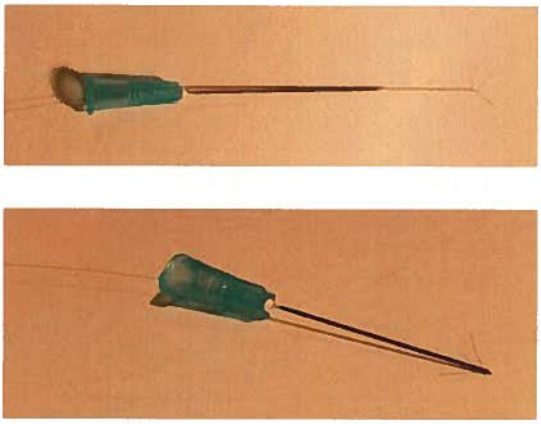

Figure A.6. The two cut ends are separated (top panel). The wire is then slid down the needle and the two loose ends are bent backwards around the tip of the needle (bottom panel).

5. The wire hooked ends were cut to 4mm and 0.5mm to maximize the electrode recording area while ensuring that both hook ends could reliably be inserted into the same group of muscle fibres. (Figure A.7). The hooked ends were cut to different lengths to prevent the two cut ends from touching and forming a closed circuit while in the muscle.

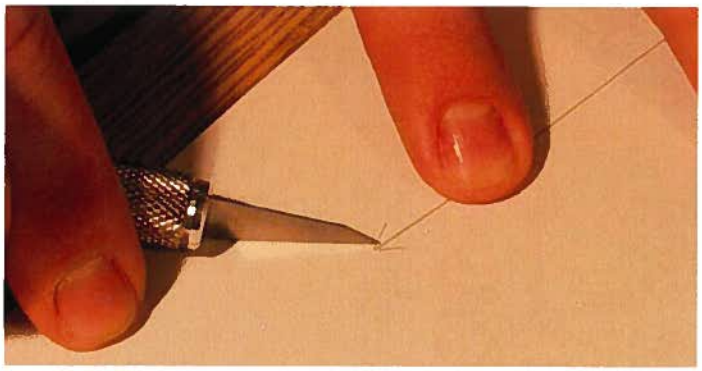

Figure A.7 The two wire "hooks" being cut to 4.0mm and 0.5mm with a sharp blade.

6. The two loose ends of wire extending out of the hypodermic needle hub were scraped with a sharp blade to remove the liquid enamel insulation (Figure A.8). Approximately 10 mm of wire was exposed by gently and repeatedly dragging the blade over the wire, then removing any additional insulation with one's fingernails.

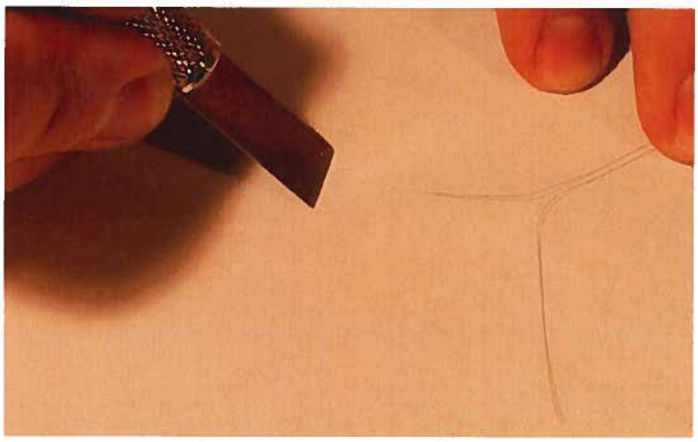

Figure A.8 Removing the liquid enamel insulation from the loose ends of each fine-wire strand.

7. After the insulation was removed, the two loose ends of exposed wire were soldered to nickel plated connectors (Figure A.9). These connectors were filled with 60/40 Rosin core solder and heated until the solder melted (Figure A.10). The exposed wire was inserted into the liquid solder (Figure A.11). The specifics of the connectors were:

- Nickel plated insulated small tip plugs
- Johnson components #105-0772-001
- 10 Amp, 0.08D male tip jack
- ohms contact resistance

These connectors were purchased from Electrosonic Inc. (product number 229-105-0772-001):

- Electrosonic Inc (e-sonic.com)
- 1100 Gordon Baker Road
  Toronto, Ontario M2H 3B3
- Phone: 800-56-SONIC
- Fax: 416-496-3030

Figure A.9. Nickel plated tip plug connector.

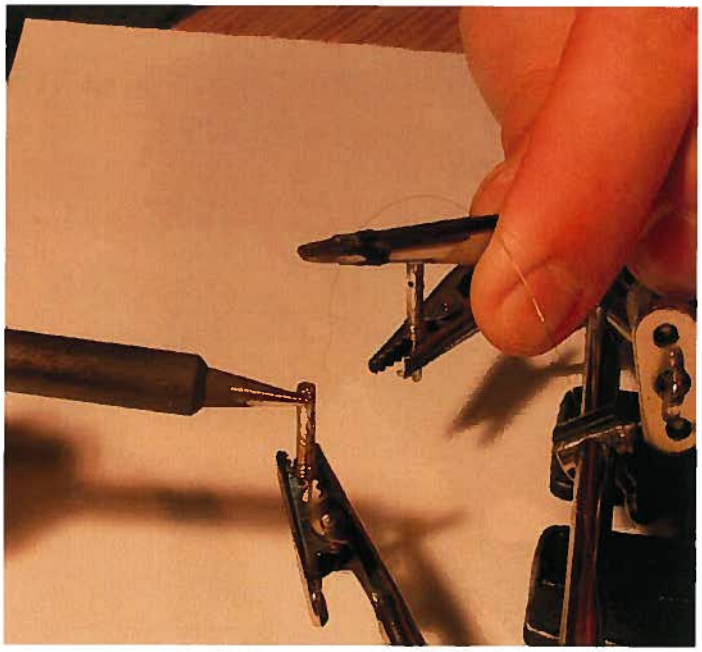

Figure A.10. The exposed loose ends of the fine-wire being soldered to the connector.

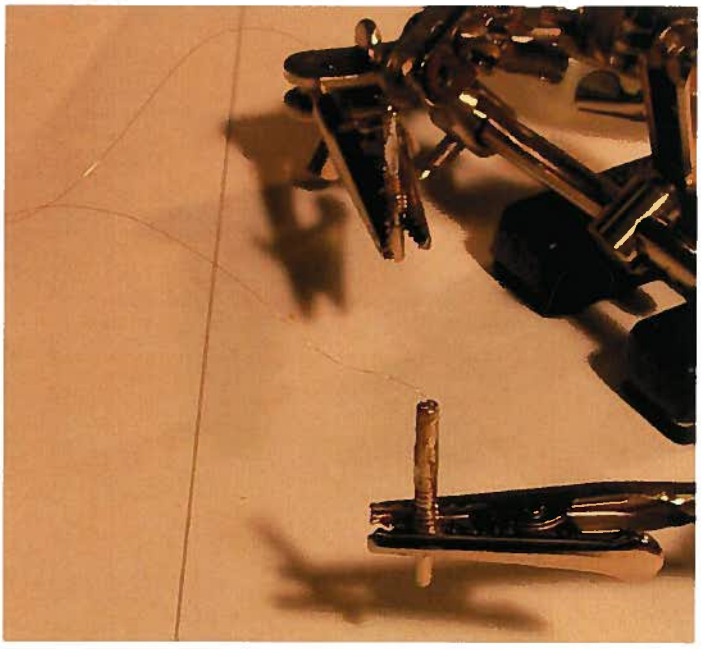

Figure A.11. Both wire ends soldered into the nickel plated connectors.

8. The closed end of the plastic needle shield was drilled through and the needle electrode was inserted into the shield (Figure A.12). The end of the shield was opened to allow sterilization gas to access the needle tip during medical sterilization.

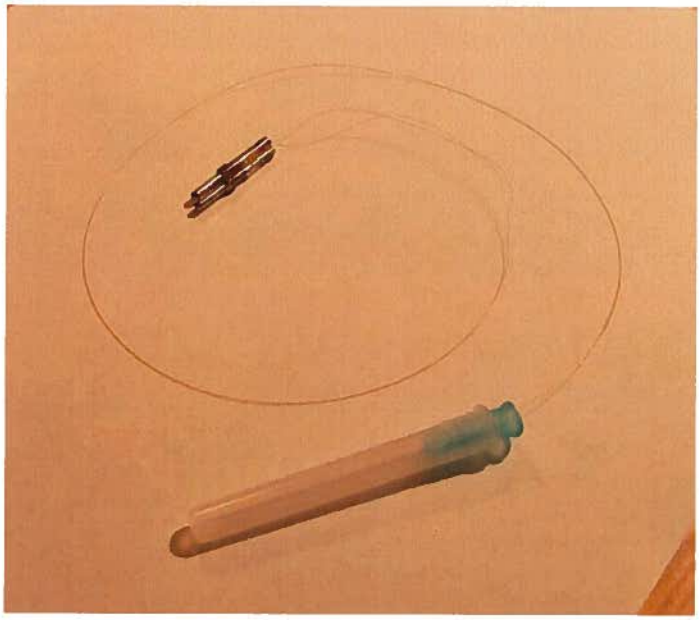

Figure A.12. Once the connectors were soldered to the wire, the needle shield near the tip was drilled through and the needle was placed into the needle shield.

9. The connectors were taped to the needle shield (Figure A.13) and the entire fine-wire electrode was placed in a self-seal sterilization bag (Figure A.14). The sterilization bag specifications were:

- Henry Schein Self Seal Sterilization bag
- Product number: 100-2973
- Bag dimensions: 3.5" x 9"

The sterilization bags were purchased from:

- Henry Schein Ash Arcona
- 1619 Fosters Way
  Delta, B.C. V3M 6S7
- Phone: 800-668-5558
- Fax: 800-263-3962
- website: www.henryschein.ca

Figure A.13. The connectors were taped to the shield to prevent the wire from being tangled during sterilization.

10. The needles were medically sterilized at the UBC Hospital Sterile Processing Department.

Figure A.14. The entire electrode and shield were placed in a self-seal sterilization bag.

Appendix B: Lumbar multifidus imaging and fine-wire electrode insertion

B.1 Lumbar multifidus imaging

A variety of techniques were used to image the lumbar paraspinal musculature using ultrasound (Sonosite Micromaxx, 13-6MHz HFL38 Transducer). Ultrasound imaging began at the level of the L4 spinous process because at this level lumbar multifidus was the most superficial muscle at the midline (Figure B.1). The L4 spinous process was landmarked by identifying the L1 spinous process and counting spinous processes caudally or identifying the sacrum and counting spinous processes cranially. The experimenter identified the lumbar multifidus muscle and then asked the study participant to perform low intensity back extension efforts or raise the ipsilateral leg to evoke a multifidus contraction. Tension in the multifidus and lumbar erector spinae muscles produce different patterns of fibre movement in the transverse plane (Stokes et al. 2005). The multifidus muscle fibres move in a circular fashion that has been described as a "lava lamp effect" (Stokes et al. 2005, p.124). The fascial borders of multifidus are roughly perpendicular to the cutaneous surface and thus are slightly more challenging to observe using ultrasound; however, these contractions assisted with fascial border identification.

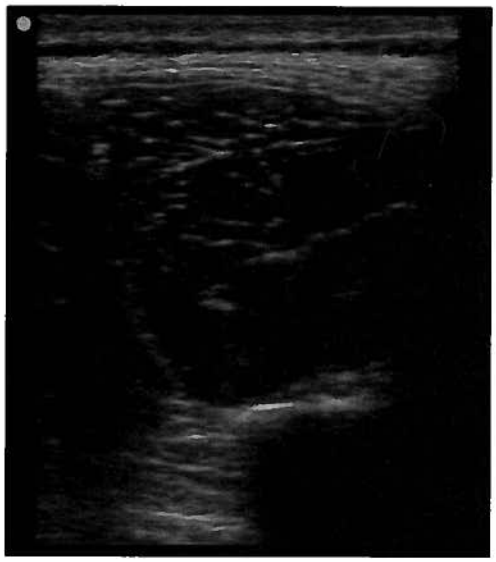

Figure B.1. Transverse plane ultrasound image at the L4 vertebral level showing the fascial border of the lumbar multifidus.

A second technique used to identify the lumbar multifidus fibres was to rotate the ultrasound transducer head and image the lumbar paraspinal musculature in the approximate longitudinal plane. The transducer head was rotated past ninety degrees to obtain a slightly oblique angle to the longitudinal plane (10-15° caudolateral direction of the inferior edge of the transducer probe) and to align the ultrasound image with the approximate orientation of lumbar multifidus fibres. At this slightly oblique angle the transducer head was placed approximately 5-10cm lateral to the L4 spinous process over the bulk of the lumbar erector spinae musculature. The lumbar erector spinae muscles have a dorsocaudal orientation due to more cranial fibres attaching progressively more dorsally on the ilium (Macintosh and Bogduk 1987). At this lateral ultrasound transducer probe location the orientation of these fibres was visible on the ultrasound image (Figure B.2a). The transducer head was then translated medially maintaining the 10-15 ° caudolateral angle to the longitudinal plane. As the transducer probe approached the midline, muscle fibres with a ventrocaudal orientation appeared at a location visceral to the erector spine muscle fibres (Figure B.2b). These ventrocaudal lumbar multifidus fibres became increasingly superficial as the probe continued to translate medially. Figure B.2 shows ultrasound images of paraspinal musculature in the approximate longitudinal plane at 5cm and 1cm lateral to the L4 spinous process.

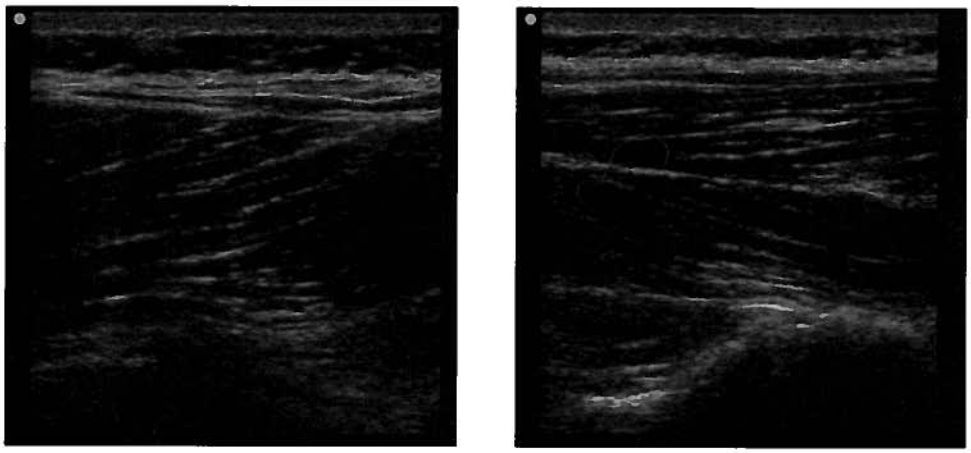

Figure B.2. Ultrasound images of the lumbar paraspinal muscles with a transducer probe orientation of 10-15° caudolateral to the longitudinal plane. The left image was taken 5cm lateral to the midline and shows the dorsocaudal orientation of the erector spinae muscles. The right image was taken 1cm lateral to the midline and shows the ventrocaudal orientation of lumbar multifidus beneath the erector spinae muscles.

Using either imaging technique, the superficial and deep fibres of multifidus were differentiated to determine the precise location of needle insertion. Once the lumbar multifidus was captured in the ultrasound image, "micro adjustments" were made to the transducer to simultaneously image the vertebral laminae. Due to the lack of rotatores muscles in the lumbar spine (Macintosh et al. 1986), deep multifidus fibres were the deepest muscle fibres visible in the lumbar spine. Imaging lumbar multifidus anatomy prior to fine-wire electrode insertion assisted in determining the most effective way to insert fine-wire electrodes into the deep and superficial multifidus fibres at the L3, L4 and L5 vertebral levels.

B.2 Fine-wire electrode insertion

The experimenter performing fine-wire electrode insertions wore sterile Sensicare non-latex powderfree gloves (Product number: 053-484402) during all needle insertions. These gloves were purchased from:

- The Stevens Company
- 8188 Swenson Way
  Delta, B.C. V4G 1J6
- Phone: 604-634-3088
- Fax: 604-585-0193
- website: www.stevens.ca

The electrode insertion sites and surrounding skin were thoroughly cleaned with gauze soaked in 70% Isopropyl alcohol. Aquasonic 100 ultrasound transmission gel (Parker Laboratories Inc, New Jersey, USA) was squeezed into a sterile ultrasound transducer probe cover (CIV-flex, latex-free, 8.9x91.5cm telescopic fold) (Figure B.3). The probe covers were secured to the ultrasound transducer using sterile elastic bands (Figure B.4) and the electrode insertion site was covered with Aquasonic 100 sterile ultrasound gel.

Figure B.3 Ultrasound transmission gel was deposited into the sterile ultrasound transducer probe cover

Figure B.4. The sterile ultrasound transducer probe cover was secured onto the ultrasound transducer probe with sterile elastic bands.

Aquasonic 100 ultrasound transmission gel was purchased from:

- Macdonald's Prescriptions and Medical Supplies
- 746 West Broadway
  Vancouver, B.C. V5Z 1G8
- Phone: (604) 872-2662
- Fax: (604) 876-0242
- website: www.macdonaldsrx.com

The sterile probe covers, sterile elastic bands and sterile ultrasound gel were purchased as a package from Cone Instruments (Item #914679).

- Cone Instruments, Inc
- PO Box 73065
  Cleveland, Ohio 44193
- Phone: 800-321-6964
- Fax: 800-987-2663
- website: www.coneinstruments.com

The electrode insertion site was covered with sterile Aquasonic 100 ultrasound transmission gel (Parker Laboratories Inc, New Jersey, USA) and the ultrasound transducer probe was placed on the low back (Figure B.5). A total of six fine-wire electrodes were inserted unilaterally into the right superficial and deep fibres at the L3, L4 and L5 vertebral laminar levels. Joel Stein (Stein et al. 1993) and Andrew Haig (Haig et al. 1991) have each developed and tested different techniques to insert needle electrodes into lumbar multifidus. Joel Stein described two separate techniques that both limit needle insertion depth to 2.5cm: the Stein midline technique and Stein paramedian technique (Stein et al.

Figure B.5 The ultrasound transducer probe inside the sterile cover was placed on the low back to image the lumbar spine.

1993). The Stein midline technique consists of a midline needle insertion directed caudolaterally in contrast to the paramedian technique which requires a needle insertion 3mm lateral to the midline (Stein et al. 1993). The Haig technique employs a medially directed insertion at 45°, 1cm superior to the inferior tip of the spinous process at 2.5cm lateral to the midline. The Haig technique appears to be more accurate with a reported accuracy rate of 81% in cadavers which they reason would have been 97% if EMG was available to guide insertion depth (Haig et al. 1991). Kim et al. (2005) compared both techniques and reported cadaver accuracy rates of 73% and 66% for the Haig and Stein techniques, respectively (Kim et al. 2005). No injections were found to penetrate the spinal canal using the Haig technique, however, 2.5% of insertions using the Stein techniques were inadvertently inserted into the spinal canal (Kim et al. 2005). These studies did not simultaneously image the lumbar musculature and these accuracy rates would have likely improved significantly with real-time ultrasound imaging.

Paul Hodges and colleagues have inserted deep and superficial lumbar multifidus fibre electrodes at L4 (Moseley et al. 2002; Moseley et al. 2003; Moseley et al. 2004; Saunders et al. 2004; Saunders et al. 2005) using a technique similar to that described by Andrew Haig (Haig et al. 1991). Needle electrodes were inserted at a distance of 40mm lateral to the midline with one set advanced medially to the L4 lamina (deep fibres) and the other set advanced 10mm into the skin (superficial fibres) (Moseley et al. 2002; Moseley et al. 2003; Moseley et al. 2004; Saunders et al. 2004; Saunders et al. 2005). Vasseljen et al. (2006) inserted intramuscular electrodes 30-40mm lateral to the midline with a medial direction to make recordings from lumbar multifidus at L5. To record from deep fibres the needle was advanced 30mm into the skin while the superficial fibre electrodes were advanced 10mm into the posterolateral multifidus fascial border (Vasseljen et al. 2006). These studies all employed a lateral insertion site with a medially directed needle to record from the deep and superficial lumbar multifidus fibres. Similar to these techniques, this study employed a modified Haig insertion with simultaneously ultrasound imaging due to its increased accuracy and safety (Kim et al. 2005).

At each vertebral level, fine-wire electrodes recording from superficial fibres were inserted prior to deep fibre electrodes and at insertion sites marginally closer to the midline. The fine-wire electrode was inserted into the skin but not the muscle and the participant was asked if the insertion site felt uncomfortable. Generally, participants did not find the insertion painful; however, on a few occasions the participant felt a stinging sensation which quickly faded. The experimenter then guided the needle through the first muscle fascial layer and into the paraspinal musculature (Figure B.6).

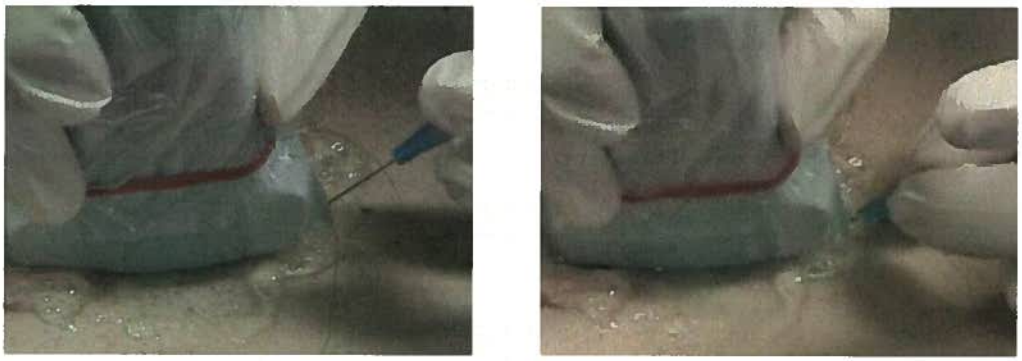

Figure B.6. The needle electrode being inserted into the skin under ultrasound guidance (left panel) and the needle being advanced into the paraspinal musculature under ultrasound guidance (right panel)

During fine-wire electrode fabrication it was determined that there was approximately 1.0-1.5mm between the tip of the hypodermic needle and the trailing edge of the beveled cannula tip. As the insertion needle penetrated through skin and muscle, the hooked wire ends protruding from the cannula tip were likely pushed toward the trailing edge of the beveled cannula tip. Accounting for the hooked wire lengths of 4.0mm and 0.5mm, it was determined that the electrode recoding site was between 1.5 and 5.0mm superficial to the needle tip visible under ultrasound. To account for this distance, the needle tip was inserted past its target location to ensure that both hooked ends were within the same muscle fibre groupings. Superficial fibre electrodes were inserted medially toward the spinous process and past the lumbar multifidus fascial layer, which was usually (depending on the participant) 10-25 mm beneath the skin (Figure B.7a). Deep fibre electrodes were inserted lateral to superficial fibre electrodes and directed medially towards the vertebral lamina (Figure B.7b).

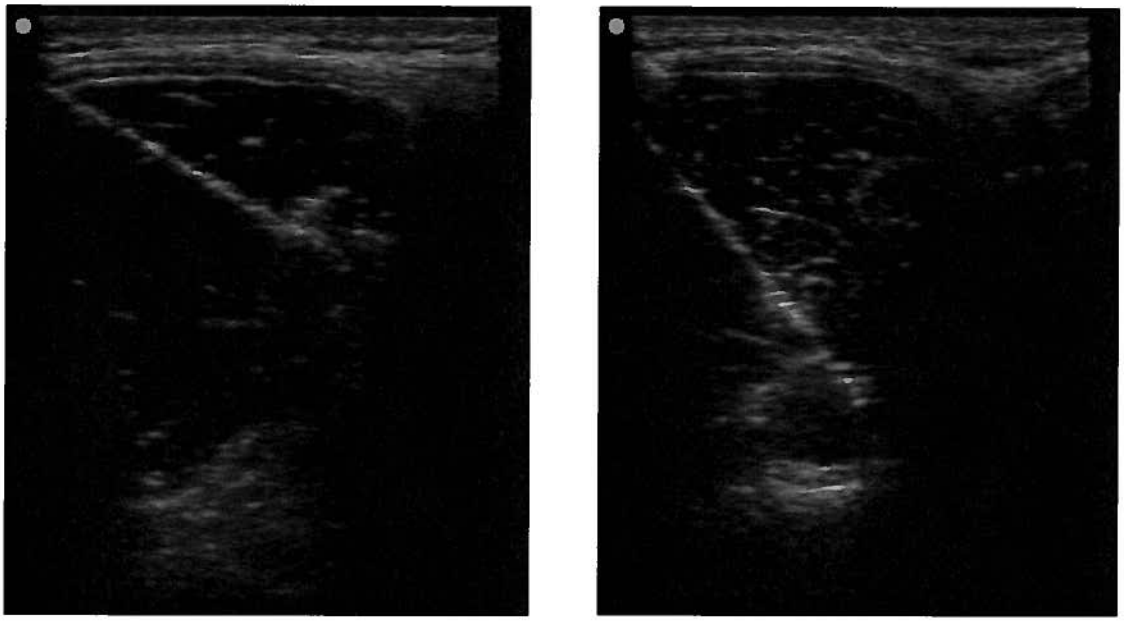

Figure B.7. Superficial and deep fine-wire needle electrode insertions. The superficial needle electrode insertion shown was at L5 of Subject 06 (left panel). Note that the superficial needle was medially directed toward the spinous process and inserted past the fascia layer surrounding lumbar multifidus. The deep needle electrode was inserted to the vertebral lamina at L5 of Subject 10 (right panel) and was usually tapped against the vertebral lamina to ensure it was within the deepest multifidus fibres.

In most subjects, the deep fibre needle electrode tip gently tapped the bony vertebral lamina before being withdrawn. This procedure was delicately performed to ensure that these fine-wire electrodes were inserted into the deepest multifidus fascicles. Once the desired muscle location was reached, the needle was removed from the skin leaving the wire in the muscle (Figure B.8).

Figure B.8. Fine-wire electrodes embedded in the superficial and deep lumbar multifidus fibres at L3, L4 and L5 after the insertion needles had been removed.

The wire was taped to the skin with sufficient slack in the wire to allow the subject's skin to move during the experimental activity. To secure the needle, hypodermic needle shields were cut along their length to allow the needle to be placed in the shield through the side of the shield (Figure B.9).

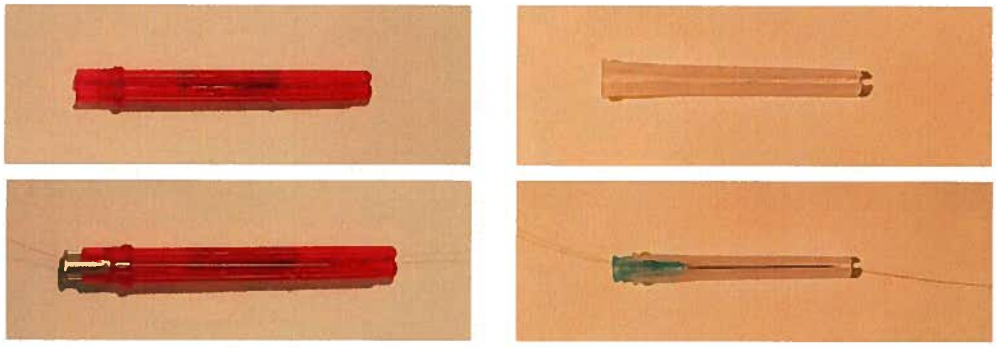

Figure B.9. The needle shield was cut along its length (top panels) to allow the insertion needle to be placed in the needle shield through the side of the shield while the fine-wire was still within the needle's cannula (bottom panels). The left panels show a Kendall Monoject needle and shield and the right panels show a Becton Dickinson needle and shield.

These exposed needle shields were taped to the participant's skin lateral to the electrode insertion sites. After the needle was withdrawn the fine-wire electrode could often be imaged with the ultrasound transducer (Figure B.10), although this was generally more difficult than imaging the fine-wire insertion needle.

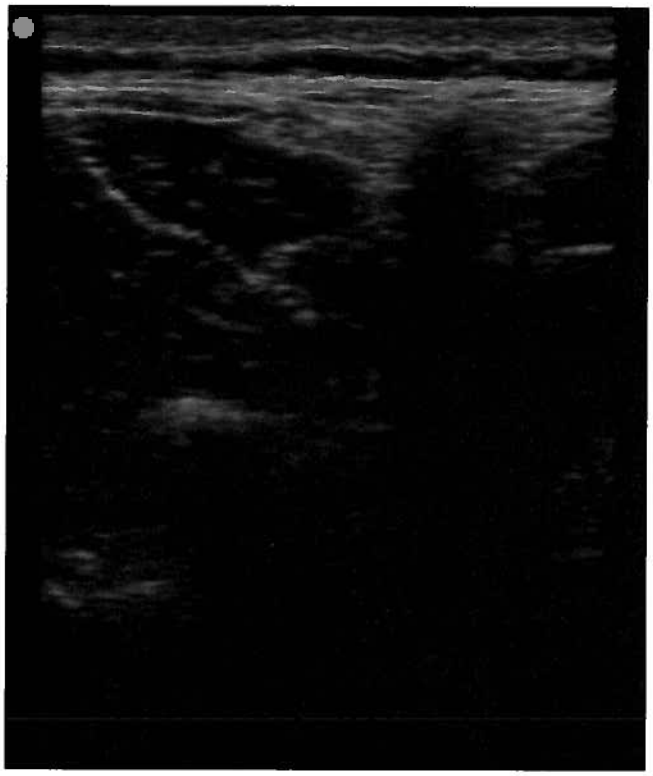

Figure B.10. Ultrasound image of a fine-wire electrode inserted into the superficial fibres of lumbar multifidus at L3 (just adjacent to the L3 spinous process). This image was taken after the needle was withdrawn from the muscle.

Appendix C: Ethical approval and participant consent form

The University of British Columbia
Office of Research Services
Clinical Research Ethics Board –
Room 210, 828 West 10th Avenue,
Vancouver, BC V5Z 1L8

ETHICS CERTIFICATE OF FULL BOARD APPROVAL: RENEWAL WITH AMENDMENTS TO THE STUDY

PRINCIPAL INVESTIGATOR:	DEPARTMENT:	UBC CREB NUMBER:
Jean-Sébastien Blouin	UBC	H04-70633

INSTITUTION(S) WHERE RESEARCH WILL BE CARRIED OUT:

Institution	Site
UBC	Vancouver (excludes UBC Hospital)

Other locations where the research will be conducted:
Not Applicable.

CO-INVESTIGATOR(S):
Scott T. Apperley
J.Timothy Inglis
Romeo Chua
Jean-Sébastien Blouin
David J. Sanderson

SPONSORING AGENCIES:
British Columbia Knowledge Development Fund - "Neurophysiology of the cervical spine; application of robotics and electroencephalography to injury prevention, assessment and rehabilitation"
Canada Foundation for Innovation
UBC Dean of Education
UBC Department of Human Kinetics - "Neurophysiology of the cervical spine; application of robotics and electroencephalography to injury prevention, assessment and rehabilitation"
UBC Faculty of Education

PROJECT TITLE:
Neural Consequences of Innocuous and Noxious Vertebral Stimulations

The current UBC CREB approval for this study expires: December 11, 2008

AMENDMENTS BELOW REVIEWED AT REB FULL BOARD MEETING DATE:
December 11, 2007

AMENDMENT(S):

Document Name	Version	Date
Protocol:		
Amendments to full protocol	5	November 6, 2007
Consent Forms:		
Subject consent form	5	November 6, 2007
Advertisements:		
Advertisement to Recruit Subjects	1	November 11, 2007

AMENDMENT APPROVAL DATE:
December 20, 2007

CERTIFICATION:
In respect of clinical trials:
1. The membership of this Research Ethics Board complies with the membership requirements for Research Ethics Boards defined in Division 5 of the Food and Drug Regulations.
2. The Research Ethics Board carries out its functions in a manner consistent with Good Clinical Practices.
3. This Research Ethics Board has reviewed and approved the clinical trial protocol and informed consent form for the trial which is to be conducted by the qualified investigator named above at the specified clinical trial site. This approval and the views of this Research Ethics Board have been documented in writing.

The UBC Clinical Research Ethics Board has reviewed the documentation for the above named project. The research study, as presented in the documentation, was found to be acceptable on ethical grounds for research involving human subjects and was approved for renewal by the UBC Clinical Research Ethics Board.

Approval of the Clinical Research Ethics Board by one of:

Dr. Gail Bellward, Chair

Appendix D: Statistical tests

"Average" rms, peak rms and time-to-peak rms were statistically tested with 2x3 repeated measures ANOVAs. In part A, the independent variables were perturbation displacement (D1, D2) and perturbation level (L3, L4, L5). In part B, the independent variables were perturbation velocity (low, high) and perturbation level (L3, L4, L5).

Table D.1 Statistical F values of the statistical repeated measures ANOVA tests for each EMG channel, independent and dependent variable.

Part A (Velocity = V1)

Dependent Measure	"Average" RMS		Peak RMS		Time-to-peak RMS	
Independent Variable	Disp	Level	Disp	Level	Disp	Level
L3 deep	1.37	1.13	2.23	1.3	3.25	2.27
L3 superficial	2.59	0.87	3.35	0.61	10.89	0.02
L4 deep	1.25	0.65	2.27	0.19	10.41	0.76
L4 superficial	0.007	1.64	0.02	1.47	32.05	0.48
L5 deep	0.34	0.94	3.36	0.62	17.85	3.23
L5 superficial	5.65	1.09	1.7	1.04	3.55	1.02

Part B (Displacement = D1)

Dependent Measure	"Average" RMS		Peak RMS		Time-to-peak RMS	
Independent Variable	Vel	Level	Vel	Level	Vel	Level
L3 deep	13.46	0.38	10.86	0.19	75.63	1.19
L3 superficial	0.24	0.85	0.11	0.72	29.19	0.27
L4 deep	4.06	0.6	5.53	0.05	221.79	1.27
L4 superficial	1.24	1.01	2.56	1.08	48.61	1.29
L5 deep	0.58	0.93	2.94	0.6	227.26	3.7
L5 superficial	2.12	1.82	2.35	1.51	73.9	1.91

Part B (Displacement = D2)

Dependent Measure	"Average" RMS		Peak RMS		Time-to-peak RMS	
Independent Variable	Vel	Level	Vel	Level	Vel	Level
L3 deep	10.23	1.04	10.48	1.12	132.64	0.12
L3 superficial	4.76	0.94	1.93	0.75	45.47	0.14
L4 deep	5.89	0.55	6.43	0.09	59.36	0.71
L4 superficial	2.1	1.08	2.73	1.03	48.28	0.21
L5 deep	8.17	0.43	6.59	0.07	277.87	1.97
L5 superficial	2.96	1.44	3.74	1.02	96.63	0.76

All degrees of freedom for perturbation displacement and velocity were (1,8) and all degrees of freedom for perturbation level were (2,16). Mauchly's test of sphericity was evaluated prior to each statistical test and greenhouse-geisser corrections were applied when this assumption was violated. The following table reports the actual degrees of freedom after greenhouse-geisser corrections (when applicable).

Table D.2 Degrees of freedom for each statistical repeated measures ANOVA test for each EMG channel, independent and dependent variable.

Part A (Velocity = V1)

Dependent Measure	"Average" RMS		Peak RMS		Time-to-peak RMS	
Independent Variable	Disp	Level	Disp	Level	Disp	Level
L3 deep	1,8	1.09, 8.75	1,8	1.18, 9.40	1,8	2, 16
L3 superficial	1,8	1.02, 8.13	1,8	1.02, 8.20	1,8	2, 16
L4 deep	1,8	1.19, 9.50	1,8	1.20, 9.60	1,8	1.25, 10.00
L4 superficial	1,8	2, 16	1,8	2, 16	1,8	2, 16
L5 deep	1,8	1.01, 8.05	1,8	1.06, 8.50	1,8	2, 16
L5 superficial	1,8	1.01, 8.09	1,8	1.03, 8.21	1,8	2, 16

Part B (Displacement = D1)

Dependent Measure	"Average" RMS		Peak RMS		Time-to-peak RMS	
Independent Variable	Vel	Level	Vel	Level	Vel	Level
L3 deep	1,8	2, 16	1,8	2, 16	1,8	2, 16
L3 superficial	1,8	1.08, 8.63	1,8	1.07, 8.59	1,8	2, 16
L4 deep	1,8	2, 16	1,8	2, 16	1,8	2, 16
L4 superficial	1,8	1.12, 8.95	1,8	1.12, 8.94	1,8	2, 16
L5 deep	1,8	1.04, 8.34	1,8	1.11, 8.89	1,8	2, 16
L5 superficial	1,8	1.18, 9.40	1,8	1.08, 8.67	1,8	2, 16

Part B (Displacement = D2)

Dependent Measure	"Average" RMS		Peak RMS		Time-to-peak RMS	
Independent Variable	Vel	Level	Vel	Level	Vel	Level
L3 deep	1,8	1.21, 9.65	1,8	1.20, 9.54	1,8	2, 16
L3 superficial	1,8	1.06, 8.46	1,8	1.04, 8.32	1,8	2, 16
L4 deep	1,8	2, 16	1,8	2, 16	1,8	1.12, 8.93
L4 superficial	1,8	2, 16	1,8	2, 16	1,8	2, 16
L5 deep	1,8	1.01, 8.11	1,8	1.08, 8.67	1,8	2, 16
L5 superficial	1,8	2, 16	1,8	2, 16	1,8	2, 16

Table D.3. Summary of statistical p values for Part A and B statistical tests. Statistically significant effects are denoted with **

Part A (Velocity = V1)

Dependent Measure	"Average" RMS		Peak RMS		Time-to-peak RMS	
Independent Variable	Disp	Level	Disp	Level	Disp	Level
L3 deep	0.28	0.32	0.17	0.29	0.11	0.14
L3 superficial	0.15	0.38	0.1	0.46	0.01**	0.98
L4 deep	0.3	0.46	0.17	0.71	0.01**	0.48
L4 superficial	0.94	0.22	0.88	0.26	<0.001**	0.63
L5 deep	0.58	0.36	0.1	0.46	0.003**	0.07
L5 superficial	0.045**	0.33	0.23	0.34	0.1	0.38

Part B (Displacement = D1)

Dependent Measure	"Average" RMS		Peak RMS		Time-to-peak RMS	
Independent Variable	Vel	Level	Vel	Level	Vel	Level
L3 deep	0.006**	0.69	0.01**	0.83	Interaction =0.04**	
L3 superficial	0.63	0.39	0.75	0.43	<0.001**	0.77
L4 deep	0.08	0.56	0.047**	0.95	<0.001**	0.31
L4 superficial	0.3	0.39	0.15	0.34	<0.001**	0.3
L5 deep	0.47	0.37	0.12	0.48	<0.001**	0.048**
L5 superficial	0.18	0.21	0.16	0.26	<0.001**	0.18

Part B (Displacement = D2)

Dependent Measure	"Average" RMS		Peak RMS		Time-to-peak RMS	
Independent Variable	Vel	Level	Vel	Level	Vel	Level
L3 deep	0.01**	0.35	0.01**	0.33	<0.001**	0.89
L3 superficial	0.06	0.36	0.2	0.42	<0.001**	0.87
L4 deep	0.04**	0.58	0.04**	0.92	<0.001**	0.44
L4 superficial	0.18	0.36	0.14	0.38	<0.001**	0.82
L5 deep	0.02**	0.53	0.03**	0.81	<0.001**	0.17
L5 superficial	0.12	0.27	0.09	0.38	<0.001**	0.48

Table D.4. Mean square error values for each statistical ANOVA test for each EMG channel, independent and dependent variable.

Part A (Velocity = V1)

Dependent Measure	"Average" RMS		Peak RMS		Time-to-peak RMS	
Independent Variable	Disp	Level	Disp	Level	Disp	Level
L3 deep	2.04	210.67	39.28	1702.4	0.008	0.014
L3 superficial	1.66	1177.14	18.98	15208.53	0.01	0.02
L4 deep	0.29	378.38	90.39	4884	0.02	0.05
L4 superficial	31.78	664.54	629.48	8925.86	0.007	0.06
L5 deep	17.26	2288.03	599.84	23702.89	0.005	0.02
L5 superficial	4.27	1067.14	332.7	6198.22	0.008	0.02

Part B (Displacement = D1)

Dependent Measure	"Average" RMS		Peak RMS		Time-to-peak RMS	
Independent Variable	Vel	Level	Vel	Level	Vel	Level
L3 deep	9.92	73.91	208.09	495.15	0.02	0.01
L3 superficial	86.92	774.7	1095.44	9558.27	0.03	0.01
L4 deep	122.4	230.3	1191.18	171.96	0.01	0.02
L4 superficial	743.38	2682.49	3527.86	20896.72	0.02	0.01
L5 deep	112.97	1231.62	1230.92	12958.19	0.004	0.01
L5 superficial	424.02	567.29	4627.88	3486	0.02	0.01

Part B (Displacement = D2)

Dependent Measure	"Average" RMS		Peak RMS		Time-to-peak RMS	
Independent Variable	Vel	Level	Vel	Level	Vel	Level
L3 deep	18.42	208.22	154.06	1647.8	0.01	0.01
L3 superficial	53.67	815.05	848.01	8551.7	0.03	0.02
L4 deep	343.42	423.38	4265.7	6654.02	0.04	0.02
L4 superficial	1291.27	1440.65	12049.13	14847.46	0.04	0.02
L5 deep	402.41	1906.88	816.58	22374.29	0.01	0.01
L5 superficial	545.46	355.77	4764.21	1848.74	0.02	0.01

Table D.5. Estimates of effect size as measured by partial eta square (n_p^2) for each EMG channel, independent and dependent variable.

Part A (Velocity = V1)

Dependent Measure	"Average" RMS		Peak RMS		Time-to-peak RMS	
Independent Variable	Disp	Level	Disp	Level	Disp	Level
L3 deep	0.15	0.12	0.22	0.14	0.29	0.22
L3 superficial	0.25	0.1	0.3	0.07	0.58	<0.01
L4 deep	0.14	0.08	0.22	0.02	0.56	0.09
L4 superficial	<0.01	0.17	<0.01	0.16	0.8	0.06
L5 deep	0.04	0.1	0.3	0.07	0.69	0.29
L5 superficial	0.41	0.12	0.18	0.12	0.31	0.11

Part B (Displacement = D1)

Dependent Measure	"Average" RMS		Peak RMS		Time-to-peak RMS	
Independent Variable	Vel	Level	Vel	Level	Vel	Level
L3 deep	0.63	0.04	0.58	0.02	0.9	0.13
L3 superficial	0.03	0.1	0.01	0.08	0.78	0.03
L4 deep	0.34	0.07	0.41	0.01	0.96	0.14
L4 superficial	0.14	0.11	0.24	0.12	0.86	0.14
L5 deep	0.07	0.1	0.27	0.07	0.97	0.32
L5 superficial	0.21	0.19	0.23	0.16	0.9	0.19

Part B (Displacement = D2)

Dependent Measure	"Average" RMS		Peak RMS		Time-to-peak RMS	
Independent Variable	Vel	Level	Vel	Level	Vel	Level
L3 deep	0.56	0.12	0.57	0.12	0.94	0.01
L3 superficial	0.37	0.11	0.19	0.08	0.85	0.02
L4 deep	0.42	0.06	0.45	0.01	0.88	0.08
L4 superficial	0.21	0.12	0.25	0.11	0.86	0.02
L5 deep	0.5	0.05	0.45	0.01	0.97	0.20
L5 superficial	0.27	0.15	0.32	0.11	0.92	0.09

Appendix E: Individual subject data

The individual subject data are presented in Appendix E. The following eighteen pages (pages 136-153) contain tables of the dependent measures for the nine study participants included in data analysis. The individual participant means are also displayed graphically in figures at the end of this appendix. Subject 07 was removed from analysis due to reasons discussed in section 7.1.1 and this participant's data were removed from the tables.

Individual Participant Means

EMG responses to perturbations of the same velocity and displacement were averaged for each subject to create nine means for each of the nine perturbation velocity-displacement combinations for each perturbation level, EMG channel and participant. These means are displayed in the following tables with each row a different participant and each column a different perturbation velocity-displacement combination. Perturbations at the V3 velocity or to the D3 displacement were excluded from analysis; however, the means for these perturbations are displayed in the following tables (refer to section 7.1.2 for the specific velocities and displacements). The means for each perturbation level are displayed in a different table with all perturbation levels for a single EMG channel displayed on the same page. The "average" RMS dependent measure is displayed first and is followed by peak RMS with the values of both of these dependent measures in microvolts (μV). The last dependent measure displayed is time-to-peak RMS with values displayed in seconds. The last two rows of each table display the mean of all individual participant means and the standard error of the participant means. It must be noted that EMG values were not normalized and thus these means may not be indicative of the general trend within each participant.

"Average" RMS: L3 deep

L3 perturbation level

μV	V1-D1	V1-D2	V1-D3	V2-D1	V2-D2	V2-D3	V3-D1	V3-D2	V3-D3
S 01	0.26	0.49	0.21	0.57	0.44	1.65	0.38	2.98	2.12
S 02	0.80	0.32	0.56	4.64	3.46	9.86	5.25	9.05	17.02
S 03	26.95	32.67	54.16	24.18	42.19	58.31	31.70	45.91	73.21
S 04	0.57	0.61	0.49	3.19	1.11	1.88	1.53	2.56	2.34
S 05	0.97	0.55	0.68	2.56	2.30	1.86	1.87	3.23	3.15
S 06	8.02	9.86	23.18	16.51	24.61	28.62	18.22	25.74	52.24
S 08	0.23	0.24	0.36	1.53	4.23	3.01	2.50	3.03	2.78
S 09	4.69	8.24	8.03	9.45	13.91	12.45	1.60	11.48	10.57
S 10	0.47	0.54	0.97	1.83	2.52	2.81	1.62	3.67	4.49
Average	4.77	5.95	9.85	7.16	10.53	13.38	7.18	11.96	18.66
Std Err	8.73	10.70	18.25	8.13	14.25	18.99	10.71	14.77	25.99

L4 perturbation level

μV	V1-D1	V1-D2	V1-D3	V2-D1	V2-D2	V2-D3	V3-D1	V3-D2	V3-D3
S 01	0.44	0.40	0.30	0.59	0.39	0.57	0.39	0.67	0.92
S 02	1.01	1.40	1.27	8.29	10.48	10.16	10.11	11.09	14.41
S 03	41.52	43.98	71.77	36.94	33.58	68.38	38.98	44.47	76.19
S 04	0.73	0.73	0.63	0.96	1.77	1.39	1.12	1.37	2.76
S 05	3.56	1.77	3.16	5.45	9.39	9.61	5.42	8.80	12.10
S 06	3.47	3.09	2.40	5.20	11.67	12.19	10.44	23.84	43.70
S 08	0.30	0.19	0.23	1.52	1.47	2.15	1.13	1.46	4.21
S 09	0.26	2.45	2.91	1.79	3.32	4.11	3.04	6.14	8.61
S 10	0.33	1.11	0.35	1.90	2.72	2.70	2.36	4.18	7.11
Average	5.74	6.12	9.22	6.96	8.31	12.36	8.11	11.34	18.89
Std Err	13.49	14.23	23.48	11.53	10.39	21.43	12.17	14.36	25.02

L5 perturbation level

μV	V1-D1	V1-D2	V1-D3	V2-D1	V2-D2	V2-D3	V3-D1	V3-D2	V3-D3
S 01	0.47	0.40	0.31	10.07	2.49	2.65	3.68	2.40	5.34
S 02	0.96	0.89	1.31	18.07	19.09	23.21	16.72	22.93	29.75
S 03	-0.28	-1.08	-0.97	16.27	2.25	60.54	1.45	6.64	48.92
S 04	0.69	0.69	0.65	0.91	1.23	1.56	2.45	2.45	3.42
S 05	5.30	3.93	10.66	7.14	7.49	6.52	6.12	5.83	7.07
S 06	1.54	1.43	4.23	3.18	4.39	5.64	3.07	9.05	11.27
S 08	0.18	0.20	0.25	0.49	0.72	1.09	0.46	0.88	0.92
S 09	0.41	1.40	0.41	2.87	5.86	3.97	3.40	5.71	6.51
S 10	0.78	0.40	1.18	3.45	4.71	4.89	4.93	6.45	7.61
Average	1.12	0.92	2.00	6.94	5.36	12.23	4.70	6.93	13.42
Std Err	1.65	1.36	3.54	6.53	5.60	19.31	4.82	6.53	15.71

"Average" RMS: L3 superficial

L3 perturbation level

μV	V1-D1	V1-D2	V1-D3	V2-D1	V2-D2	V2-D3	V3-D1	V3-D2	V3-D3
S 01	0.39	0.37	0.23	0.32	0.37	0.37	0.39	0.35	0.39
S 02	0.82	0.53	0.57	1.02	0.64	1.32	1.04	1.48	1.36
S 03	43.13	69.34	150.19	39.38	101.28	141.18	56.38	105.58	171.65
S 04	0.46	0.57	0.52	0.66	0.76	0.62	0.61	0.76	0.65
S 05	1.07	0.92	1.05	1.41	1.45	1.54	1.13	1.50	2.14
S 06	14.33	17.46	63.83	27.03	38.59	48.95	26.34	39.81	68.05
S 08	0.39	0.86	2.48	9.32	12.78	14.69	6.25	15.48	15.83
S 09	0.81	1.82	1.84	2.23	7.57	7.23	2.67	5.22	11.17
S 10	0.18	0.19	0.35	0.30	0.45	0.75	0.45	0.78	0.52
Average	6.84	10.23	24.56	9.07	18.21	24.07	10.59	19.00	30.20
Std Err	14.35	22.85	51.49	14.30	33.51	46.62	19.08	34.92	57.31

L4 perturbation level

μV	V1-D1	V1-D2	V1-D3	V2-D1	V2-D2	V2-D3	V3-D1	V3-D2	V3-D3
S 01	0.51	0.44	0.35	0.72	0.75	0.69	0.77	0.77	1.16
S 02	0.68	0.67	0.56	0.83	1.21	1.92	1.03	1.14	1.61
S 03	111.79	95.46	209.90	63.94	47.61	141.58	53.92	82.37	171.89
S 04	0.65	0.58	0.48	0.64	0.61	0.63	0.58	0.70	0.77
S 05	1.47	0.82	1.20	1.38	4.00	2.69	2.52	3.19	3.93
S 06	10.59	11.49	16.37	8.95	14.43	22.96	8.78	16.46	27.52
S 08	0.33	1.73	0.83	21.20	24.84	23.23	28.31	17.72	35.78
S 09	0.29	0.32	0.69	7.84	11.18	12.25	8.18	8.85	12.21
S 10	0.34	0.39	0.38	4.14	4.45	3.59	4.88	5.09	7.42
Average	14.07	12.43	25.64	12.18	12.12	23.28	12.11	15.14	29.14
Std Err	36.79	31.34	69.29	20.51	15.54	45.29	17.91	26.04	54.96

L5 perturbation level

μV	V1-D1	V1-D2	V1-D3	V2-D1	V2-D2	V2-D3	V3-D1	V3-D2	V3-D3
S 01	0.69	0.45	0.29	8.49	4.69	6.35	11.83	6.83	2.16
S 02	0.73	0.62	1.22	0.50	0.75	0.64	0.58	0.74	0.86
S 03	2.09	0.92	6.02	5.13	10.65	25.43	-0.09	9.58	40.39
S 04	0.52	0.52	0.52	0.54	0.55	0.60	0.60	0.66	0.64
S 05	0.89	0.71	1.22	2.00	2.87	3.06	2.40	2.91	5.03
S 06	8.26	8.35	11.56	9.80	12.19	13.21	11.89	11.71	17.02
S 08	8.74	10.02	3.24	16.05	23.32	22.94	18.10	26.56	30.08
S 09	0.41	0.63	0.56	9.02	13.23	15.73	7.94	13.72	12.93
S 10	0.70	0.32	1.33	2.36	2.71	2.98	3.67	3.49	4.52
Average	2.56	2.50	2.88	5.99	7.89	10.10	6.33	8.47	12.63
Std Err	3.40	3.81	3.72	5.26	7.58	9.59	6.44	8.26	14.18

"Average" RMS: L4 deep

L3 perturbation level

μV	V1-D1	V1-D2	V1-D3	V2-D1	V2-D2	V2-D3	V3-D1	V3-D2	V3-D3
S 01	0.63	0.68	0.83	1.18	1.54	1.45	1.16	1.96	2.16
S 02	0.88	0.73	1.08	3.43	5.90	6.83	3.95	6.98	14.34
S 03	35.13	40.06	90.66	33.53	59.97	77.22	43.76	60.80	101.70
S 04	0.16	0.19	0.22	0.20	0.21	0.22	0.12	0.49	0.31
S 05	10.99	10.53	11.87	20.35	19.96	29.23	23.82	26.00	41.87
S 06	34.04	34.84	89.50	61.29	69.90	84.15	55.54	76.45	104.62
S 08	0.20	0.13	1.10	0.34	1.31	0.53	0.63	0.97	0.91
S 09	0.49	0.93	1.09	8.11	11.65	12.47	7.80	14.96	29.22
S 10	0.65	0.66	0.67	0.87	1.42	2.77	1.08	1.36	1.91
Average	9.24	9.86	21.89	14.37	19.10	23.87	15.32	21.11	33.00
Std Err	14.78	16.03	38.83	20.97	26.87	33.50	21.02	28.47	42.29

L4 perturbation level

μV	V1-D1	V1-D2	V1-D3	V2-D1	V2-D2	V2-D3	V3-D1	V3-D2	V3-D3
S 01	0.49	0.64	0.86	11.84	9.73	11.27	8.47	14.86	13.94
S 02	0.89	0.89	0.73	5.88	10.10	9.88	6.07	10.23	16.12
S 03	60.06	59.48	116.86	37.26	36.73	83.44	48.29	58.41	101.07
S 04	0.13	0.15	0.18	0.14	0.17	0.60	0.19	0.20	0.39
S 05	15.08	17.35	28.25	27.00	68.47	76.31	53.76	54.69	92.91
S 06	22.56	10.43	33.62	19.30	21.82	59.24	26.86	39.43	58.75
S 08	0.15	0.19	0.19	0.59	2.17	1.63	0.58	1.10	1.81
S 09	2.69	3.30	11.99	50.69	90.08	147.47	72.98	91.81	186.68
S 10	0.35	1.63	0.28	1.00	1.65	1.86	1.15	2.29	4.09
Average	11.38	10.45	21.44	17.08	26.77	43.52	24.26	30.34	52.86
Std Err	19.96	19.30	38.07	18.07	32.37	51.51	27.57	32.47	63.71

L5 perturbation level

μV	V1-D1	V1-D2	V1-D3	V2-D1	V2-D2	V2-D3	V3-D1	V3-D2	V3-D3
S 01	0.58	0.59	0.61	5.42	7.23	8.11	6.42	10.20	14.47
S 02	0.71	1.25	1.41	3.13	6.24	6.98	3.45	8.00	14.25
S 03	1.99	0.29	0.07	11.51	8.93	26.93	3.03	11.81	31.68
S 04	0.14	0.14	0.16	0.62	1.06	1.14	0.20	1.16	1.82
S 05	18.10	17.32	32.49	56.54	70.63	96.02	61.30	74.54	163.77
S 06	21.11	30.45	53.30	21.13	43.24	60.05	30.85	57.37	62.50
S 08	0.92	0.62	0.68	3.07	3.82	5.30	3.15	3.91	5.23
S 09	0.52	1.25	2.12	8.97	10.63	10.84	7.40	11.32	11.73
S 10	1.19	0.52	3.20	1.25	1.25	3.21	2.79	1.86	1.96
Average	5.03	5.83	10.45	12.41	17.00	24.29	13.18	20.02	34.16
Std Err	8.31	10.76	19.14	17.75	23.87	32.62	20.25	26.68	52.22

"Average" RMS: L4 superficial

L3 perturbation level

μV	V1-D1	V1-D2	V1-D3	V2-D1	V2-D2	V2-D3	V3-D1	V3-D2	V3-D3
S 01	0.31	0.32	0.22	0.27	0.32	0.27	0.35	0.33	0.25
S 02	1.95	0.27	1.04	1.00	1.32	2.46	1.31	1.96	1.40
S 03	35.11	50.58	112.48	31.47	68.20	98.71	43.92	73.82	120.55
S 04	0.39	0.36	0.50	0.94	1.39	1.72	0.47	1.48	2.25
S 05	5.80	5.58	6.72	13.07	21.68	17.51	12.26	22.91	34.01
S 06	63.08	20.18	57.66	52.18	71.91	74.51	56.22	76.96	100.60
S 08	0.53	0.58	1.26	1.01	2.42	1.99	0.98	2.65	3.47
S 09	0.28	0.92	0.58	0.62	3.16	1.09	0.56	1.07	1.53
S 10	0.55	0.79	0.80	0.93	1.03	0.97	1.04	1.17	1.46
Average	12.00	8.84	20.14	11.27	19.05	22.14	13.01	20.26	29.50
Std Err	22.23	16.94	39.33	18.52	29.68	37.43	21.56	32.05	47.43

L4 perturbation level

μV	V1-D1	V1-D2	V1-D3	V2-D1	V2-D2	V2-D3	V3-D1	V3-D2	V3-D3
S 01	1.53	23.01	1.65	32.46	38.34	36.00	43.89	44.07	46.21
S 02	0.20	0.52	0.26	0.54	0.83	3.03	0.57	1.04	1.41
S 03	72.88	70.86	134.32	39.49	36.60	99.02	50.48	60.83	110.88
S 04	0.16	0.12	0.15	0.25	0.20	0.19	0.17	0.19	0.41
S 05	94.46	76.89	157.17	215.61	237.89	334.85	276.50	277.07	348.37
S 06	10.79	20.78	20.27	12.66	24.69	33.62	11.81	21.89	54.22
S 08	0.59	0.73	0.79	1.19	2.67	3.73	1.73	1.15	2.57
S 09	0.25	0.18	0.17	0.42	0.75	1.13	0.68	1.14	1.28
S 10	0.59	2.80	0.62	4.98	4.67	11.75	6.52	12.98	16.53
Average	20.16	21.77	35.04	34.18	38.52	58.15	43.59	46.71	64.65
Std Err	36.57	30.90	63.35	69.62	76.40	108.45	89.45	89.04	112.58

L5 perturbation level

μV	V1-D1	V1-D2	V1-D3	V2-D1	V2-D2	V2-D3	V3-D1	V3-D2	V3-D3
S 01	0.43	0.42	0.30	0.44	0.65	2.94	0.43	0.56	0.49
S 02	1.96	3.33	6.37	1.42	5.35	5.28	1.35	3.54	4.70
S 03	3.23	1.78	4.30	10.72	10.74	20.19	5.84	12.30	25.40
S 04	0.15	0.15	0.19	0.24	0.20	0.55	0.20	0.77	0.66
S 05	21.75	27.95	45.52	91.11	114.69	127.15	96.76	129.71	171.46
S 06	16.61	21.55	39.97	41.53	56.58	79.55	20.07	38.01	68.70
S 08	1.16	0.93	0.92	3.03	5.02	8.18	4.12	5.15	7.00
S 09	0.17	0.20	0.14	0.80	1.10	1.25	1.00	1.41	1.93
S 10	1.09	0.73	0.97	1.17	2.62	1.80	1.07	1.19	2.53
Average	5.17	6.34	10.96	16.72	21.88	27.43	14.54	21.40	31.43
Std Err	8.10	10.61	18.19	30.90	39.09	45.05	31.46	42.34	56.96

"Average" RMS: L5 deep

L3 perturbation level

μV	V1-D1	V1-D2	V1-D3	V2-D1	V2-D2	V2-D3	V3-D1	V3-D2	V3-D3
S 01	0.18	0.15	0.17	0.31	0.29	0.24	0.23	0.22	0.31
S 02	0.57	0.69	0.93	4.51	5.05	10.42	4.14	7.18	21.42
S 03	78.71	113.49	298.03	70.79	158.36	255.50	95.64	165.35	338.94
S 04	0.55	0.80	0.94	1.18	1.56	2.27	1.00	3.04	4.20
S 05	0.52	0.16	1.11	1.35	1.06	1.52	1.40	1.02	3.89
S 06	13.81	15.11	60.59	31.07	25.33	42.53	23.21	46.63	50.68
S 08	0.20	0.29	0.99	0.29	0.84	0.31	0.61	0.98	0.40
S 09	0.13	0.20	0.13	1.12	2.61	1.43	1.19	2.55	3.43
S 10	0.08	-0.04	0.10	0.89	2.16	2.55	1.41	2.95	6.08
Average	10.53	14.54	40.33	12.39	21.92	35.20	14.31	25.55	47.71
Std Err	25.95	37.43	98.65	24.03	51.77	83.71	31.36	54.45	110.40

L4 perturbation level

μV	V1-D1	V1-D2	V1-D3	V2-D1	V2-D2	V2-D3	V3-D1	V3-D2	V3-D3
S 01	0.55	0.65	0.66	3.03	2.46	3.97	11.92	9.49	2.95
S 02	0.79	0.82	1.04	8.51	10.92	16.77	9.06	12.85	18.97
S 03	154.47	148.40	340.16	92.96	78.10	241.37	98.09	146.26	292.43
S 04	0.47	0.74	5.06	6.68	9.17	10.97	6.66	11.34	12.23
S 05	8.89	6.93	17.35	18.00	22.71	26.14	24.63	36.06	31.00
S 06	26.80	8.58	23.79	20.96	24.13	31.93	21.28	16.40	32.07
S 08	0.31	0.34	0.44	0.70	2.59	4.11	0.91	1.24	2.06
S 09	0.20	0.22	0.14	5.33	5.80	6.29	4.79	5.49	8.63
S 10	0.56	2.66	0.64	4.21	4.84	6.31	5.23	6.86	8.54
Average	21.45	18.81	43.25	17.82	17.86	38.65	20.28	27.33	45.43
Std Err	50.64	48.69	111.67	28.98	23.98	76.67	30.20	45.69	93.27

L5 perturbation level

μV	V1-D1	V1-D2	V1-D3	V2-D1	V2-D2	V2-D3	V3-D1	V3-D2	V3-D3
S 01	0.20	0.21	0.30	4.27	0.83	0.97	0.26	3.58	1.54
S 02	1.22	5.52	3.41	22.32	21.24	23.03	12.65	29.47	18.77
S 03	12.02	7.02	14.64	25.87	30.05	53.31	15.51	32.68	60.86
S 04	1.93	4.85	1.06	11.55	14.53	9.77	10.51	15.13	17.42
S 05	5.91	8.35	13.55	28.88	40.14	31.71	11.41	32.51	22.37
S 06	17.08	17.70	23.86	18.98	24.05	32.45	14.04	23.07	31.01
S 08	0.32	0.39	0.30	0.35	0.46	1.66	1.19	0.88	1.25
S 09	0.12	0.12	0.23	0.25	0.49	0.82	0.27	0.58	0.61
S 10	0.39	0.39	-0.53	1.89	2.38	4.26	2.44	3.30	6.57
Average	4.35	4.95	6.31	12.71	14.91	17.55	7.59	15.69	17.82
Std Err	6.18	5.77	8.82	11.53	14.84	18.63	6.40	13.98	19.40

"Average" RMS: L5 superficial

L3 perturbation level

μV	V1-D1	V1-D2	V1-D3	V2-D1	V2-D2	V2-D3	V3-D1	V3-D2	V3-D3
S 01	0.26	0.21	0.23	0.21	0.23	0.34	0.24	0.30	0.47
S 02	0.83	0.59	1.33	5.13	4.29	6.48	4.40	5.74	7.27
S 03	55.01	69.34	107.37	59.74	84.83	105.17	74.51	91.12	139.94
S 04	0.46	1.60	3.88	2.38	1.58	2.64	1.34	1.83	2.50
S 05	0.82	0.94	1.78	2.23	2.50	4.01	2.89	3.19	4.01
S 06	19.17	25.37	85.99	31.33	42.07	60.30	42.44	44.74	106.62
S 08	0.19	0.36	0.85	0.28	0.92	0.66	0.50	0.76	0.60
S 09	0.38	1.26	0.42	6.16	15.87	7.56	6.32	12.99	16.80
S 10	3.51	3.58	5.65	32.24	45.18	32.91	43.83	66.14	85.93
Average	8.96	11.47	23.06	15.52	21.94	24.45	19.61	25.20	40.46
Std Err	18.32	23.15	42.12	20.91	29.48	36.27	27.12	33.87	54.73

L4 perturbation level

μV	V1-D1	V1-D2	V1-D3	V2-D1	V2-D2	V2-D3	V3-D1	V3-D2	V3-D3
S 01	0.42	0.48	0.50	1.43	1.35	1.41	1.08	1.99	2.94
S 02	0.78	1.30	0.78	2.59	4.28	4.51	4.12	4.99	5.26
S 03	111.59	112.93	148.50	79.35	75.62	129.51	85.55	95.56	133.65
S 04	0.15	0.19	0.19	0.19	0.26	0.25	0.23	0.37	2.01
S 05	2.43	4.22	6.04	8.20	10.18	12.05	9.02	10.04	14.38
S 06	12.85	17.19	21.89	15.10	19.45	30.19	13.47	54.06	59.96
S 08	0.32	0.37	0.43	0.78	1.49	1.52	0.74	0.81	1.44
S 09	0.04	-0.29	-0.49	29.34	28.93	31.12	25.10	28.48	37.76
S 10	5.80	17.97	3.65	90.53	93.19	75.46	99.34	110.02	155.86
Average	14.93	17.15	20.17	25.28	26.08	31.78	26.52	34.03	45.92
Std Err	36.49	36.65	48.63	35.19	34.68	43.91	38.36	42.83	59.63

L5 perturbation level

μV	V1-D1	V1-D2	V1-D3	V2-D1	V2-D2	V2-D3	V3-D1	V3-D2	V3-D3
S 01	2.03	0.38	0.30	2.67	2.08	2.56	8.24	2.22	2.71
S 02	0.96	1.19	1.33	1.74	5.32	2.88	1.61	3.35	2.94
S 03	16.88	11.52	28.85	31.71	38.83	57.43	19.50	38.60	62.03
S 04	0.15	0.14	0.15	2.01	0.50	0.16	-0.89	1.96	0.41
S 05	2.19	2.96	5.50	11.64	15.30	14.59	6.24	15.31	9.72
S 06	20.62	20.38	37.53	18.88	31.08	48.60	14.35	36.74	46.82
S 08	0.41	0.32	0.82	1.16	1.02	1.45	1.08	1.20	1.17
S 09	-0.49	0.47	0.78	-0.03	0.36	1.26	4.23	0.42	1.08
S 10	2.17	1.04	1.59	43.00	64.55	47.59	31.32	66.22	75.15
Average	4.99	4.27	8.54	12.53	17.67	19.61	9.52	18.45	22.45
Std Err	7.92	7.04	14.23	15.61	22.63	24.22	10.49	23.50	30.13

Peak RMS: L3 deep

L3 perturbation level

μV	V1-D1	V1-D2	V1-D3	V2-D1	V2-D2	V2-D3	V3-D1	V3-D2	V3-D3
S 01	4.50	7.30	4.52	6.24	4.78	15.11	4.85	25.44	16.98
S 02	7.89	8.60	8.23	27.11	20.03	50.53	30.13	46.71	76.94
S 03	118.99	138.45	176.24	102.50	142.82	179.48	114.42	174.71	217.96
S 04	20.75	17.36	19.15	32.19	23.24	30.50	28.55	29.85	31.63
S 05	8.32	7.44	10.49	13.90	12.90	15.39	13.03	21.37	18.39
S 06	34.80	47.09	110.05	46.92	77.43	88.30	58.08	80.40	158.84
S 08	3.99	3.98	5.59	10.72	20.04	14.44	13.81	14.98	12.01
S 09	43.10	52.68	53.11	55.01	60.07	64.87	12.50	56.39	49.77
S 10	6.49	7.04	11.70	12.80	14.46	15.59	12.17	16.46	18.96
Average	27.65	32.22	44.34	34.16	41.75	52.69	31.95	51.81	66.83
Std Err	37.06	43.83	60.24	30.65	44.80	54.35	34.80	50.84	73.37

L4 perturbation level

μV	V1-D1	V1-D2	V1-D3	V2-D1	V2-D2	V2-D3	V3-D1	V3-D2	V3-D3
S 01	8.37	8.35	8.52	8.82	8.65	8.99	8.19	9.59	11.27
S 02	9.74	13.35	12.12	36.21	39.07	39.84	40.94	39.58	50.47
S 03	136.68	133.45	212.00	112.23	112.49	199.72	131.52	139.27	205.51
S 04	13.58	15.12	13.98	15.38	24.58	20.49	18.57	19.91	25.91
S 05	16.89	11.10	22.79	23.96	44.60	37.73	27.83	34.78	47.72
S 06	19.37	25.74	19.55	25.46	45.91	42.49	58.40	117.74	206.70
S 08	5.77	4.82	4.79	12.52	12.65	15.92	9.74	14.25	24.04
S 09	6.00	27.06	30.02	11.69	16.22	31.92	16.12	32.79	39.91
S 10	3.65	8.89	4.76	8.52	11.64	10.50	9.09	16.58	23.91
Average	24.45	27.54	36.50	28.31	35.09	45.29	35.60	47.17	70.60
Std Err	42.42	40.43	66.35	32.78	32.47	59.30	39.69	47.51	77.83

L5 perturbation level

μV	V1-D1	V1-D2	V1-D3	V2-D1	V2-D2	V2-D3	V3-D1	V3-D2	V3-D3
S 01	8.66	8.70	8.37	67.14	16.34	17.82	23.01	17.38	24.43
S 02	14.03	13.48	18.94	83.29	71.99	96.79	76.70	84.72	99.79
S 03	24.35	24.95	36.54	131.77	45.87	373.17	39.16	62.94	274.53
S 04	13.44	13.28	13.35	15.00	18.27	22.25	29.38	25.71	35.49
S 05	32.26	27.59	59.11	25.40	33.14	29.25	23.90	26.23	29.90
S 06	9.76	8.25	29.45	17.05	21.80	25.21	15.71	48.34	54.18
S 08	3.75	3.72	3.95	5.49	6.35	9.17	5.56	8.14	7.66
S 09	5.70	15.99	5.83	15.79	30.18	23.47	19.29	29.94	29.65
S 10	11.17	6.93	14.87	18.26	20.40	20.56	21.79	26.49	27.99
Average	13.68	13.65	21.16	42.13	29.37	68.63	28.28	36.66	64.85
Std Err	9.14	8.10	17.84	42.73	19.57	117.04	20.34	24.24	82.83

Peak RMS: L3 superficial

L3 perturbation level

μV	V1-D1	V1-D2	V1-D3	V2-D1	V2-D2	V2-D3	V3-D1	V3-D2	V3-D3
S 01	3.83	3.66	3.46	3.39	3.60	3.36	3.51	3.45	3.60
S 02	14.12	14.93	12.05	14.09	11.90	18.23	15.56	17.06	19.17
S 03	199.77	293.36	410.28	171.76	365.79	404.21	217.66	345.30	507.63
S 04	16.55	17.58	17.41	18.43	18.00	18.83	18.31	17.38	19.02
S 05	37.16	38.22	39.39	39.39	40.96	41.97	37.45	41.57	43.62
S 06	73.27	84.07	273.61	109.10	133.85	178.20	105.15	138.45	224.25
S 08	5.33	9.66	22.88	35.78	49.31	65.49	24.29	61.38	59.17
S 09	9.89	19.50	18.14	16.59	39.57	34.65	22.57	27.71	55.69
S 10	3.41	3.92	6.05	4.12	5.29	7.15	5.54	7.07	4.97
Average	40.37	53.88	89.25	45.85	74.25	85.79	50.00	73.26	104.13
Std Err	63.85	93.21	147.65	57.18	116.34	130.82	69.87	110.12	165.71

L4 perturbation level

μV	V1-D1	V1-D2	V1-D3	V2-D1	V2-D2	V2-D3	V3-D1	V3-D2	V3-D3
S 01	4.56	4.50	4.16	6.05	7.68	6.87	7.98	6.85	9.51
S 02	12.46	12.54	12.58	13.00	16.05	20.18	13.77	16.59	19.50
S 03	437.02	367.39	674.62	260.82	148.94	408.55	201.40	273.18	471.73
S 04	12.49	12.84	12.46	12.64	12.52	12.90	12.63	12.72	13.87
S 05	18.38	17.06	24.07	17.72	35.78	26.35	24.66	28.10	29.76
S 06	80.33	74.46	92.50	62.26	69.63	90.03	57.78	80.65	107.22
S 08	4.22	14.69	8.74	88.64	114.36	96.21	124.17	85.17	141.82
S 09	8.28	8.31	10.58	46.92	54.11	56.99	40.69	45.40	53.99
S 10	3.82	4.14	3.78	17.56	15.41	19.27	15.88	20.24	24.71
Average	64.62	57.33	93.72	58.40	52.72	81.93	55.44	63.21	96.90
Std Err	141.70	118.26	219.58	80.82	50.02	126.88	65.75	83.79	147.78

L5 perturbation level

μV	V1-D1	V1-D2	V1-D3	V2-D1	V2-D2	V2-D3	V3-D1	V3-D2	V3-D3
S 01	5.29	4.22	3.82	29.75	19.56	19.89	36.97	24.21	12.96
S 02	17.13	16.81	21.73	16.65	17.70	16.72	16.43	16.68	17.84
S 03	45.72	44.57	83.15	67.52	95.00	156.84	47.45	80.28	217.48
S 04	11.89	11.99	11.98	11.94	12.21	12.34	12.36	12.39	13.33
S 05	26.63	27.63	31.75	35.10	40.53	45.55	35.95	40.19	55.29
S 06	66.21	62.58	72.78	68.19	70.51	68.37	84.03	67.79	84.09
S 08	66.38	76.39	34.10	65.29	96.06	109.40	73.62	129.96	137.82
S 09	7.71	9.82	7.84	37.75	50.65	59.59	36.91	50.40	41.83
S 10	9.27	4.85	19.60	10.15	11.69	13.72	13.59	12.90	19.26
Average	28.47	28.76	31.86	38.04	45.99	55.82	39.70	48.31	66.66
Std Err	24.76	26.51	28.11	23.75	34.24	49.79	25.43	39.15	70.02

Peak RMS: L4 deep

L3 perturbation level

µV	V1-D1	V1-D2	V1-D3	V2-D1	V2-D2	V2-D3	V3-D1	V3-D2	V3-D3
S 01	16.11	15.98	17.41	20.00	24.05	19.73	20.03	26.80	25.68
S 02	12.30	12.72	14.70	22.99	36.71	40.77	26.58	34.21	77.52
S 03	149.82	147.39	263.88	123.57	187.87	217.18	153.50	182.18	296.58
S 04	3.11	3.67	3.25	3.16	5.13	3.59	3.58	5.33	4.51
S 05	159.04	170.67	170.18	182.34	155.04	233.80	207.54	216.40	251.59
S 06	141.99	173.70	347.61	262.88	313.17	313.13	253.79	329.68	341.45
S 08	4.17	5.21	13.85	5.50	12.12	6.78	6.57	10.47	9.14
S 09	7.88	12.00	12.12	30.34	49.04	50.40	45.82	59.89	121.97
S 10	13.82	14.08	14.30	16.03	22.03	35.24	17.81	19.00	25.83
Average	56.47	61.71	95.26	74.09	89.46	102.29	81.69	98.22	128.25
Std Err	70.61	77.09	131.74	93.78	106.28	118.11	96.54	116.12	133.29

L4 perturbation level

µV	V1-D1	V1-D2	V1-D3	V2-D1	V2-D2	V2-D3	V3-D1	V3-D2	V3-D3
S 01	10.61	10.58	11.32	52.48	52.39	50.36	45.86	68.81	63.93
S 02	13.13	14.45	12.26	35.55	50.00	49.43	36.67	49.49	80.09
S 03	189.38	200.08	365.61	134.07	120.08	237.79	162.87	192.87	278.56
S 04	2.57	2.62	2.83	2.61	2.65	5.57	2.81	2.73	4.04
S 05	110.50	120.49	170.19	123.51	280.22	298.20	217.41	216.60	340.45
S 06	86.31	68.45	180.41	104.64	112.96	243.92	128.56	206.30	218.04
S 08	4.51	4.47	5.30	6.58	17.10	12.48	6.27	8.59	12.17
S 09	16.96	18.99	59.39	171.33	395.76	641.04	288.80	330.48	738.37
S 10	5.33	15.22	5.28	8.08	14.72	14.70	10.17	16.74	24.31
Average	48.81	50.60	90.29	70.98	116.21	172.61	99.94	121.40	195.55
Std Err	65.87	68.13	125.34	63.56	135.34	210.10	104.54	117.68	238.05

L5 perturbation level

µV	V1-D1	V1-D2	V1-D3	V2-D1	V2-D2	V2-D3	V3-D1	V3-D2	V3-D3
S 01	10.57	10.90	10.34	35.45	40.66	42.81	38.16	51.88	66.40
S 02	36.82	44.36	45.53	50.21	66.89	67.97	52.80	77.19	107.02
S 03	22.35	8.95	11.70	65.08	61.25	135.35	22.97	75.78	144.11
S 04	2.58	2.65	2.73	6.19	9.06	9.91	4.16	10.73	11.87
S 05	173.94	177.70	237.97	319.37	394.49	475.85	299.94	376.78	747.55
S 06	123.30	178.20	243.11	114.78	195.94	228.20	163.26	273.68	221.82
S 08	11.60	9.29	10.32	17.20	19.01	26.15	17.58	18.87	23.18
S 09	9.39	12.19	13.07	27.05	27.33	36.72	30.02	34.55	45.23
S 10	29.91	18.26	59.06	23.46	24.47	38.95	36.79	30.84	29.56
Average	46.72	51.39	70.42	73.20	93.23	117.99	73.97	105.59	155.19
Std Err	60.11	72.72	98.23	97.84	126.22	150.68	96.65	129.20	232.25

Peak RMS: L4 superficial

L3 perturbation level

µV	V1-D1	V1-D2	V1-D3	V2-D1	V2-D2	V2-D3	V3-D1	V3-D2	V3-D3
S 01	4.02	4.08	3.51	3.50	3.58	3.62	3.78	3.62	3.52
S 02	12.00	4.93	8.26	7.07	8.37	11.81	10.21	16.42	9.43
S 03	132.83	194.96	302.27	107.67	227.04	262.69	136.82	212.38	312.57
S 04	8.56	8.42	9.59	13.23	14.78	20.38	10.44	18.77	22.12
S 05	84.52	72.40	74.09	96.77	126.46	102.61	83.04	123.21	141.69
S 06	253.07	124.12	209.66	244.14	329.61	288.94	300.33	385.88	352.28
S 08	15.23	19.57	26.92	20.29	29.66	26.76	20.19	30.37	33.73
S 09	3.75	9.53	6.98	5.10	17.69	6.80	4.67	6.46	8.02
S 10	32.14	31.15	31.23	32.81	33.98	32.01	33.68	37.26	39.31
Average	60.68	52.13	74.72	58.95	87.91	83.96	67.02	92.71	102.52
Std Err	84.56	66.85	107.52	79.87	116.88	112.88	98.22	129.82	137.21

L4 perturbation level

µV	V1-D1	V1-D2	V1-D3	V2-D1	V2-D2	V2-D3	V3-D1	V3-D2	V3-D3
S 01	14.16	132.99	17.15	182.48	206.32	207.07	236.61	250.97	258.04
S 02	4.28	5.59	4.44	5.98	7.85	15.47	5.70	8.57	10.54
S 03	211.66	206.30	382.25	117.12	123.24	290.04	178.71	196.34	279.87
S 04	3.20	3.14	3.20	4.08	3.50	3.37	3.44	3.31	4.83
S 05	403.47	279.63	611.53	607.11	794.83	964.36	776.70	746.43	1135.58
S 06	142.13	166.18	157.14	172.47	190.20	194.28	139.17	183.97	277.77
S 08	19.75	20.97	22.73	22.75	33.53	36.85	27.91	22.94	31.73
S 09	3.32	3.46	3.41	4.76	5.83	7.31	5.49	7.42	7.69
S 10	9.04	26.04	8.70	35.98	36.45	64.48	42.64	70.22	77.24
Average	90.11	93.81	134.51	128.08	155.75	198.14	157.37	165.58	231.48
Std Err	139.38	104.89	218.77	193.52	252.47	305.62	247.57	237.54	359.96

L5 perturbation level

µV	V1-D1	V1-D2	V1-D3	V2-D1	V2-D2	V2-D3	V3-D1	V3-D2	V3-D3
S 01	4.38	4.24	4.01	4.16	6.15	15.68	4.14	5.19	5.21
S 02	19.19	28.94	39.76	16.10	37.71	39.68	15.41	24.76	38.03
S 03	31.58	28.02	42.03	65.57	52.58	75.58	39.88	58.91	94.01
S 04	3.16	3.52	4.91	4.03	3.56	6.85	4.35	7.89	7.87
S 05	147.59	191.78	258.00	324.88	405.63	476.56	364.91	457.79	616.39
S 06	145.98	181.26	208.31	305.15	342.54	377.07	166.50	238.44	335.98
S 08	25.03	20.43	26.02	32.40	40.97	56.22	40.93	41.56	51.22
S 09	3.52	3.40	3.13	5.93	7.51	8.89	7.53	9.55	12.01
S 10	41.80	33.44	32.92	35.66	51.14	40.13	33.81	36.08	47.58
Average	46.91	55.00	68.79	88.21	105.31	121.85	75.27	97.80	134.26
Std Err	58.16	75.50	95.22	130.19	154.37	176.10	119.70	153.15	207.97

Peak RMS: L5 deep

L3 perturbation level

μV	V1-D1	V1-D2	V1-D3	V2-D1	V2-D2	V2-D3	V3-D1	V3-D2	V3-D3
S 01	3.61	3.58	3.88	4.91	5.08	4.45	4.11	4.14	5.24
S 02	10.53	12.07	15.50	23.14	34.23	55.83	25.24	37.48	118.40
S 03	245.46	405.72	866.51	211.74	544.38	736.85	274.21	470.65	977.46
S 04	29.86	31.80	34.32	36.79	37.98	47.84	34.21	47.08	65.58
S 05	15.68	14.14	20.23	20.72	18.39	24.64	20.60	18.61	37.59
S 06	98.79	101.89	290.09	163.85	135.50	234.61	124.22	252.04	229.72
S 08	7.07	9.59	16.31	7.02	11.65	7.43	9.75	12.36	7.57
S 09	2.68	3.83	2.73	7.29	12.69	8.74	7.68	11.80	15.10
S 10	12.57	12.58	16.11	21.19	27.40	25.42	22.52	29.61	40.99
Average	47.36	66.13	140.63	55.18	91.92	127.31	58.06	98.20	166.41
Std Err	80.08	130.99	287.09	76.78	174.17	239.51	88.88	159.45	312.39

L4 perturbation level

μV	V1-D1	V1-D2	V1-D3	V2-D1	V2-D2	V2-D3	V3-D1	V3-D2	V3-D3
S 01	6.80	8.21	7.79	20.47	17.44	26.45	71.33	55.69	17.18
S 02	12.73	11.88	15.33	38.32	40.33	79.29	38.17	53.94	82.06
S 03	470.06	517.73	993.27	331.16	227.89	741.24	320.13	474.95	805.99
S 04	9.36	11.74	56.11	39.50	44.06	55.11	35.38	53.78	59.70
S 05	49.73	44.25	110.49	73.31	94.02	107.25	85.22	151.34	105.16
S 06	168.89	169.93	254.93	170.64	240.33	210.32	163.55	155.71	230.31
S 08	8.94	9.00	10.51	11.31	21.96	31.41	10.73	13.11	18.78
S 09	3.77	4.42	3.13	24.13	25.55	28.37	21.74	23.10	37.91
S 10	8.40	26.93	9.17	22.56	24.77	30.01	24.92	29.65	32.51
Average	82.07	89.34	162.30	81.27	81.82	145.49	85.68	112.36	154.40
Std Err	154.83	168.90	322.17	105.70	89.38	231.13	99.64	145.59	253.13

L5 perturbation level

μV	V1-D1	V1-D2	V1-D3	V2-D1	V2-D2	V2-D3	V3-D1	V3-D2	V3-D3
S 01	2.99	3.04	4.09	25.64	6.39	6.85	3.76	21.50	7.81
S 02	49.02	101.36	70.70	206.80	187.11	177.51	125.29	237.75	150.99
S 03	57.26	39.19	78.37	110.14	153.81	239.45	68.53	152.78	220.03
S 04	22.64	54.62	16.65	62.19	81.23	58.32	70.54	76.13	94.47
S 05	51.44	66.78	96.37	129.61	196.60	165.33	61.02	148.23	98.79
S 06	158.48	172.41	175.64	180.09	175.84	197.77	138.62	169.85	180.91
S 08	6.94	8.01	5.87	5.30	5.79	11.90	11.27	8.92	11.47
S 09	2.67	2.86	4.36	3.77	5.11	7.74	3.76	5.70	5.59
S 10	8.81	7.57	13.56	15.97	18.56	29.35	18.04	24.03	32.87
Average	40.03	50.65	51.73	82.17	92.27	99.36	55.65	93.87	89.21
Std Err	49.60	57.04	58.87	77.61	85.63	94.18	51.14	85.38	80.85

Peak RMS: L5 superficial

L3 perturbation level

μV	V1-D1	V1-D2	V1-D3	V2-D1	V2-D2	V2-D3	V3-D1	V3-D2	V3-D3
S 01	4.23	4.26	4.28	4.24	4.54	4.81	4.29	4.52	5.74
S 02	8.49	8.93	12.55	20.46	21.43	26.64	19.92	26.34	31.40
S 03	183.03	202.43	274.71	176.85	252.57	249.10	209.97	232.55	396.23
S 04	5.35	11.14	25.49	17.06	14.32	17.30	10.39	14.27	17.83
S 05	8.37	9.71	13.33	13.04	13.20	20.47	16.01	15.71	17.88
S 06	72.16	141.82	375.21	144.78	188.23	265.45	208.67	228.76	369.84
S 08	10.68	14.70	19.30	11.05	14.54	13.01	12.64	13.89	12.49
S 09	10.22	20.77	10.93	38.79	75.50	39.34	38.43	62.68	71.75
S 10	42.81	45.28	63.58	172.64	235.77	158.31	239.30	292.84	400.22
Average	38.37	51.00	88.82	66.55	91.12	88.27	84.40	99.06	147.04
Std Err	58.84	71.32	137.29	74.76	104.20	106.43	101.98	116.80	182.46

L4 perturbation level

μV	V1-D1	V1-D2	V1-D3	V2-D1	V2-D2	V2-D3	V3-D1	V3-D2	V3-D3
S 01	5.28	5.65	5.36	9.34	9.83	8.71	8.68	11.12	14.50
S 02	6.29	9.64	7.98	12.04	18.27	21.18	18.18	22.28	19.52
S 03	324.94	289.04	369.86	209.54	211.20	308.44	254.18	243.90	311.92
S 04	2.84	2.85	2.95	2.87	3.66	3.20	3.23	4.10	9.49
S 05	17.49	27.74	47.54	35.06	42.01	53.67	42.88	40.94	56.66
S 06	89.67	123.04	113.88	101.81	111.23	132.05	85.83	286.00	275.78
S 08	13.72	14.44	15.10	17.35	21.60	20.51	14.47	18.34	18.26
S 09	10.52	9.80	9.53	128.46	130.60	145.85	110.68	121.07	173.29
S 10	48.14	127.70	19.54	284.16	255.01	287.08	248.44	335.25	449.53
Average	57.65	67.77	65.75	88.96	89.27	108.97	87.40	120.33	147.66
Std Err	104.11	96.74	119.33	101.28	93.55	118.97	99.79	132.60	163.34

L5 perturbation level

μV	V1-D1	V1-D2	V1-D3	V2-D1	V2-D2	V2-D3	V3-D1	V3-D2	V3-D3
S 01	22.08	5.88	5.33	20.75	16.06	14.89	52.98	13.58	13.27
S 02	17.11	19.54	18.23	22.01	46.01	25.95	19.98	32.67	25.10
S 03	84.44	65.67	112.03	128.10	153.01	180.01	105.58	146.85	183.63
S 04	2.75	2.77	2.83	10.55	5.92	2.75	5.45	9.96	6.24
S 05	14.57	18.62	41.13	41.51	69.49	67.00	26.37	68.49	34.53
S 06	118.01	128.18	171.03	134.75	149.31	197.99	105.79	176.66	200.59
S 08	23.60	21.23	31.08	24.12	28.92	30.36	24.58	28.81	27.21
S 09	9.39	15.31	14.62	11.13	13.21	13.01	37.19	11.99	15.41
S 10	48.56	33.55	34.10	178.35	255.66	208.68	136.93	217.47	284.97
Average	37.83	34.53	47.82	63.47	81.95	82.29	57.20	78.50	87.88
Std Err	39.01	39.68	56.60	64.78	85.78	87.09	46.84	80.33	105.28

Time-to-peak RMS: L3 deep

L3 perturbation level

sec	V1-D1	V1-D2	V1-D3	V2-D1	V2-D2	V2-D3	V3-D1	V3-D2	V3-D3
S 01	0.64	0.51	0.30	0.24	0.20	0.15	0.17	0.15	0.13
S 02	0.46	0.38	0.54	0.15	0.15	0.15	0.14	0.17	0.18
S 03	0.56	0.56	0.78	0.23	0.24	0.35	0.26	0.26	0.37
S 04	0.51	0.71	0.64	0.12	0.15	0.16	0.17	0.19	0.12
S 05	0.68	0.38	0.48	0.11	0.11	0.09	0.08	0.12	0.09
S 06	0.68	0.61	0.99	0.26	0.27	0.27	0.17	0.25	0.21
S 08	0.51	0.55	0.85	0.10	0.18	0.14	0.18	0.19	0.14
S 09	0.41	0.68	0.57	0.12	0.26	0.27	0.07	0.26	0.29
S 10	0.38	0.48	0.81	0.13	0.15	0.15	0.11	0.13	0.12
Average	0.54	0.54	0.66	0.16	0.19	0.19	0.15	0.19	0.18
Std Err	0.11	0.12	0.22	0.06	0.06	0.08	0.06	0.05	0.09

L4 perturbation level

sec	V1-D1	V1-D2	V1-D3	V2-D1	V2-D2	V2-D3	V3-D1	V3-D2	V3-D3
S 01	0.47	0.51	0.66	0.14	0.28	0.14	0.20	0.14	0.12
S 02	0.29	0.39	0.41	0.14	0.11	0.14	0.19	0.13	0.15
S 03	0.50	0.62	0.73	0.23	0.29	0.24	0.22	0.24	0.26
S 04	0.43	0.43	0.51	0.17	0.06	0.09	0.14	0.10	0.06
S 05	0.66	0.55	0.62	0.17	0.30	0.18	0.27	0.12	0.18
S 06	0.20	0.57	0.81	0.16	0.28	0.24	0.12	0.16	0.16
S 08	0.43	0.44	0.56	0.11	0.10	0.11	0.11	0.13	0.13
S 09	0.53	0.40	0.48	0.25	0.24	0.27	0.25	0.25	0.28
S 10	0.31	0.48	0.52	0.22	0.21	0.21	0.22	0.22	0.27
Average	0.43	0.49	0.59	0.18	0.21	0.18	0.19	0.17	0.18
Std Err	0.14	0.08	0.13	0.05	0.09	0.06	0.06	0.06	0.08

L5 perturbation level

sec	V1-D1	V1-D2	V1-D3	V2-D1	V2-D2	V2-D3	V3-D1	V3-D2	V3-D3
S 01	0.46	0.48	0.70	0.10	0.13	0.18	0.10	0.16	0.18
S 02	0.34	0.42	0.54	0.19	0.29	0.26	0.23	0.25	0.19
S 03	0.21	0.42	0.55	0.15	0.22	0.23	0.08	0.11	0.23
S 04	0.56	0.70	0.35	0.09	0.15	0.10	0.23	0.13	0.09
S 05	0.62	0.74	0.77	0.12	0.13	0.17	0.24	0.13	0.21
S 06	0.56	0.63	0.96	0.10	0.13	0.17	0.10	0.12	0.13
S 08	0.56	0.62	0.87	0.17	0.17	0.18	0.08	0.23	0.22
S 09	0.54	0.51	0.45	0.16	0.15	0.14	0.11	0.12	0.20
S 10	0.40	0.34	0.58	0.22	0.25	0.21	0.30	0.19	0.18
Average	0.47	0.54	0.64	0.14	0.18	0.18	0.16	0.16	0.18
Std Err	0.13	0.14	0.20	0.04	0.06	0.05	0.09	0.05	0.04

Time-to-peak RMS: L3 superficial

L3 perturbation level

sec	V1-D1	V1-D2	V1-D3	V2-D1	V2-D2	V2-D3	V3-D1	V3-D2	V3-D3
S 01	0.11	0.23	0.58	0.19	0.29	0.28	0.25	0.19	0.26
S 02	0.35	0.76	0.49	0.22	0.20	0.26	0.18	0.21	0.17
S 03	0.63	0.68	0.79	0.32	0.30	0.39	0.32	0.25	0.23
S 04	0.58	0.47	0.71	0.23	0.19	0.23	0.19	0.14	0.11
S 05	0.68	0.58	0.55	0.16	0.13	0.17	0.29	0.17	0.19
S 06	0.70	0.84	0.93	0.27	0.24	0.29	0.14	0.26	0.32
S 08	0.33	0.41	0.81	0.14	0.12	0.18	0.09	0.21	0.16
S 09	0.50	0.60	0.44	0.13	0.26	0.21	0.14	0.18	0.14
S 10	0.21	0.20	0.84	0.20	0.17	0.13	0.21	0.19	0.16
Average	0.45	0.53	0.68	0.21	0.21	0.24	0.20	0.20	0.19
Std Err	0.22	0.22	0.17	0.06	0.06	0.08	0.08	0.04	0.07

L4 perturbation level

sec	V1-D1	V1-D2	V1-D3	V2-D1	V2-D2	V2-D3	V3-D1	V3-D2	V3-D3
S 01	0.09	0.09	0.39	0.13	0.03	0.03	0.02	0.02	0.04
S 02	0.39	0.51	0.78	0.16	0.11	0.14	0.14	0.18	0.12
S 03	0.61	0.84	0.94	0.23	0.41	0.31	0.24	0.21	0.39
S 04	0.47	0.59	0.66	0.30	0.21	0.13	0.29	0.34	0.15
S 05	0.54	0.60	0.75	0.14	0.22	0.15	0.18	0.28	0.19
S 06	0.75	0.80	0.87	0.24	0.27	0.38	0.20	0.28	0.40
S 08	0.56	0.49	0.57	0.15	0.14	0.14	0.16	0.15	0.15
S 09	0.40	0.44	0.44	0.11	0.09	0.13	0.10	0.09	0.14
S 10	0.28	0.48	0.58	0.21	0.27	0.20	0.29	0.21	0.23
Average	0.46	0.54	0.66	0.19	0.19	0.18	0.18	0.19	0.20
Std Err	0.19	0.22	0.19	0.06	0.11	0.11	0.09	0.10	0.12

L5 perturbation level

sec	V1-D1	V1-D2	V1-D3	V2-D1	V2-D2	V2-D3	V3-D1	V3-D2	V3-D3
S 01	0.35	0.46	0.51	0.23	0.20	0.19	0.31	0.24	0.13
S 02	0.49	0.67	0.73	0.17	0.23	0.24	0.22	0.22	0.21
S 03	0.32	0.58	0.87	0.25	0.26	0.27	0.23	0.23	0.26
S 04	0.50	0.67	0.34	0.17	0.23	0.16	0.27	0.12	0.12
S 05	0.44	0.39	0.63	0.13	0.16	0.14	0.10	0.16	0.13
S 06	0.59	0.87	0.98	0.27	0.35	0.37	0.24	0.36	0.26
S 08	0.45	0.45	1.10	0.10	0.15	0.16	0.11	0.11	0.12
S 09	0.30	0.52	0.43	0.19	0.19	0.14	0.15	0.16	0.15
S 10	0.38	0.35	0.36	0.22	0.21	0.22	0.22	0.18	0.19
Average	0.42	0.55	0.66	0.19	0.22	0.21	0.21	0.20	0.17
Std Err	0.09	0.16	0.28	0.06	0.06	0.08	0.07	0.07	0.06

Time-to-peak RMS: L4 deep

L3 perturbation level

sec	V1-D1	V1-D2	V1-D3	V2-D1	V2-D2	V2-D3	V3-D1	V3-D2	V3-D3
S 01	0.53	0.70	0.61	0.14	0.10	0.12	0.10	0.11	0.14
S 02	0.34	0.38	0.33	0.12	0.10	0.10	0.11	0.17	0.11
S 03	0.64	0.72	0.82	0.23	0.28	0.33	0.26	0.23	0.36
S 04	0.32	0.68	0.62	0.22	0.12	0.23	0.15	0.08	0.09
S 05	0.69	0.59	0.64	0.16	0.20	0.12	0.10	0.15	0.29
S 06	0.46	0.95	0.94	0.14	0.18	0.28	0.13	0.11	0.19
S 08	0.49	0.52	0.84	0.21	0.12	0.18	0.17	0.15	0.14
S 09	0.55	0.42	0.54	0.16	0.25	0.18	0.03	0.20	0.13
S 10	0.44	0.67	0.57	0.09	0.08	0.07	0.09	0.12	0.08
Average	0.50	0.62	0.65	0.16	0.16	0.18	0.13	0.15	0.17
Std Err	0.12	0.17	0.18	0.05	0.07	0.09	0.06	0.05	0.10

L4 perturbation level

sec	V1-D1	V1-D2	V1-D3	V2-D1	V2-D2	V2-D3	V3-D1	V3-D2	V3-D3
S 01	0.45	0.70	0.83	0.18	0.18	0.18	0.16	0.15	0.12
S 02	0.31	0.28	0.38	0.11	0.13	0.14	0.11	0.11	0.10
S 03	0.67	0.70	0.90	0.23	0.29	0.33	0.32	0.29	0.24
S 04	0.52	0.57	0.61	0.24	0.19	0.14	0.15	0.14	0.13
S 05	0.33	0.55	0.67	0.12	0.13	0.12	0.10	0.12	0.13
S 06	0.59	0.90	0.92	0.09	0.14	0.18	0.14	0.12	0.25
S 08	0.52	0.52	0.75	0.13	0.19	0.19	0.13	0.18	0.17
S 09	0.31	0.27	0.37	0.20	0.26	0.29	0.24	0.22	0.19
S 10	0.57	0.49	1.00	0.07	0.28	0.08	0.15	0.11	0.11
Average	0.47	0.55	0.71	0.15	0.20	0.18	0.17	0.16	0.16
Std Err	0.13	0.20	0.23	0.06	0.06	0.08	0.07	0.06	0.06

L5 perturbation level

sec	V1-D1	V1-D2	V1-D3	V2-D1	V2-D2	V2-D3	V3-D1	V3-D2	V3-D3
S 01	0.51	0.67	0.66	0.12	0.14	0.14	0.14	0.14	0.18
S 02	0.44	0.62	0.78	0.12	0.15	0.16	0.15	0.15	0.14
S 03	0.17	0.25	0.53	0.11	0.17	0.23	0.08	0.16	0.30
S 04	0.53	0.38	0.67	0.15	0.10	0.15	0.21	0.10	0.10
S 05	0.41	0.68	0.80	0.09	0.08	0.20	0.08	0.09	0.13
S 06	0.66	0.82	0.88	0.11	0.16	0.22	0.11	0.20	0.32
S 08	0.39	0.46	0.60	0.15	0.13	0.17	0.12	0.12	0.20
S 09	0.52	0.56	0.55	0.18	0.22	0.16	0.13	0.18	0.12
S 10	0.10	0.63	0.69	0.03	0.04	0.10	0.03	0.03	0.03
Average	0.41	0.56	0.68	0.12	0.13	0.17	0.12	0.13	0.17
Std Err	0.18	0.17	0.12	0.04	0.05	0.04	0.05	0.05	0.09

Time-to-peak RMS: L4 superficial

L3 perturbation level

sec	V1-D1	V1-D2	V1-D3	V2-D1	V2-D2	V2-D3	V3-D1	V3-D2	V3-D3
S 01	0.11	0.10	0.58	0.21	0.35	0.27	0.31	0.19	0.21
S 02	0.44	0.80	0.77	0.18	0.19	0.13	0.16	0.13	0.13
S 03	0.62	0.67	0.91	0.30	0.35	0.39	0.36	0.39	0.28
S 04	0.29	0.46	0.83	0.14	0.13	0.10	0.12	0.04	0.04
S 05	0.35	0.39	0.51	0.12	0.12	0.21	0.15	0.18	0.19
S 06	0.69	0.94	1.00	0.13	0.11	0.34	0.20	0.15	0.22
S 08	0.54	0.66	0.81	0.11	0.15	0.15	0.18	0.19	0.16
S 09	0.38	0.54	0.40	0.16	0.25	0.28	0.13	0.21	0.15
S 10	0.50	0.69	0.93	0.20	0.15	0.09	0.10	0.11	0.10
Average	0.43	0.58	0.75	0.18	0.20	0.22	0.19	0.18	0.16
Std Err	0.18	0.25	0.20	0.06	0.09	0.11	0.09	0.09	0.07

L4 perturbation level

sec	V1-D1	V1-D2	V1-D3	V2-D1	V2-D2	V2-D3	V3-D1	V3-D2	V3-D3
S 01	0.32	0.26	0.39	0.03	0.03	0.07	0.03	0.03	0.03
S 02	0.54	0.56	0.44	0.11	0.14	0.15	0.11	0.13	0.12
S 03	0.75	0.92	0.69	0.24	0.39	0.28	0.31	0.29	0.40
S 04	0.40	0.75	0.70	0.19	0.13	0.11	0.12	0.15	0.08
S 05	0.47	0.52	0.70	0.18	0.12	0.13	0.22	0.10	0.12
S 06	0.59	0.67	0.81	0.13	0.14	0.19	0.21	0.10	0.20
S 08	0.52	0.53	0.66	0.17	0.18	0.20	0.15	0.13	0.15
S 09	0.25	0.38	0.31	0.16	0.13	0.14	0.15	0.12	0.14
S 10	0.60	0.64	0.61	0.15	0.12	0.15	0.16	0.17	0.20
Average	0.49	0.58	0.59	0.15	0.15	0.16	0.16	0.14	0.16
Std Err	0.15	0.20	0.17	0.06	0.10	0.06	0.08	0.07	0.10

L5 perturbation level

sec	V1-D1	V1-D2	V1-D3	V2-D1	V2-D2	V2-D3	V3-D1	V3-D2	V3-D3
S 01	0.34	0.54	0.65	0.24	0.26	0.34	0.10	0.39	0.20
S 02	0.34	0.58	0.77	0.18	0.26	0.32	0.20	0.28	0.24
S 03	0.51	0.56	1.02	0.13	0.27	0.25	0.21	0.22	0.19
S 04	0.55	0.70	0.55	0.10	0.18	0.13	0.23	0.11	0.09
S 05	0.35	0.46	0.89	0.14	0.10	0.12	0.10	0.10	0.09
S 06	0.61	0.79	0.82	0.10	0.18	0.20	0.12	0.13	0.22
S 08	0.44	0.57	0.85	0.15	0.15	0.17	0.12	0.14	0.16
S 09	0.28	0.22	0.45	0.12	0.15	0.17	0.14	0.13	0.14
S 10	0.33	0.58	0.52	0.17	0.13	0.13	0.08	0.12	0.11
Average	0.42	0.56	0.72	0.15	0.19	0.20	0.15	0.18	0.16
Std Err	0.11	0.16	0.19	0.05	0.06	0.08	0.05	0.10	0.06

Time-to-peak RMS: L5 deep

L3 perturbation level

sec	V1-D1	V1-D2	V1-D3	V2-D1	V2-D2	V2-D3	V3-D1	V3-D2	V3-D3
S 01	0.51	0.55	0.47	0.22	0.17	0.26	0.27	0.27	0.23
S 02	0.38	0.61	0.66	0.15	0.09	0.16	0.16	0.19	0.12
S 03	0.75	0.65	0.82	0.36	0.31	0.37	0.37	0.36	0.35
S 04	0.48	0.65	0.60	0.11	0.14	0.13	0.09	0.13	0.11
S 05	0.48	0.68	0.72	0.13	0.11	0.09	0.11	0.12	0.15
S 06	0.77	0.67	0.76	0.20	0.16	0.27	0.19	0.20	0.14
S 08	0.43	0.53	0.78	0.21	0.20	0.24	0.29	0.28	0.29
S 09	0.59	0.60	0.59	0.38	0.35	0.31	0.29	0.30	0.25
S 10	0.24	0.42	0.68	0.08	0.11	0.10	0.10	0.11	0.10
Average	0.51	0.59	0.68	0.20	0.18	0.21	0.21	0.22	0.19
Std Err	0.17	0.08	0.11	0.11	0.09	0.10	0.10	0.09	0.09

L4 perturbation level

sec	V1-D1	V1-D2	V1-D3	V2-D1	V2-D2	V2-D3	V3-D1	V3-D2	V3-D3
S 01	0.47	0.51	0.66	0.14	0.28	0.14	0.20	0.14	0.12
S 02	0.29	0.39	0.41	0.14	0.11	0.14	0.19	0.13	0.15
S 03	0.50	0.62	0.73	0.23	0.29	0.24	0.22	0.24	0.26
S 04	0.43	0.43	0.51	0.17	0.06	0.09	0.14	0.10	0.06
S 05	0.66	0.55	0.62	0.17	0.30	0.18	0.27	0.12	0.18
S 06	0.20	0.57	0.81	0.16	0.28	0.24	0.12	0.16	0.16
S 08	0.43	0.44	0.56	0.11	0.10	0.11	0.11	0.13	0.13
S 09	0.53	0.40	0.48	0.25	0.24	0.27	0.25	0.25	0.28
S 10	0.31	0.48	0.52	0.22	0.21	0.21	0.22	0.22	0.27
Average	0.43	0.49	0.59	0.18	0.21	0.18	0.19	0.17	0.18
Std Err	0.14	0.08	0.13	0.05	0.09	0.06	0.06	0.06	0.08

L5 perturbation level

sec	V1-D1	V1-D2	V1-D3	V2-D1	V2-D2	V2-D3	V3-D1	V3-D2	V3-D3
S 01	0.53	0.64	0.57	0.19	0.12	0.13	0.25	0.20	0.13
S 02	0.38	0.56	0.48	0.04	0.12	0.12	0.08	0.07	0.06
S 03	0.40	0.64	0.86	0.18	0.15	0.23	0.16	0.17	0.22
S 04	0.27	0.15	0.39	0.07	0.07	0.07	0.07	0.06	0.09
S 05	0.46	0.44	0.57	0.13	0.11	0.16	0.21	0.14	0.14
S 06	0.34	0.58	0.59	0.19	0.20	0.15	0.17	0.17	0.21
S 08	0.31	0.59	0.80	0.25	0.19	0.20	0.24	0.18	0.16
S 09	0.48	0.47	0.39	0.17	0.11	0.11	0.12	0.14	0.16
S 10	0.36	0.45	0.56	0.09	0.11	0.12	0.09	0.12	0.12
Average	0.39	0.50	0.58	0.15	0.13	0.14	0.15	0.14	0.14
Std Err	0.08	0.15	0.16	0.07	0.04	0.05	0.07	0.05	0.05

Time-to-peak RMS: L5 superficial

L3 perturbation level

sec	V1-D1	V1-D2	V1-D3	V2-D1	V2-D2	V2-D3	V3-D1	V3-D2	V3-D3
S 01	0.70	0.49	0.46	0.18	0.20	0.12	0.11	0.11	0.09
S 02	0.40	0.48	0.45	0.20	0.23	0.16	0.13	0.20	0.15
S 03	0.48	0.63	0.89	0.20	0.26	0.31	0.29	0.38	0.41
S 04	0.48	0.58	0.77	0.15	0.32	0.29	0.15	0.21	0.26
S 05	0.41	0.44	0.48	0.10	0.11	0.10	0.09	0.11	0.11
S 06	0.62	0.68	0.81	0.19	0.23	0.27	0.17	0.18	0.27
S 08	0.60	0.57	0.88	0.18	0.22	0.20	0.16	0.21	0.25
S 09	0.66	0.42	0.50	0.25	0.24	0.26	0.18	0.22	0.23
S 10	0.37	0.48	0.65	0.11	0.13	0.15	0.15	0.13	0.10
Average	0.52	0.53	0.65	0.17	0.22	0.21	0.16	0.19	0.21
Std Err	0.12	0.09	0.19	0.05	0.06	0.08	0.06	0.08	0.10

L4 perturbation level

sec	V1-D1	V1-D2	V1-D3	V2-D1	V2-D2	V2-D3	V3-D1	V3-D2	V3-D3
S 01	0.78	0.83	0.93	0.23	0.16	0.27	0.18	0.18	0.19
S 02	0.35	0.54	0.57	0.12	0.15	0.11	0.10	0.06	0.14
S 03	0.75	0.70	0.98	0.30	0.39	0.35	0.29	0.28	0.44
S 04	0.48	0.63	0.71	0.21	0.21	0.11	0.18	0.14	0.12
S 05	0.46	0.58	0.55	0.21	0.13	0.12	0.16	0.12	0.12
S 06	0.75	0.73	0.81	0.10	0.20	0.26	0.09	0.18	0.23
S 08	0.48	0.34	0.87	0.12	0.15	0.18	0.16	0.26	0.21
S 09	0.23	0.42	0.06	0.26	0.29	0.28	0.24	0.30	0.33
S 10	0.41	0.46	0.69	0.22	0.25	0.21	0.23	0.23	0.23
Average	0.52	0.58	0.69	0.20	0.21	0.21	0.18	0.19	0.22
Std Err	0.19	0.16	0.28	0.07	0.08	0.09	0.06	0.08	0.10

L5 perturbation level

sec	V1-D1	V1-D2	V1-D3	V2-D1	V2-D2	V2-D3	V3-D1	V3-D2	V3-D3
S 01	0.50	0.51	0.60	0.08	0.08	0.11	0.09	0.12	0.14
S 02	0.48	0.80	0.64	0.11	0.18	0.21	0.08	0.16	0.16
S 03	0.35	0.37	0.73	0.12	0.22	0.24	0.16	0.26	0.24
S 04	0.49	0.46	0.65	0.32	0.28	0.24	0.20	0.18	0.27
S 05	0.29	0.33	0.62	0.12	0.12	0.09	0.16	0.11	0.16
S 06	0.65	0.74	0.86	0.18	0.24	0.22	0.15	0.26	0.31
S 08	0.49	0.60	0.65	0.09	0.26	0.30	0.21	0.15	0.21
S 09	0.28	0.31	0.35	0.05	0.11	0.12	0.11	0.10	0.11
S 10	0.44	0.52	0.38	0.14	0.19	0.17	0.13	0.23	0.24
Average	0.44	0.51	0.61	0.14	0.19	0.19	0.14	0.17	0.20
Std Err	0.12	0.17	0.16	0.08	0.07	0.07	0.04	0.06	0.07

Individual Participant Plots

The following pages contain individual plots of the participant means with standard deviation bars for each dependent measure, EMG channel and perturbation level. The participant displayed in each plot is identified at the top of each plot by the number following the "S" (ie. S03 refers to participant 03). Each plot displays the participant mean of all trials for each of the V1-D1, V1-D2, V2-D1 and V2-D2 indentation perturbations. The V1 and V2 perturbation velocities are labeled along the x-axis as "low" or "high" perturbation velocities (see section 7.1.2 for an explanation of these labels). The D1 perturbation displacement is represented by the solid line while the D2 perturbation displacement is represented by the dashed line on each of the individual participant plots. The "average" and peak RMS values are plotted on the following pages in microvolts (μV). The amplitude of each EMG channel was not normalized and thus the y-axis scale for each participant was different and is not displayed in the plots. To determine the actual mean values for each participant refer to the preceding tables in this appendix. The last set of plots display the time-to-peak RMS values in seconds for each participant, EMG channel and perturbation level. The time-to-peak RMS plots for all participants, levels and EMG channels are displayed with a y-axis scale of 1 second. To evaluate the difference between the D1 and D2 displacement at the V1 perturbation velocity (Part A analysis, section 7.2.1), the difference between the solid and dashed lines at the "low" perturbation velocity (left side of each plot) must be examined. To evaluate the difference between the "low" and "high" perturbation velocities at each perturbation displacement (Part B analysis, section 7.2.2), the slope of each perturbation displacement line (D1 and D2) must be examined across the "low" and "high" perturbation velocities.

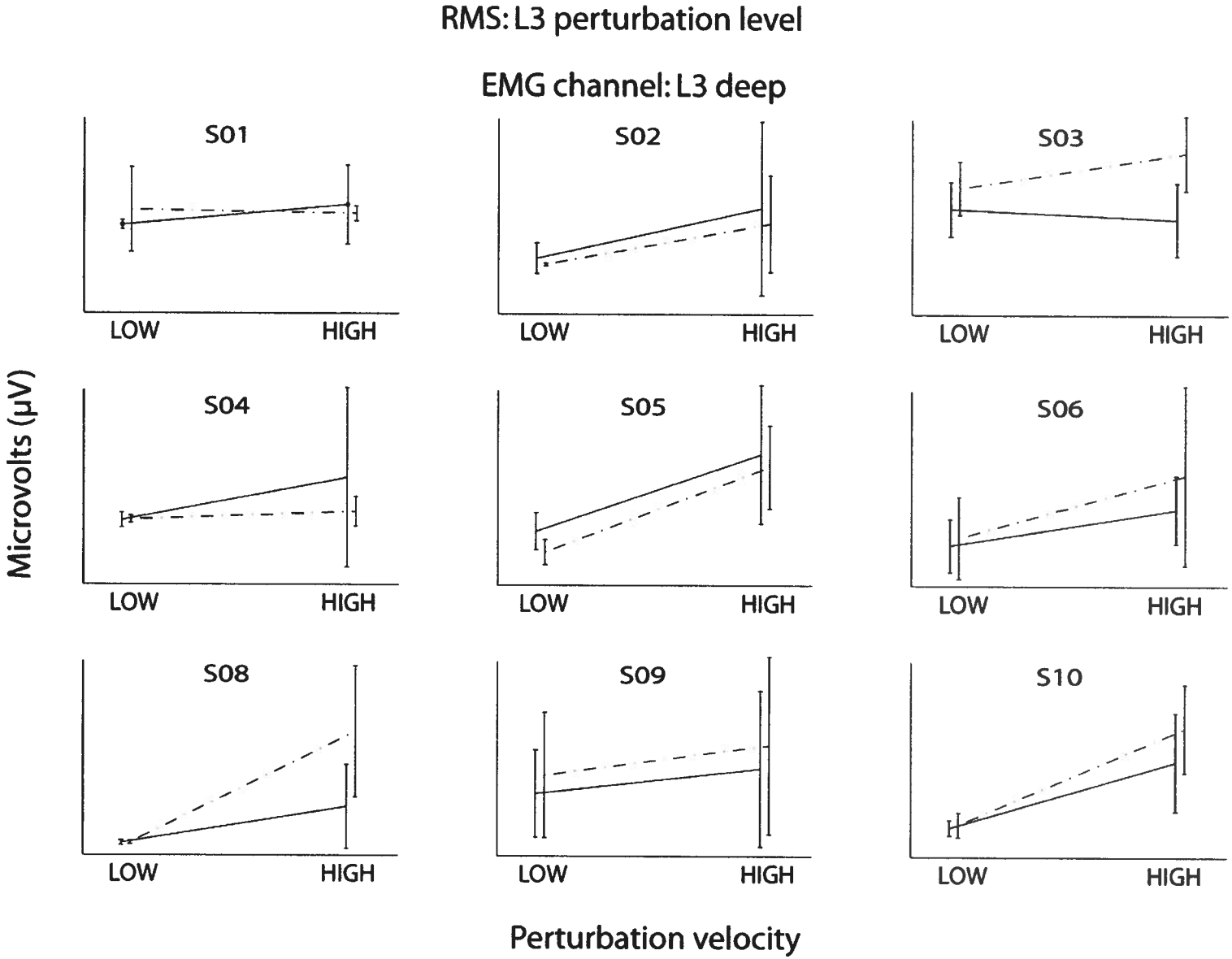
RMS: L3 perturbation level
EMG channel: L3 deep
S01
S02
S03
S04
S05
S06
S08
S09
S10
LOW
HIGH
Microvolts (μV)
Perturbation velocity

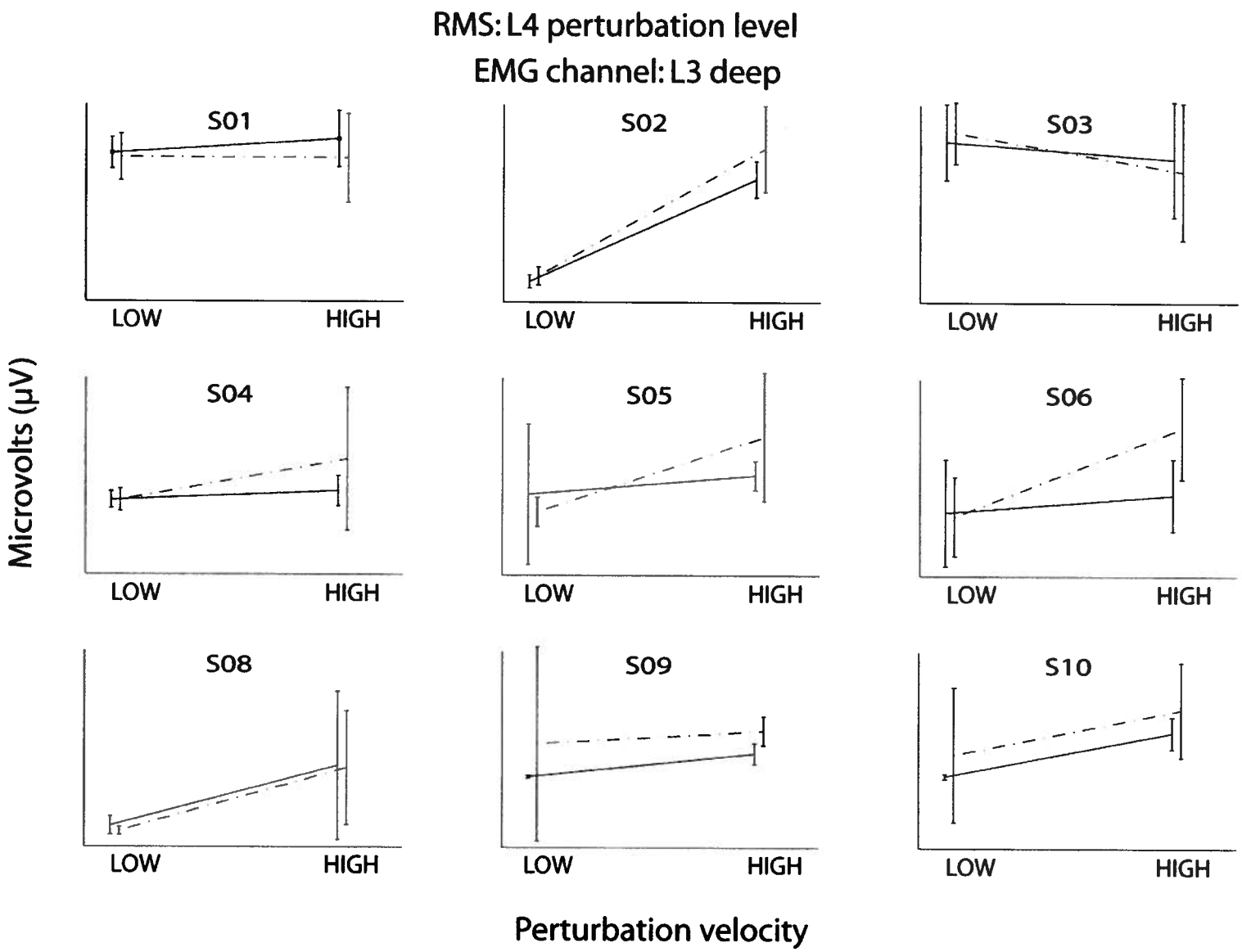
RMS: L4 perturbation level
EMG channel: L3 deep
S01
S02
S03
S04
S05
S06
S08
S09
S10
LOW
HIGH
Microvolts (μV)
Perturbation velocity

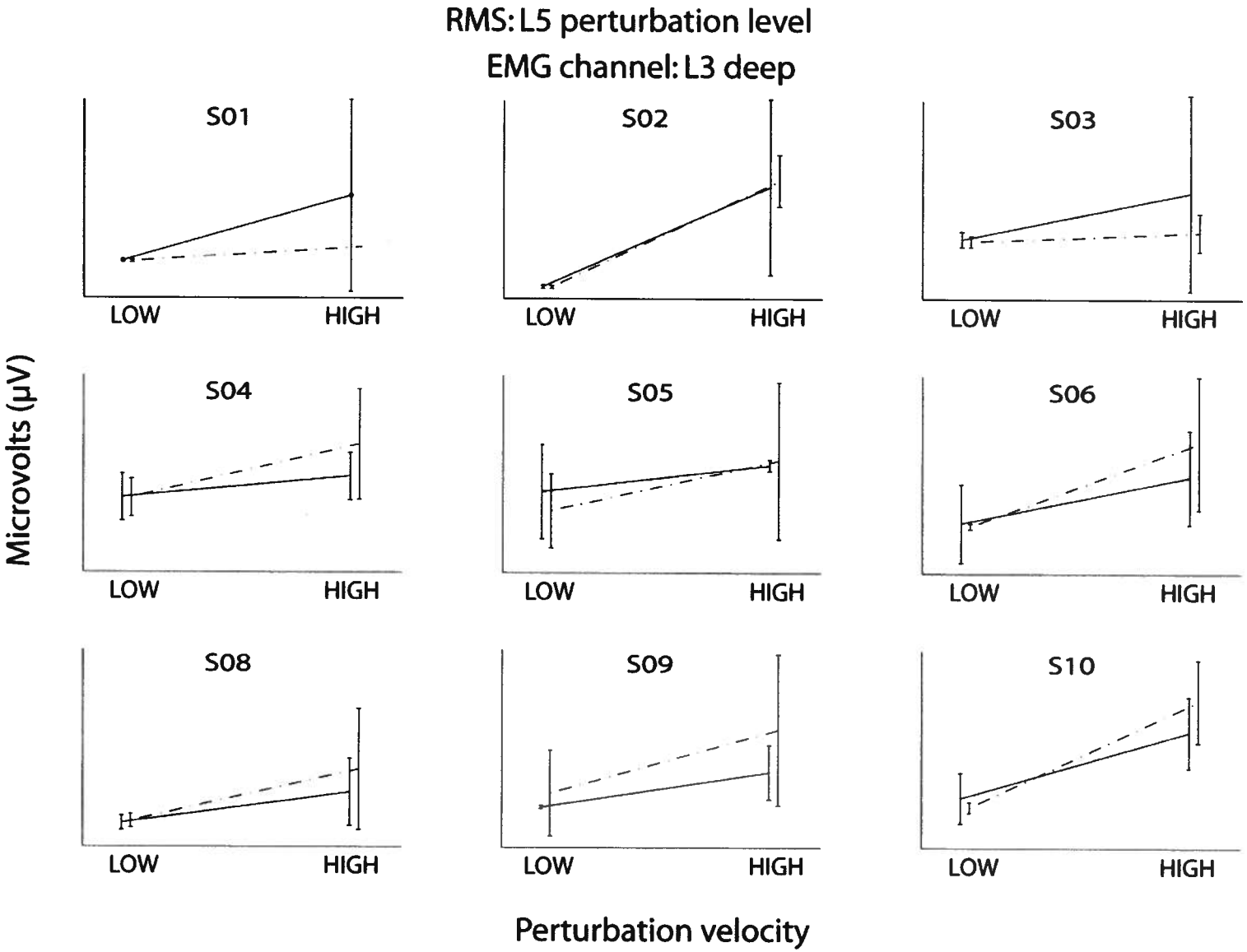
RMS: L5 perturbation level
EMG channel: L3 deep
S01
S02
S03
S04
S05
S06
S08
S09
S10
LOW
HIGH
Microvolts (μV)
Perturbation velocity

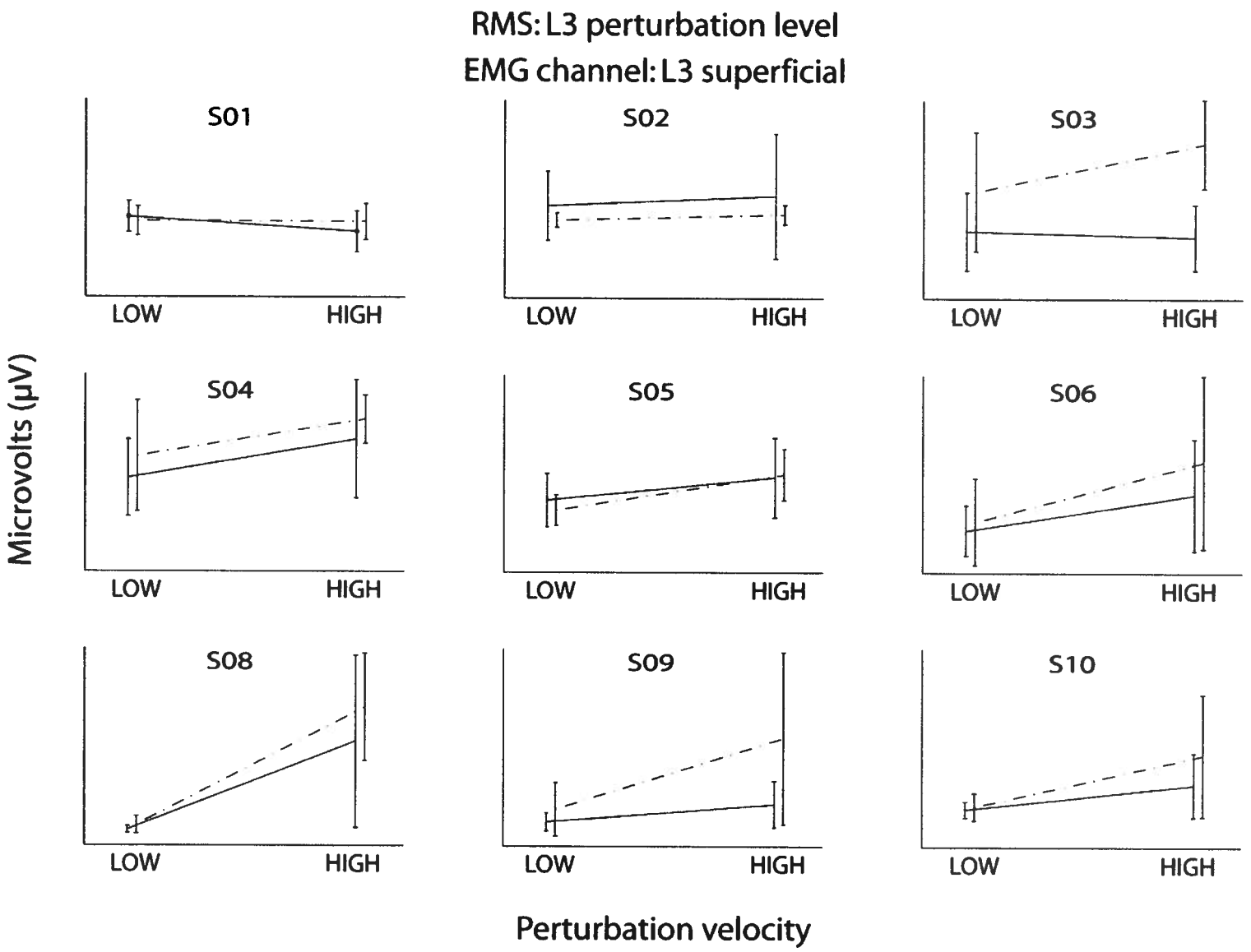
RMS: L3 perturbation level
EMG channel: L3 superficial
S01
S02
S03
S04
S05
S06
S08
S09
S10
LOW
HIGH
Microvolts (μV)
Perturbation velocity

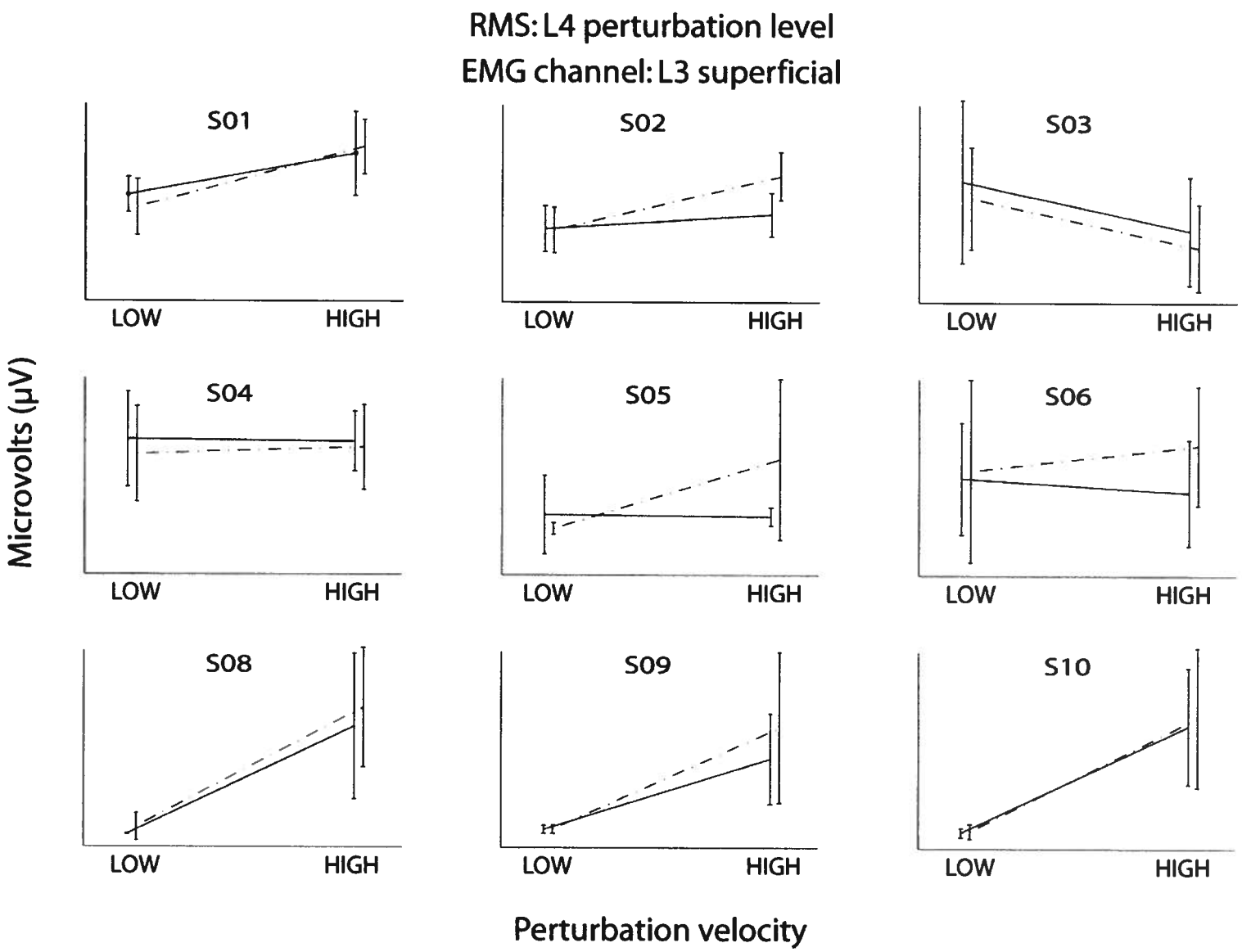
RMS: L4 perturbation level
EMG channel: L3 superficial
S01
S02
S03
S04
S05
S06
S08
S09
S10
LOW
HIGH
Microvolts (μV)
Perturbation velocity

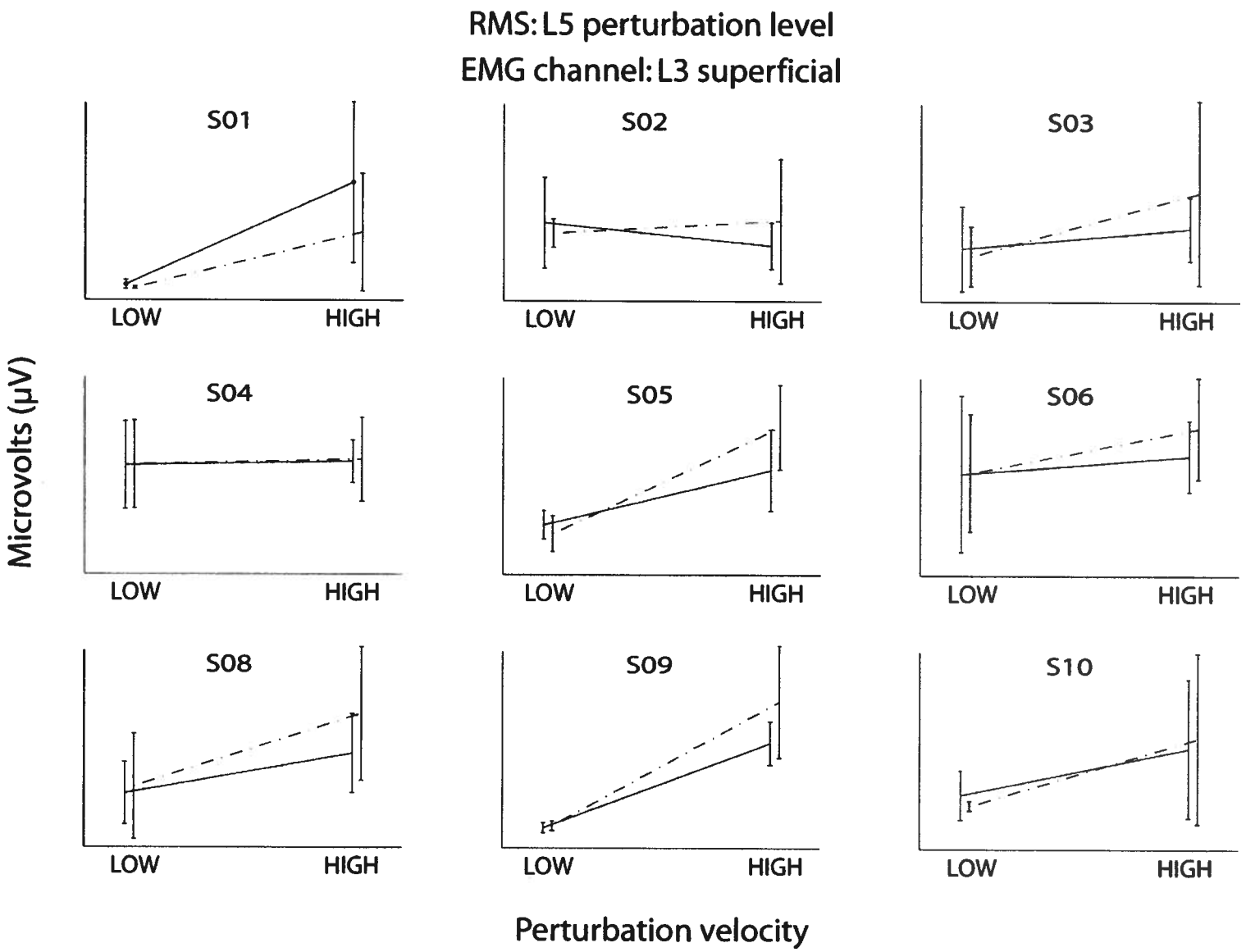
RMS: L5 perturbation level
EMG channel: L3 superficial
S01
S02
S03
S04
S05
S06
S08
S09
S10
LOW
HIGH
Microvolts (μV)
Perturbation velocity

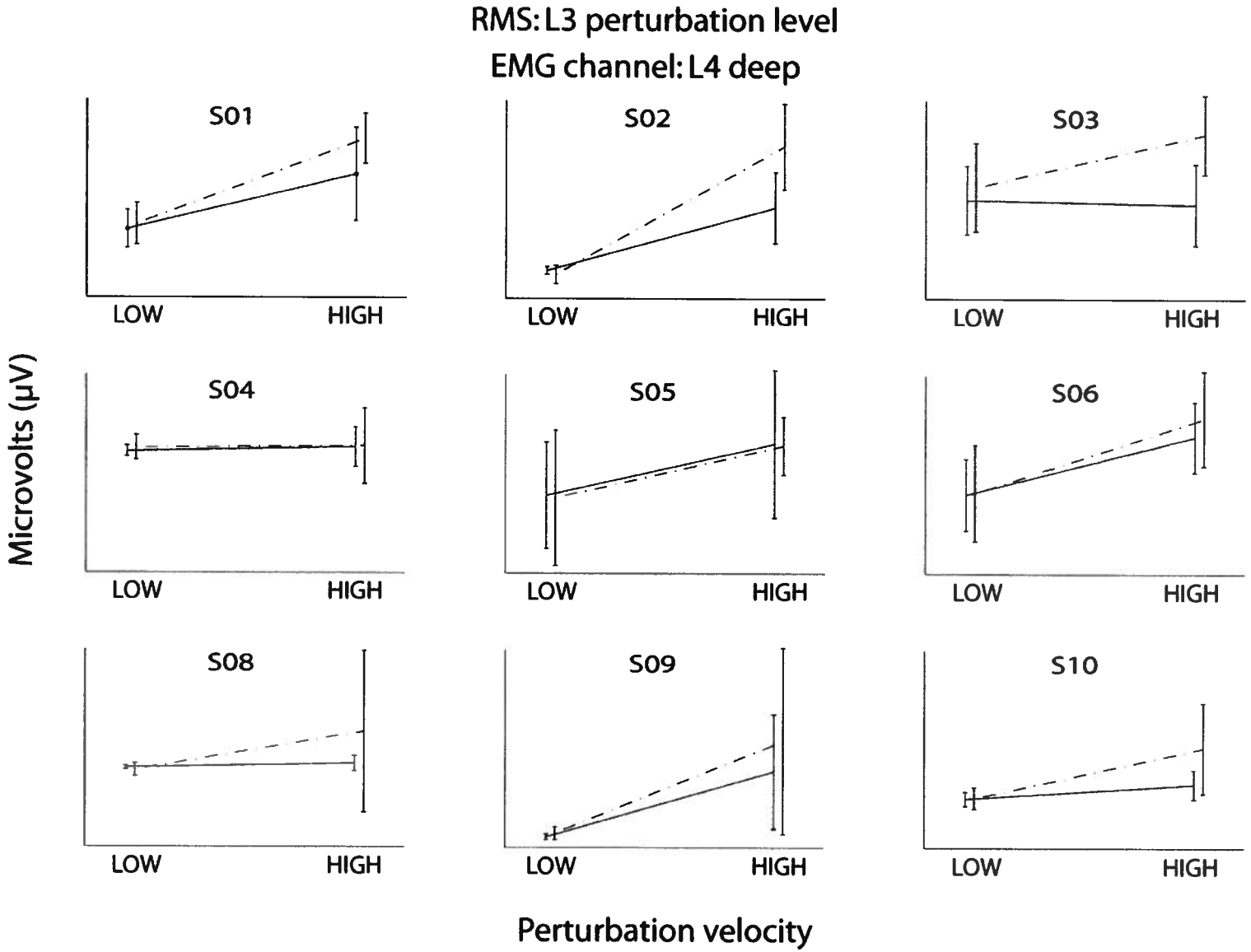
RMS: L3 perturbation level
EMG channel: L4 deep
S01
S02
S03
S04
S05
S06
S08
S09
S10
LOW
HIGH
Microvolts (μV)
Perturbation velocity

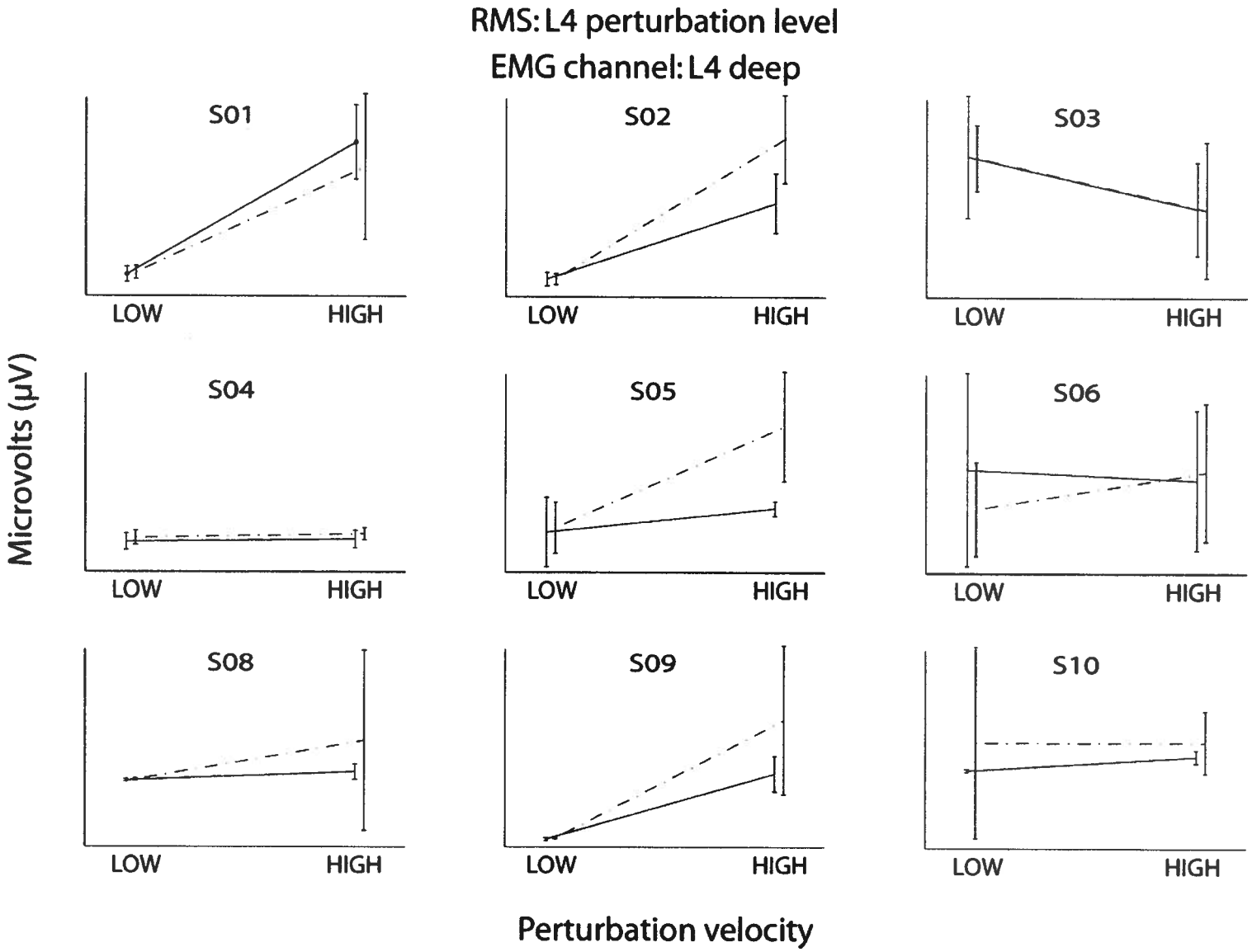
RMS: L4 perturbation level
EMG channel: L4 deep
S01
S02
S03
S04
S05
S06
S08
S09
S10
LOW
HIGH
Microvolts (μV)
Perturbation velocity

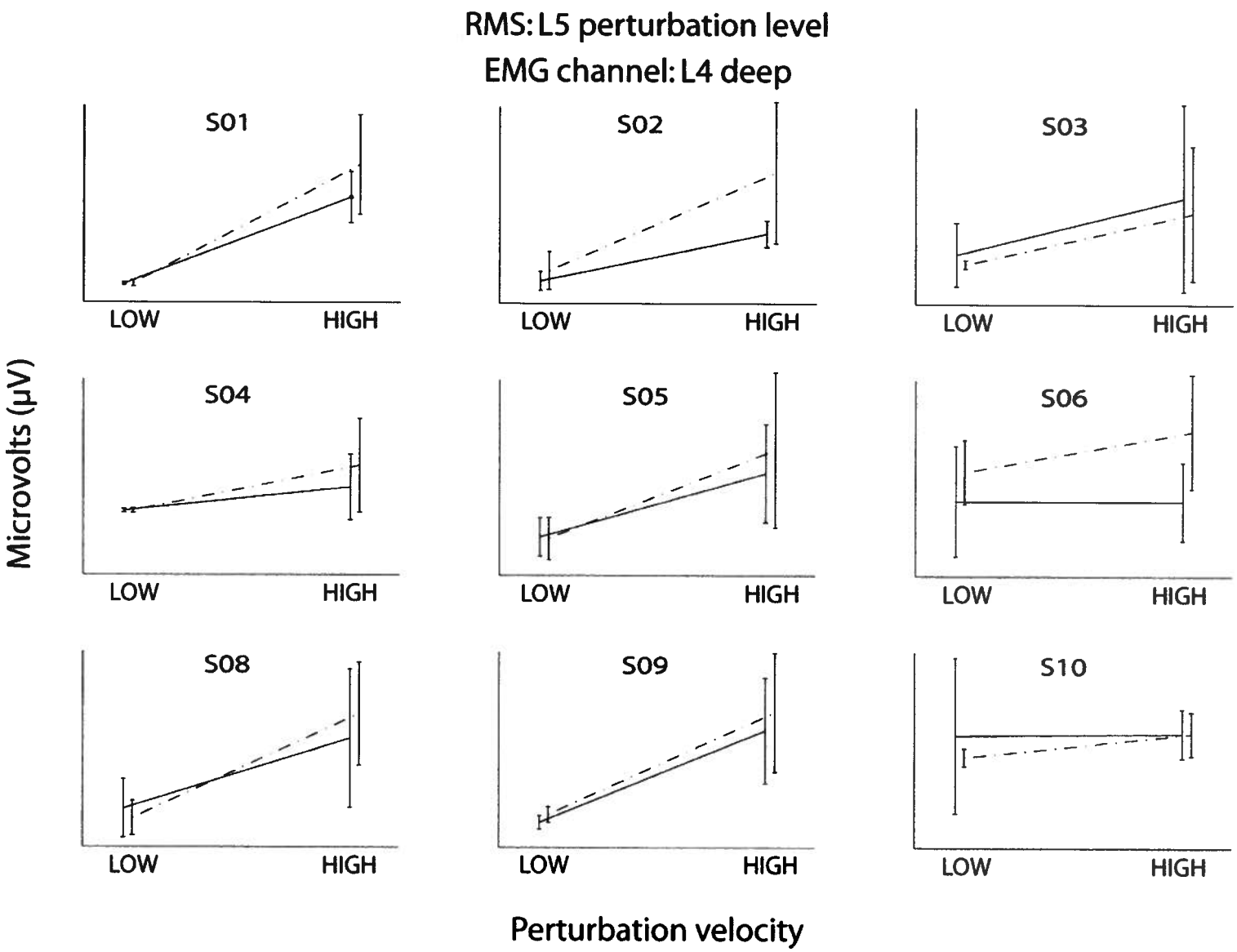
RMS: L5 perturbation level
EMG channel: L4 deep
S01
S02
S03
S04
S05
S06
S08
S09
S10
LOW
HIGH
Microvolts (μV)
Perturbation velocity

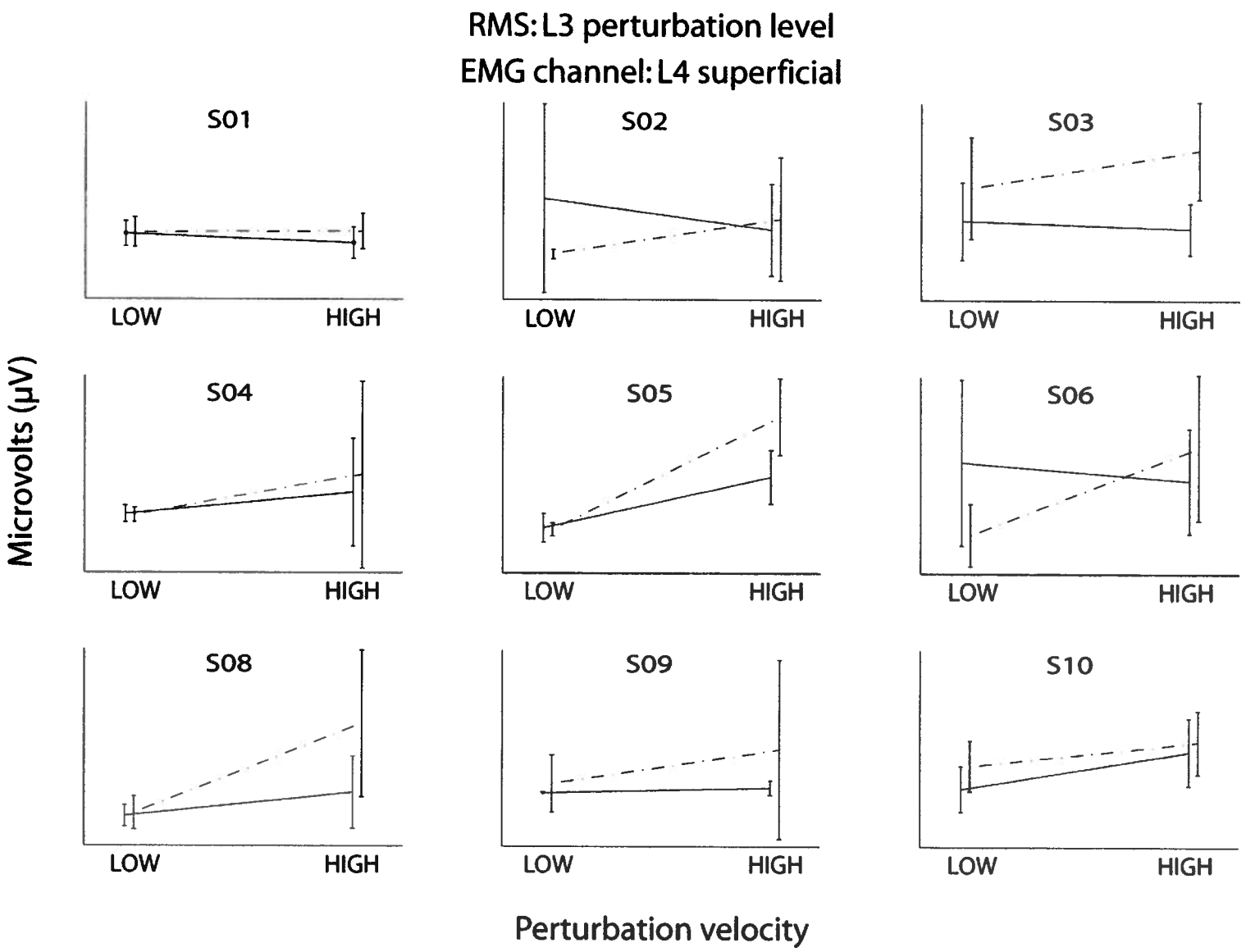
RMS: L3 perturbation level
EMG channel: L4 superficial
S01
S02
S03
S04
S05
S06
S08
S09
S10
LOW
HIGH
Microvolts (μV)
Perturbation velocity

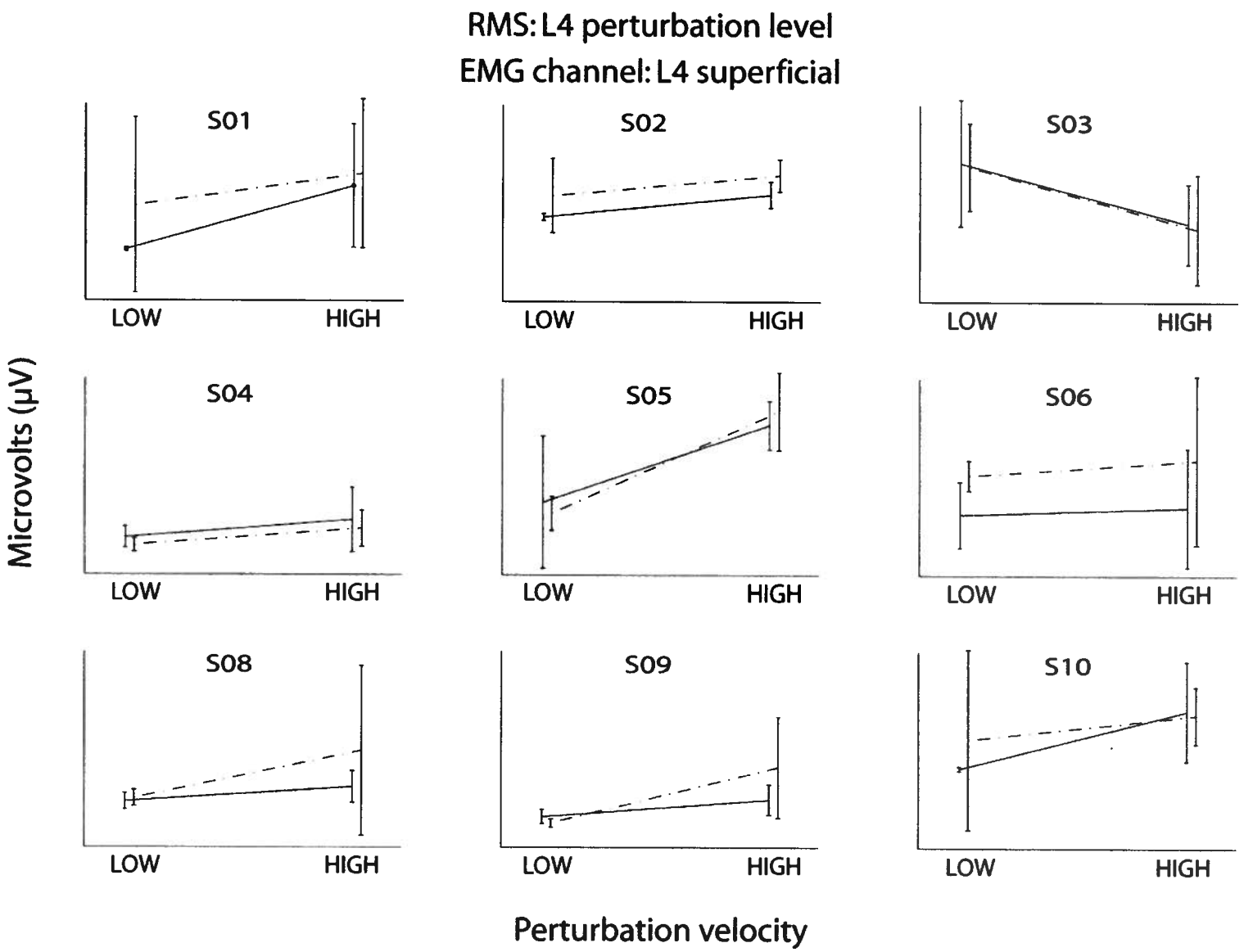
RMS: L4 perturbation level
EMG channel: L4 superficial
S01
S02
S03
S04
S05
S06
S08
S09
S10
LOW
HIGH
Microvolts (μV)
Perturbation velocity

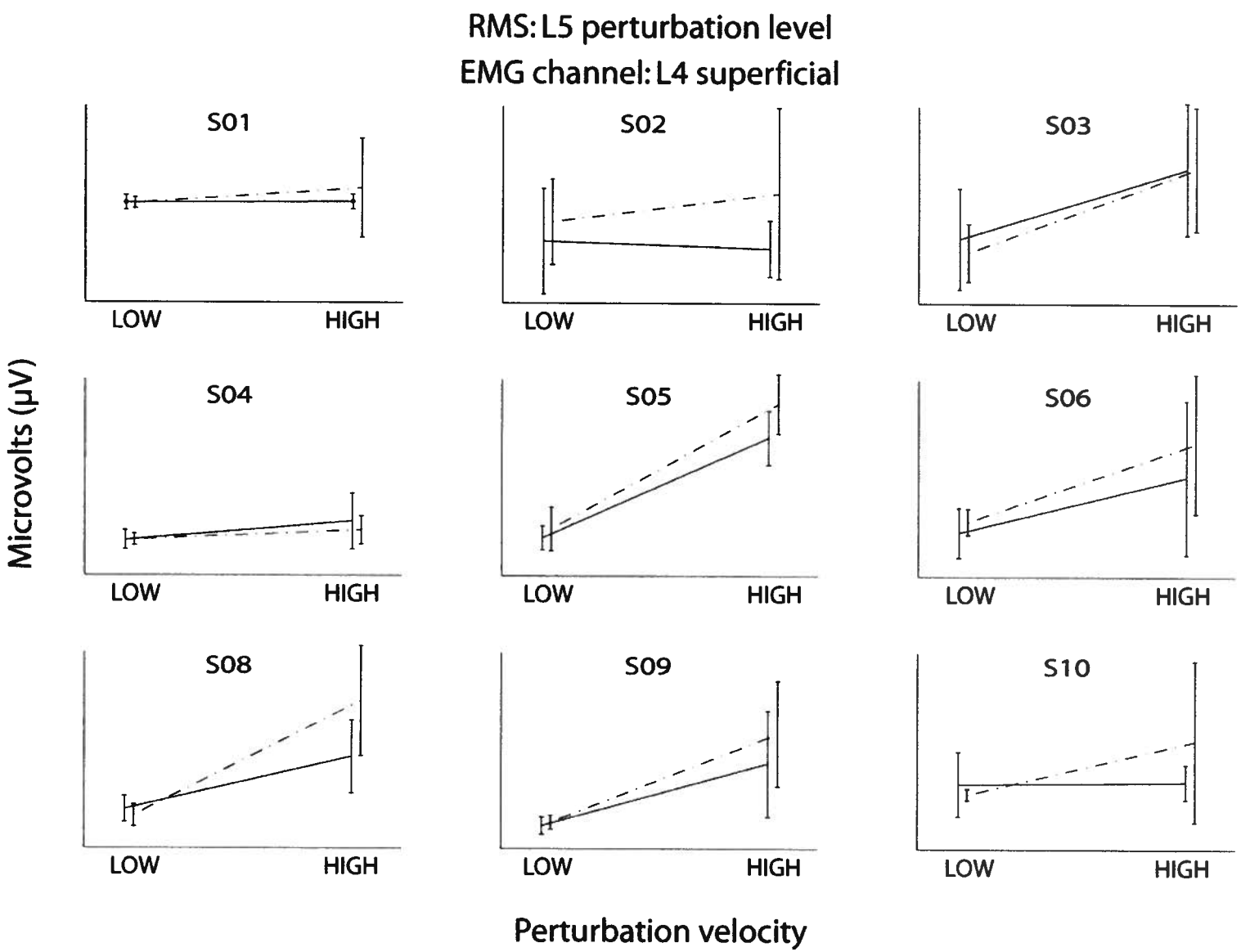
RMS: L5 perturbation level
EMG channel: L4 superficial
S01
S02
S03
S04
S05
S06
S08
S09
S10
LOW
HIGH
Microvolts (μV)
Perturbation velocity

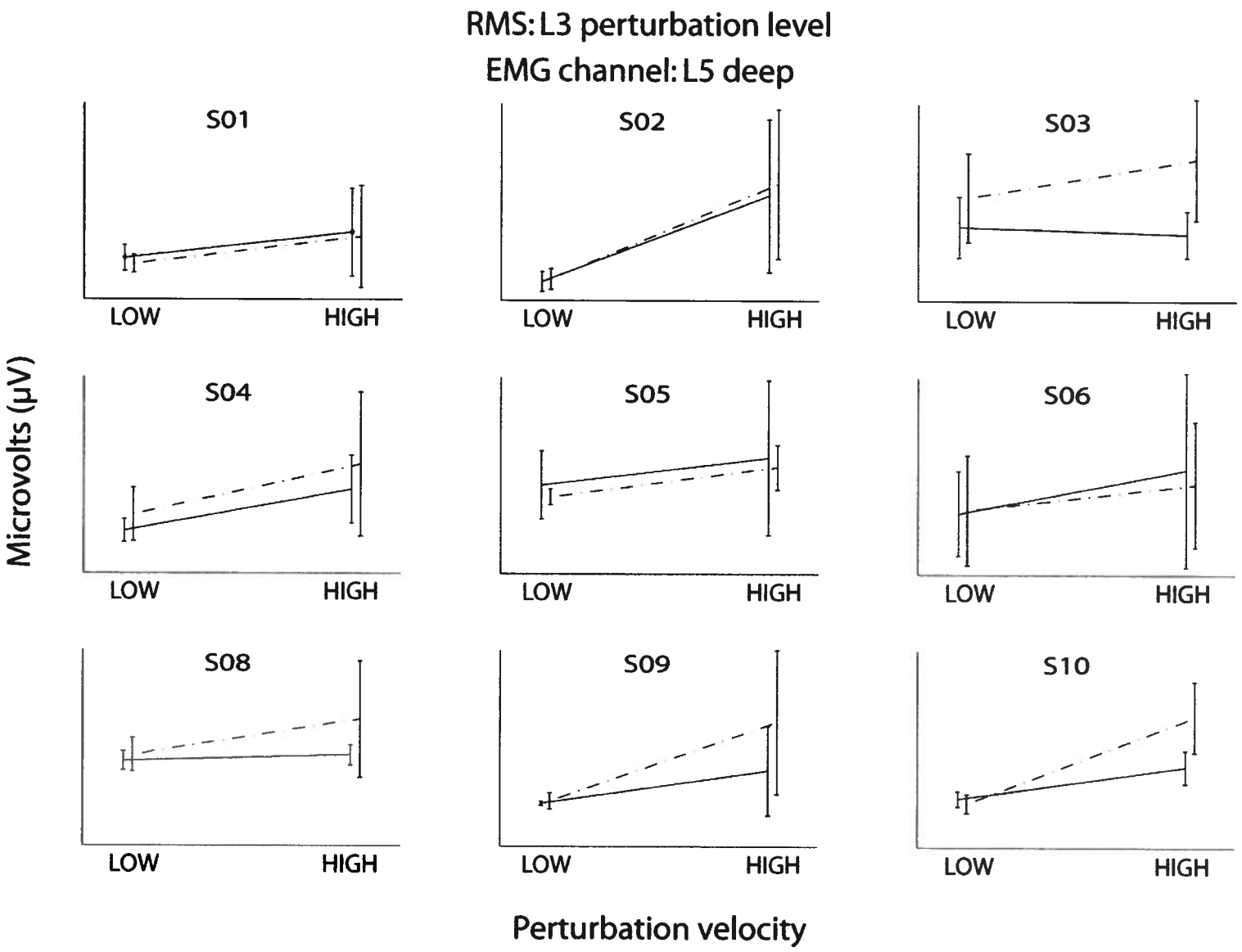
RMS: L3 perturbation level
EMG channel: L5 deep
S01
S02
S03
S04
S05
S06
S08
S09
S10
LOW
HIGH
Microvolts (μV)
Perturbation velocity

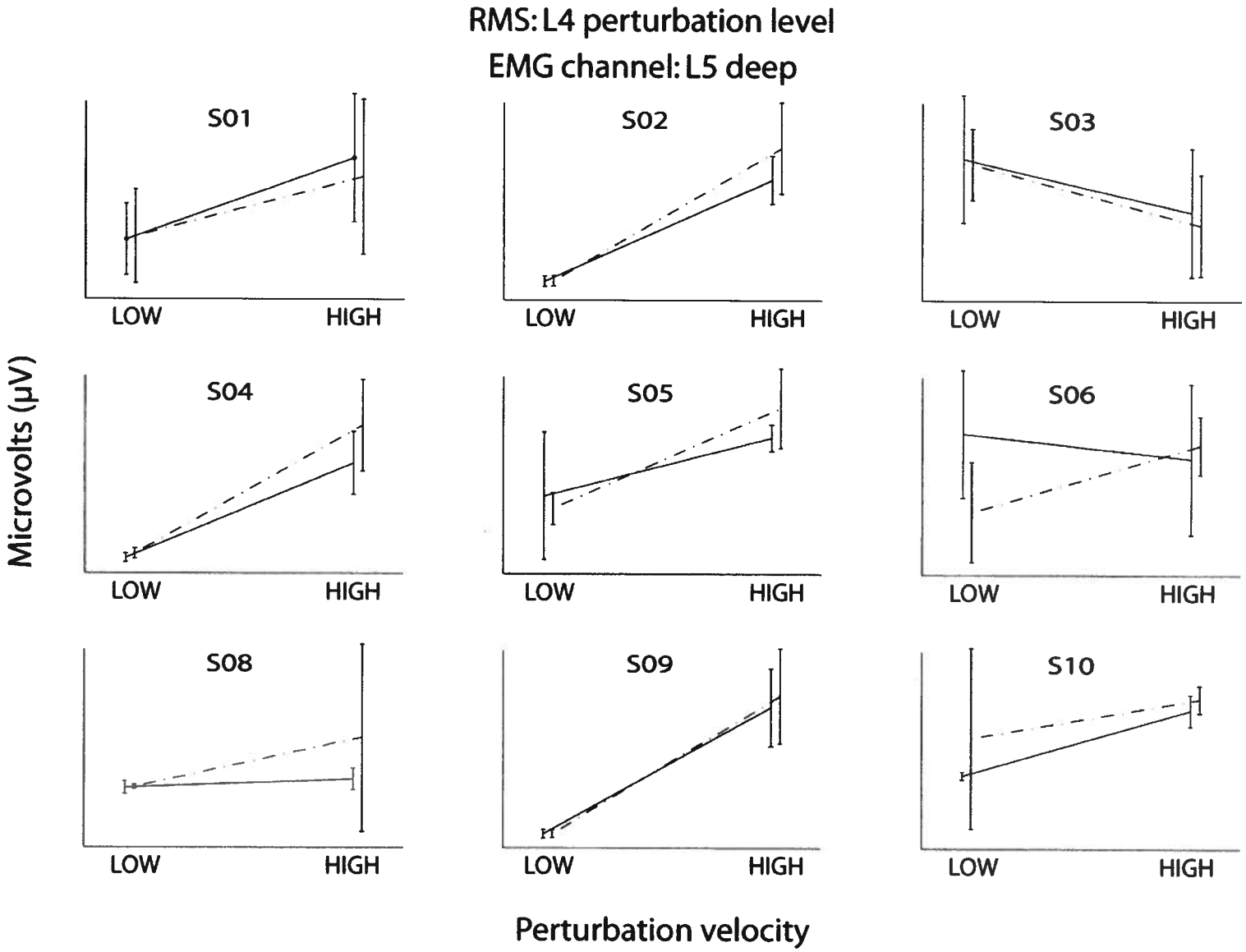
RMS: L4 perturbation level
EMG channel: L5 deep
Microvolts (μV)
S01
S02
S03
S04
S05
S06
S08
S09
S10
LOW
HIGH
Perturbation velocity

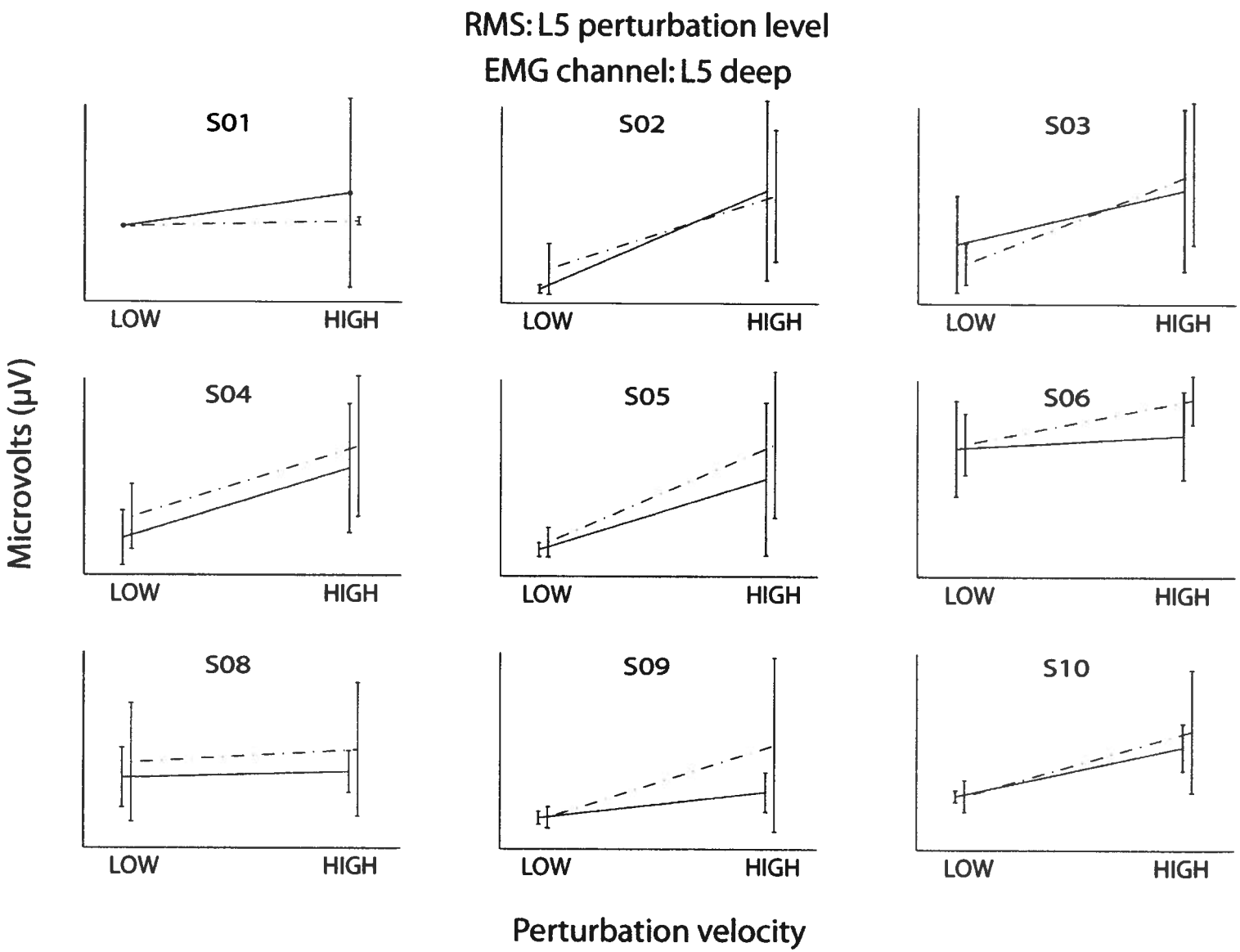
RMS: L5 perturbation level
EMG channel: L5 deep
S01
S02
S03
S04
S05
S06
S08
S09
S10
LOW
HIGH
Microvolts (μV)
Perturbation velocity

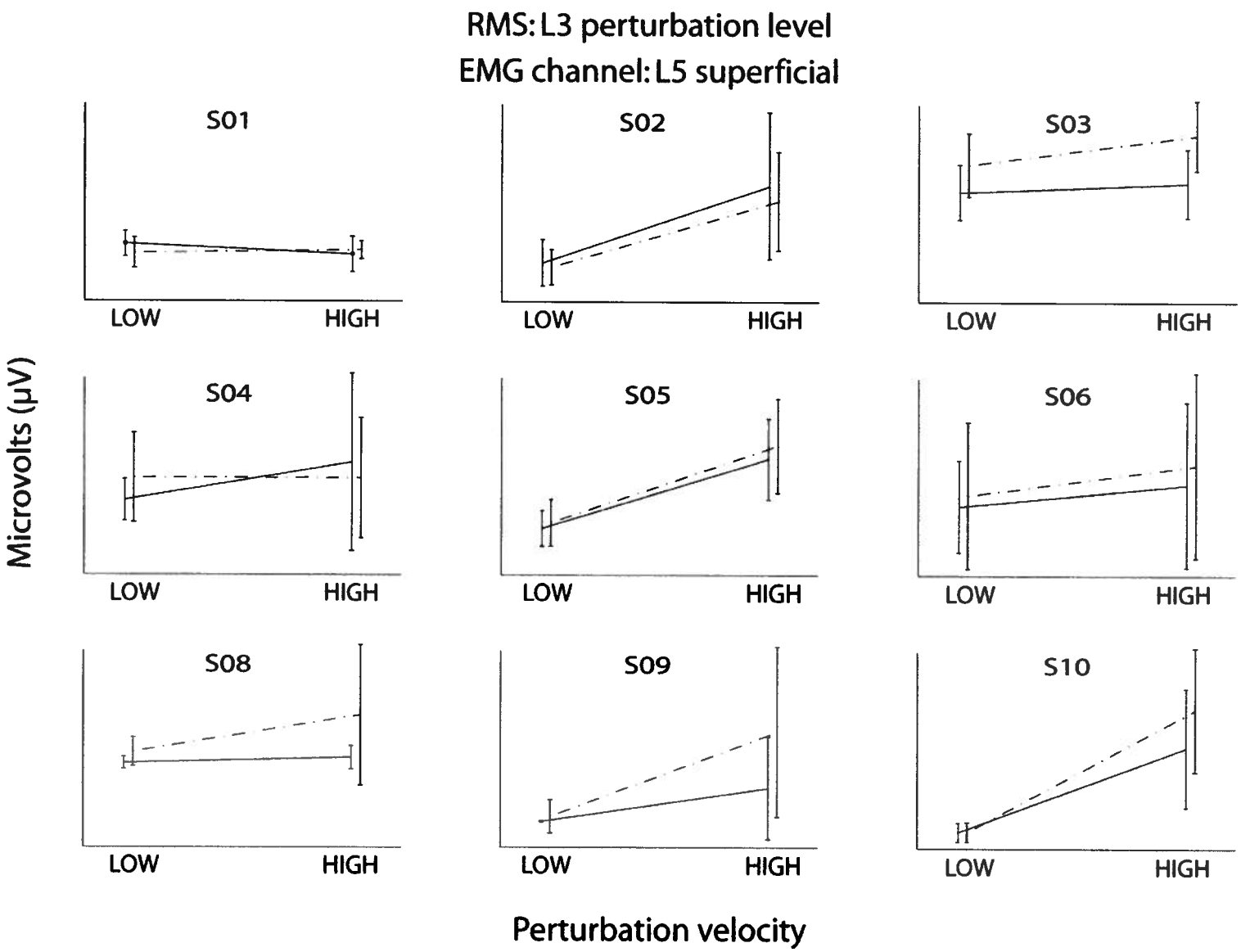
RMS: L3 perturbation level
EMG channel: L5 superficial
S01
S02
S03
S04
S05
S06
S08
S09
S10
LOW
HIGH
Microvolts (μV)
Perturbation velocity

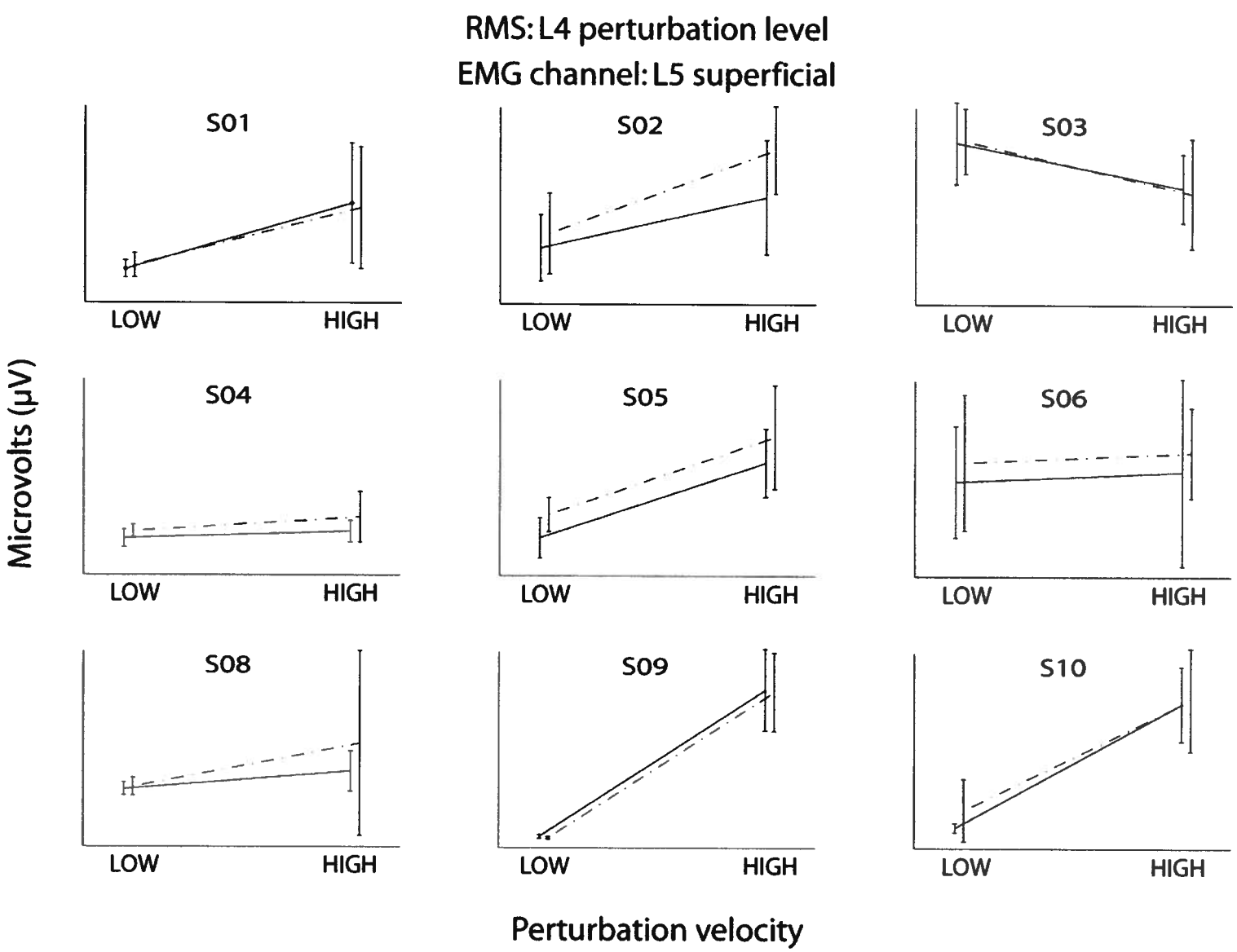
RMS: L4 perturbation level
EMG channel: L5 superficial
S01
S02
S03
S04
S05
S06
S08
S09
S10
LOW
HIGH
Microvolts (μV)
Perturbation velocity

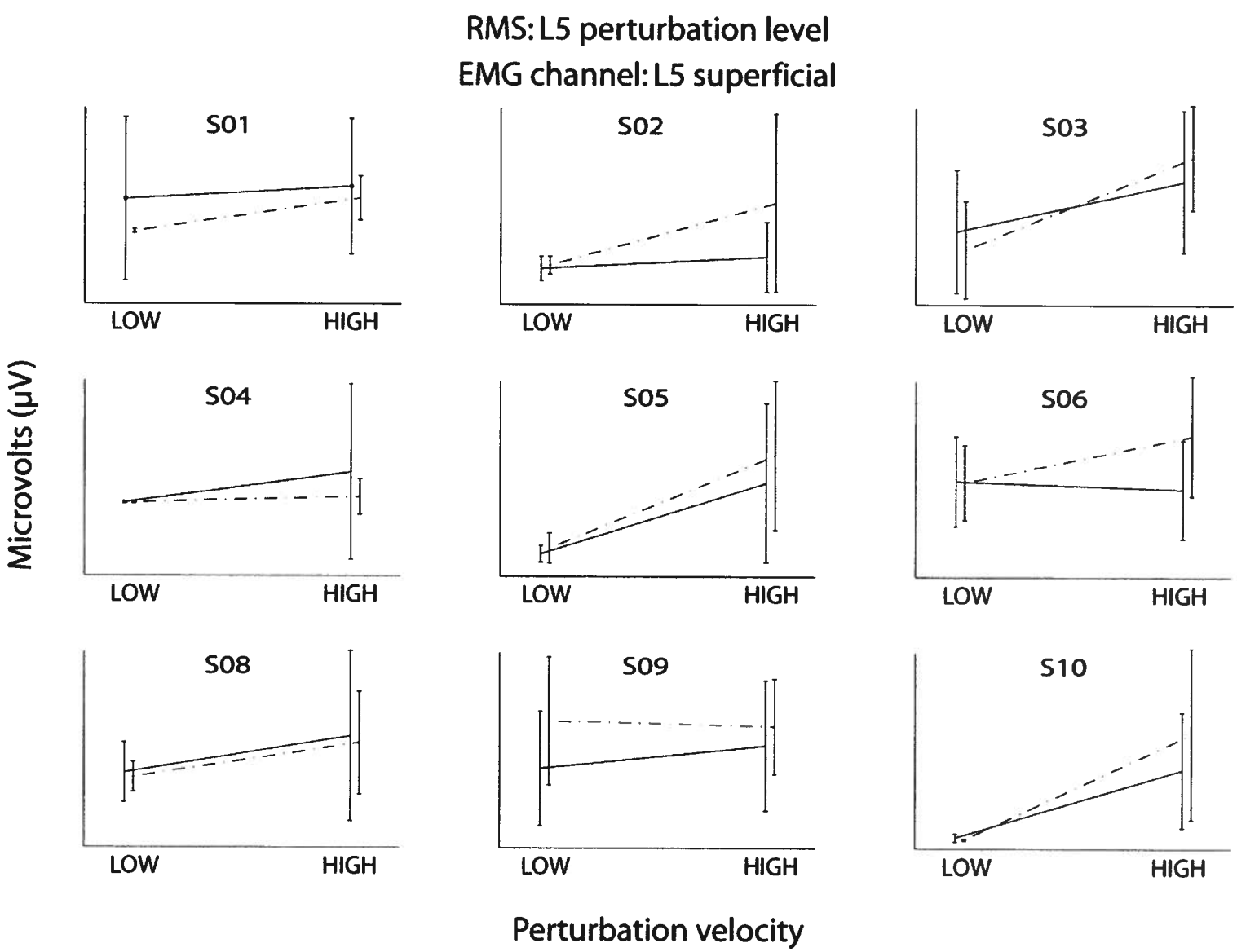
RMS: L5 perturbation level
EMG channel: L5 superficial
S01
S02
S03
S04
S05
S06
S08
S09
S10
LOW
HIGH
Microvolts (μV)
Perturbation velocity

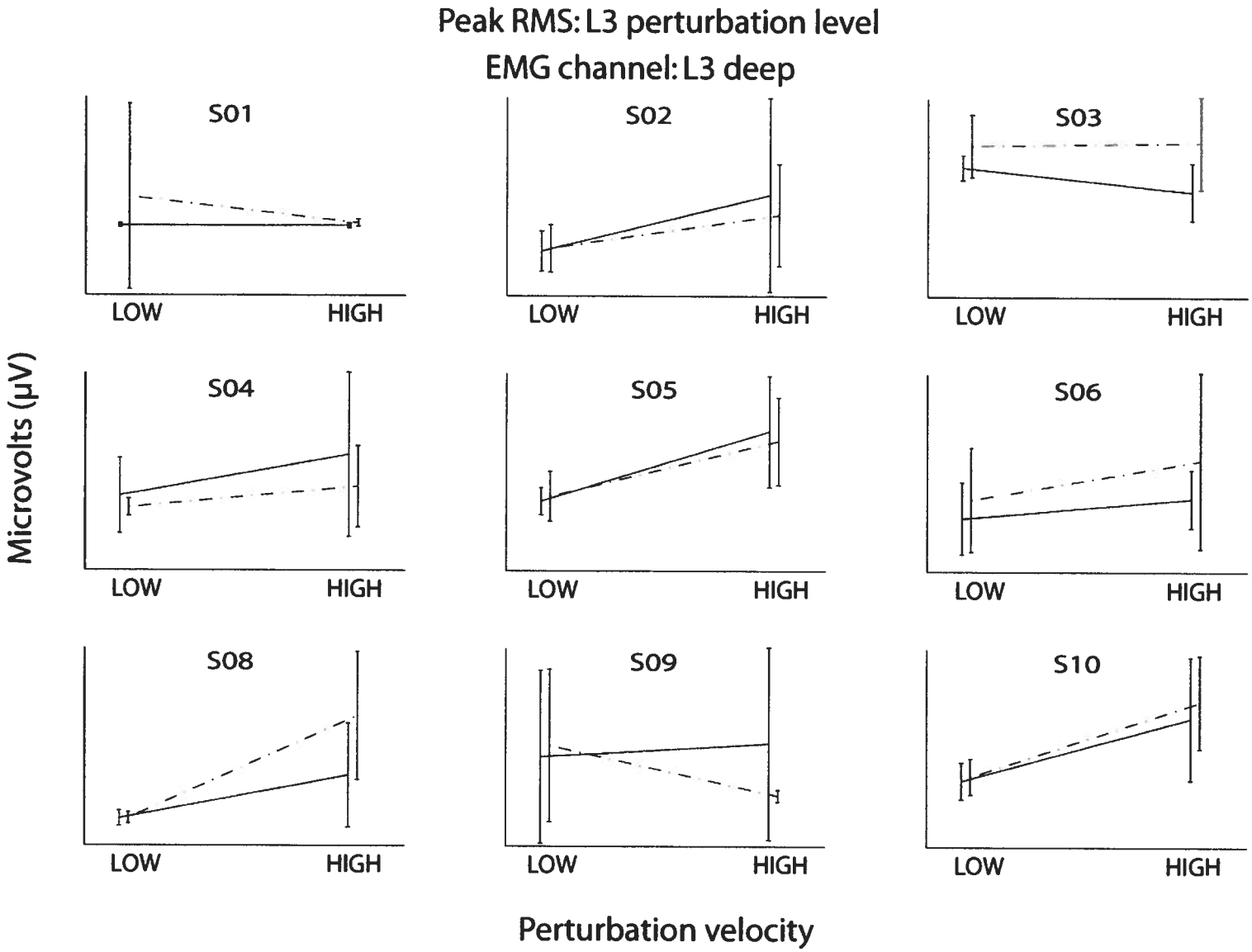
Peak RMS: L3 perturbation level
EMG channel: L3 deep
S01
S02
S03
S04
S05
S06
S08
S09
S10
LOW
HIGH
Microvolts (μV)
Perturbation velocity

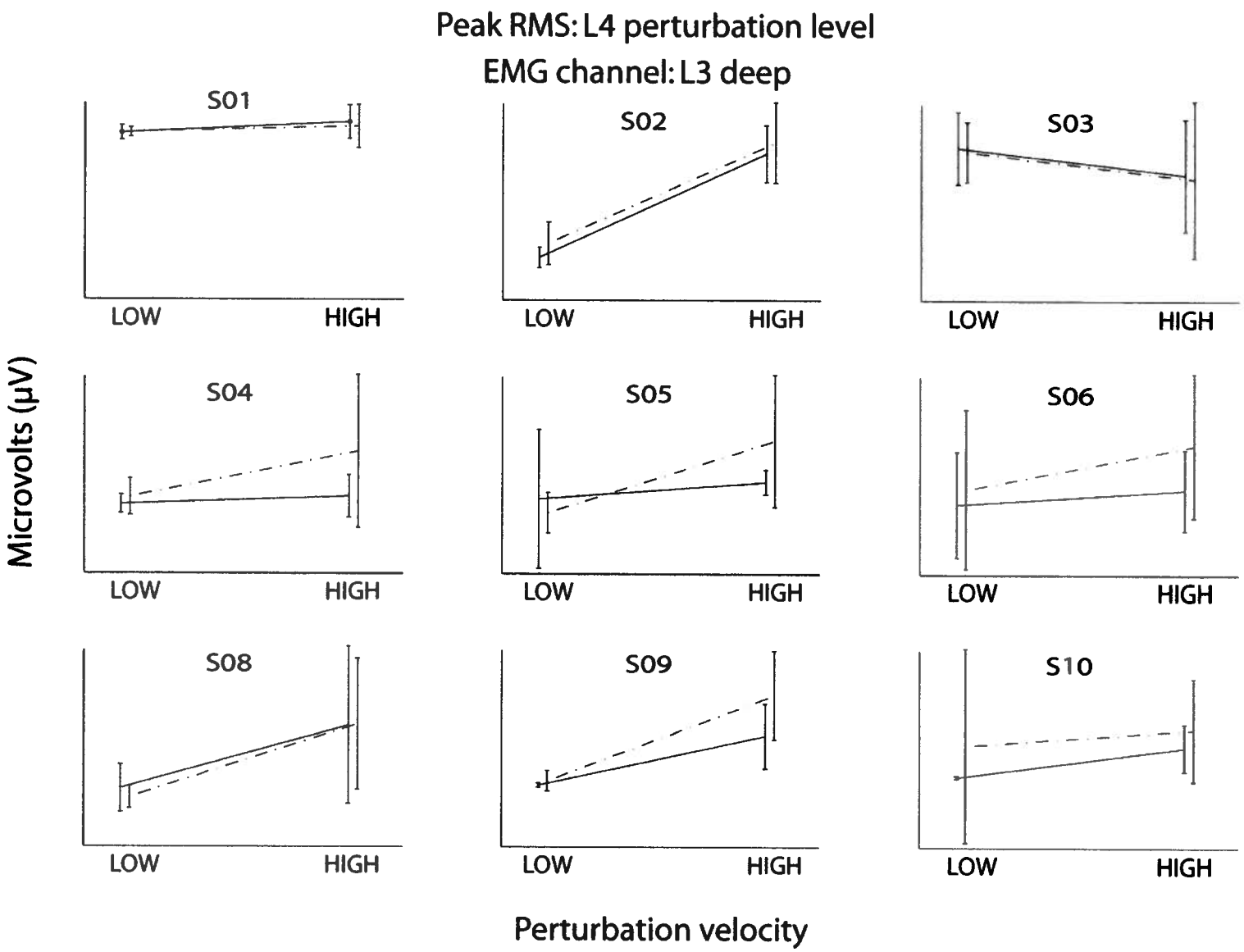
Peak RMS: L4 perturbation level
EMG channel: L3 deep
S01
S02
S03
S04
S05
S06
S08
S09
S10
LOW
HIGH
Microvolts (μV)
Perturbation velocity

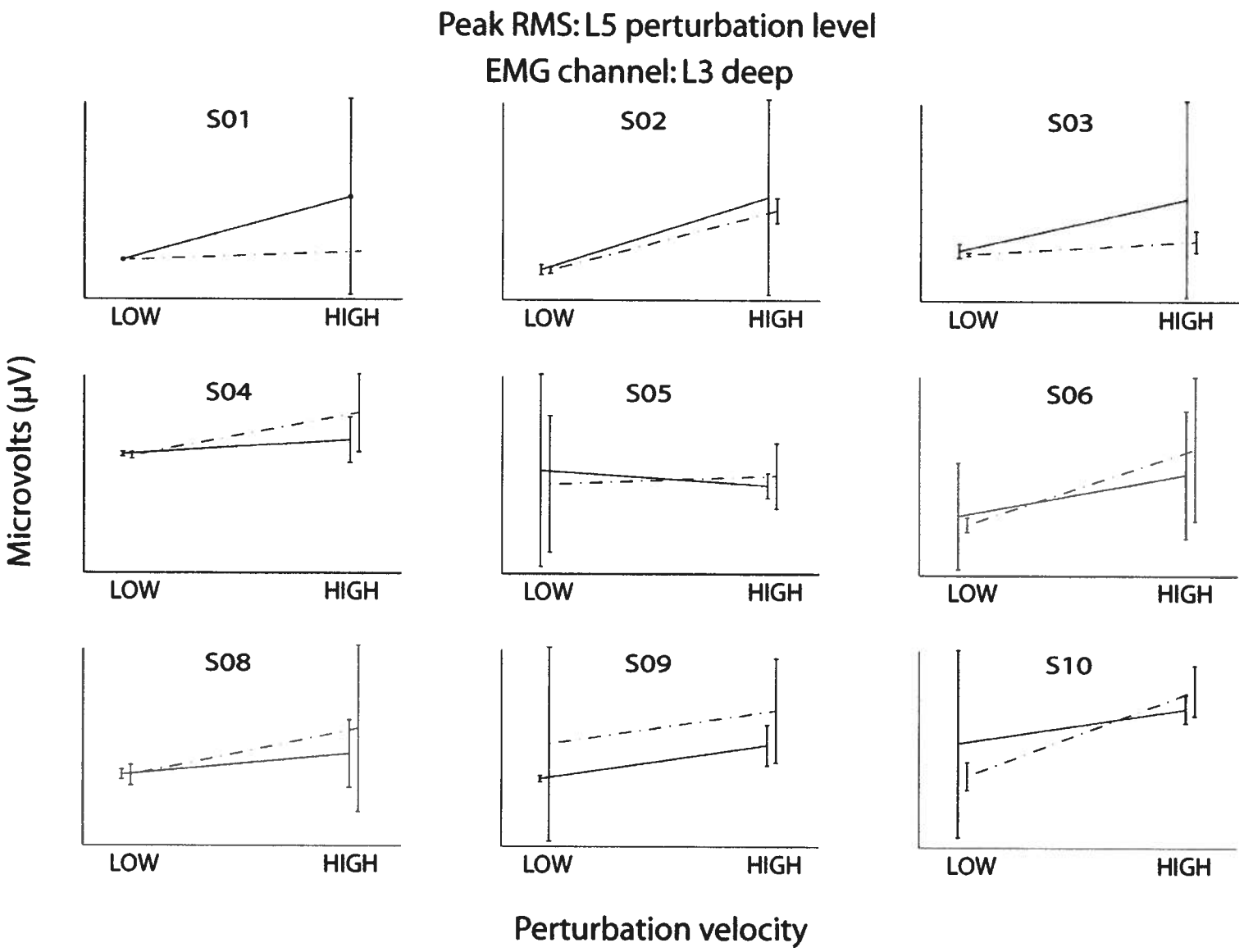
Peak RMS: L5 perturbation level
EMG channel: L3 deep
S01
S02
S03
S04
S05
S06
S08
S09
S10
LOW
HIGH
Microvolts (μV)
Perturbation velocity

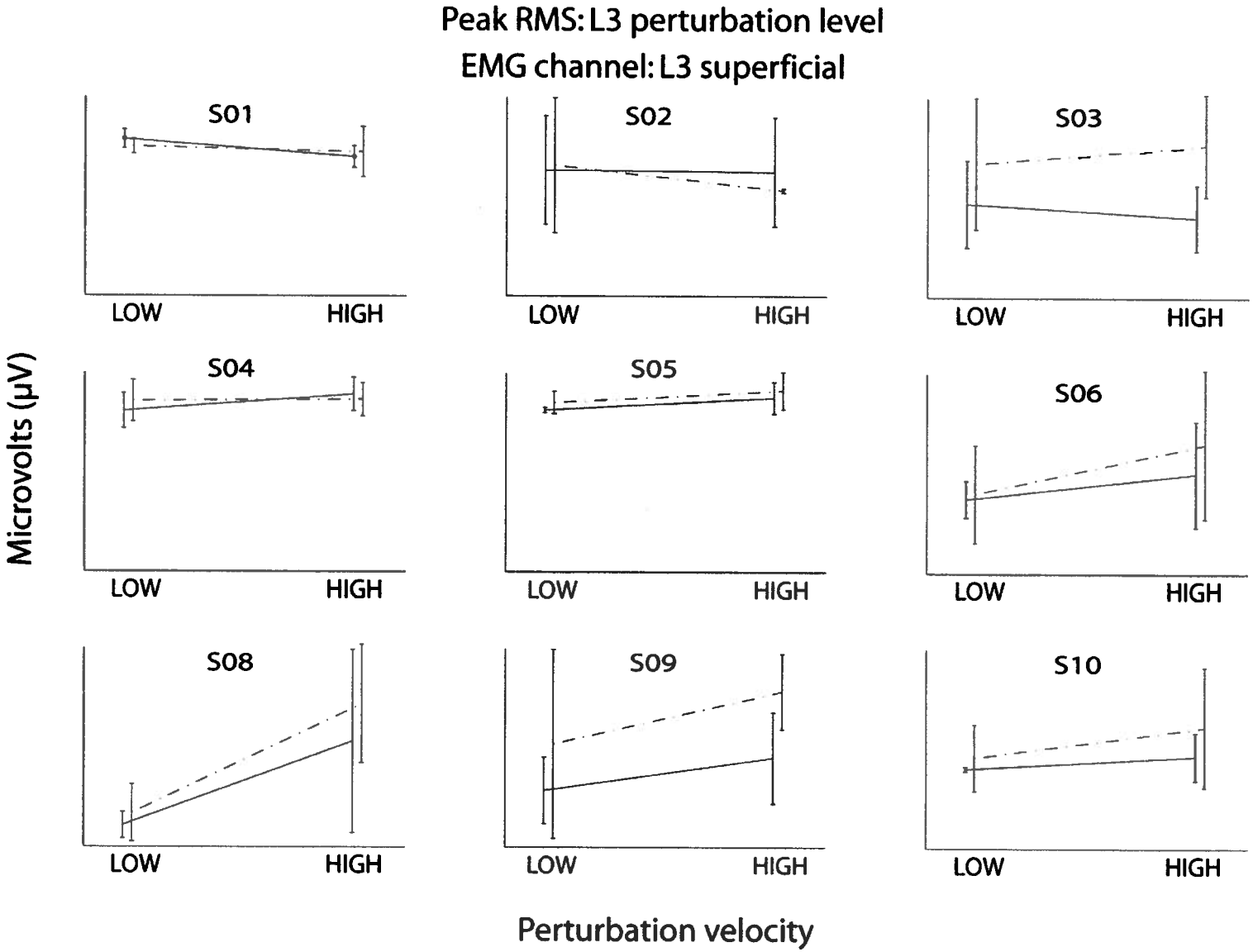
Peak RMS: L3 perturbation level
EMG channel: L3 superficial
S01
S02
S03
S04
S05
S06
S08
S09
S10
LOW
HIGH
Microvolts (μV)
Perturbation velocity

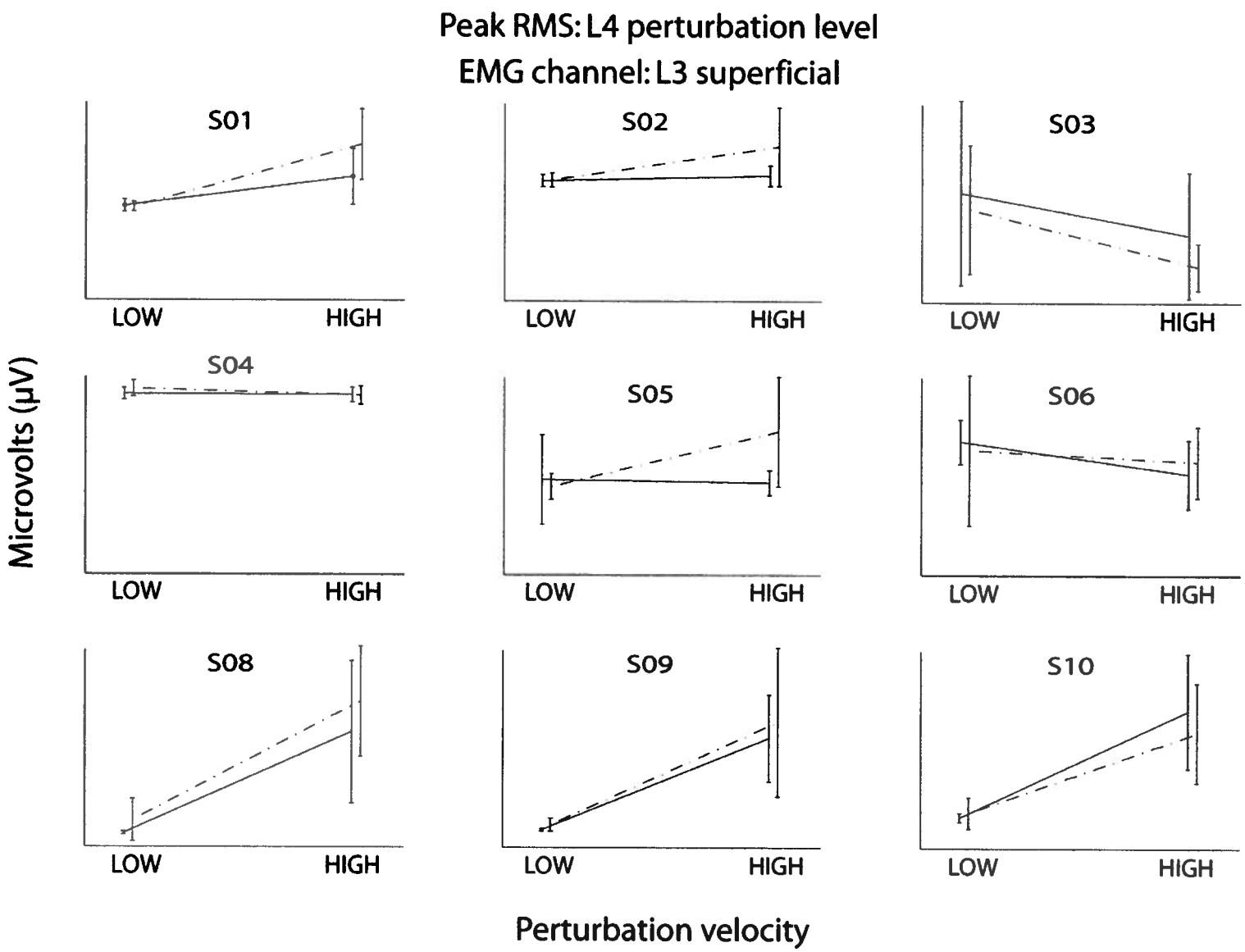
Peak RMS: L4 perturbation level
EMG channel: L3 superficial
S01
S02
S03
S04
S05
S06
S08
S09
S10
LOW
HIGH
Microvolts (μV)
Perturbation velocity

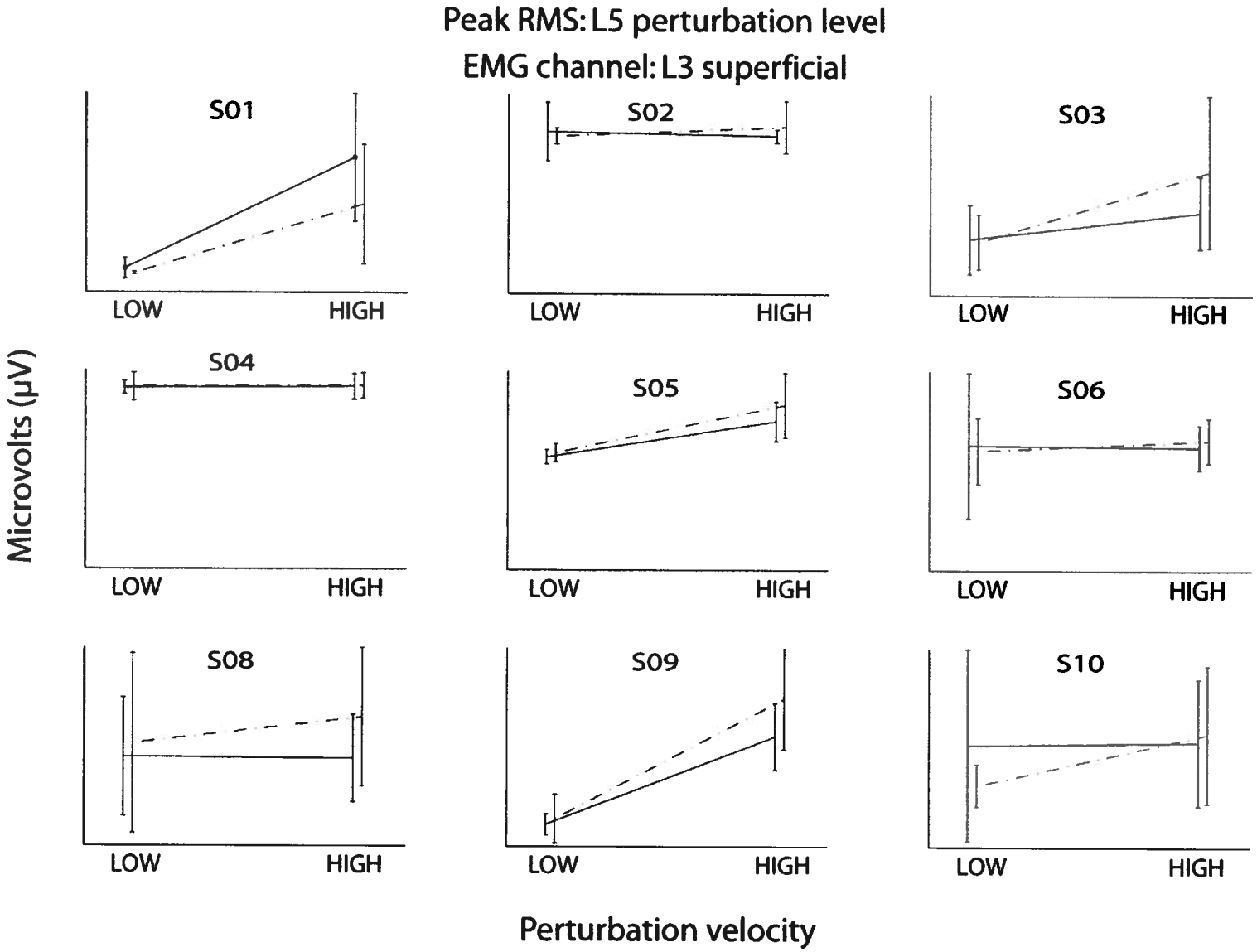
Peak RMS: L5 perturbation level
EMG channel: L3 superficial
S01
S02
S03
S04
S05
S06
S08
S09
S10
LOW
HIGH
Microvolts (μV)
Perturbation velocity

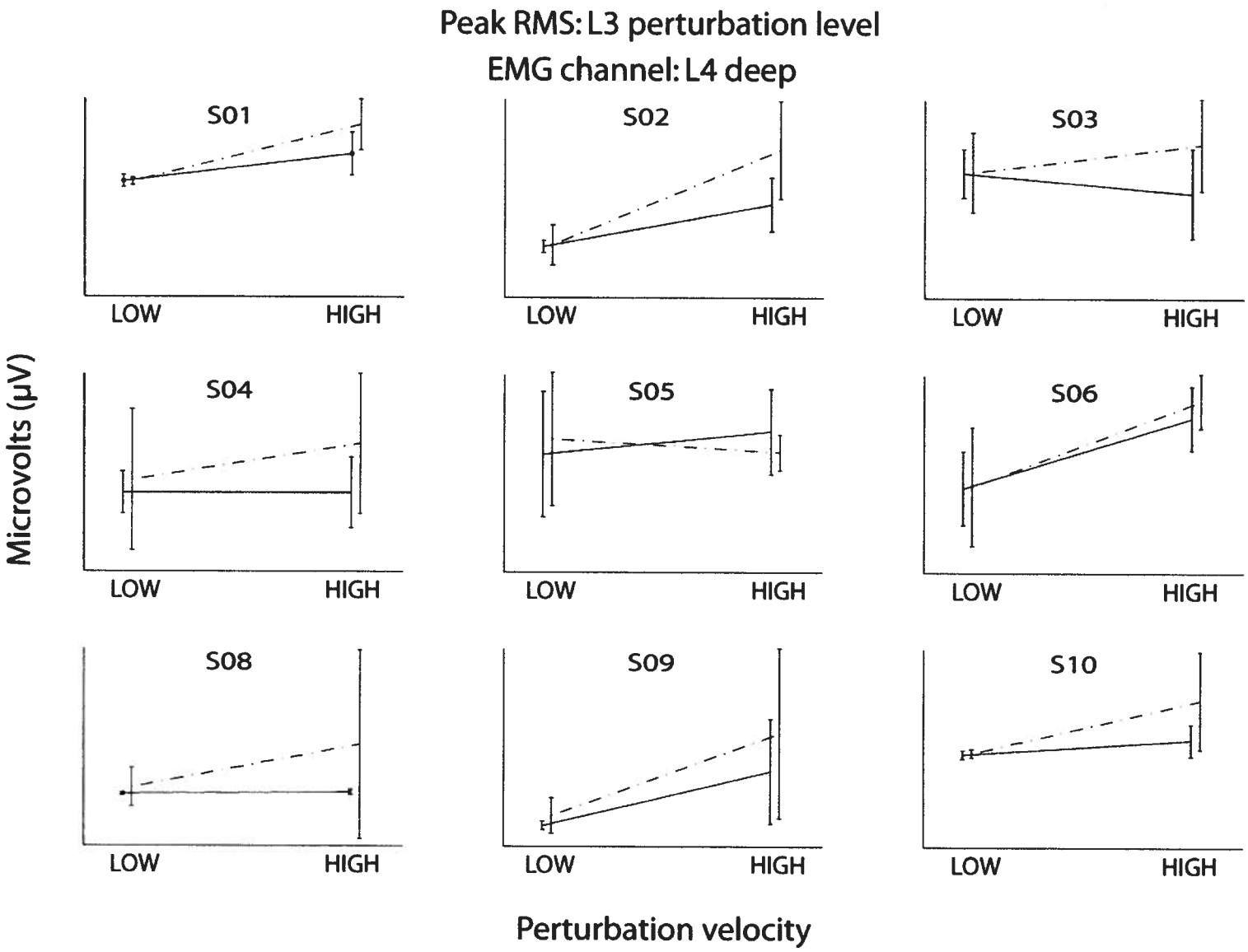
Peak RMS: L3 perturbation level
EMG channel: L4 deep
S01
S02
S03
S04
S05
S06
S08
S09
S10
LOW
HIGH
Microvolts (μV)
Perturbation velocity

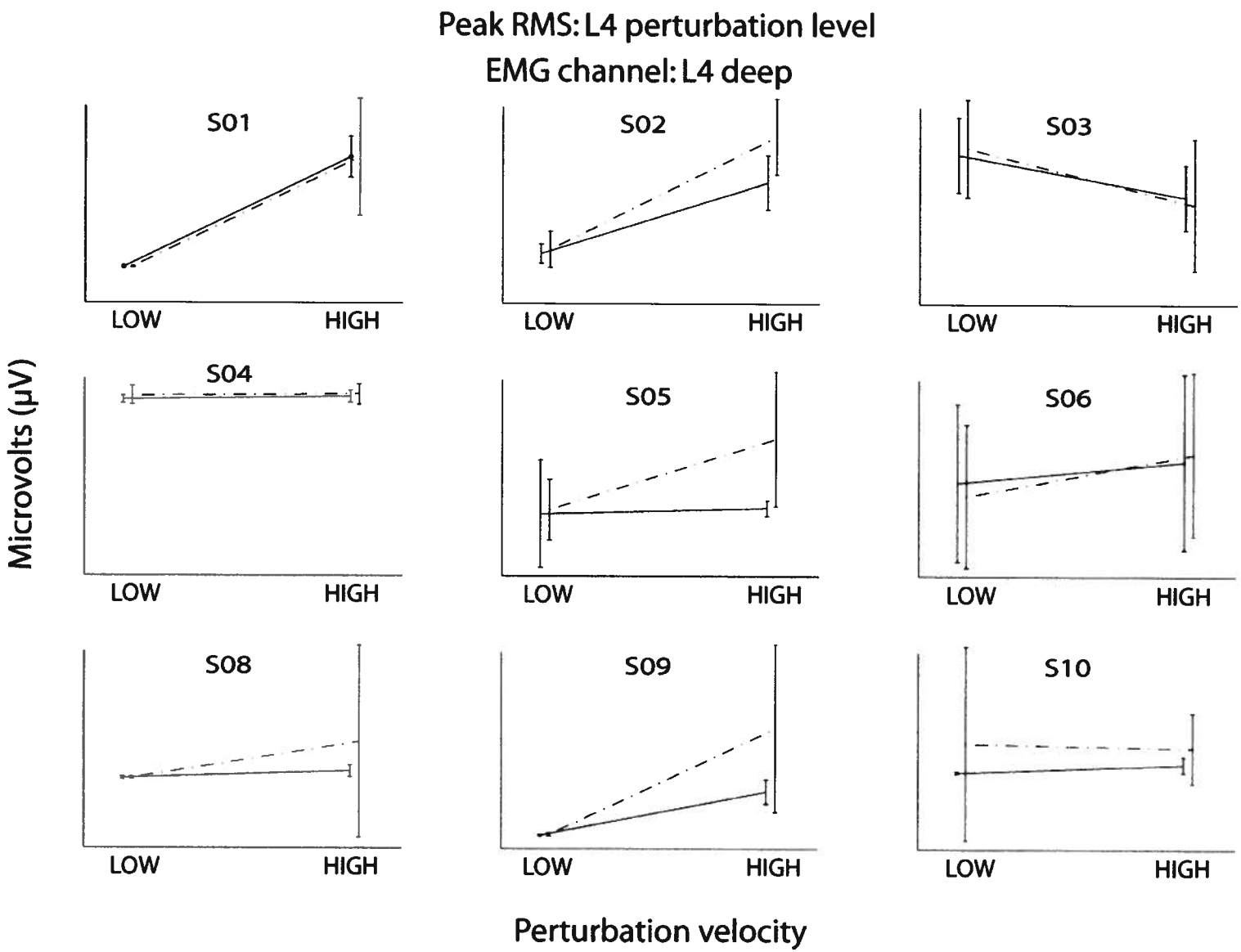
Peak RMS: L4 perturbation level
EMG channel: L4 deep
S01
S02
S03
S04
S05
S06
S08
S09
S10
LOW
HIGH
Microvolts (μV)
Perturbation velocity

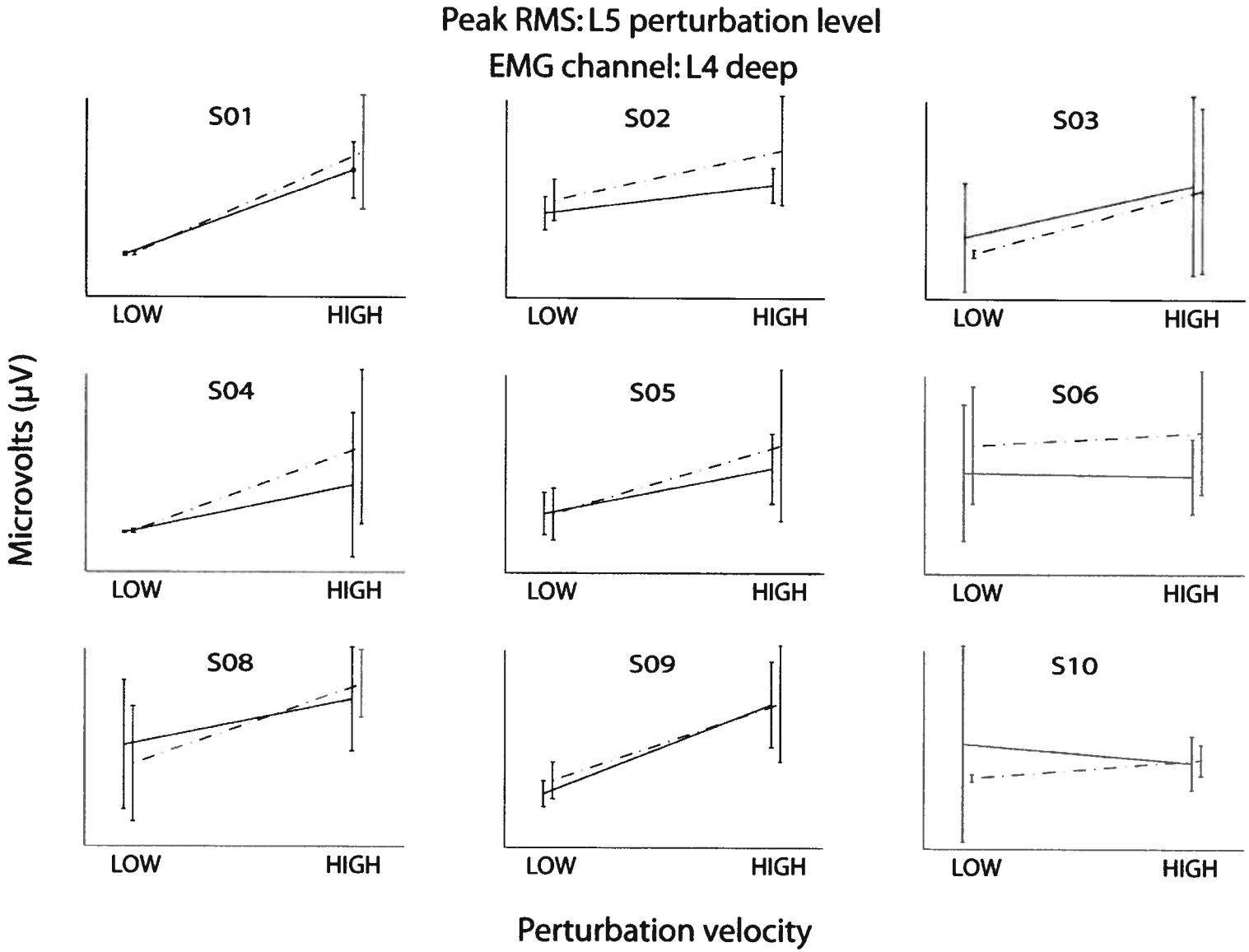
Peak RMS: L5 perturbation level
EMG channel: L4 deep
S01
S02
S03
S04
S05
S06
S08
S09
S10
LOW
HIGH
Microvolts (μV)
Perturbation velocity

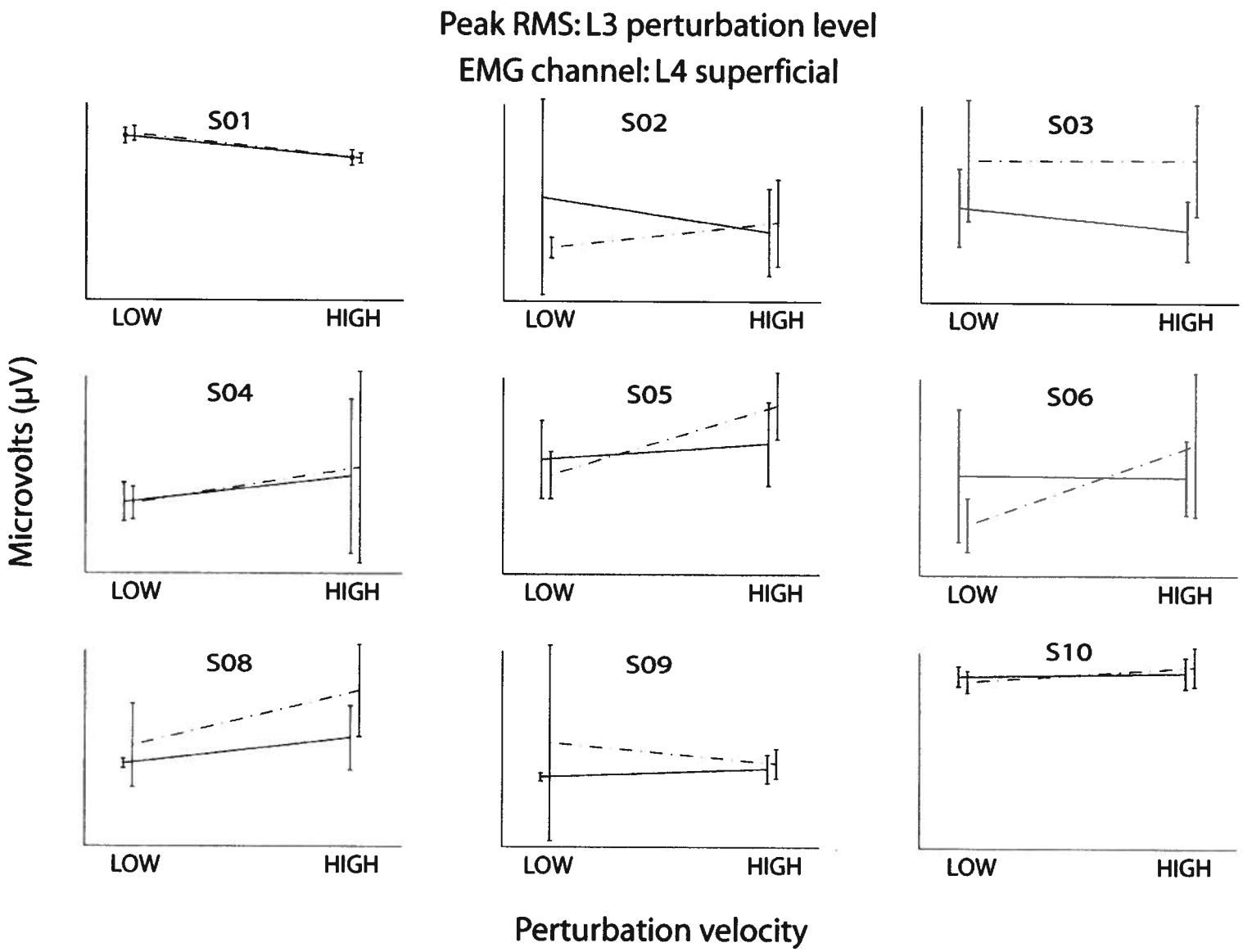
Peak RMS: L3 perturbation level
EMG channel: L4 superficial
S01
S02
S03
S04
S05
S06
S08
S09
S10
LOW
HIGH
Microvolts (μV)
Perturbation velocity

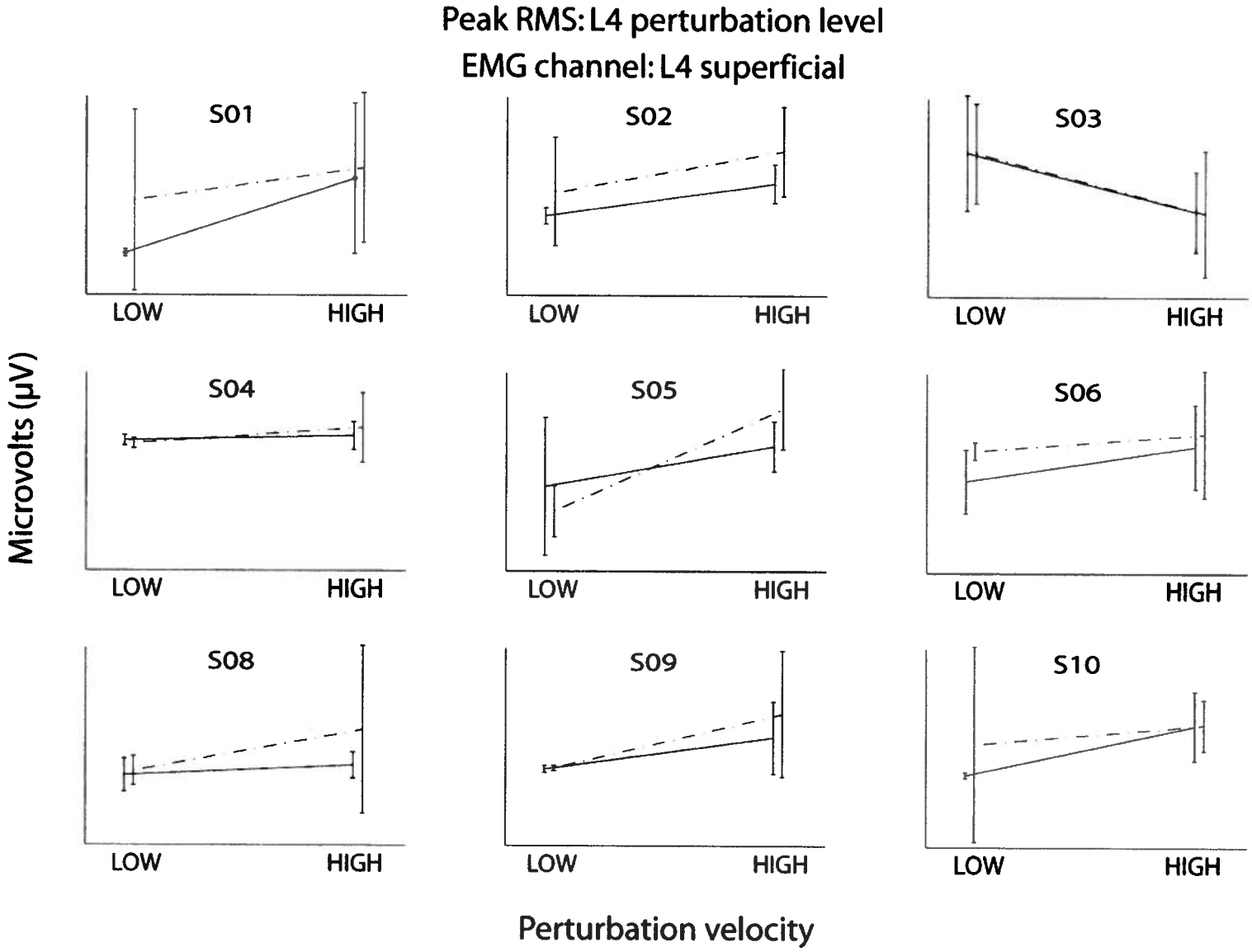
Peak RMS: L4 perturbation level
EMG channel: L4 superficial
S01
S02
S03
S04
S05
S06
S08
S09
S10
LOW
HIGH
Microvolts (μV)
Perturbation velocity

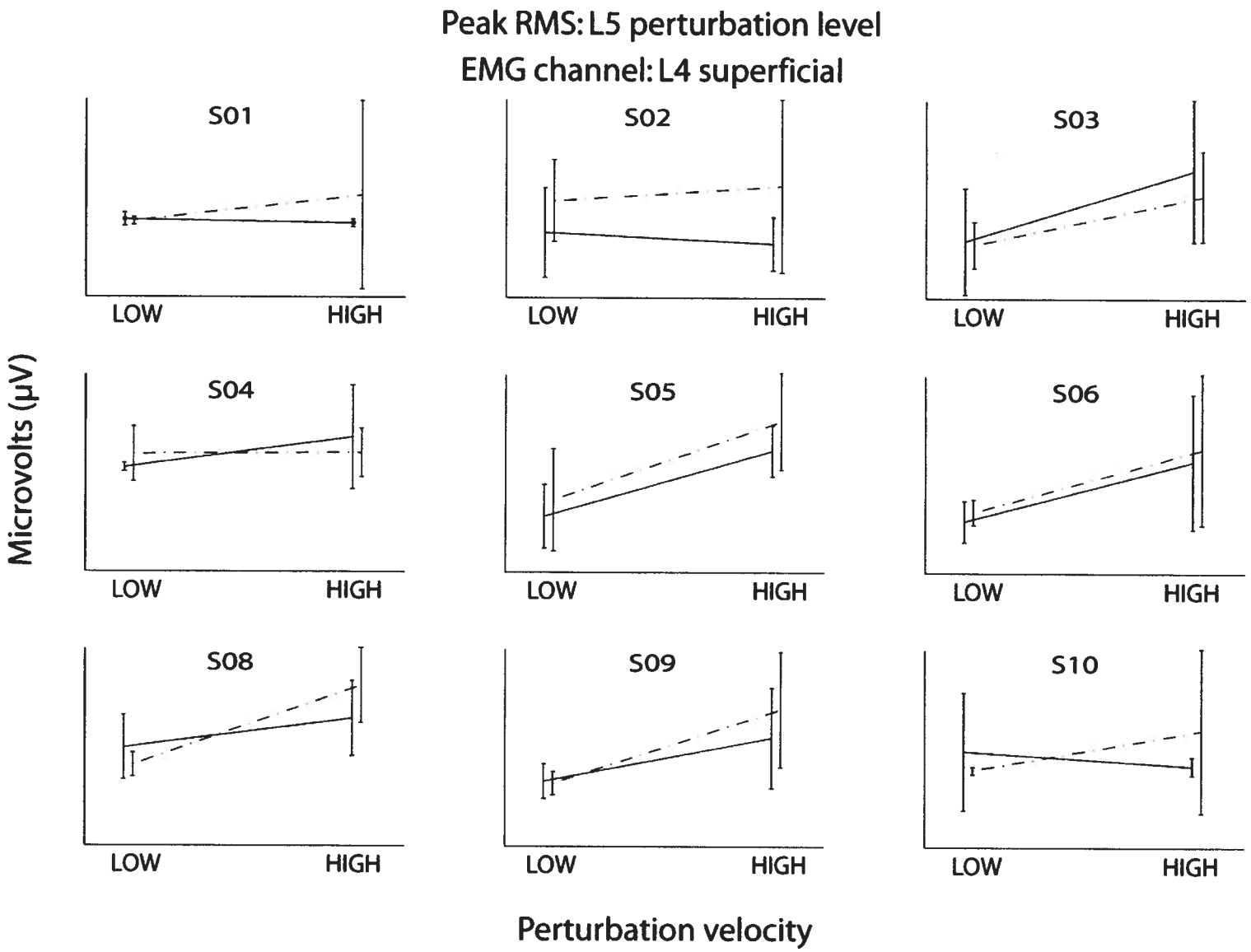
Peak RMS: L5 perturbation level
EMG channel: L4 superficial
S01
S02
S03
S04
S05
S06
S08
S09
S10
LOW
HIGH
Microvolts (μV)
Perturbation velocity

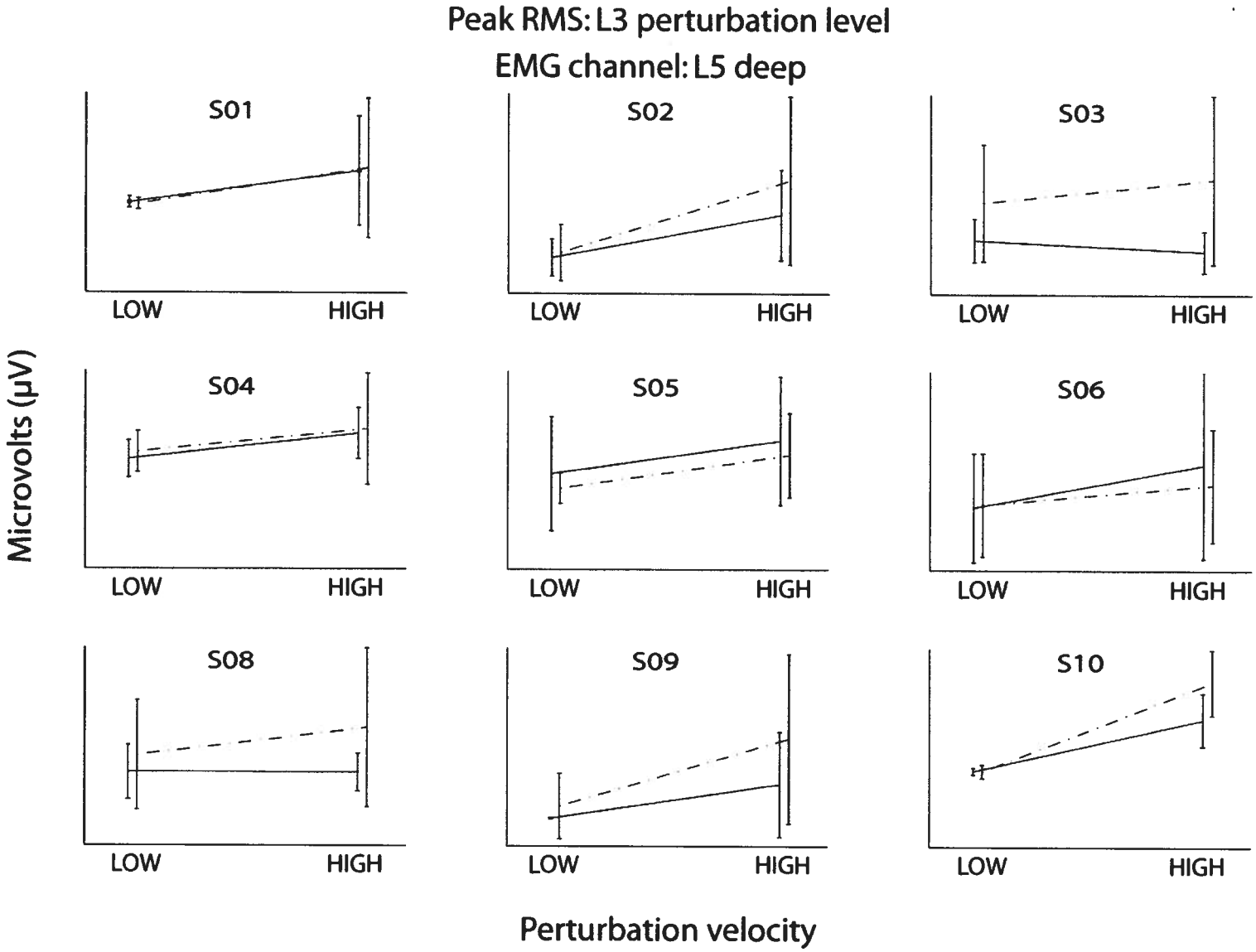
Peak RMS: L3 perturbation level
EMG channel: L5 deep
S01
S02
S03
S04
S05
S06
S08
S09
S10
LOW
HIGH
Microvolts (μV)
Perturbation velocity

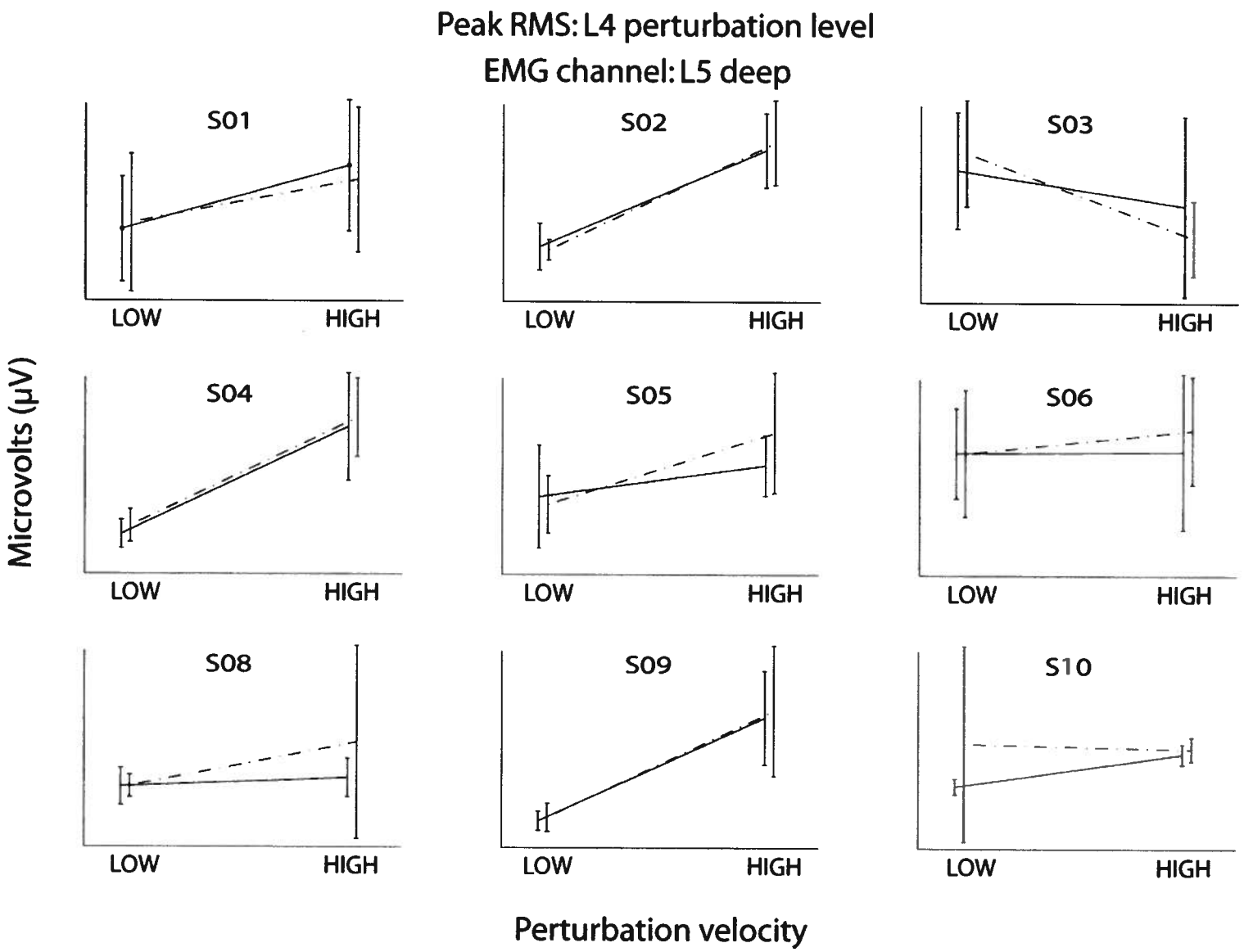
Peak RMS: L4 perturbation level
EMG channel: L5 deep
S01
S02
S03
S04
S05
S06
S08
S09
S10
LOW
HIGH
Microvolts (μV)
Perturbation velocity

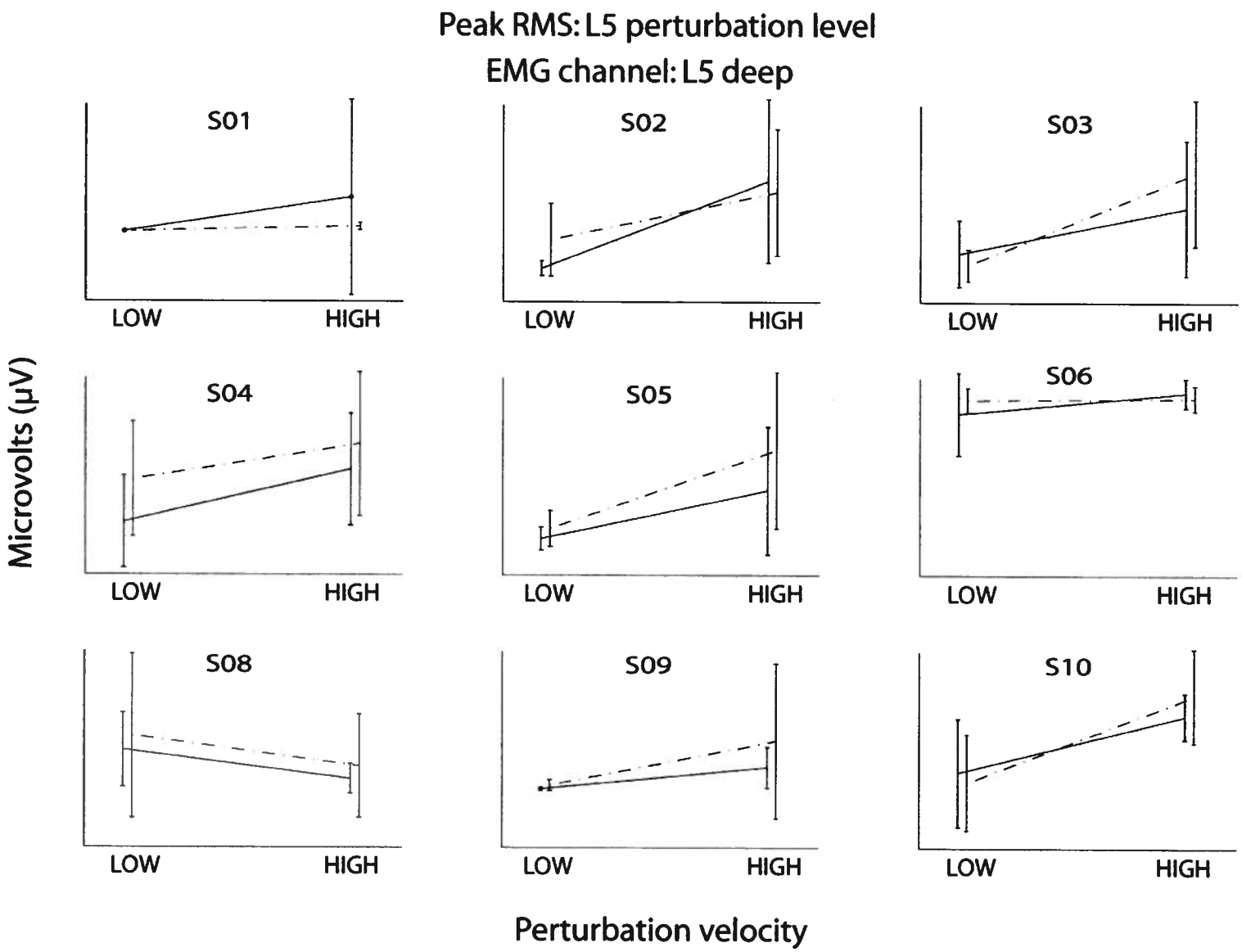
Peak RMS: L5 perturbation level
EMG channel: L5 deep
S01
S02
S03
S04
S05
S06
S08
S09
S10
LOW
HIGH
Microvolts (μV)
Perturbation velocity

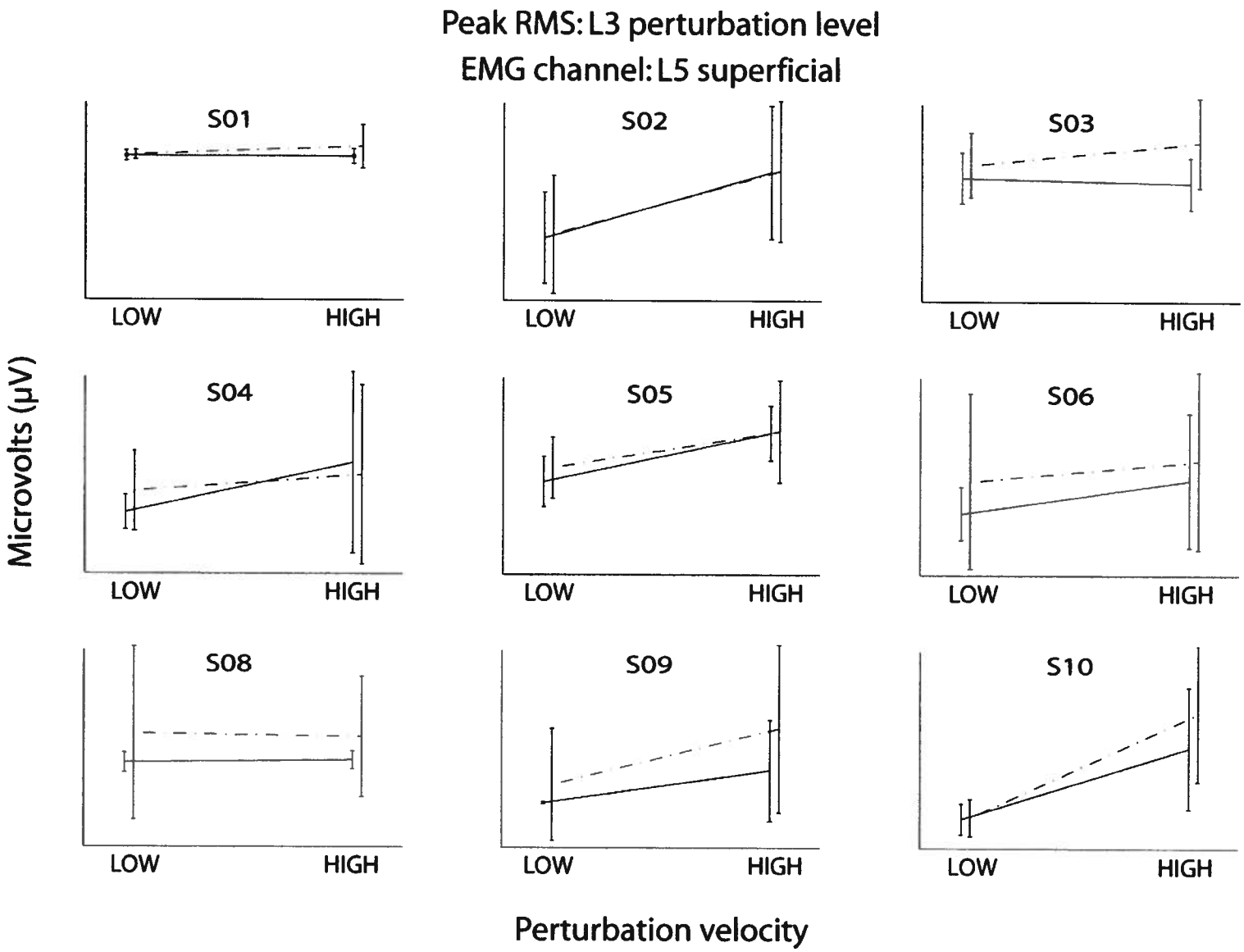
Peak RMS: L3 perturbation level
EMG channel: L5 superficial
S01
S02
S03
S04
S05
S06
S08
S09
S10
LOW
HIGH
Microvolts (μV)
Perturbation velocity

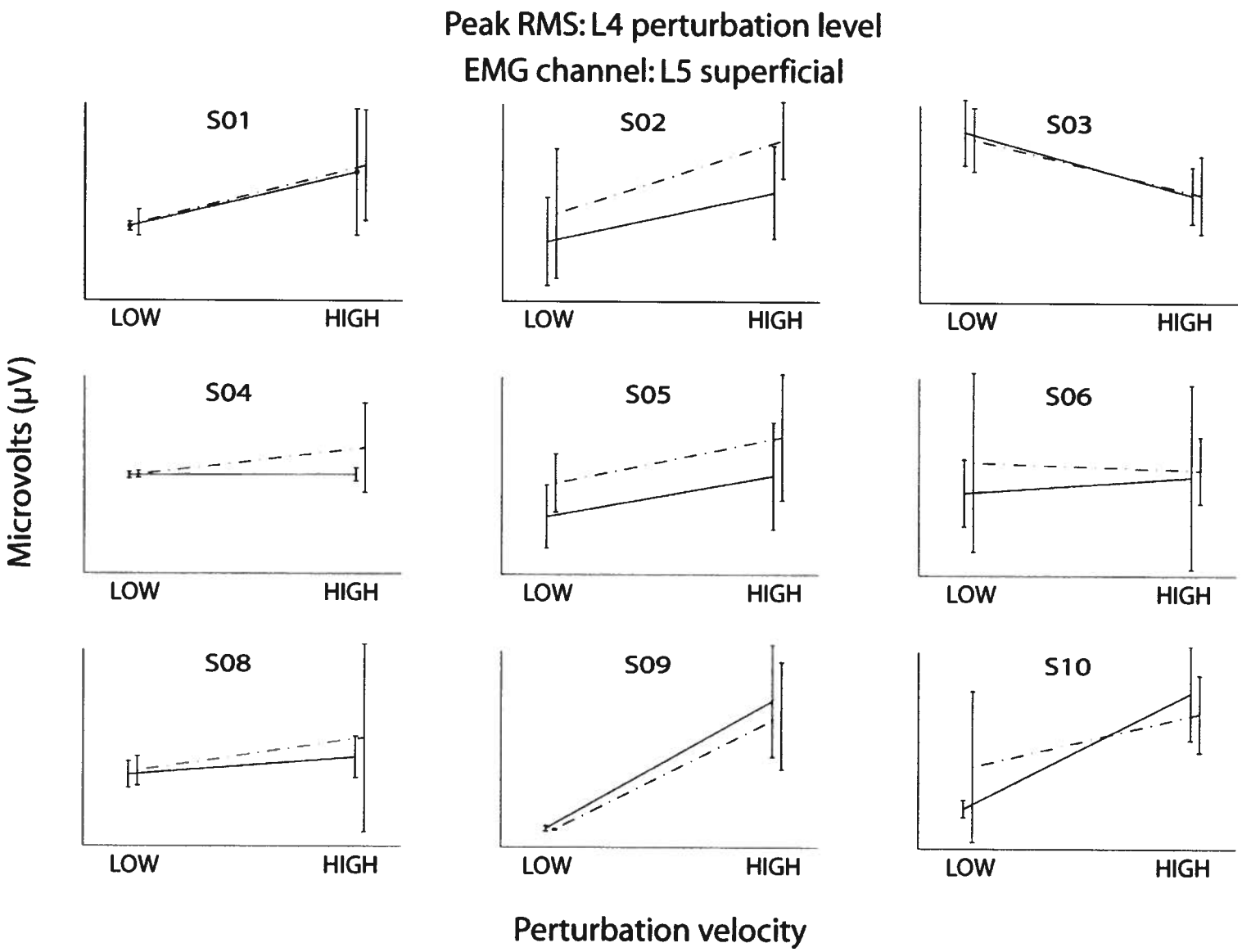
Peak RMS: L4 perturbation level
EMG channel: L5 superficial
S01
S02
S03
S04
S05
S06
S08
S09
S10
LOW
HIGH
Microvolts (μV)
Perturbation velocity

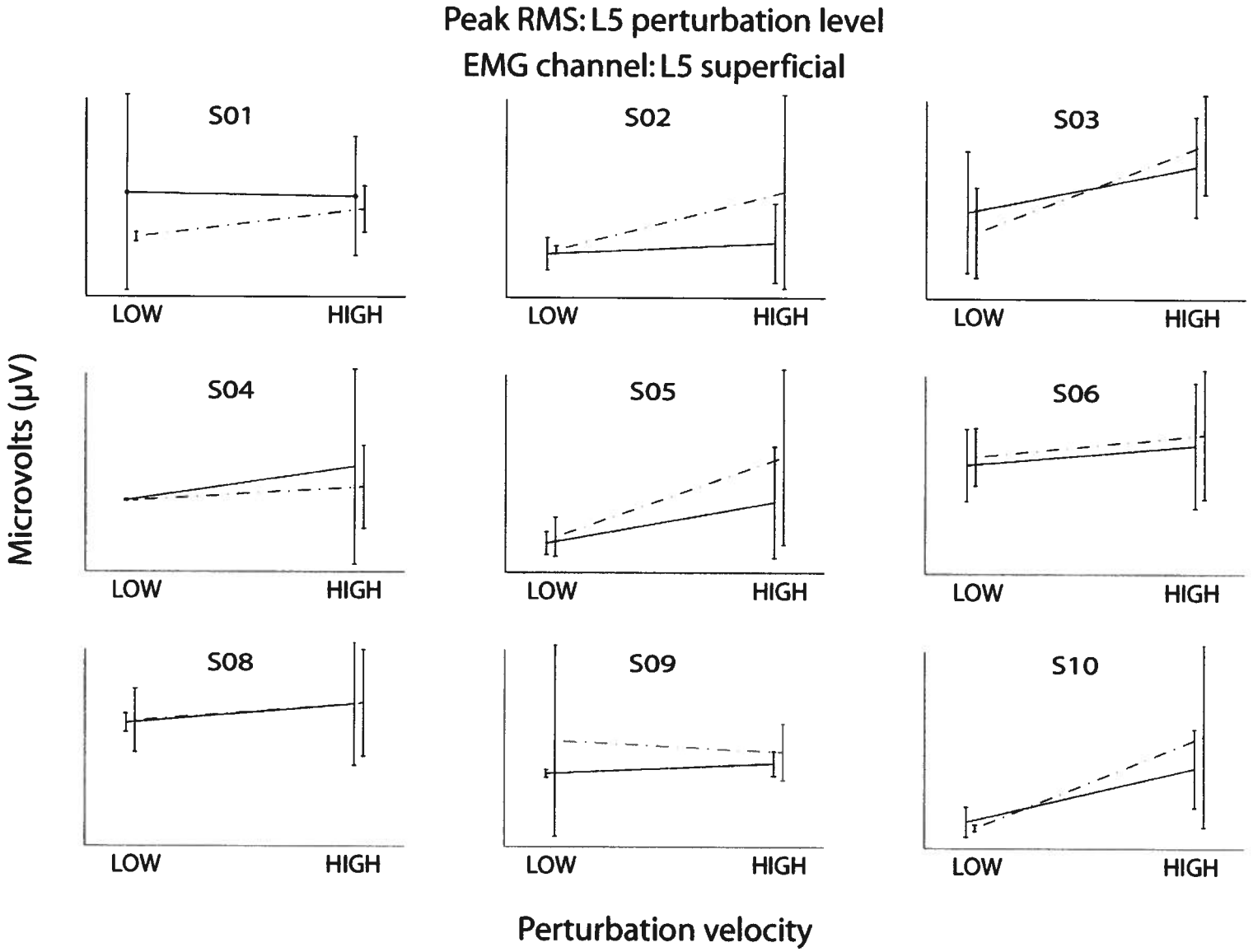
Peak RMS: L5 perturbation level
EMG channel: L5 superficial
S01
S02
S03
S04
S05
S06
S08
S09
S10
LOW
HIGH
Microvolts (μV)
Perturbation velocity

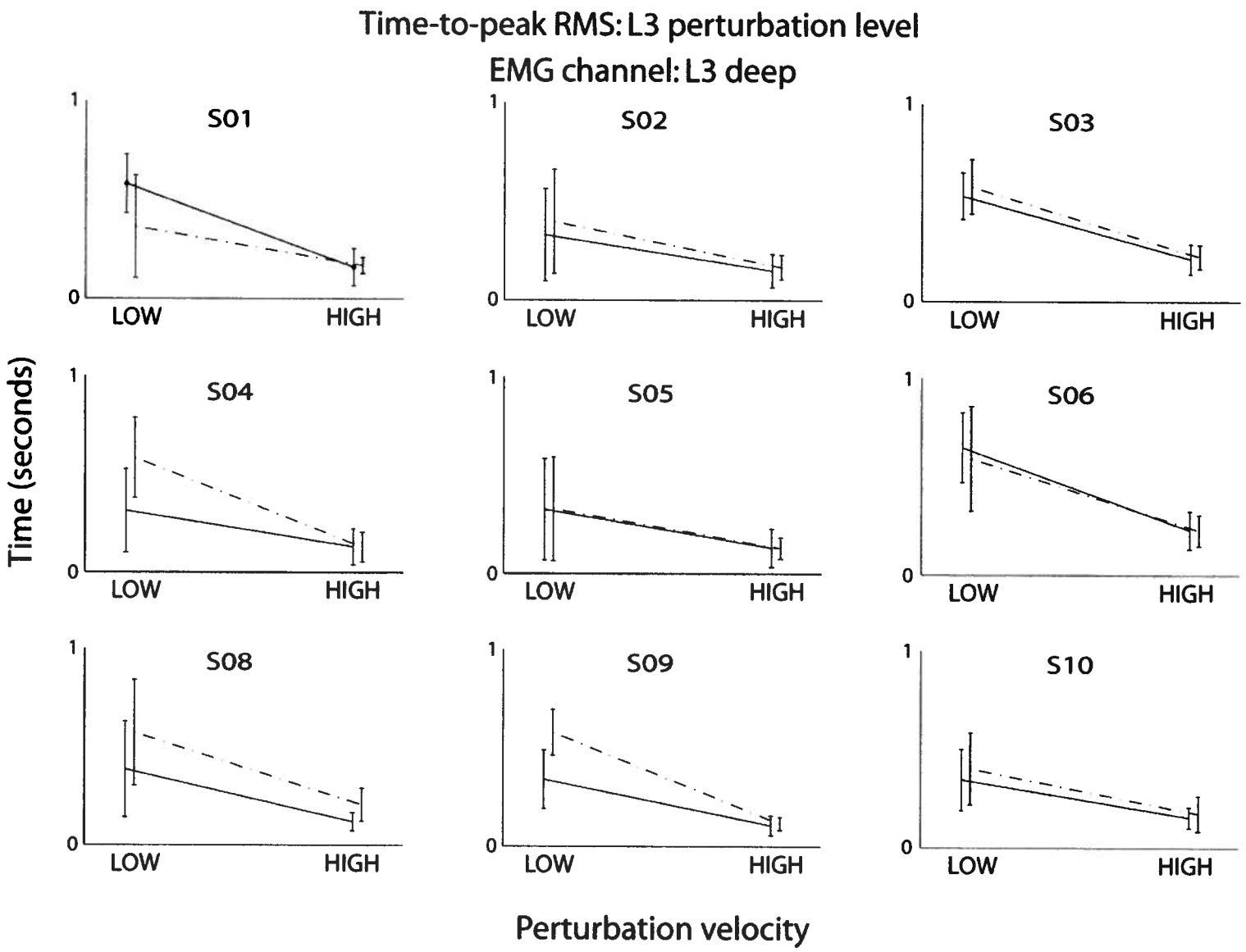
Time-to-peak RMS: L3 perturbation level
EMG channel: L3 deep
S01
S02
S03
S04
S05
S06
S08
S09
S10
1
0
LOW
HIGH
Time (seconds)
Perturbation velocity

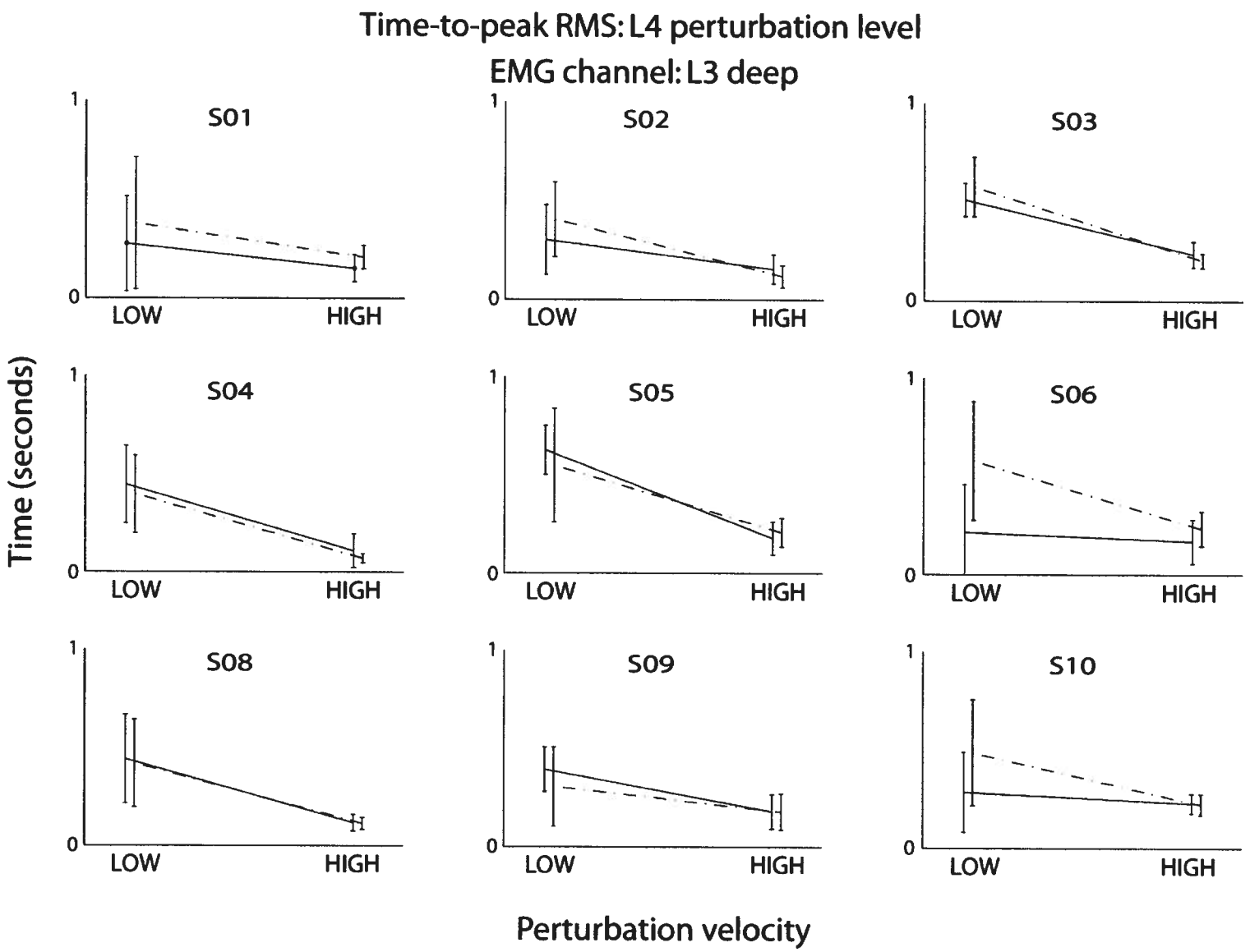
Time-to-peak RMS: L4 perturbation level
EMG channel: L3 deep
S01
S02
S03
S04
S05
S06
S08
S09
S10
1
0
LOW
HIGH
Time (seconds)
Perturbation velocity

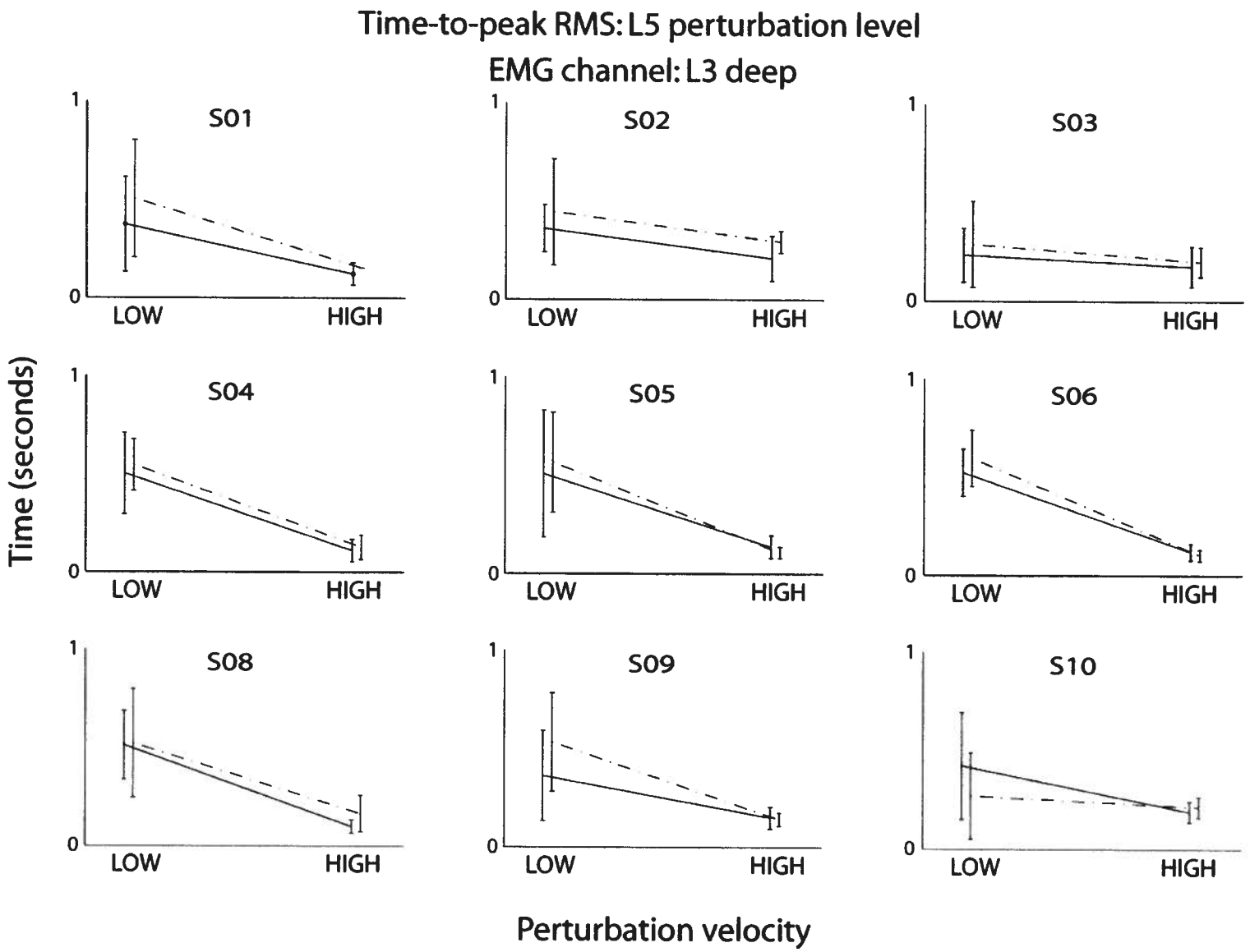
Time-to-peak RMS: L5 perturbation level
EMG channel: L3 deep
S01
S02
S03
S04
S05
S06
S08
S09
S10
1
0
LOW
HIGH
Time (seconds)
Perturbation velocity

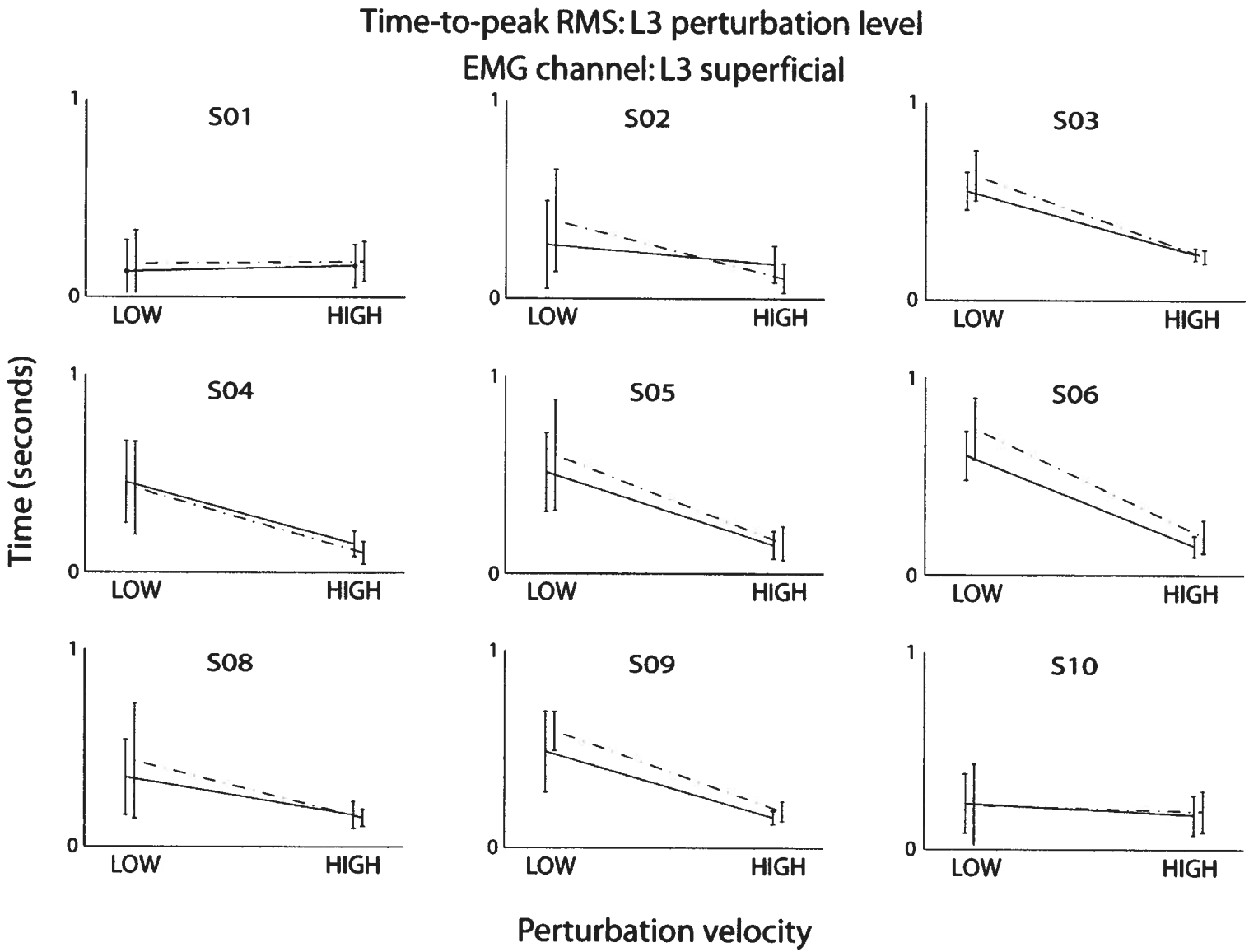
Time-to-peak RMS: L3 perturbation level
EMG channel: L3 superficial
S01
S02
S03
S04
S05
S06
S08
S09
S10
1
0
LOW
HIGH
Time (seconds)
Perturbation velocity

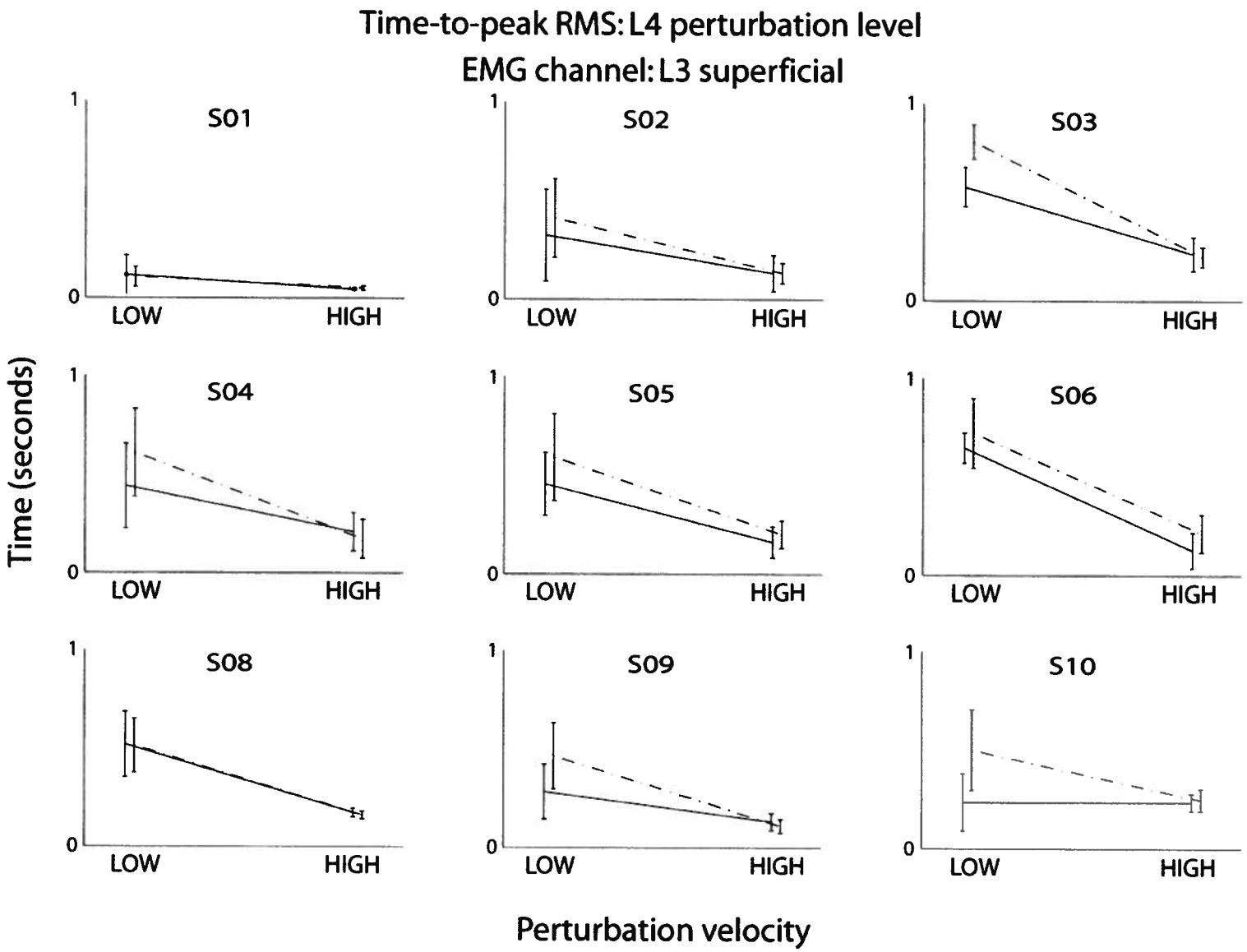
Time-to-peak RMS: L4 perturbation level
EMG channel: L3 superficial
S01
S02
S03
S04
S05
S06
S08
S09
S10
1
0
LOW
HIGH
Time (seconds)
Perturbation velocity

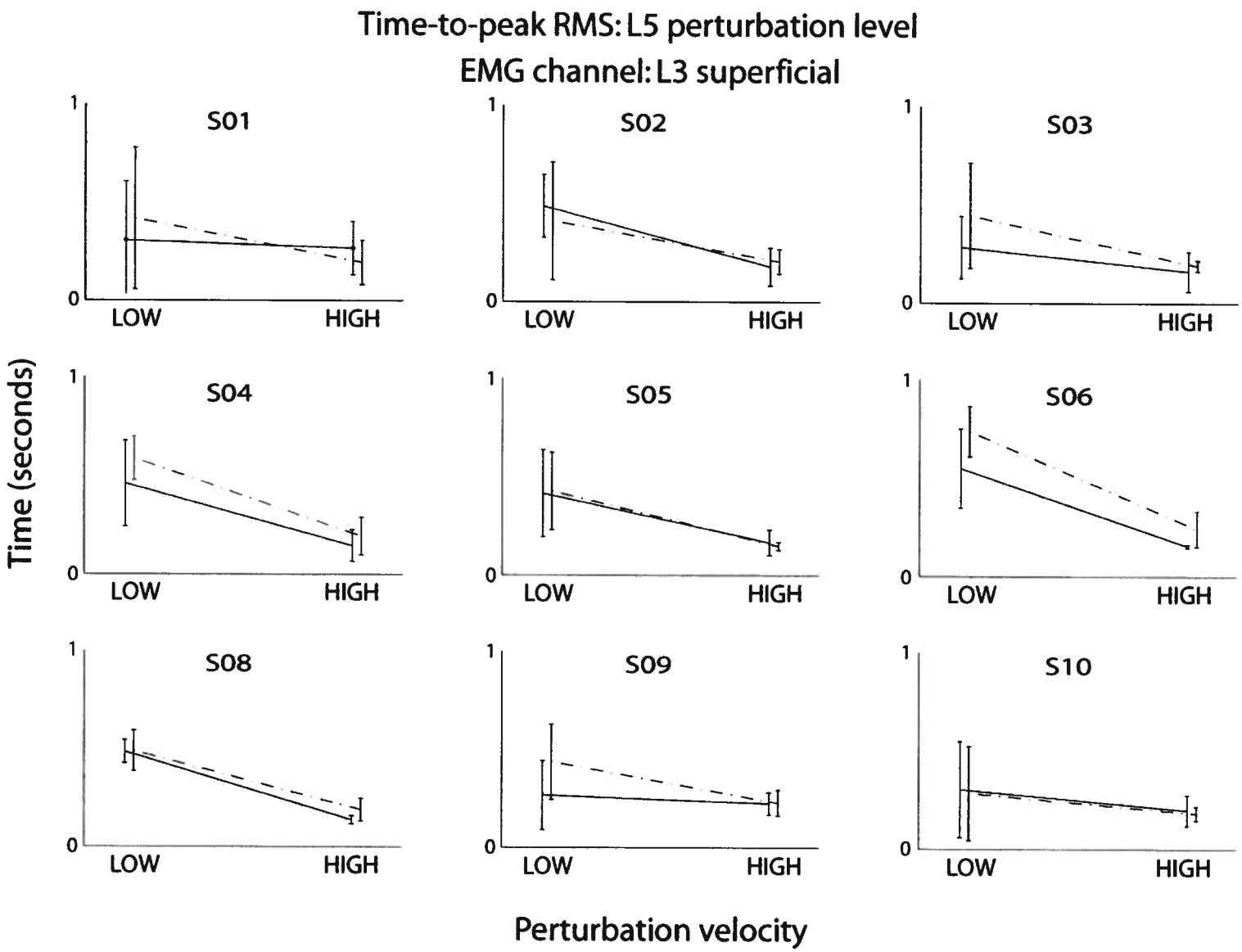
Time-to-peak RMS: L5 perturbation level
EMG channel: L3 superficial
S01
S02
S03
S04
S05
S06
S08
S09
S10
1
0
LOW
HIGH
Time (seconds)
Perturbation velocity

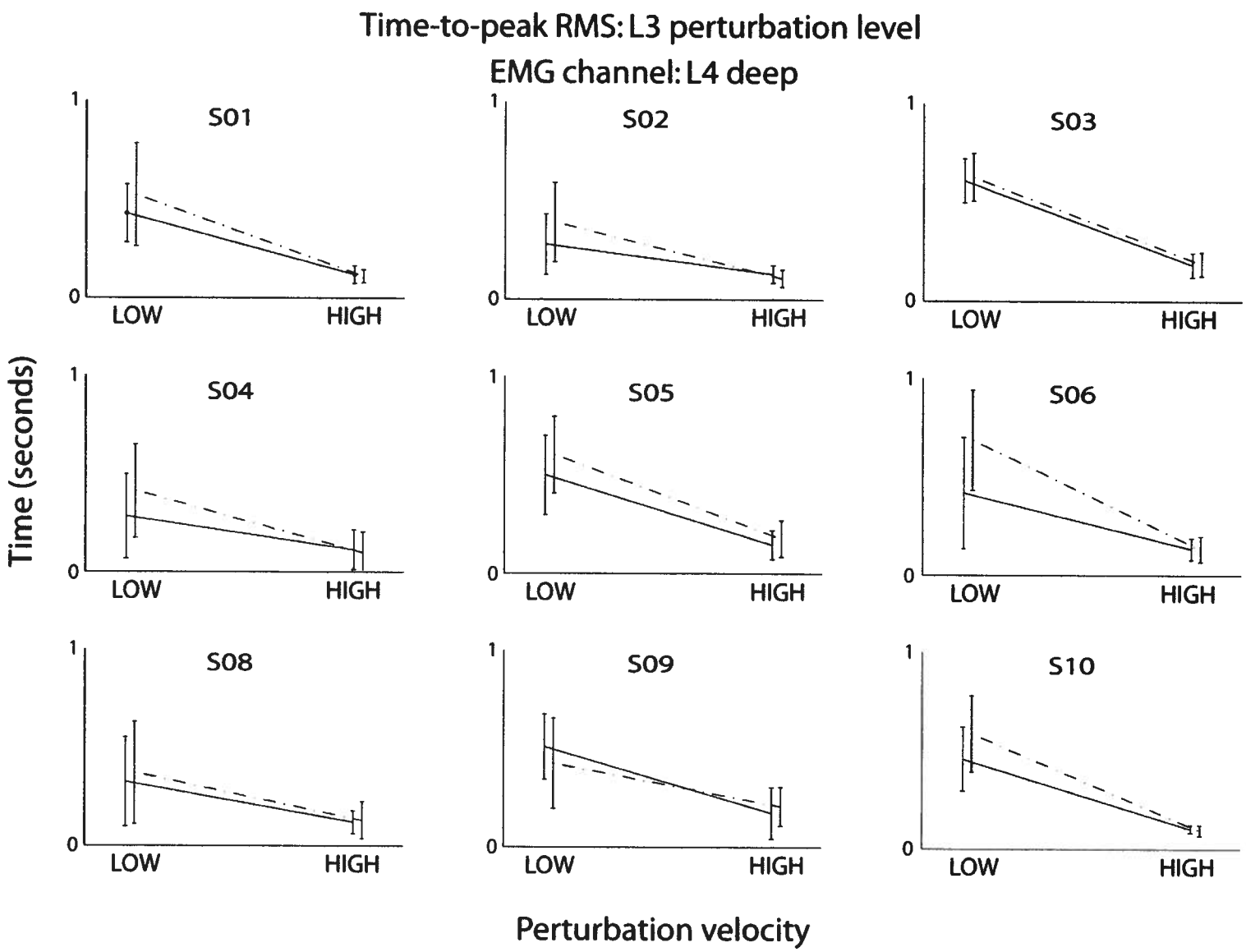
Time-to-peak RMS: L3 perturbation level
EMG channel: L4 deep
S01
S02
S03
S04
S05
S06
S08
S09
S10
1
0
LOW
HIGH
Time (seconds)
Perturbation velocity

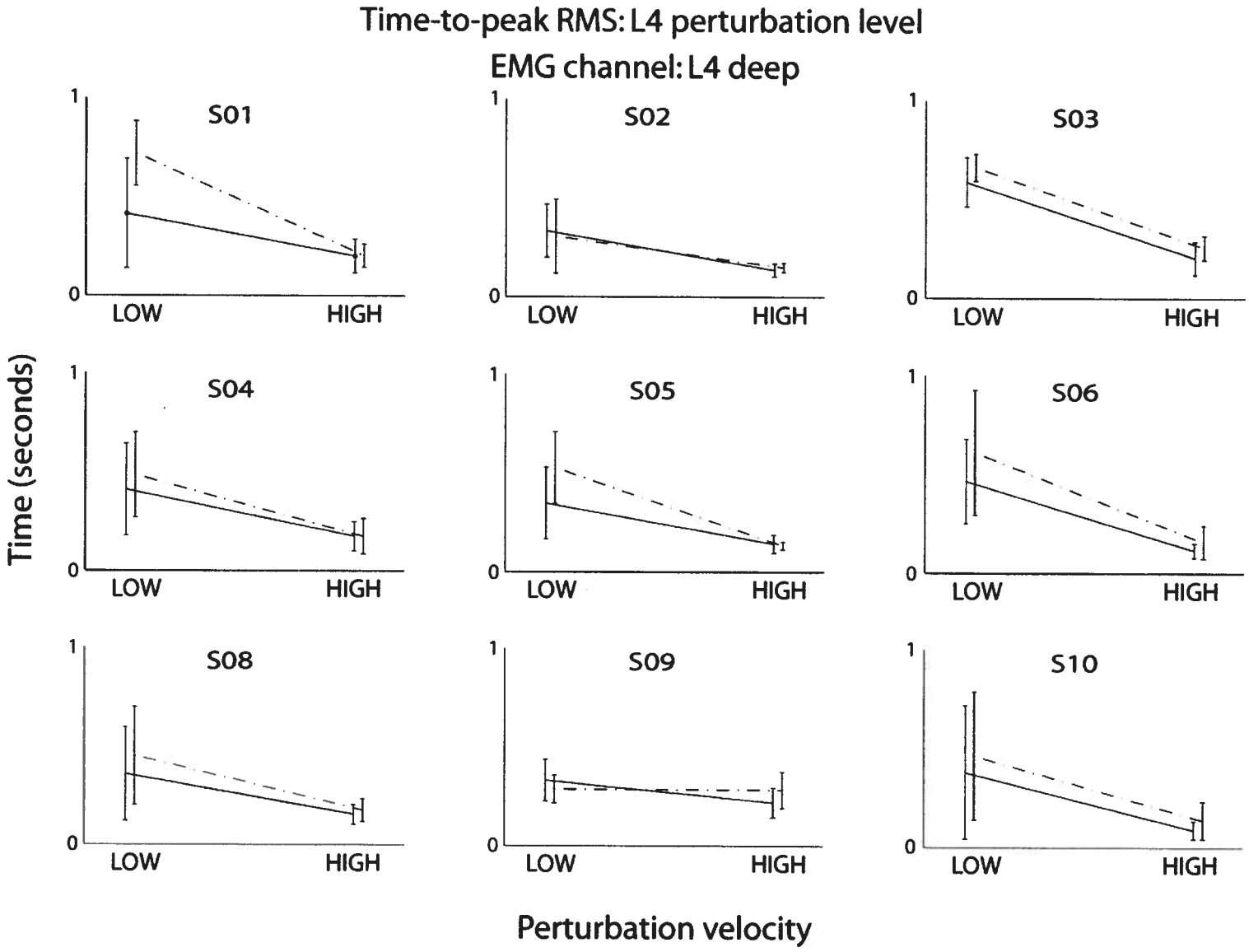
Time-to-peak RMS: L4 perturbation level
EMG channel: L4 deep
S01
S02
S03
S04
S05
S06
S08
S09
S10
1
0
LOW
HIGH
Time (seconds)
Perturbation velocity

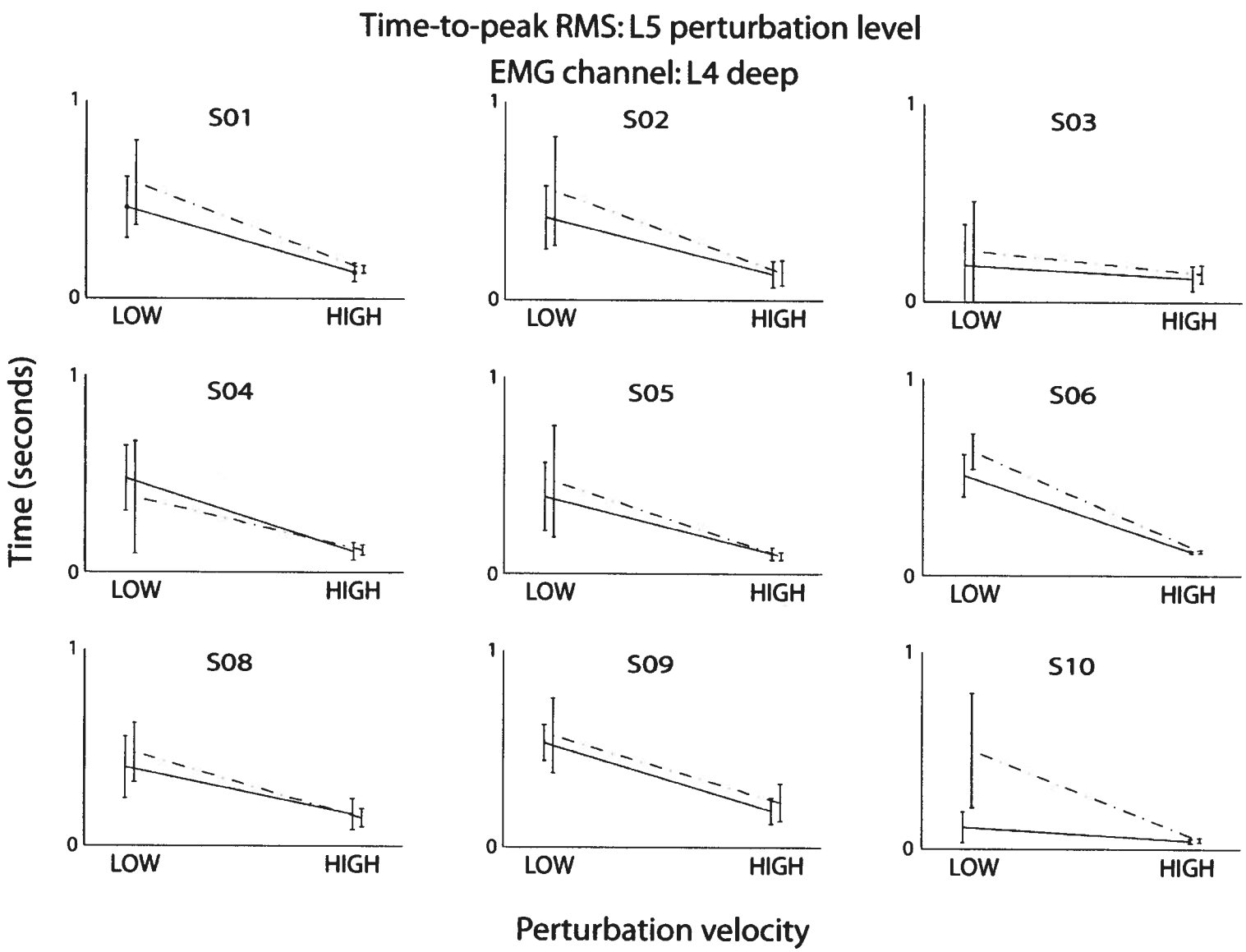
Time-to-peak RMS: L5 perturbation level
EMG channel: L4 deep
S01
S02
S03
S04
S05
S06
S08
S09
S10
1
0
LOW
HIGH
Time (seconds)
Perturbation velocity

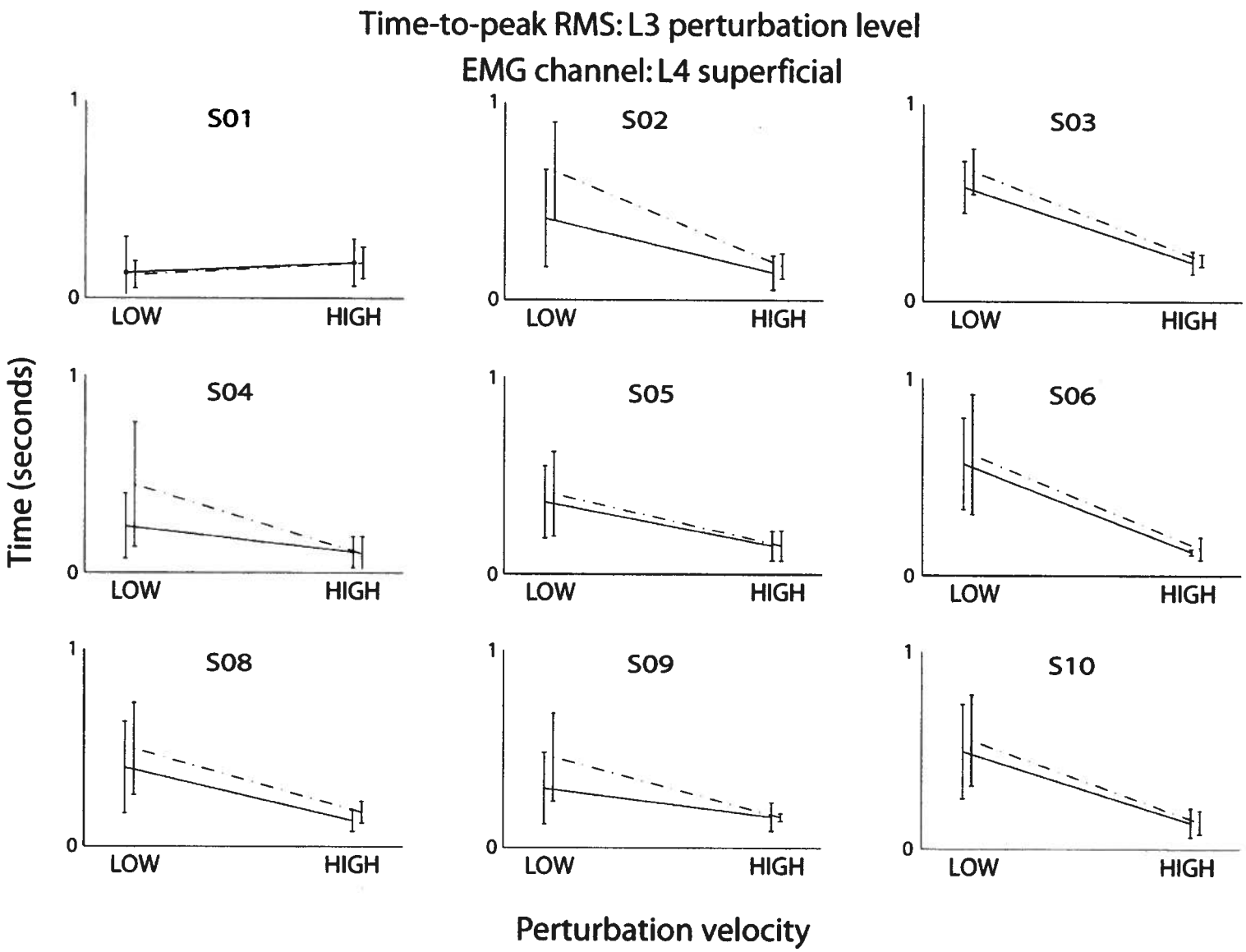
Time-to-peak RMS: L3 perturbation level
EMG channel: L4 superficial
S01
S02
S03
S04
S05
S06
S08
S09
S10
1
0
LOW
HIGH
Time (seconds)
Perturbation velocity

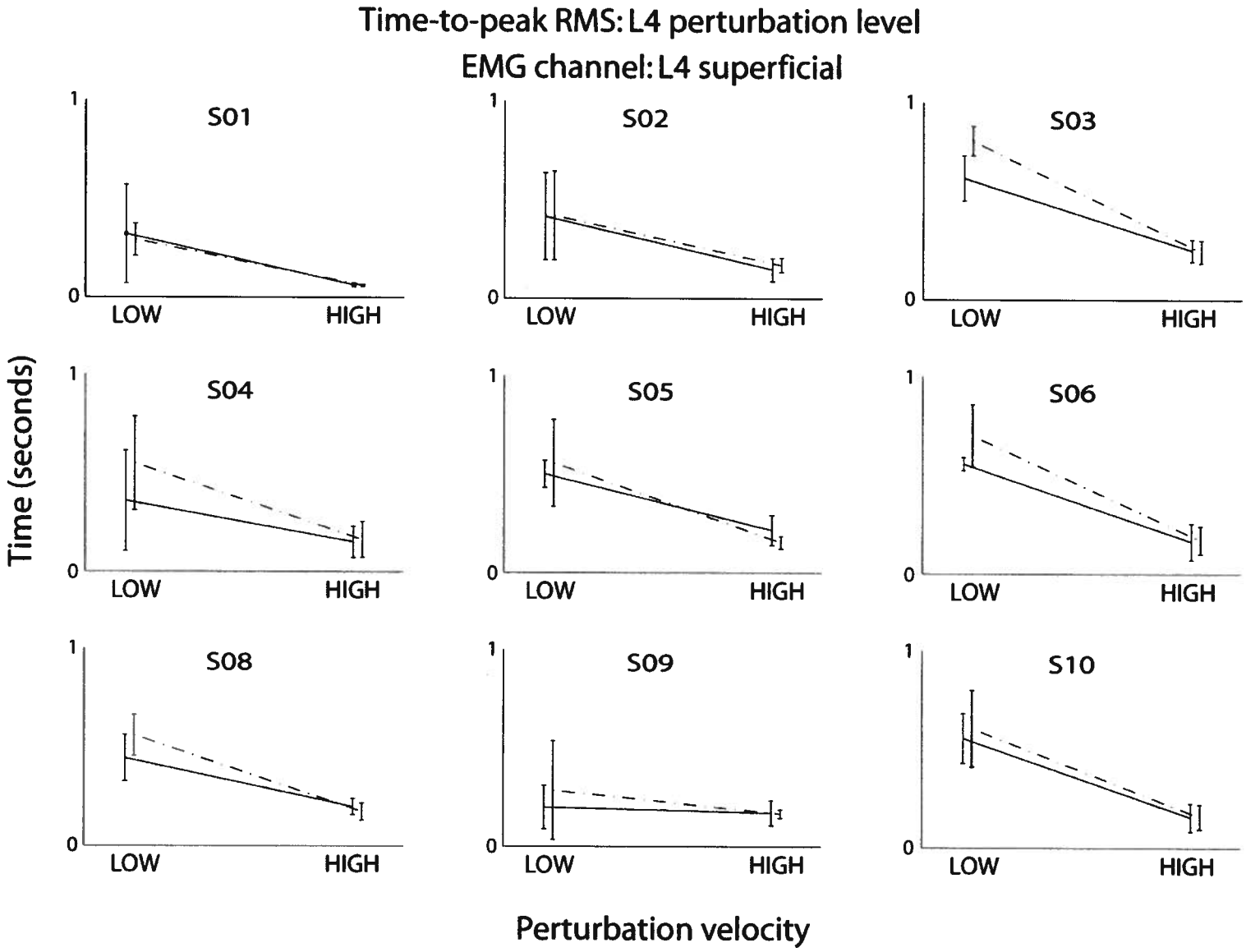
Time-to-peak RMS: L4 perturbation level
EMG channel: L4 superficial
S01
S02
S03
S04
S05
S06
S08
S09
S10
1
0
LOW
HIGH
Time (seconds)
Perturbation velocity

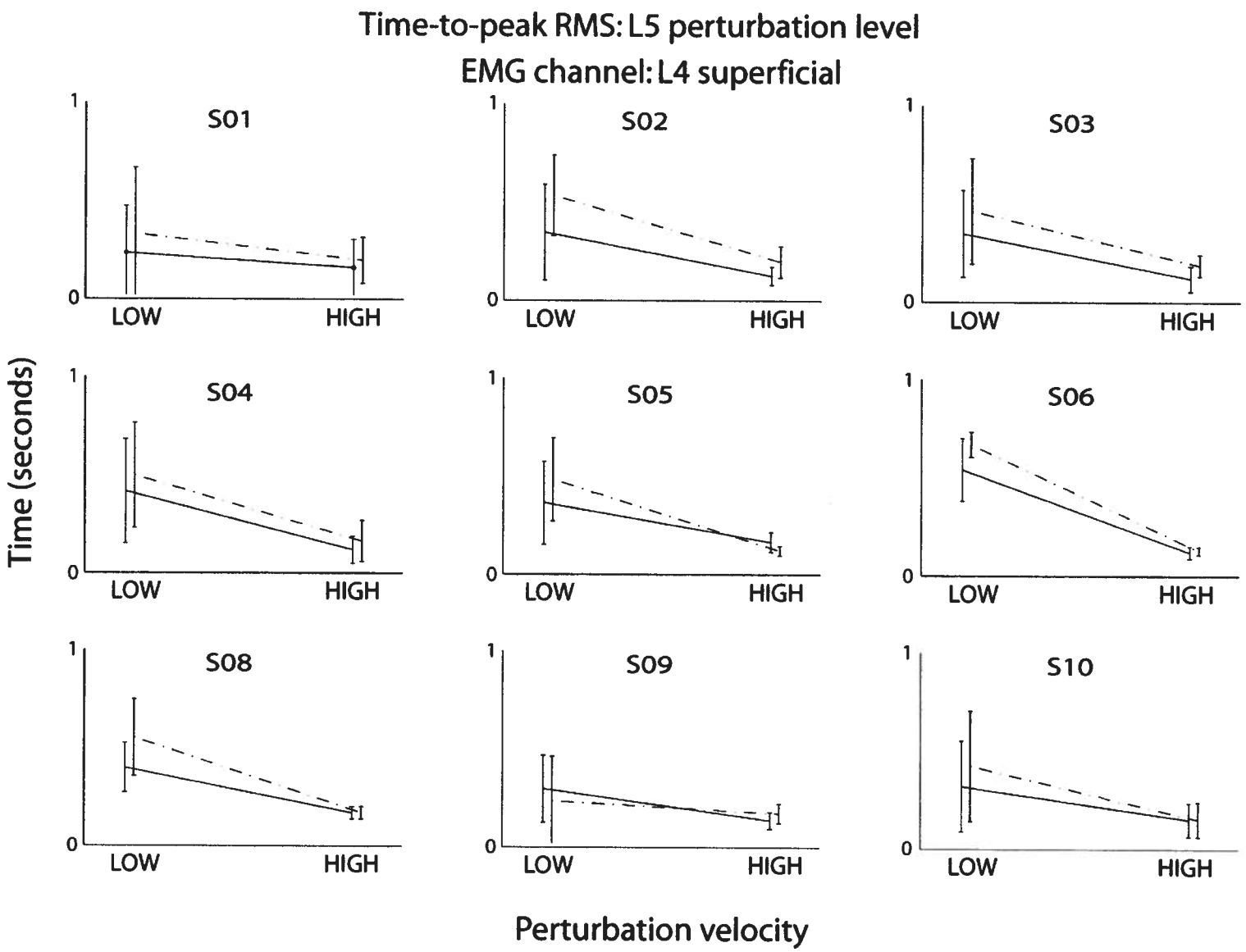
Time-to-peak RMS: L5 perturbation level
EMG channel: L4 superficial
S01
S02
S03
S04
S05
S06
S08
S09
S10
1
0
LOW
HIGH
Time (seconds)
Perturbation velocity

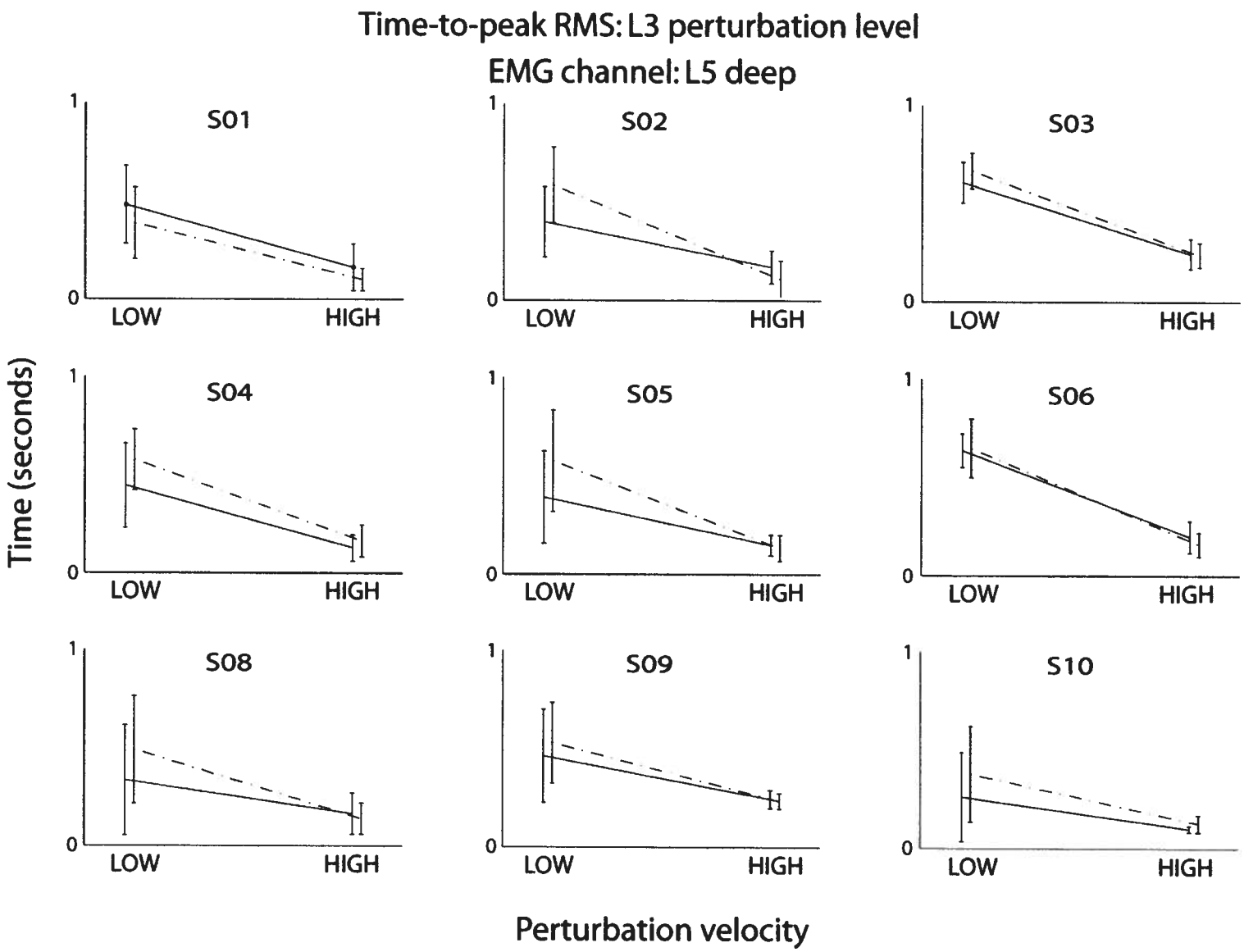
Time-to-peak RMS: L3 perturbation level
EMG channel: L5 deep
S01
S02
S03
S04
S05
S06
S08
S09
S10
1
0
LOW
HIGH
Time (seconds)
Perturbation velocity

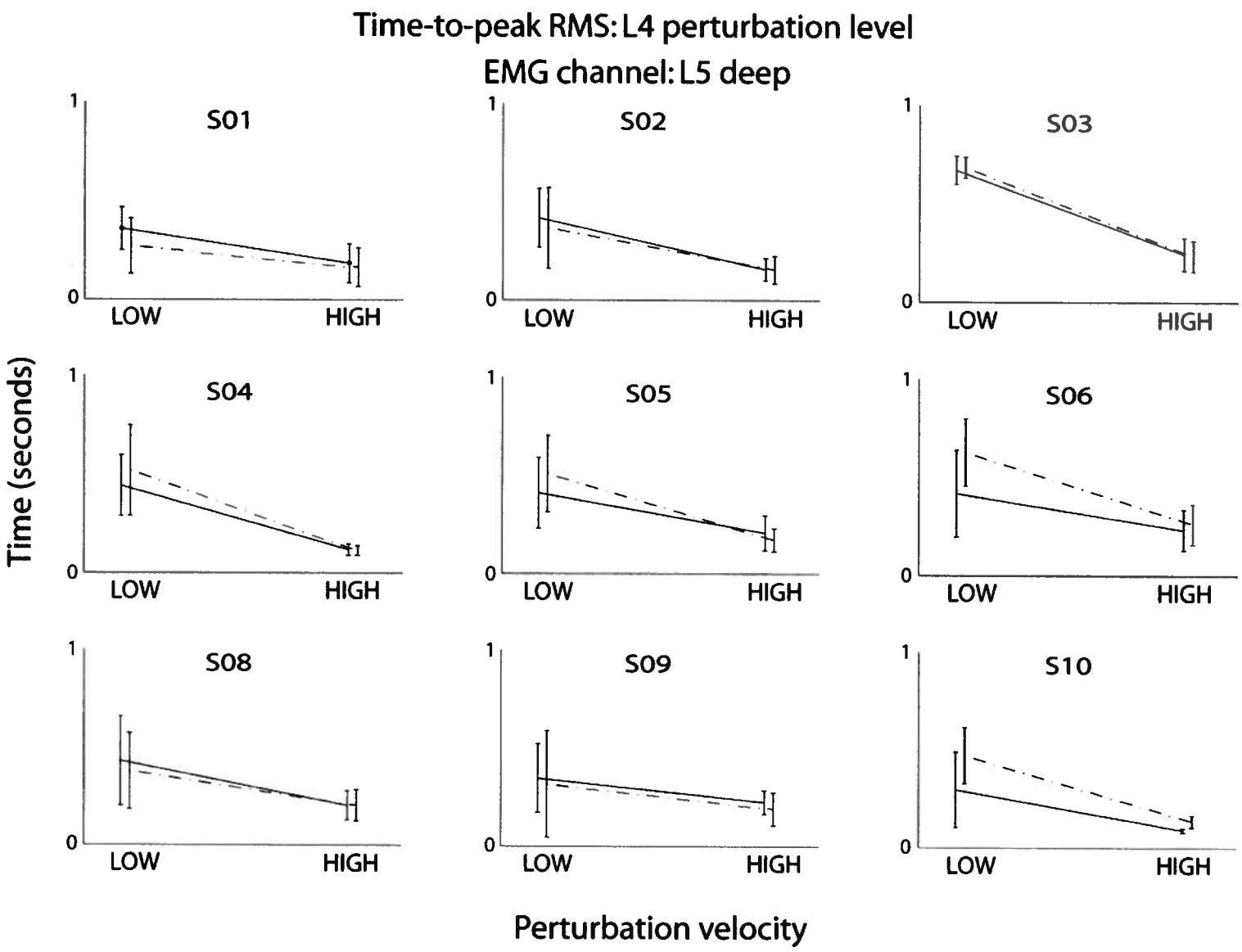
Time-to-peak RMS: L4 perturbation level
EMG channel: L5 deep
S01
S02
S03
S04
S05
S06
S08
S09
S10
1
0
LOW
HIGH
Time (seconds)
Perturbation velocity

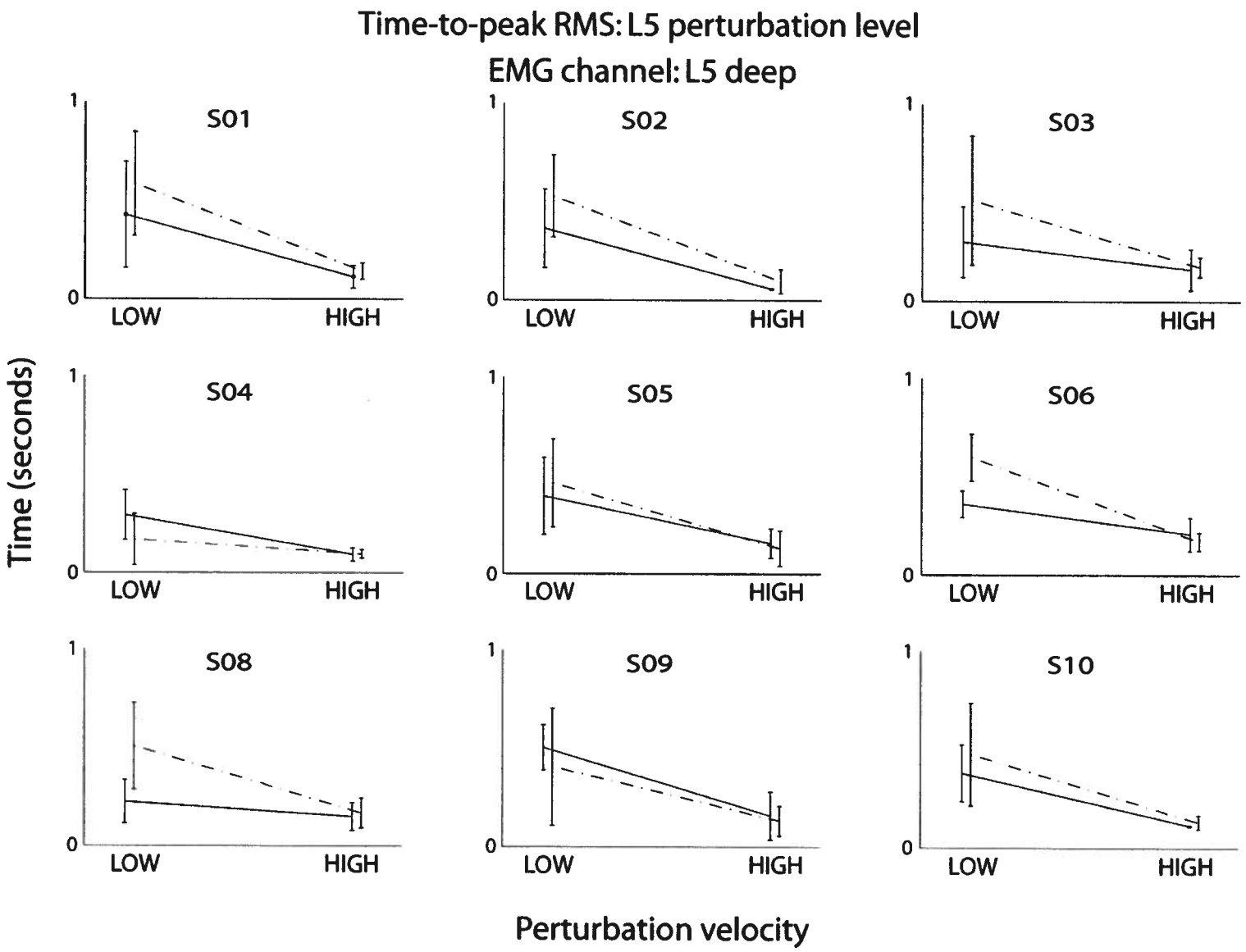
Time-to-peak RMS: L5 perturbation level
EMG channel: L5 deep
S01
S02
S03
S04
S05
S06
S08
S09
S10
1
0
LOW
HIGH
Time (seconds)
Perturbation velocity

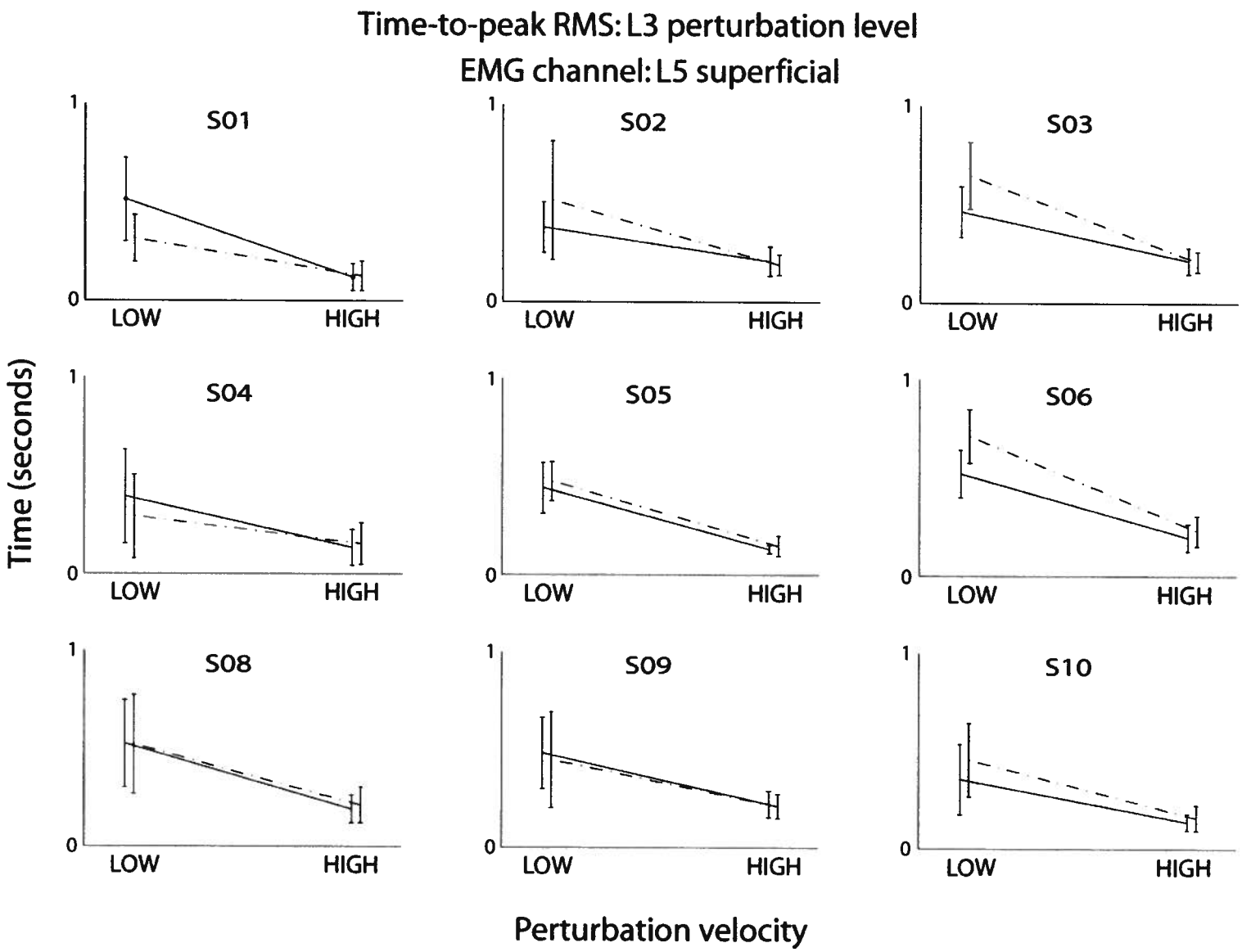
Time-to-peak RMS: L3 perturbation level
EMG channel: L5 superficial
S01
S02
S03
S04
S05
S06
S08
S09
S10
1
0
LOW
HIGH
Time (seconds)
Perturbation velocity

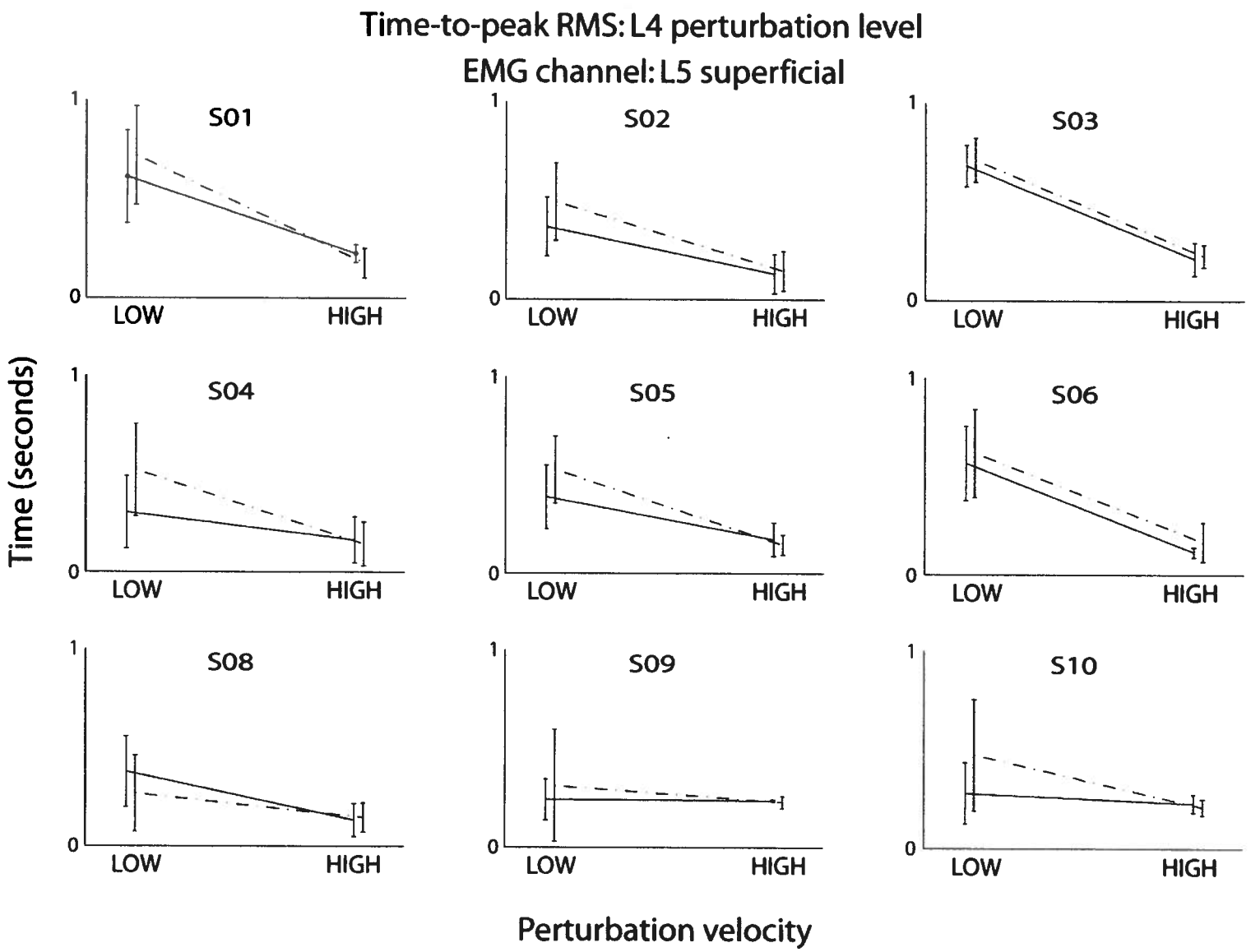
Time-to-peak RMS: L4 perturbation level
EMG channel: L5 superficial
S01
S02
S03
S04
S05
S06
S08
S09
S10
1
0
LOW
HIGH
Time (seconds)
Perturbation velocity

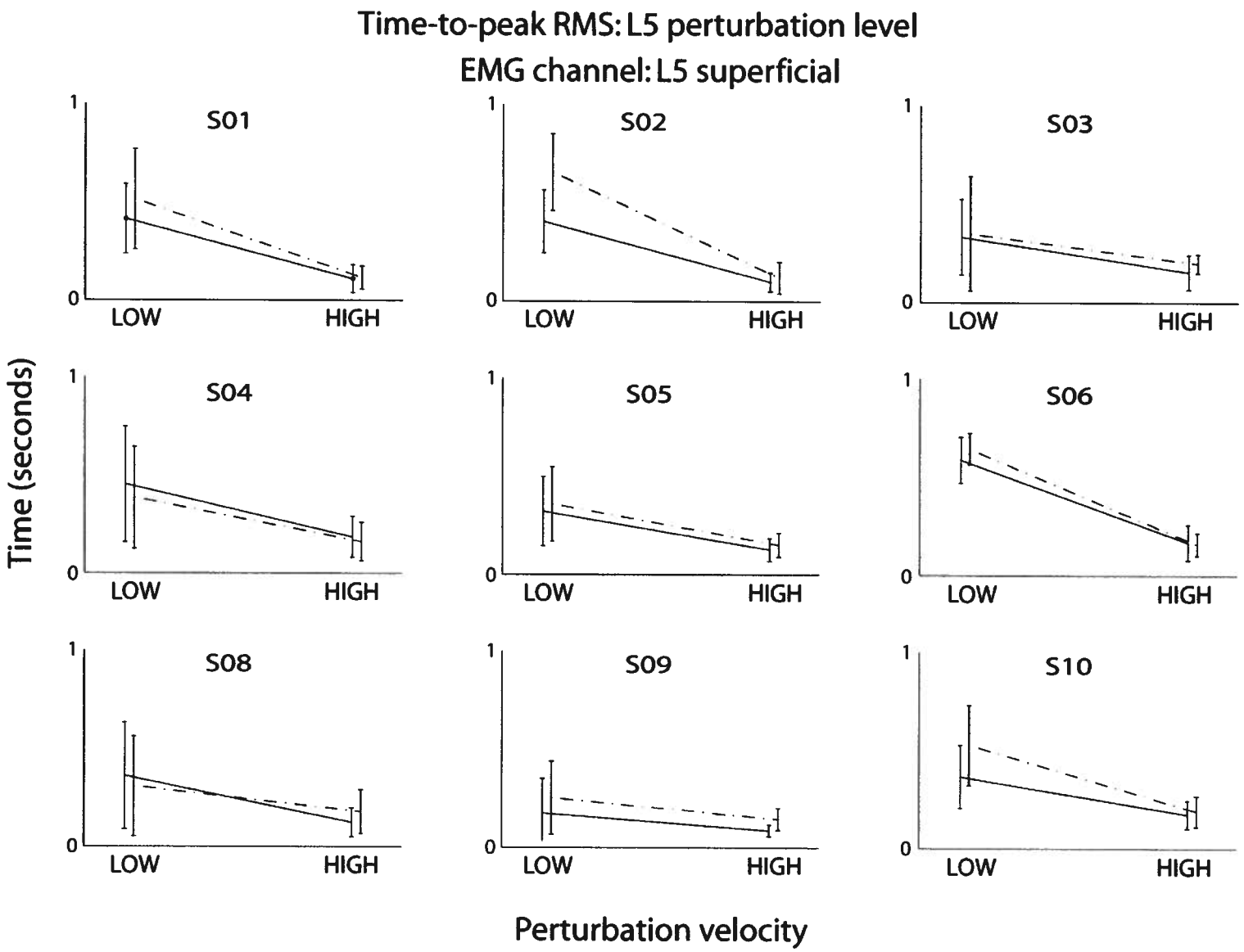
Time-to-peak RMS: L5 perturbation level
EMG channel: L5 superficial
S01
S02
S03
S04
S05
S06
S08
S09
S10
1
0
LOW
HIGH
Time (seconds)
Perturbation velocity